

# Deep Learning For Climate Studies

M.Sc. Thesis

By  
**MANISH KUMAR SINGH**



**DISCIPLINE OF Astronomy, Astrophysics and Space Engineering**  
**INDIAN INSTITUTE OF TECHNOLOGY INDORE**  
May, 2022

# Deep Learning For Climate Studies

A THESIS

*Submitted in partial fulfillment of the  
requirements for the award of the degree of*  
**Master of Science**

*by*

**MANISH KUMAR SINGH**



**DISCIPLINE OF Astronomy, Astrophysics and Space Engineering**  
**INDIAN INSTITUTE OF TECHNOLOGY INDORE**

**May, 2022**



# INDIAN INSTITUTE OF TECHNOLOGY INDORE

## CANDIDATE'S DECLARATION

I hereby certify that the work which is being presented in the thesis entitled “**Deep Learning For Climate Studies**” in the partial fulfillment of the requirements for the award of the degree of **Master of Science** and submitted in the **Discipline of Astronomy, Astrophysics and Space Engineering, Indian Institute of Technology Indore**, is an authentic record of my own work carried out during the time period from August 2020 to May 2022 under the supervision of Dr. Saurabh Das, Assistant Professor, IIT Indore. The matter presented in this thesis has not been submitted by me for the award of any other degree of this or any other institute.

*Manish Kumar Singh 23/05/2022*

Signature of the student with date  
(**MANISH KUMAR SINGH**)

-----  
This is to certify that the above statement made by the candidate is correct to the best of my/our knowledge.

*S. Das*  
23/05/2022

Signature(s) of the Supervisor(s) of

M.Sc. (with date)

(**DR. SAURABH DAS**)

-----  
Manish Kumar Singh has successfully given his/her M.Sc. Oral Examination held on **05 May 2022**.

*S. Das*  
24-05-2022

Signature of PSPC Member #1  
Date:

*Somnath Dey* 25.05.2022

Signature of PSPC Member #2  
Date:

Signature of PSPC Member #3  
Date:

*S. Das*  
23/05/2022  
Signature(s) of Supervisor(s).  
Date:

*S. Das*  
Signature of M.Sc. Co-Ordinator  
Date: 25/05/2022

*S. Das*  
23/05/2022  
Convener, DPGC  
Date:

*Manusweta Chakraborty*  
Signature of HoD (Officiating)  
Date: 26/05/2022

## **ACKNOWLEDGEMENTS**

I would like to acknowledge my supervisor Dr. Saurabh Das. His guidance has been very helpful for my learning and research.

## **Abstract**

Numerical Weather Prediction is the basis for weather forecasting which require interpretation by experts to generate weather forecasts for a local area. NWP's predictions have very low spatial resolution like 30-50 kms or more. For disaster management, agriculture, etc we often need weather prediction for local regions, in some cases for a particular location. Deep learning models like CNN can be used to downscale the global NWP's predictions to produce local forecasts.

In this project, I have used different convolutional neural network models to interpret numerical weather prediction model data. Also, different architectures are compared against each other to find which gives the best performance. Here the measure of the performance is mean absolute error (MAE). We show that CNNs can learn certain configurations of the atmospheric pressure system and connect them with wind speed and visibility. There is a possibility CNN-based models can be used to automatically generate derived products, in addition to numerical weather model interpretation.

## Contents

|  |      |
|--|------|
| LIST OF FIGURES .....                              | VIII |
| LIST OF TABLES .....                               | XVII |
| Chapter 1- Introduction .....                      | 1    |
| Chapter 2- Literature review .....                 | 5    |
| Chapter 3- DATA.....                               | 7    |
| Data characteristics .....                         | 10   |
| Wind Speed (mph) data for airport VABB .....       | 10   |
| Wind Speed (mph) data for airport VOTV .....       | 11   |
| Wind Speed (mph) data for airport VOBL .....       | 12   |
| Wind Speed (mph) data for airport VECC.....        | 14   |
| Wind Speed (mph) data for airport VIDP .....       | 15   |
| Visibility (miles) data for airport VABB .....     | 16   |
| Visibility (miles) data for airport VOTV .....     | 18   |
| Visibility (miles) data for airport VOBL .....     | 19   |
| Visibility (miles) data for airport VECC.....      | 20   |
| Visibility (miles) data for airport VIDP .....     | 22   |
| Chapter 4- Methodology .....                       | 24   |
| VGG16, 2D CNN, 3D CNN .....                        | 24   |
| Hyperparameters used:.....                         | 26   |
| Chapter 5- Results .....                           | 27   |
| Result (Mean Absolute Error) for Visibility: ..... | 27   |
| For station VABB, .....                            | 28   |
| For station VOTV, .....                            | 37   |

|  |     |
|--|-----|
| For station VOBL.....                              | 45  |
| For station VECC,.....                             | 52  |
| For station VIDP,.....                             | 60  |
| Result (Mean Absolute Error) for Wind Speed: ..... | 67  |
| For station VABB, .....                            | 68  |
| For station VOTV, .....                            | 77  |
| For station VOBL,.....                             | 85  |
| For station VECC,.....                             | 93  |
| For station VIDP, .....                            | 101 |
| CHAPTER 6 – Conclusions and Future work .....      | 109 |
| REFERENCES.....                                    | 110 |

# LIST OF FIGURES

|   |    |
|---|----|
| Figure 3.1(a): wind speed Vs frequency for VABB .....         | 10 |
| Figure 3.1(b): wind speed in different seasons for VABB ..... | 10 |
| Figure 3.1(c): wind speed in winter for VABB .....            | 10 |
| Figure 3.1(d): wind speed in summer for VABB .....            | 10 |
| Figure 3.1(e): wind speed in monsoon for VABB .....           | 11 |
| Figure 3.1(f): wind speed in autumn for VABB .....            | 11 |
| Figure 3.2(a): wind speed Vs frequency for VOTV .....         | 11 |
| Figure 3.2(b): wind speed in different seasons for VOTV ..... | 11 |
| Figure 3.2(c): wind speed in winter for VOTV .....            | 12 |
| Figure 3.2(d): wind speed in summer for VOTV .....            | 12 |
| Figure 3.2(e): wind speed in monsoon for VOTV .....           | 12 |
| Figure 3.2(f): wind speed in autumn for VOTV .....            | 12 |
| Figure 3.3(a): wind speed Vs frequency for VOBL .....         | 13 |
| Figure 3.3(b): wind speed in different seasons for VOBL ..... | 13 |
| Figure 3.3(c): wind speed in winter for VOBL .....            | 13 |
| Figure 3.3(d): wind speed in summer for VOBL .....            | 13 |
| Figure 3.3(e): wind speed in monsoon for VOBL .....           | 13 |
| Figure 3.3(f): wind speed in autumn for VOBL .....            | 13 |
| Figure 3.4(a): wind speed Vs frequency for VECC .....         | 14 |
| Figure 3.4(b): wind speed in different seasons for VECC ..... | 14 |
| Figure 3.4(c): wind speed in winter for VECC .....            | 14 |
| Figure 3.4(d): wind speed in summer for VECC .....            | 14 |
| Figure 3.4(e): wind speed in monsoon for VECC .....           | 15 |
| Figure 3.4(f): wind speed in autumn for VECC .....            | 15 |
| Figure 3.5(a): wind speed Vs frequency for VIDP .....         | 15 |
| Figure 3.5(b): wind speed in different seasons for VIDP ..... | 15 |
| Figure 3.5(c): wind speed in winter for VIDP .....            | 16 |
| Figure 3.5(d): wind speed in summer for VIDP .....            | 16 |
| Figure 3.5(e): wind speed in monsoon for VIDP .....           | 16 |
| Figure 3.5(f): wind speed in autumn for VIDP .....            | 16 |
| Figure 3.6(a): visibility Vs frequency for VABB .....         | 17 |

|   |    |
|---|----|
| Figure 3.6(b): visibility in different seasons for VABB .....           | 17 |
| Figure 3.6(c): visibility in winter for VABB .....                      | 17 |
| Figure 3.6(d): visibility in summer for VABB .....                      | 17 |
| Figure 3.6(e): visibility in monsoon for VABB .....                     | 17 |
| Figure 3.6(f): visibility in autumn for VABB .....                      | 17 |
| Figure 3.7(a): visibility Vs frequency for VOTV .....                   | 18 |
| Figure 3.7(b): visibility in different seasons for VOTV .....           | 18 |
| Figure 3.7(c): visibility in winter for VOTV .....                      | 18 |
| Figure 3.7(d): visibility in summer for VOTV .....                      | 18 |
| Figure 3.7(e): visibility in monsoon for VOTV .....                     | 19 |
| Figure 3.7(f): visibility in autumn for VOTV .....                      | 19 |
| Figure 3.8(a): visibility Vs frequency for VOBL .....                   | 19 |
| Figure 3.8(b): visibility in different seasons for VOBL .....           | 19 |
| Figure 3.8(c): visibility in winter for VOBL .....                      | 20 |
| Figure 3.8(d): visibility in summer for VOBL .....                      | 20 |
| Figure 3.8(e): visibility in monsoon for VOBL .....                     | 20 |
| Figure 3.8(f): visibility in autumn for VOBL .....                      | 20 |
| Figure 3.9(a): visibility Vs frequency for VECC .....                   | 21 |
| Figure 3.9(b): visibility in different seasons for VECC .....           | 21 |
| Figure 3.9(c): visibility in winter for VECC .....                      | 21 |
| Figure 3.9(d): visibility in summer for VECC .....                      | 21 |
| Figure 3.9(e): visibility in monsoon for VECC .....                     | 21 |
| Figure 3.9(f): visibility in autumn for VECC .....                      | 21 |
| Figure 3.10(a): visibility Vs frequency for VIDP .....                  | 22 |
| Figure 3.10(b): visibility in different seasons for VIDP .....          | 22 |
| Figure 3.10(c): visibility in winter for VIDP .....                     | 22 |
| Figure 3.10(d): visibility in summer for VIDP .....                     | 22 |
| Figure 3.10(e): visibility in monsoon for VIDP .....                    | 23 |
| Figure 3.10(f): visibility in autumn for VIDP .....                     | 23 |
| Figure 4.1: VGG16 .....   | 24 |
| Figure 5.1(a): epoch Vs loss for VABB, visibility with 2D CNN .....     | 28 |
| Figure 5.1(b): epoch Vs accuracy for VABB, visibility with 2D CNN ..... | 28 |
| Figure 5.1(c): histogram of errors .....                                | 29 |

|   |    |
|---|----|
| Figure 5.1(d): observation and prediction plot for monsoon season .....                 | 30 |
| Figure 5.1(e): histogram of errors on 1 year independent dataset .....                  | 30 |
| Figure 5.1(f): percentage error histogram for the same 1 year independent dataset ..... | 31 |
| Figure 5.1(g): error histogram for summer .....   | 31 |
| Figure 5.1(h): error histogram for monsoon .....  | 31 |
| Figure 5.1(i): error histogram for autumn .....   | 32 |
| Figure 5.1(j): error histogram for winter .....   | 32 |
| Figure 5.1(k): epoch Vs loss for VABB, visibility with VGG16 .....                      | 33 |
| Figure 5.1(l): epoch Vs accuracy for VABB, visibility with VGG16 .....                  | 33 |
| Figure 5.1(m): histogram of errors .....  | 33 |
| Figure 5.1(n): observation and prediction plot for monsoon season .....                 | 34 |
| Figure 5.1(o): histogram of errors on 1 year independent dataset .....                  | 35 |
| Figure 5.1(p): percentage error histogram for the same 1 year independent dataset ..... | 35 |
| Figure 5.1(q): error histogram for summer .....   | 35 |
| Figure 5.1(r): error histogram for monsoon .....  | 35 |
| Figure 5.1(s): error histogram for autumn .....   | 36 |
| Figure 5.1(t): error histogram for winter .....   | 36 |
| Figure 5.1(u): epoch Vs loss for VABB, visibility with 3D CNN .....                     | 37 |
| Figure 5.1(v): epoch Vs accuracy for VABB, visibility with 3D CNN .....                 | 37 |
| Figure 5.2(a): epoch Vs loss for VABB, visibility with 2D CNN .....                     | 37 |
| Figure 5.2(b): epoch Vs accuracy for VABB, visibility with 2D CNN .....                 | 37 |
| Figure 5.2(c): histogram of errors .....  | 38 |
| Figure 5.2(d): observation and prediction plot for monsoon season .....                 | 39 |
| Figure 5.2(e): histogram of errors on 1 year independent dataset .....                  | 39 |
| Figure 5.2(f): percentage error histogram for the same 1 year independent dataset ..... | 39 |
| Figure 5.2(g): error histogram for summer .....   | 40 |
| Figure 5.2(h): error histogram for monsoon .....  | 40 |
| Figure 5.2(i): error histogram for autumn .....   | 40 |
| Figure 5.2(j): error histogram for winter .....   | 40 |
| Figure 5.2(k): epoch Vs loss for VABB, visibility with VGG16 .....                      | 41 |
| Figure 5.2(l): epoch Vs accuracy for VABB, visibility with VGG16 .....                  | 41 |
| Figure 5.2(m): histogram of errors .....  | 41 |
| Figure 5.2(n): observation and prediction plot for monsoon season .....                 | 42 |

|   |    |
|---|----|
| Figure 5.2(o): histogram of errors on 1 year independent dataset .....                  | 43 |
| Figure 5.2(p): percentage error histogram for the same 1 year independent dataset ..... | 43 |
| Figure 5.2(q): error histogram for summer .....   | 43 |
| Figure 5.2(r): error histogram for monsoon .....  | 43 |
| Figure 5.2(s): error histogram for autumn .....   | 44 |
| Figure 5.2(t): error histogram for winter .....   | 44 |
| Figure 5.2(u): epoch Vs loss for VABB, visibility with 3D CNN .....                     | 44 |
| Figure 5.2(v): epoch Vs accuracy for VABB, visibility with 3D CNN .....                 | 44 |
| Figure 5.3(a): epoch Vs loss for VABB, visibility with 2D CNN .....                     | 45 |
| Figure 5.3(b): epoch Vs accuracy for VABB, visibility with 2D CNN .....                 | 45 |
| Figure 5.3(c): histogram of errors .....  | 45 |
| Figure 5.3(d): observation and prediction plot for monsoon season .....                 | 46 |
| Figure 5.3(e): histogram of errors on 1 year independent dataset .....                  | 47 |
| Figure 5.3(f): percentage error histogram for the same 1 year independent dataset ..... | 47 |
| Figure 5.3(g): error histogram for summer .....   | 47 |
| Figure 5.3(h): error histogram for monsoon .....  | 47 |
| Figure 5.3(i): error histogram for autumn .....   | 48 |
| Figure 5.3(j): error histogram for winter .....   | 48 |
| Figure 5.3(k): epoch Vs loss for VABB, visibility with VGG16 .....                      | 48 |
| Figure 5.3(l): epoch Vs accuracy for VABB, visibility with VGG16 .....                  | 48 |
| Figure 5.3(m): histogram of errors .....  | 49 |
| Figure 5.3(n): observation and prediction plot for monsoon season .....                 | 50 |
| Figure 5.3(o): histogram of errors on 1 year independent dataset .....                  | 50 |
| Figure 5.3(p): percentage error histogram for the same 1 year independent dataset ..... | 50 |
| Figure 5.3(q): error histogram for summer .....   | 51 |
| Figure 5.3(r): error histogram for monsoon .....  | 51 |
| Figure 5.3(s): error histogram for autumn .....   | 51 |
| Figure 5.3(t): error histogram for winter .....   | 51 |
| Figure 5.3(u): epoch Vs loss for VABB, visibility with 3D CNN .....                     | 52 |
| Figure 5.3(v): epoch Vs accuracy for VABB, visibility with 3D CNN .....                 | 52 |
| Figure 5.4(a): epoch Vs loss for VABB, visibility with 2D CNN .....                     | 52 |
| Figure 5.4(b): epoch Vs accuracy for VABB, visibility with 2D CNN .....                 | 52 |
| Figure 5.4(c): histogram of errors .....  | 53 |

|   |    |
|---|----|
| Figure 5.4(d): observation and prediction plot for monsoon season .....                 | 54 |
| Figure 5.4(e): histogram of errors on 1 year independent dataset .....                  | 54 |
| Figure 5.4(f): percentage error histogram for the same 1 year independent dataset ..... | 54 |
| Figure 5.4(g): error histogram for summer .....   | 55 |
| Figure 5.4(h): error histogram for monsoon .....  | 55 |
| Figure 5.4(i): error histogram for autumn .....   | 55 |
| Figure 5.4(j): error histogram for winter .....   | 55 |
| Figure 5.4(k): epoch Vs loss for VABB, visibility with VGG16 .....                      | 56 |
| Figure 5.4(l): epoch Vs accuracy for VABB, visibility with VGG16 .....                  | 56 |
| Figure 5.4(m): histogram of errors .....  | 56 |
| Figure 5.4(n): observation and prediction plot for monsoon season .....                 | 57 |
| Figure 5.4(o): histogram of errors on 1 year independent dataset .....                  | 58 |
| Figure 5.4(p): percentage error histogram for the same 1 year independent dataset ..... | 58 |
| Figure 5.4(q): error histogram for summer .....   | 58 |
| Figure 5.4(r): error histogram for monsoon .....  | 58 |
| Figure 5.4(s): error histogram for autumn .....   | 59 |
| Figure 5.4(t): error histogram for winter .....   | 59 |
| Figure 5.4(u): epoch Vs loss for VABB, visibility with 3D CNN .....                     | 59 |
| Figure 5.4(v): epoch Vs accuracy for VABB, visibility with 3D CNN .....                 | 59 |
| Figure 5.5(a): epoch Vs loss for VABB, visibility with 2D CNN .....                     | 60 |
| Figure 5.5(b): epoch Vs accuracy for VABB, visibility with 2D CNN .....                 | 60 |
| Figure 5.5(c): histogram of errors .....  | 61 |
| Figure 5.5(d): observation and prediction plot for monsoon season .....                 | 62 |
| Figure 5.5(e): histogram of errors on 1 year independent dataset .....                  | 62 |
| Figure 5.5(f): percentage error histogram for the same 1 year independent dataset ..... | 62 |
| Figure 5.5(g): error histogram for summer .....   | 63 |
| Figure 5.5(h): error histogram for monsoon .....  | 63 |
| Figure 5.5(i): error histogram for autumn .....   | 63 |
| Figure 5.5(j): error histogram for winter .....   | 63 |
| Figure 5.5(k): epoch Vs loss for VABB, visibility with VGG16 .....                      | 64 |
| Figure 5.5(l): epoch Vs accuracy for VABB, visibility with VGG16 .....                  | 64 |
| Figure 5.5(m): histogram of errors .....  | 64 |
| Figure 5.5(n): observation and prediction plot for monsoon season .....                 | 65 |

|   |    |
|---|----|
| Figure 5.5(o): histogram of errors on 1 year independent dataset .....                  | 66 |
| Figure 5.5(p): percentage error histogram for the same 1 year independent dataset ..... | 66 |
| Figure 5.5(q): error histogram for summer .....   | 66 |
| Figure 5.5(r): error histogram for monsoon .....  | 66 |
| Figure 5.5(s): error histogram for autumn .....   | 66 |
| Figure 5.5(t): error histogram for winter .....   | 66 |
| Figure 5.5(u): epoch Vs loss for VABB, visibility with 3D CNN .....                     | 67 |
| Figure 5.5(v): epoch Vs accuracy for VABB, visibility with 3D CNN .....                 | 67 |
| Figure 5.6(a): epoch Vs loss for VABB, wind speed with 2D CNN .....                     | 68 |
| Figure 5.6(b): epoch Vs accuracy for VABB, wind speed with 2D CNN .....                 | 68 |
| Figure 5.6(c): histogram of errors .....  | 69 |
| Figure 5.6(d): observation and prediction plot for monsoon season .....                 | 70 |
| Figure 5.6(e): histogram of errors on 1 year independent dataset .....                  | 71 |
| Figure 5.6(f): percentage error histogram for the same 1 year independent dataset ..... | 71 |
| Figure 5.6(g): error histogram for summer .....   | 71 |
| Figure 5.6(h): error histogram for monsoon .....  | 71 |
| Figure 5.6(i): error histogram for autumn .....   | 72 |
| Figure 5.6(j): error histogram for winter .....   | 72 |
| Figure 5.6(k): epoch Vs loss for VABB, wind speed with VGG16 .....                      | 73 |
| Figure 5.6(l): epoch Vs accuracy for VABB, wind speed with VGG16 .....                  | 73 |
| Figure 5.6(m): histogram of errors .....  | 73 |
| Figure 5.6(n): observation and prediction plot for monsoon season .....                 | 74 |
| Figure 5.6(o): histogram of errors on 1 year independent dataset .....                  | 75 |
| Figure 5.6(p): percentage error histogram for the same 1 year independent dataset ..... | 75 |
| Figure 5.6(q): error histogram for summer .....   | 75 |
| Figure 5.6(r): error histogram for monsoon .....  | 75 |
| Figure 5.6(s): error histogram for autumn .....   | 76 |
| Figure 5.6(t): error histogram for winter .....   | 76 |
| Figure 5.6(u): epoch Vs loss for VABB, wind speed with 3D CNN .....                     | 77 |
| Figure 5.6(v): epoch Vs accuracy for VABB, wind speed with 3D CNN .....                 | 77 |
| Figure 5.7(a): epoch Vs loss for VOTV, wind speed with 2D CNN .....                     | 77 |
| Figure 5.7(b): epoch Vs accuracy for VOTV, wind speed with 2D CNN .....                 | 77 |
| Figure 5.7(c): histogram of errors .....  | 78 |

|   |    |
|---|----|
| Figure 5.7(d): observation and prediction plot for monsoon season .....                 | 79 |
| Figure 5.7(e): histogram of errors on 1 year independent dataset .....                  | 79 |
| Figure 5.7(f): percentage error histogram for the same 1 year independent dataset ..... | 79 |
| Figure 5.7(g): error histogram for summer .....   | 80 |
| Figure 5.7(h): error histogram for monsoon .....  | 80 |
| Figure 5.7(i): error histogram for autumn .....   | 80 |
| Figure 5.7(j): error histogram for winter .....   | 80 |
| Figure 5.7(k): epoch Vs loss for VOTV, wind speed with VGG16 .....                      | 81 |
| Figure 5.7(l): epoch Vs accuracy for VOTV, wind speed with VGG16 .....                  | 81 |
| Figure 5.7(m): histogram of errors .....  | 81 |
| Figure 5.7(n): observation and prediction plot for monsoon season .....                 | 82 |
| Figure 5.7(o): histogram of errors on 1 year independent dataset .....                  | 83 |
| Figure 5.7(p): percentage error histogram for the same 1 year independent dataset ..... | 83 |
| Figure 5.7(q): error histogram for summer .....   | 83 |
| Figure 5.7(r): error histogram for monsoon .....  | 83 |
| Figure 5.7(s): error histogram for autumn .....   | 84 |
| Figure 5.7(t): error histogram for winter .....   | 84 |
| Figure 5.7(u): epoch Vs loss for VOTV, wind speed with 3D CNN .....                     | 84 |
| Figure 5.7(v): epoch Vs accuracy for VOTV, wind speed with 3D CNN .....                 | 84 |
| Figure 5.8(a): epoch Vs loss for VOBL, wind speed with 2D CNN .....                     | 85 |
| Figure 5.8(b): epoch Vs accuracy for VOBL, wind speed with 2D CNN .....                 | 85 |
| Figure 5.8(c): histogram of errors .....  | 86 |
| Figure 5.8(d): observation and prediction plot for monsoon season .....                 | 87 |
| Figure 5.8(e): histogram of errors on 1 year independent dataset .....                  | 87 |
| Figure 5.8(f): percentage error histogram for the same 1 year independent dataset ..... | 87 |
| Figure 5.8(g): error histogram for summer .....   | 88 |
| Figure 5.8(h): error histogram for monsoon .....  | 88 |
| Figure 5.8(i): error histogram for autumn .....   | 88 |
| Figure 5.8(j): error histogram for winter .....   | 89 |
| Figure 5.8(k): epoch Vs loss for VOBL, wind speed with VGG16 .....                      | 89 |
| Figure 5.8(l): epoch Vs accuracy for VOBL, wind speed with VGG16 .....                  | 89 |
| Figure 5.8(m): histogram of errors .....  | 89 |
| Figure 5.8(n): observation and prediction plot for monsoon season .....                 | 90 |

|   |     |
|---|-----|
| Figure 5.8(o): histogram of errors on 1 year independent dataset .....                  | 90  |
| Figure 5.8(p): percentage error histogram for the same 1 year independent dataset ..... | 90  |
| Figure 5.8(q): error histogram for summer .....   | 91  |
| Figure 5.8(r): error histogram for monsoon .....  | 91  |
| Figure 5.8(s): error histogram for autumn .....   | 91  |
| Figure 5.8(t): error histogram for winter .....   | 91  |
| Figure 5.8(u): epoch Vs loss for VOBL, wind speed with 3D CNN .....                     | 92  |
| Figure 5.8(v): epoch Vs accuracy for VOBL, wind speed with 3D CNN .....                 | 92  |
| Figure 5.9(a): epoch Vs loss for VECC, wind speed with 2D CNN .....                     | 93  |
| Figure 5.9(b): epoch Vs accuracy for VECC, wind speed with 2D CNN .....                 | 93  |
| Figure 5.9(c): histogram of errors .....  | 94  |
| Figure 5.9(d): observation and prediction plot for monsoon season .....                 | 95  |
| Figure 5.9(e): histogram of errors on 1 year independent dataset .....                  | 95  |
| Figure 5.9(f): percentage error histogram for the same 1 year independent dataset ..... | 95  |
| Figure 5.9(g): error histogram for summer .....   | 96  |
| Figure 5.9(h): error histogram for monsoon .....  | 96  |
| Figure 5.9(i): error histogram for autumn .....   | 96  |
| Figure 5.9(j): error histogram for winter .....   | 96  |
| Figure 5.9(k): epoch Vs loss for VECC, wind speed with VGG16 .....                      | 97  |
| Figure 5.9(l): epoch Vs accuracy for VECC, wind speed with VGG16 .....                  | 97  |
| Figure 5.9(m): histogram of errors .....  | 97  |
| Figure 5.9(n): observation and prediction plot for monsoon season .....                 | 98  |
| Figure 5.9(o): histogram of errors on 1 year independent dataset .....                  | 98  |
| Figure 5.9(p): percentage error histogram for the same 1 year independent dataset ..... | 98  |
| Figure 5.9(q): error histogram for summer .....   | 99  |
| Figure 5.9(r): error histogram for monsoon .....  | 99  |
| Figure 5.9(s): error histogram for autumn .....   | 99  |
| Figure 5.9(t): error histogram for winter .....   | 99  |
| Figure 5.9(u): epoch Vs loss for VECC, wind speed with 3D CNN .....                     | 100 |
| Figure 5.9(v): epoch Vs accuracy for VECC, wind speed with 3D CNN .....                 | 100 |
| Figure 5.10(a): epoch Vs loss for VIDP, wind speed with 2D CNN .....                    | 101 |
| Figure 5.10(b): epoch Vs accuracy for VIDP, wind speed with 2D CNN .....                | 101 |
| Figure 5.10(c): histogram of errors .....   | 101 |

|  |     |
|--|-----|
| Figure 5.10(d): observation and prediction plot for monsoon season .....                 | 102 |
| Figure 5.10(e): histogram of errors on 1 year independent dataset .....                  | 103 |
| Figure 5.10(f): percentage error histogram for the same 1 year independent dataset ..... | 103 |
| Figure 5.10(g): error histogram for summer .....   | 103 |
| Figure 5.10(h): error histogram for monsoon .....  | 103 |
| Figure 5.10(i): error histogram for autumn .....   | 104 |
| Figure 5.10(j): error histogram for winter .....   | 104 |
| Figure 5.10(k): epoch Vs loss for VIDP, wind speed with VGG16 .....                      | 104 |
| Figure 5.10(l): epoch Vs accuracy for VIDP, wind speed with VGG16 .....                  | 104 |
| Figure 5.10(m): histogram of errors .....  | 105 |
| Figure 5.10(n): observation and prediction plot for monsoon season .....                 | 106 |
| Figure 5.10(o): histogram of errors on 1 year independent dataset .....                  | 106 |
| Figure 5.10(p): percentage error histogram for the same 1 year independent dataset ..... | 106 |
| Figure 5.10(q): error histogram for summer .....   | 107 |
| Figure 5.10(r): error histogram for monsoon .....  | 107 |
| Figure 5.10(s): error histogram for autumn .....   | 107 |
| Figure 5.10(t): error histogram for winter .....   | 107 |
| Figure 5.10(u): epoch Vs loss for VIDP, wind speed with 3D CNN .....                     | 108 |
| Figure 5.10(v): epoch Vs accuracy for VIDP, wind speed with 3D CNN .....                 | 108 |

# LIST OF TABLES

|  |    |
|--|----|
| Table 1: description of Era-5 data .....         | 7  |
| Table 2: description of geopotential data .....  | 8  |
| Table 3: wind speed data for airport VABB .....  | 10 |
| Table 4: wind speed data for airport VOTV .....  | 11 |
| Table 5: wind speed data for airport VOBL .....  | 12 |
| Table 6: wind speed data for airport VECC .....  | 14 |
| Table 7: wind speed data for airport VIDP .....  | 15 |
| Table 8: visibility data for airport VABB .....  | 16 |
| Table 9: visibility data for airport VOTV .....  | 18 |
| Table 10: visibility data for airport VOBL ..... | 19 |
| Table 11: visibility data for airport VECC ..... | 20 |
| Table 12: visibility data for airport VIDP ..... | 22 |
| Table 13: hyperparameters used .....             | 26 |

Table 14: visibility forecasting accuracy for several stations comparing 2D CNN, 3D CNN and pretrained model VGG16 with the reference accuracy of climatology .....27

Table 15: Wind speed forecasting accuracy for several stations comparing 2D CNN, 3D CNN and pretrained model VGG16 with the reference accuracy of climatology .....68

# ACRONYMS

NWP- Numerical Weather Prediction

VABB- Chhatrapati Shivaji Maharaj International Airport

VOTV- Trivandrum International Airport

VOBL- Kempegowda International Airport Bengaluru

VECC- Netaji Subhash Chandra Bose International Airport

VIDP- Indira Gandhi International Airport

RCM- Regional Climate Model

GCM- Global Climate Model

SDM- Statistical Downscaling Method

ECMWF- European Centre for Medium Range Weather Forecasts

METARs- Meteorological Variables for Every Commercial Airport in the World

hPa- Hectopascal

# Chapter 1- Introduction

Predicting and comprehending the atmospheric status in the future and the past requires numerical modelling. Numerical Weather Predictions (NWP) models are the most common techniques for forecasting weather. These are computer models that take the atmospheric condition and simulate its development using models that are both physical and chemical that mathematically depict numerous physical processes of the global weather system. In most cases, NWPs provide a significant number of parameters that reflect various physical quantities such as humidity, temperature, pressure, wind speed, etc. Because the interactions between the quantities are described by equations in physics, such as mass conservation, momentum conservation, and energy conservation, these processes are well understood, but due to computational resource constraints, they are not fully represented in the models. Many numerical simulations operate at grid spacings of approximately 20-50 km. This resolves mainly weather phenomena at large scales. NWPs are only evaluated for weather forecasting at global or continental scales due to their coarse spatial resolution, and to make forecasts for any specific region (downscaling), the predictions must be downscaled to a greater spatial resolution (3-5 kilometres).

For atmospheric modeling's real-world applications, such as climate risk assessment, and natural resource planning, atmospheric variables (e.g., precipitation, 2-m temperature, wind speed) with very fine spatiotemporal scales and, updates in near-real-time are required, which goes beyond what many meteorological centres in operation can provide right now.. Agriculture, transportation, and energy all require high-resolution estimates (between 1 and 5 kilometres). Predicting wind speed accurately, for example, enhances wind power generating planning, lowering costs and maximising resource utilisation. It can also be utilised to ensure the air traffic flow safety and to help airports construct a power generation system that is both reliable and secure. A post-processing approach called Statistical Downscaling (SD) can offer localised information on the weather based on reanalysis data or crude numerical model outputs, has the ability to address this issue and has sparked considerable interest since the 1990s.

Downscaling, or at a small scale, inferring information about physical properties from publicly accessible simulation data with a poor resolution utilising appropriate refining techniques, is one way to avoid simulations

with a high resolution (costing a lot of money) over wide scales of space. It's the umbrella term for a method for using data from vast scales to create predictions at smaller scales. Many scientific disciplines have long been interested in downscaling, and there are numerous methods for downscaling physical parameters in meteorological research. Two main classification of these methods are Dynamical and statistical downscaling.

1. Dynamical: A higher resolution climate model is utilised for dynamic downscaling. These models are frequently referred to as regional climate models (RCM). To mimic local climate, RCM use lower resolution climate models (in most instances GCMs) as boundary conditions and physical principles. It is computationally expensive and necessitates a vast amount of information as well as a high degree of understanding to apply and assess results, which is often beyond the scope of institutional capacities in developing countries.
2. Statistical: establishing statistical linkages between large-scale climate features provided by NWP and local climate circumstances. In contrast to dynamical methods, statistical methods are easy to apply and interpret. They only require a little amount of computing power, but they rely mostly on historical climate records and the assumption that present conditions would remain similar to those previously observed. With improved quality and longer duration of previously observed weather data, the statistical downscaling findings improve. High-quality historical weather data, on the other hand, is not always available.

CNNs are deep learning networks that can be used to statistically downscale weather predictions provided by global numerical models like the NWP. CNNs have convolutional layers that receive inputs that are gridded. The convolutional layer output channels of CNNs correspond to an activation function for each channel and a convolution kernel. Picture classification, image segmentation, and object recognition have all been found to be quite effective with CNNs. Deep learning-based downscaling algorithms can be a powerful and effective way to extract fine-scale local weather data from coarse resolution global NWP data. CNNs extract spatial information from images, enabling for the creation of higher-level structures from fine-grained input. Without the need for huge computation needs, CNNs can give a model for directly reading numerical weather model fields and creating local weather forecasts, as is the case with dynamical downscaling.

The employment of cutting-edge CNNs in downscaling techniques is still in its early stages. Downscaling based on CNN has the potential to deliver novel insights in the context of SD. For starters, CNNs excel at gridded

data learning. Based on their achievements in the field of computer vision, such as semantic segmentation, and single-image super resolution which figures out how low-resolution and high-resolution images are related, in gridded downscaling situations that are similar to image-to-image learning, CNNs are likely to perform well. This is evidenced by the recent progress of sea surface temperature and precipitation downscaling. Second, although developing creating deep-learning models from the ground up is costly, porting deep-learning models that already exist is quick and simple. CNNs and other deep-learning models that are cutting-edge are modular and has the ability to extract hierarchical representations for a variety of tasks for learning.

CNNs work best with regular-gridded data in multi-dimensional array representations, enabling for quick and efficient concurrent calculation of optimization problems on computer hardware equipped with graphics processing units (GPUs). One of CNN's primary selling factors is their computational efficiency via parallelization, which is taken into account during model building and preparation of data. In addition, more complex mappings can be learned, by stacking together many layers of convolution operations (increasing the model depth) and applying them consecutively to get feature representations that is more abstract. The model can learn nonlinear mappings by using activation functions that are non-linear, between consecutive convolution layers, as in traditional artificial neural networks.

Beyond sequential feature processing, more complex design patterns, such as skip connections in between convolution layers, residual learning can be employed to increase model performance. As a result, CNNs are especially well adapted to learning tasks employing data that is spatially scattered, which are common in meteorology. Despite the fact that CNN based model architectures are becoming more widely used in Earth-system sciences, their application in downscaling applications has received less attention. Earlier research has concentrated on simplistic CNN designs that do not leverage modern model design trends and so do not fully harness the possibilities of cutting-edge CNN architectures.

In computer vision, single-image super-resolution is a problem setting that is similar to downscaling in meteorology and climatology and is the basis of many technological advances in machine learning. The goal is to develop mappings that allow a single image with a low resolution as an input to be increased in resolution while avoiding pixel distortions and blurriness and keeping visual quality. Deep learning has resulted in significant gains over traditional statistical models in this situation. CNNs, in particular, have been shown to be quite effective. This project shows how CNNs may be employed to automatically understand the Numerical Weather Prediction's output to produce forecasts for the local area.

A variety of statistical downscaling approaches and techniques are now available as a consequence of decades of thorough investigation. The predictands of interest in the local area (for example, temperature and pressure) are known from Global Climate Model (GCM) outputs by making use of statistical models based on a set of predictors (atmospheric variables at large scales, for e.g., fraction of cloud cover, temperature, relative humidity or geopotential) that explain a significant portion of local climate variation.

Bao-Medina et al. (2019) used large-scale reanalysis predictions to investigate the viability of downscaling temperature and precipitation with deep CNNs, throughout Europe. To do so, they compared the CNNs provided results with those produced through a variety of other more traditional, well-established methods, such as generalised linear models giving the conclusion that CNNs are highly suited for applications on continental scale, according to the researchers. Similar studies in China (Sun and Lan 2020) and North America (Pan et al 2019) have all found that convolutional neural networks perform similarly or superior to regular Statistical Downscaling Methods (SDMs). Furthermore, the issue of feature selection is avoided by CNNs, which is very dependent on case and becomes a difficult process in traditional downscaling approaches. These prior studies, on the other hand, did not examine the appropriateness and drawbacks of CNNs for use in applications related to climate change. This is especially important because these "black-box" models have poor interpretability, which can make analysis of extrapolation difficult. As a consequence, people are wary of using these techniques, and regular SDMs remain the primary method for downscaling climate change scenarios.

# Chapter 2- Literature review

Maraun et al. (2019) and Gutierrez et al. (2019) conducted a thorough analysis and compared different statistical models for downscaling climatic variables, finding that several of the techniques perform well in general but have room for improvement. Pryor (2005) and Michelangeli et al. (2009) suggested inference of wind fields using distribution-based methods and Huang et al. (2015) for downscaling, presented a physical-statistical hybrid technique, all addressing the topic of wind field downscaling and forecasting. Only a few smaller model comparison studies have attempted to answer which strategies produce the best results and added benefit over traditional approaches, with mixed findings. While Mao (2018) and Monahan (2018), and Vandal et al. (2019) showed little or no benefit from using non-traditional machine learning techniques, Gaitan et al. (2014) discovered that non-traditional methods outperform classical methods, with ANNs (artificial neural networks) as an example. Buzzi et al. (2019) employed neural networks to nowcast (prediction of very near future) wind speed in the Swiss Alps and produced highly accurate models. These seemingly contradicting findings ask when and under what circumstances deep learning technologies can be used to downscale effectively.

Only a few research in meteorology have looked at the use of CNNs in applications of downscaling. Vandal et al. (2018) suggested "DeepSD," a CNN for precipitation downscaling over wide domains of space, while Bao-Medina et al. (2019) recently investigated the performance of a collection of CNNs for temperature and precipitation downscaling over Europe. Pan et al. (2019) presented a similar architecture, focusing on precipitation once again. While Bao-Medina et al. (2019) investigated the impact of model complexity on model depth, the used models did not take advantage of the most latest design trends such as skip connections (e.g., Srivastava et al., 2015; He et al., 2016) or the fully-convolutional U-Net-like architecture (Ronneberger et al., 2015), which makes it possible for network models to attain cutting-edge results in tasks related to computer vision.

To test different CNN model settings, Pablo Rozas Larraondo et al., 2017, recommend using NWP and observed precipitation data from several locations. The purpose was training a model that forecasts the presence of rain for a specific area by making use of data from a numerical weather model as input. They used the ERA Interim dataset from the European Centre for Medium Range Weather Forecasts (ECMWF), which is a publicly available meteorological reanalysis dataset, as input data. This data was compiled by making use of a numerical weather model that mimics the atmospheric state for the entire planet with a space resolution of around 50 miles. This available data has a three-hour temporal resolution since 1979. The form of the

presented output is traditional numerical grids, with geopotential, relative humidity, wind speed among the physical attributes to pick from. They used METARs (Meteorological Variables for Every Commercial Airport in the World) for their target data, which are text reports on operational aviation weather that encodes every commercial airport's observed meteorological variables.

METARs are issued every hour or half-hour and made available to the public via the World Meteorological Organization's (WMO) communications system.

# Chapter 3- DATA

Our task is to use numerical weather model ERA-5 geopotential data as input and METAR observations (wind velocity, visibility, etc) as target to train the CNN models.

Estimates of a large variety of air, land, and oceanic climate variables on an hourly basis are provided by ERA5. The data has 30 km grid resolution and atmosphere is resolved with 137 pressure levels ranging from the ground to 80 km in altitude. ERA5 uses complex modelling and data assimilation technologies to turn massive volumes of historical data into global estimations. The ECMWF's ERA 5 is a publicly available meteorological reanalysis dataset. It is reanalysis product of the global weather and climate during the previous 40 to 70 years. This dataset was created with the help of a numerical weather model that simulates the atmospheric state for the entire Earth with a space resolution of about 30 kilometres. Since 1979, data has been accessible with a hourly temporal resolution. The result is given in form of conventional grids of numbers, and there are several physical characteristics to choose from, including relative humidity, geopotential, and temperature. Using the rules of physics, reanalysis combines observations from around the world and data from the model to create a dataset that is globally comprehensive and consistent. This is known as data assimilation. It is based on the method, in which a a previous prediction is integrated with newly available data/observation in an optimal way every few hours (for e.g., 12 hours at ECMWF) in order to generate a fresh best estimate of the status of the atmosphere, known as analysis, based on which a revised and enhanced prediction is supplied. Because reanalysis is not constrained by the need to issue forecasts that are timely, time to gather information and data is more which benefit the reanalysis product's quality. For the reanalysis, data is regridded to a normal latitude-longitude grid of 0.25 degrees.

## **Data description of Era-5:**

|                                    |                                    |
|------------------------------------|------------------------------------|
| Type of data                       | Gridded                            |
| Projection                         | Grid with latitudes and longitudes |
| Coverage on the horizontal plane   | Global                             |
| Resolution on the horizontal plane | 0.25° x 0.25° reanalysis           |
| Vertical coverage                  | 1000 hPa to 1 hPa                  |
| Resolution in the vertical plane   | 37 different pressure levels       |

|                 |                          |
|-----------------|--------------------------|
| Time coverage   | From 1979 to the present |
| Time resolution | hourly                   |

Table 1: description of Era-5 data

A unit mass's gravitational potential energy at a given location in relation to mean sea level is known as geopotential. Its also the amount of effort required to elevate a unit mass from mean sea level to that point against the force of gravity. The geopotential height is the ratio of geopotential and Earth's gravitational acceleration,  $g$  ( $9.80 \text{ ms}^{-2}$ ). In the study of weather patterns, the geopotential height plays very essential role. Weather systems for e.g., cyclones, anticyclones can be identified using geopotential height charts drawn at constant pressure levels (e.g., 500, 700, or 1000 hPa).

METAR is a weather information reporting format. This weather report is primarily utilised by pilots and meteorologists to help forecast weather. For every commercial airport in the globe, they encode observed meteorological variables. METARs are issued every hour or half hour and are made available to public via the WMO's (World Meteorological Organization) communications system. The header of each report comprises the ICAO (International Civil Aviation Organization) airport code as well as a time stamp in UTC, allowing it to be understood in many parts of the world. Raw METAR is the most widely used format for transmitting observational weather data around the world. Permanent weather monitoring stations or airports are the most common sources of METARs. Temperature, wind speed and direction, precipitation, cloud cover, cloud heights, visibility, and pressure are all included in a typical METAR that may be useful to pilots or meteorologists.

**Input (geopotential) data used:**

|                      |   |
|----------------------|---|
| Spatial resolution   | $0.25^\circ \times 0.25^\circ$  |
| Temporal resolution  | Hourly  |
| Area covered         | $63^\circ\text{W} - 102^\circ\text{E}$ and $3^\circ\text{S} - 42^\circ\text{N}$ |
| Time period covered  | 3 years from 01/01/2018 to 30/12/2020   |
| Pressure levels used | 500, 700, 1000 hPa  |

Table 2: description of geopotential data

We extract the entire area of India and some sections of the Indian subcontinent using Era-5, resulting in an hourly sequence of images made up of three bands that correspond to the geopotential height at the 500, 700 and 1000 atmospheric pressure levels. This variable defines the altitude at which a specific pressure value is reached in the atmosphere, and the levels correspond to approximately 5.5, 3, and 1 km above mean sea level, respectively. These fields were chosen because they are commonly used by weather forecasters to make

forecasts. They contain information regarding the location, shape and evolution of atmospheric pressure systems.

The goal is to use as input ERA Interim geopotential data and METAR observations to predict the wind speed and visibility for the airports in question.

Five airports are used.

- Trivandrum International Airport(VOTV)
- Chhatrapati Shivaji Maharaj International Airport(VABB)
- Kempegowda International Airport Bengaluru(VOBL)
- Indira Gandhi International Airport (VIDP)
- Netaji Subhash Chandra Bose International Airport (VECC)

# Data characteristics

## Wind Speed (mph) data for airport VABB

| No. Of samples | Mean | Median | Mode | std  | max    | min | range  |
|----------------|------|--------|------|------|--------|-----|--------|
| 26280          | 7.26 | 6.9    | 5.75 | 4.27 | 150.64 | 0   | 150.64 |

Table 3: wind speed data for airport VABB

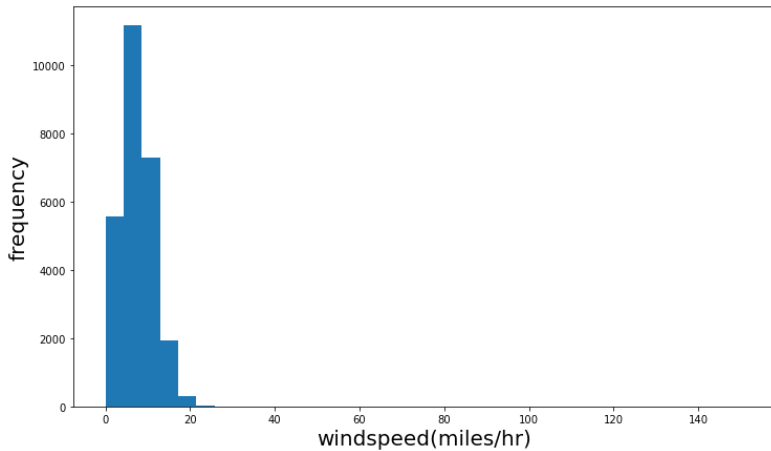


fig 3.1(a) wind speed Vs frequency

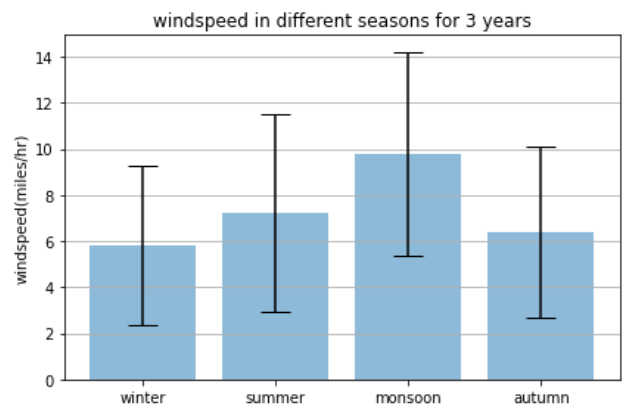


fig 3.1(b) histogram of wind speed in seasons

We can see that wind speed is highest in monsoon. For most times, wind speed is confined to 20 miles/hr.

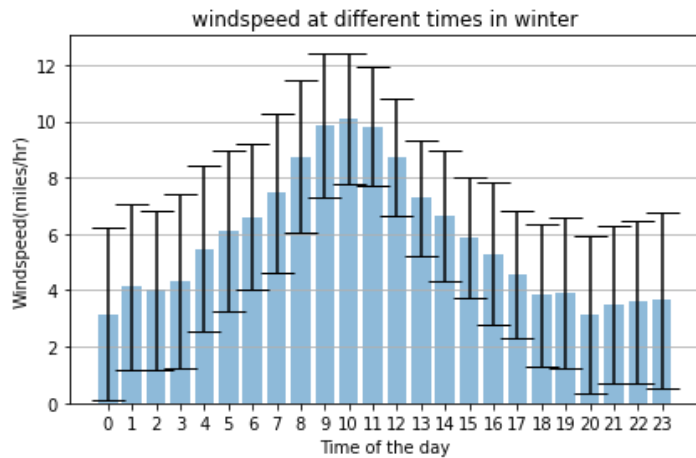


fig 3.1(c) wind speed in winter

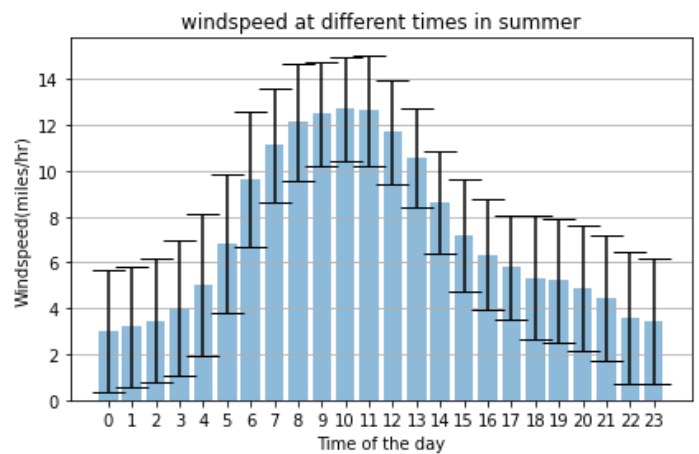


fig 3.1(d) wind speed in summer

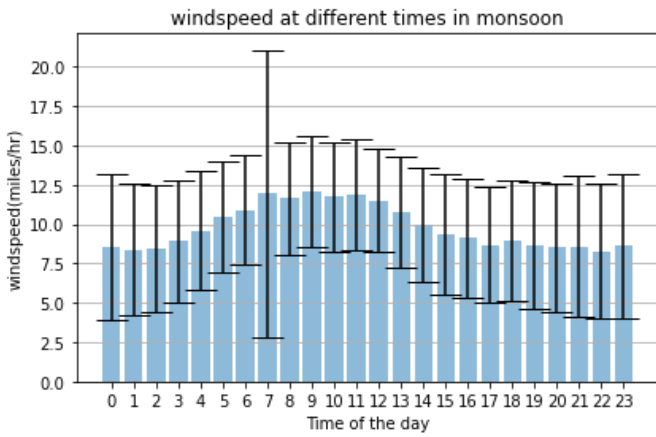


fig 3.1(e) wind speed in monsoon

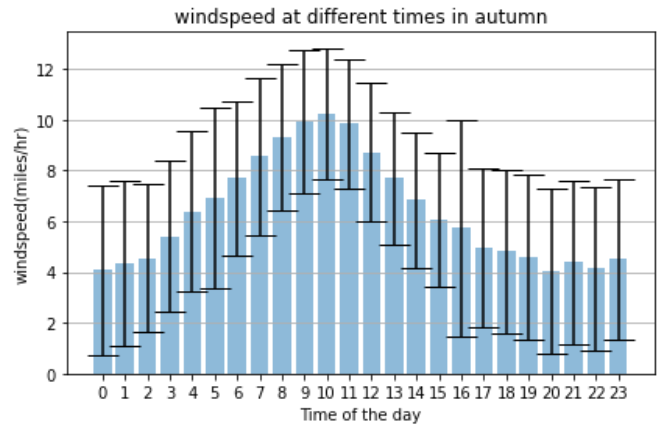


fig 3.1(f) wind speed in autumn

In the above 4 plots, on x-axis, “time of the day” is in UTC and interval between two consecutive “time of the day” is 1 hour.

We can see that wind speed is highest in monsoon. For most times, wind speed is confined to 15 miles/hr. During monsoon, speed is highest around 12:30 pm.

### Wind Speed (mph) data for airport VOTV

| No. Of samples | Mean | Median | Mode | std dev | max   | min | range |
|----------------|------|--------|------|---------|-------|-----|-------|
| 26280          | 5.48 | 4.59   | 3.45 | 3.34    | 85.09 | 0   | 85.09 |

Table 4: wind speed data for airport VOTV

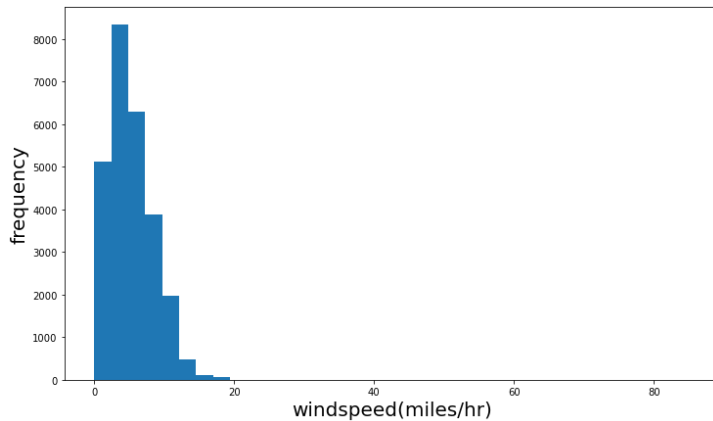


fig 3.2(a) histogram of wind speed

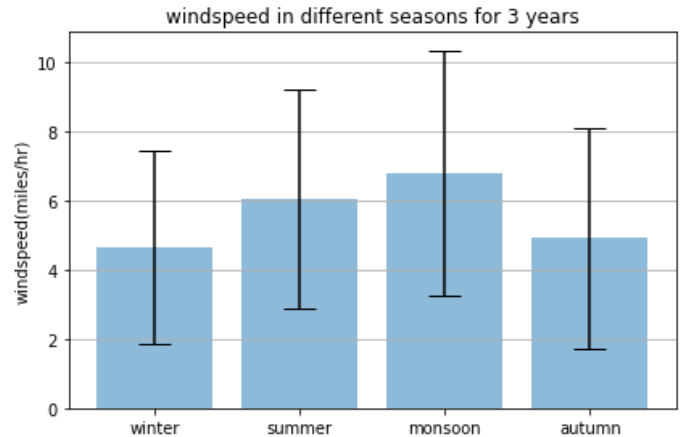


fig 3.2(b) histogram of wind speed in different seasons

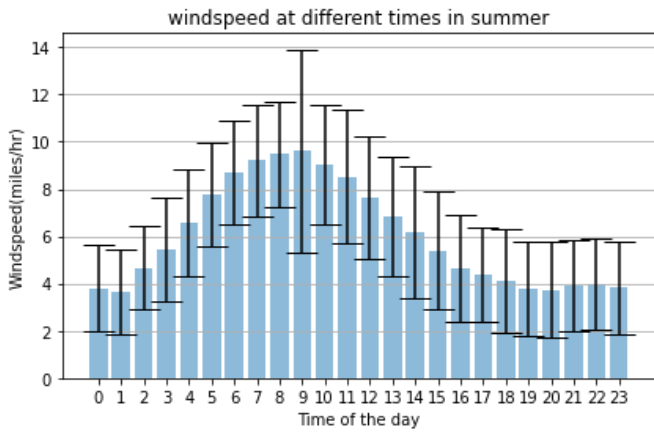


fig 3.2(c) wind speed in summer

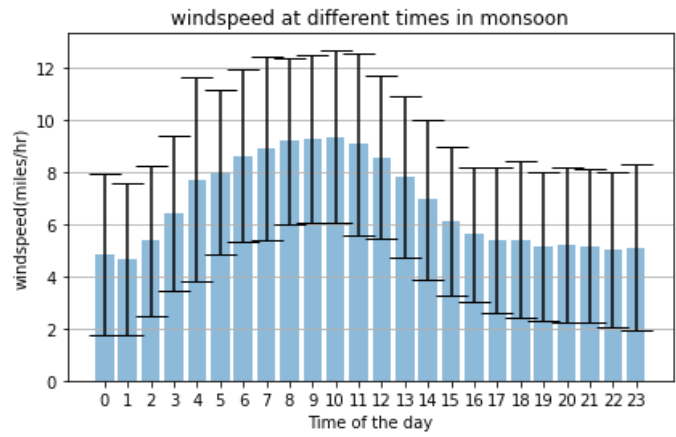


fig 3.2(d) wind speed in monsoon

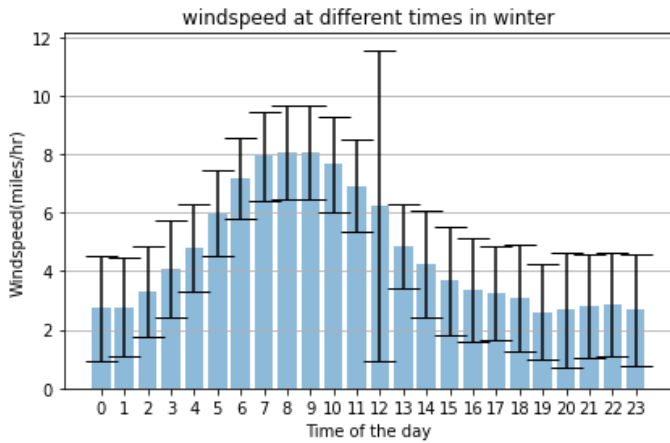


fig 3.2(e) wind speed in winter

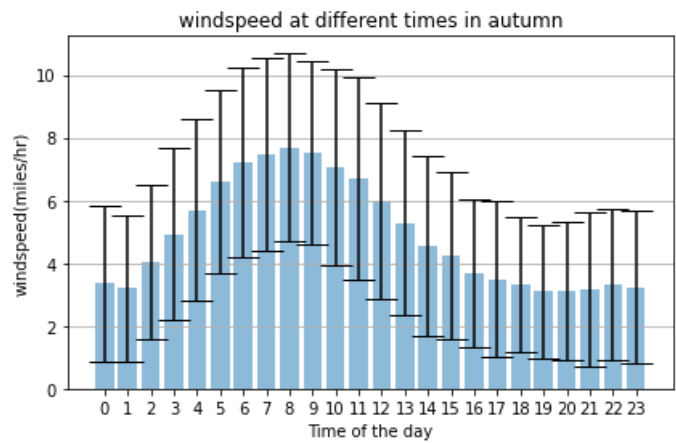


fig 3.2(f) wind speed in autumn

In the above 4 plots, on x-axis, “time of the day” is in UTC and interval between two consecutive “time of the day” is 1 hour.

We can see that wind speed is highest in monsoon. For most times, wind speed is confined to 15 miles/hr. In winter, autumn and summer, wind speed is highest around 2:30 pm. During monsoon, wind speed is highest around 2:30 pm.

### Wind Speed (mph) data for airport VOBL

| No. Of samples | Mean  | Median | Mode | std  | max    | min | range  |
|----------------|-------|--------|------|------|--------|-----|--------|
| 26280          | 8.006 | 6.9    | 5.75 | 4.65 | 102.34 | 0   | 102.34 |

Table 5: wind speed data for airport VOBL

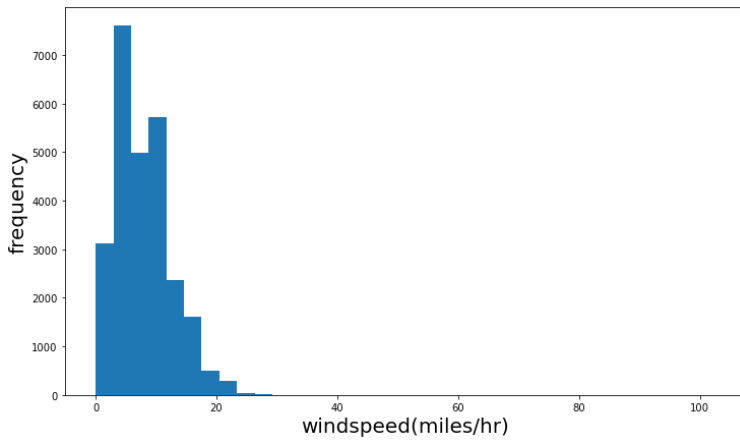


fig 3.3(a) histogram of wind speed

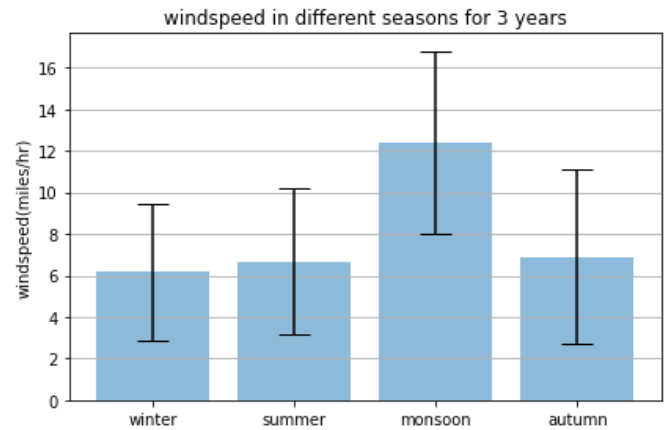


fig 3.3(b) histogram of wind speed in seasons

We can see that wind speed is highest in monsoon. For most times, wind speed is confined to about 22 miles/hr.

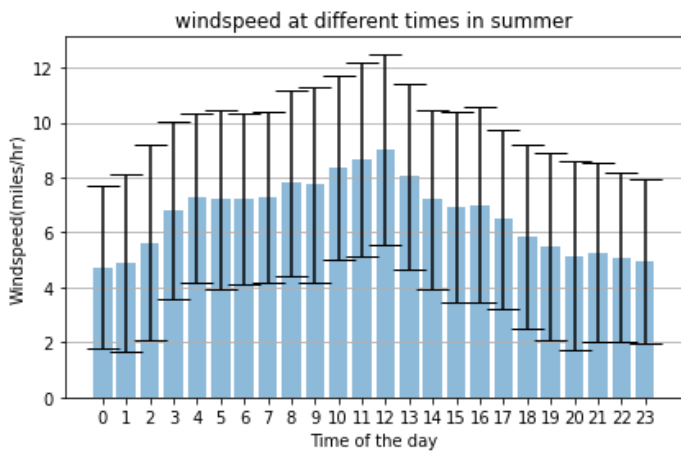


fig 3.3(c) wind speed in summer

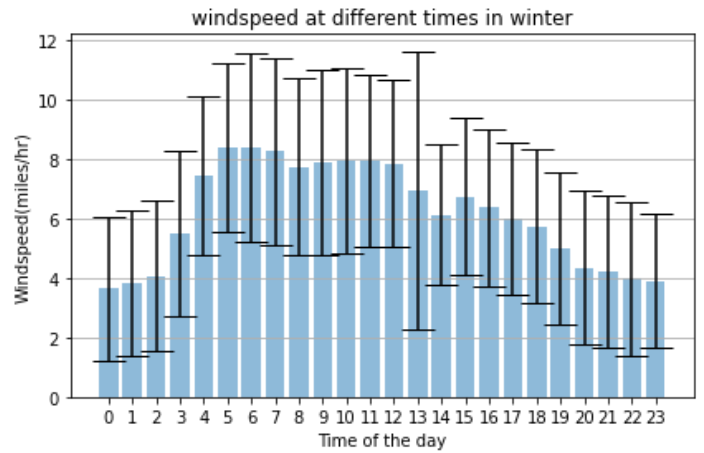


fig 3.3(d) wind speed in winter

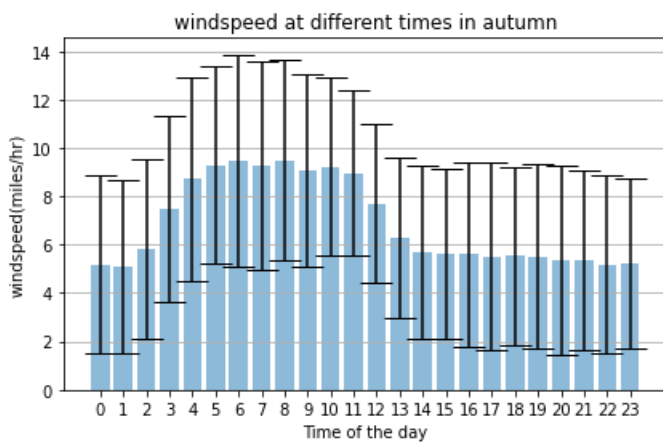


fig 3.3(e) wind speed in autumn

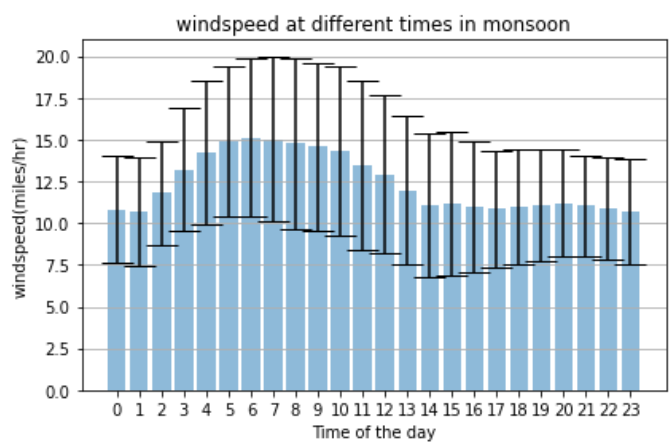


fig 3.3(f) wind speed in monsoon

In the above 4 plots, on x-axis, “time of the day” is in UTC and interval between two consecutive “time of the day” is 1 hour.

In summer, wind speed is highest around 5:30 pm. During monsoon, winter and autumn, wind speed is highest around 11:30 am.

We can see that wind speed is highest in monsoon. For most times, wind speed is confined to 20 miles/hr. In winter, summer and autumn, wind speed is highest around 3:30 pm.

### Wind Speed (mph) data for airport VECC

| No. Of samples | Mean | Median | Mode | std  | max    | min | range  |
|----------------|------|--------|------|------|--------|-----|--------|
| 26280          | 5.51 | 5.75   | 0    | 4.52 | 123.05 | 0   | 123.05 |

Table 6: wind speed data for airport VECC

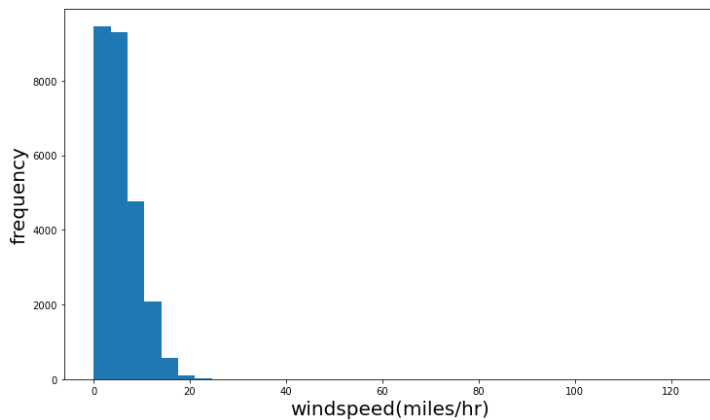


fig 3.4(a) histogram of wind speed

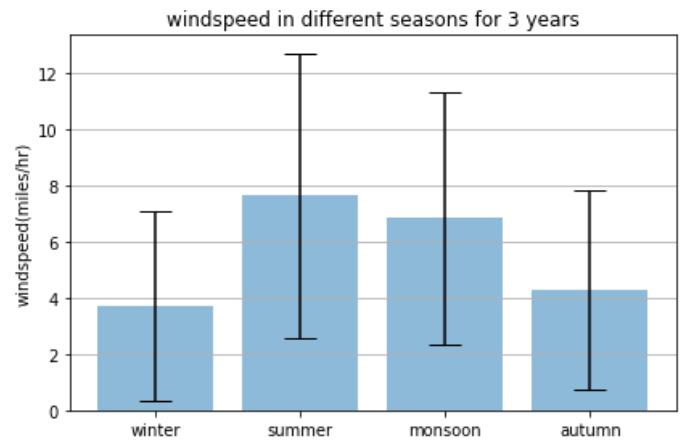


fig 3.4(b) histogram of wind speed in seasons

We can see that wind speed is highest in summer. For most times, wind speed is confined to about 18 miles/hr.

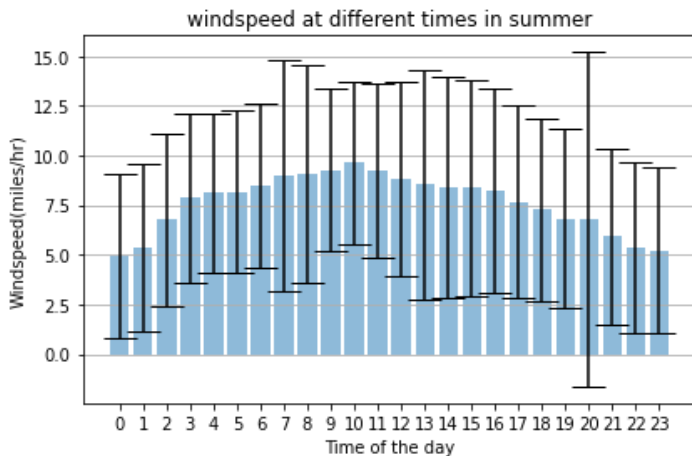


fig 3.4(c) wind speed in summer

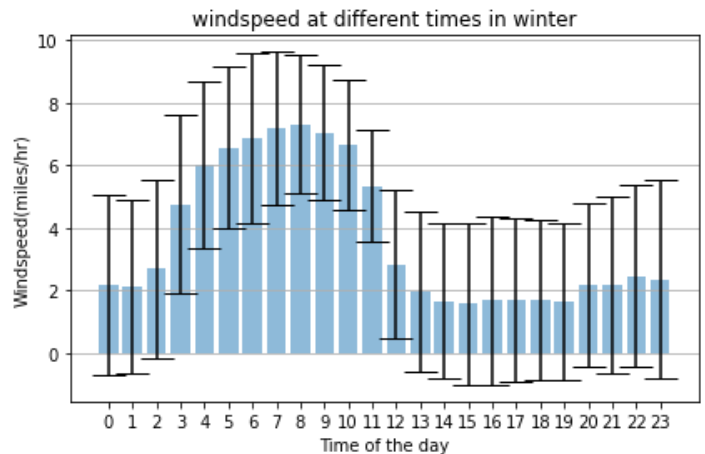


fig 3.4(d) wind speed in winter

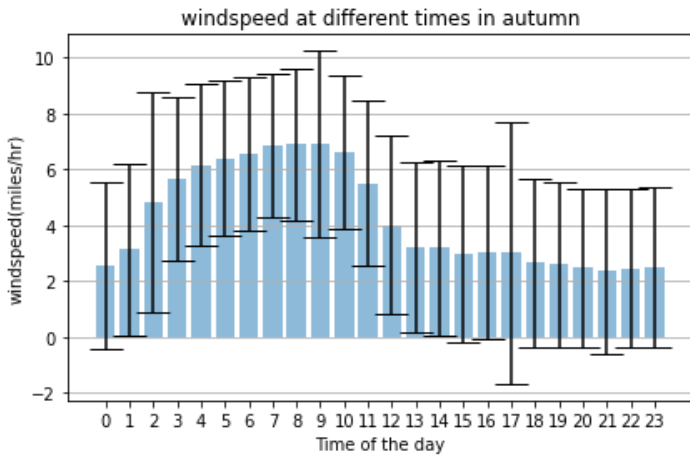


fig 3.4(e) wind speed in autumn

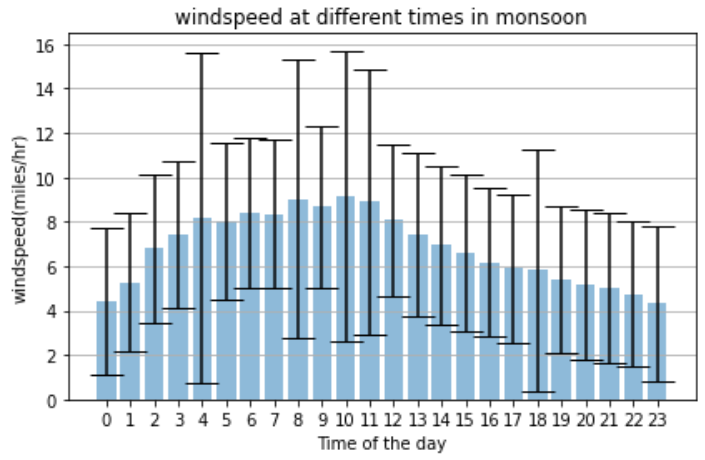


fig 3.4(f) wind speed in monsoon

In the above 4 plots, on x-axis, “time of the day” is in UTC and interval between two consecutive “time of the day” is 1 hour.

In winter and autumn, wind speed is generally highest around 1:30 pm. During monsoon and summer, wind speed is highest around 3:30 pm.

### Wind Speed (mph) data for airport VIDP

Table 7: wind speed data for airport VIDP

| No. of samples | Mean | Median | Mode | std dev | max   | min | range |
|----------------|------|--------|------|---------|-------|-----|-------|
| 26280          | 5.30 | 5.75   | 0    | 3.87    | 126.5 | 0   | 126.5 |

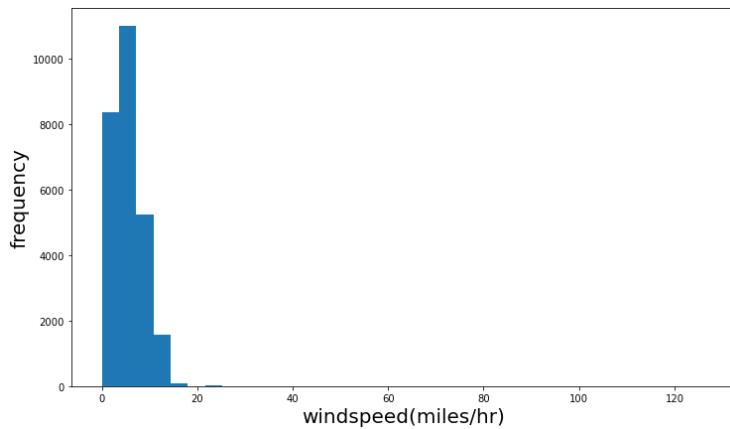


fig 3.5(a) histogram of wind speed

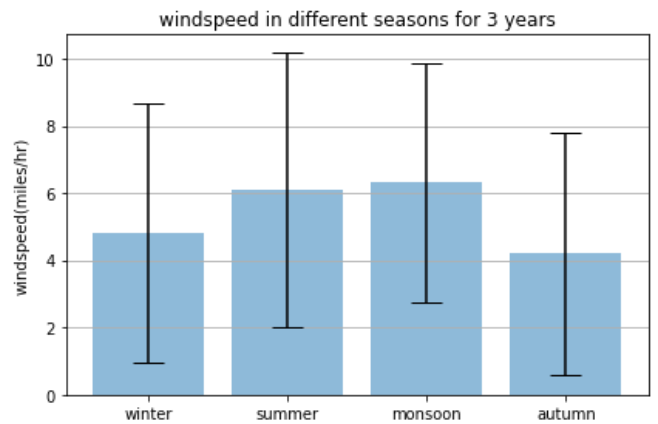


fig 3.5(b) wind speed in different seasons

We can see that wind speed is generally highest in monsoon. For most times, wind speed is confined to 15 miles/hr.

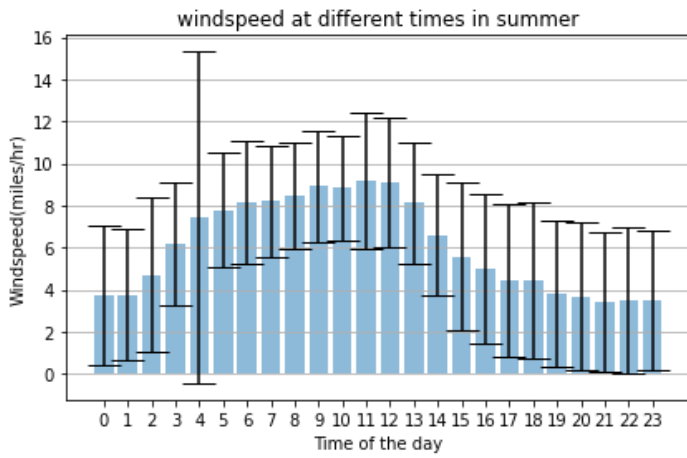


fig 3.5(c) wind speed in summer

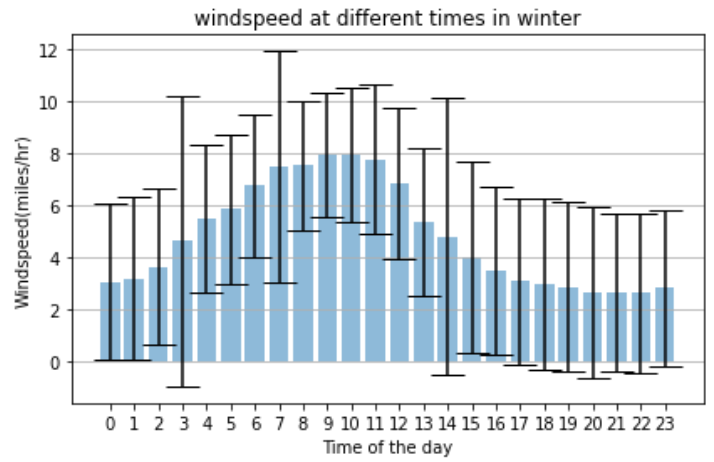


fig 3.5(d) wind speed in winter

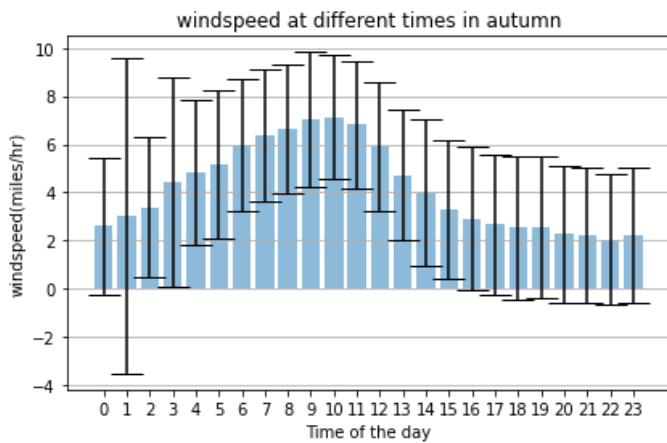


fig 3.5(e) wind speed in autumn

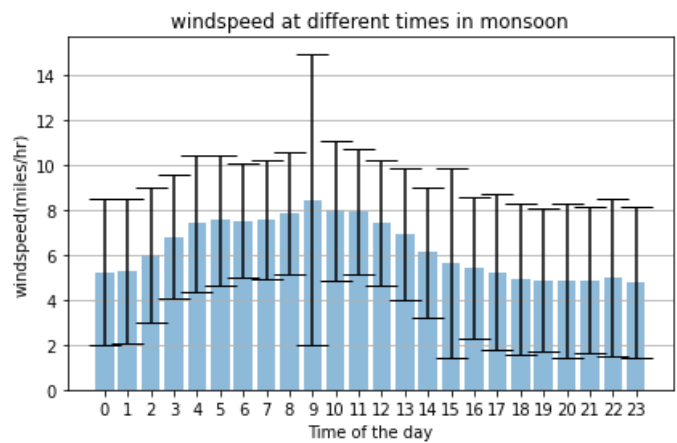


fig 3.5(f) wind speed in monsoon

In the above 4 plots, on x-axis, “time of the day” is in UTC and interval between two consecutive “time of the day” is 1 hour.

In winter and autumn, wind speed is generally highest around 3:30 pm. During monsoon, wind speed is highest around 2:30 pm and for summer it is 4:30 pm.

### Visibility (miles) data for airport VABB

| No. Of samples | Mean | Median | Mode | std. dev. | max  | min  | range |
|----------------|------|--------|------|-----------|------|------|-------|
| 26280          | 2.63 | 2.49   | 1.86 | 0.82      | 6.21 | 0.37 | 5.84  |

Table 8: visibility data for airport VABB

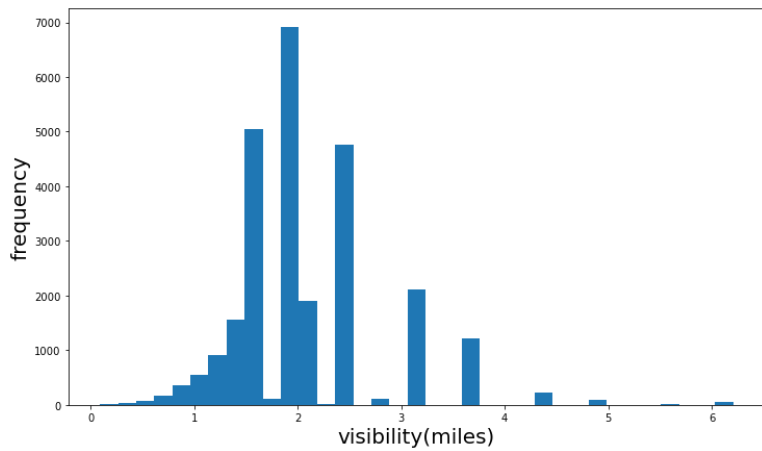


fig 3.6(a) histogram of visibility

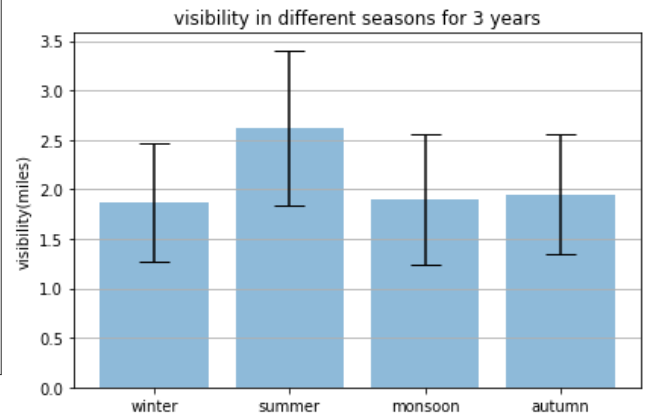


fig 3.6(b) visibility in different seasons

We can see that visibility is generally highest in summer. For most times, visibility is confined to about 5 miles.

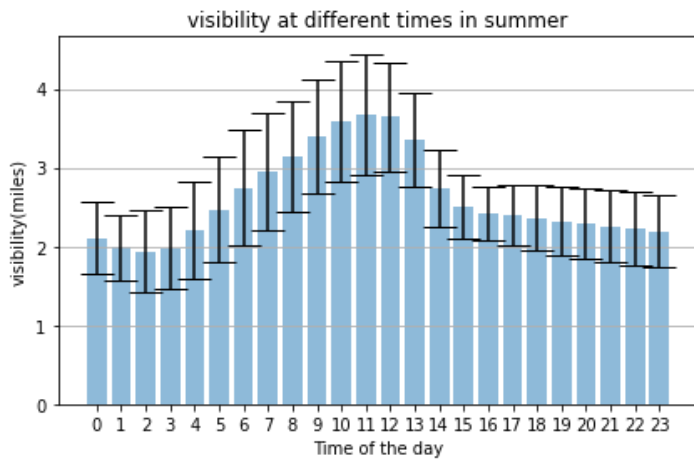


fig 3.6(c) visibility in summer

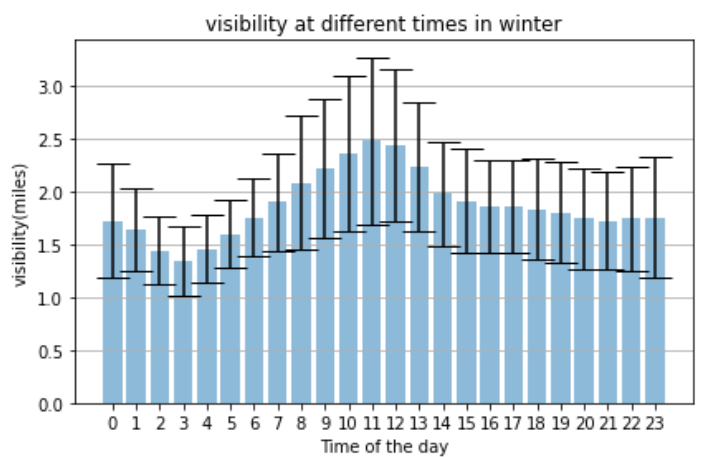


fig 3.6(d) visibility in winter

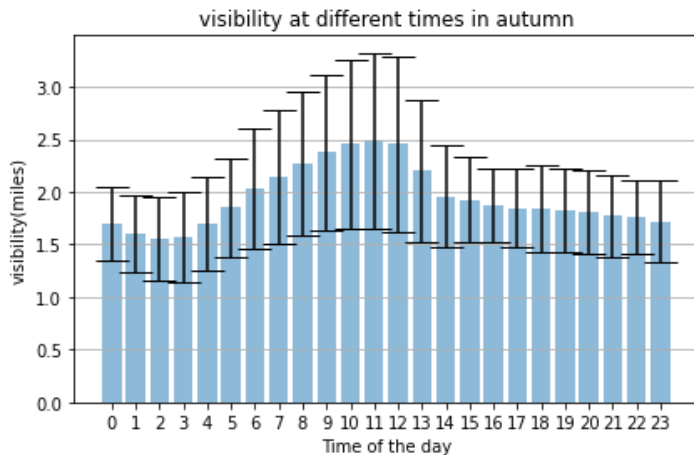


fig 3.6(e) visibility in autumn

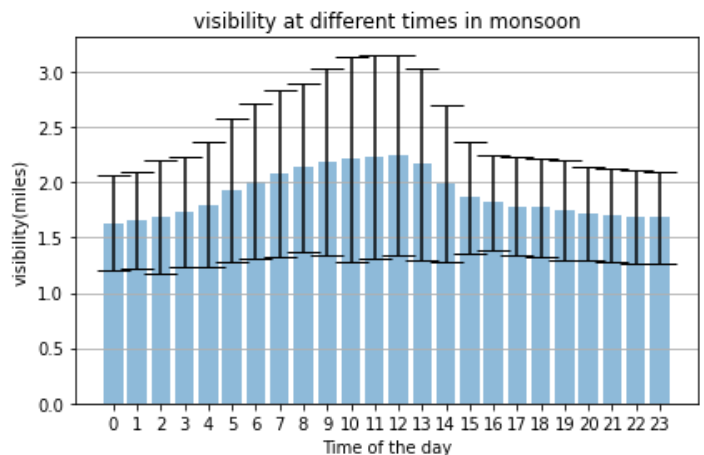


fig 3.6(f) visibility in monsoon

In the above 4 plots, on x-axis, “time of the day” is in UTC and interval between two consecutive “time of the day” is 1 hour.

In all the seasons, visibility is generally highest around 4:30 pm.

## Visibility (miles) data for airport VOTV

| No. Of samples | Mean | Median | Mode | std.dev. | max  | min  | range |
|----------------|------|--------|------|----------|------|------|-------|
| 26280          | 2.63 | 2.49   | 1.86 | 0.82     | 6.21 | 0.37 | 5.84  |

Table 9: visibility data for airport VOTV

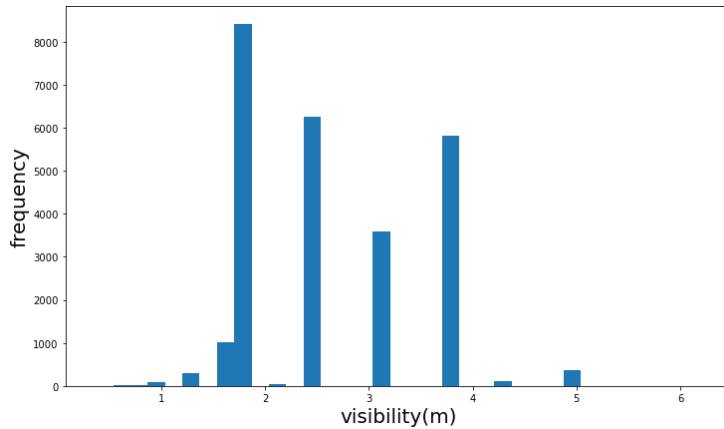


fig 3.7(a) histogram of visibility

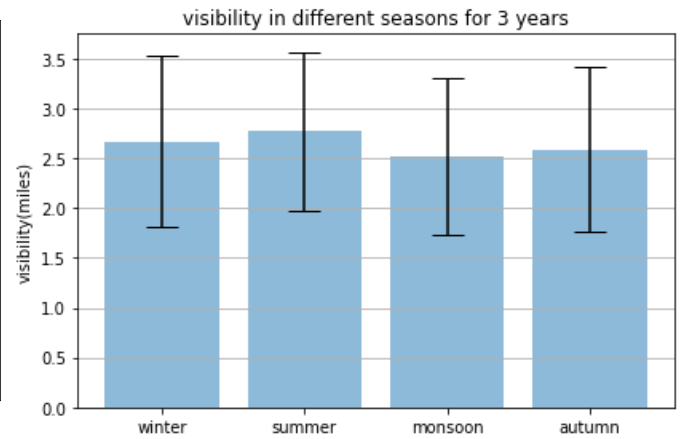


fig 3.7(b) visibility in different seasons

We can see that visibility is generally highest in summer. For most times, visibility is confined to about 5 miles.

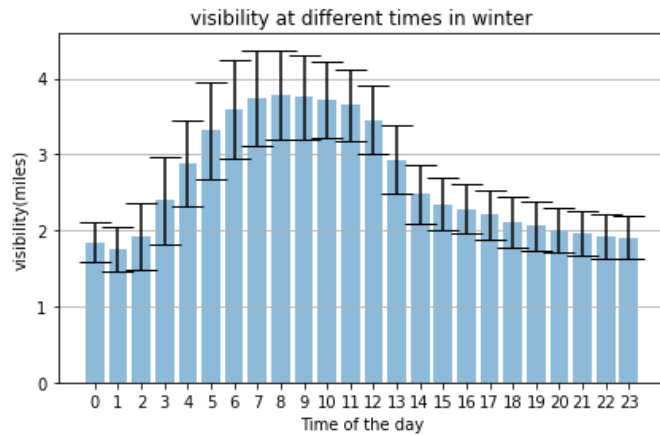


fig 3.7(c) visibility in winter

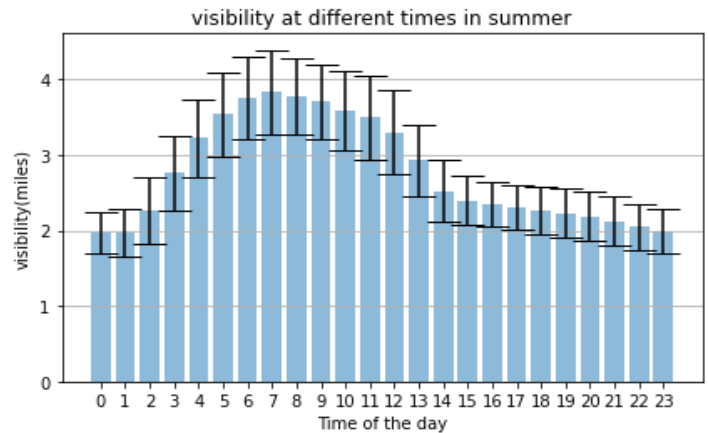


fig 3.7(d) visibility in summer

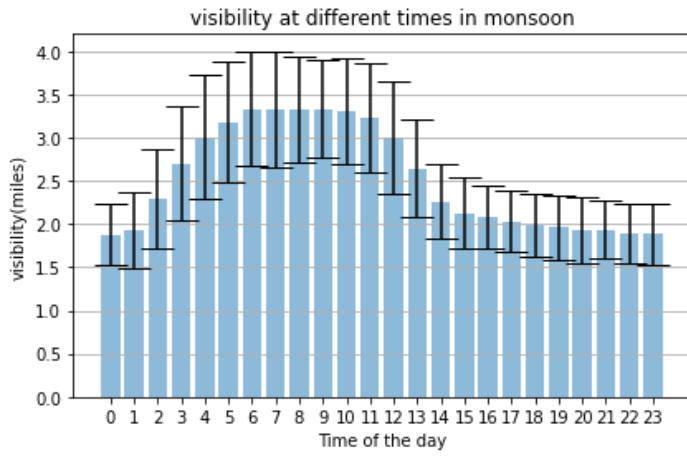


fig 3.7(e) visibility in monsoon

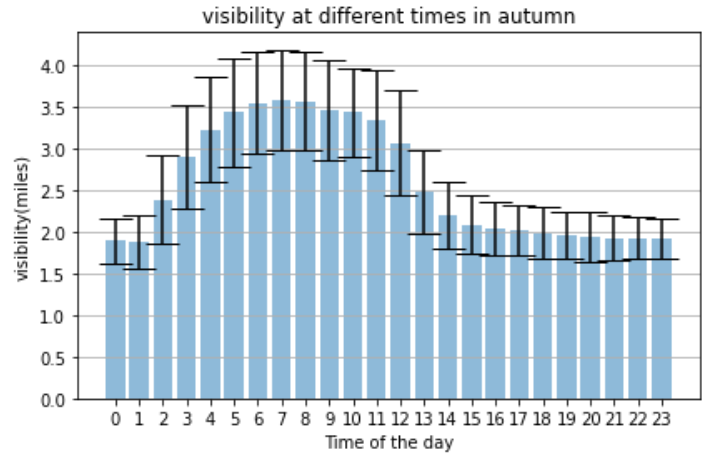


fig 3.7(f) visibility in autumn

In the above 4 plots, on x-axis, “time of the day” is in UTC and interval between two consecutive “time of the day” is 1 hour.

In autumn and summer, visibility is generally highest around 12:30 pm. In winter and monsoon, visibility is highest around 1:30 pm.

### Visibility (miles) data for airport VOBL

| No. Of samples | Mean | Median | Mode | std. dev. | max  | min  | range |
|----------------|------|--------|------|-----------|------|------|-------|
| 26280          | 3.99 | 3.73   | 3.73 | 1.34      | 6.21 | 0.02 | 6.18  |

Table 10: visibility data for airport VOBL

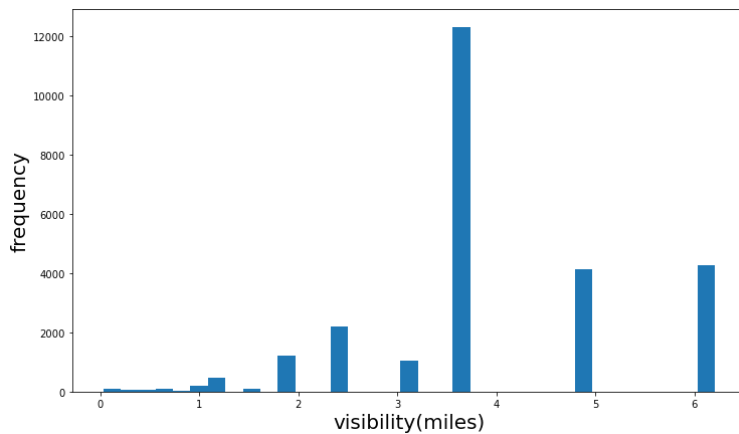


fig 3.8(a) histogram of visibility

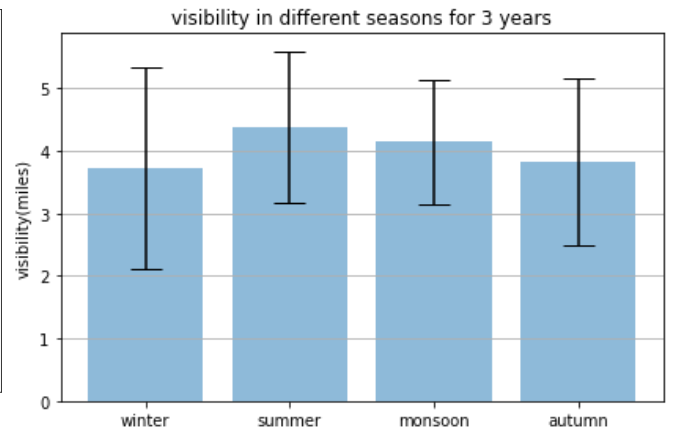


fig 3.8(b) visibility in different seasons

We can see that visibility is generally highest in summer. For most times, visibility is confined to about 8 miles.

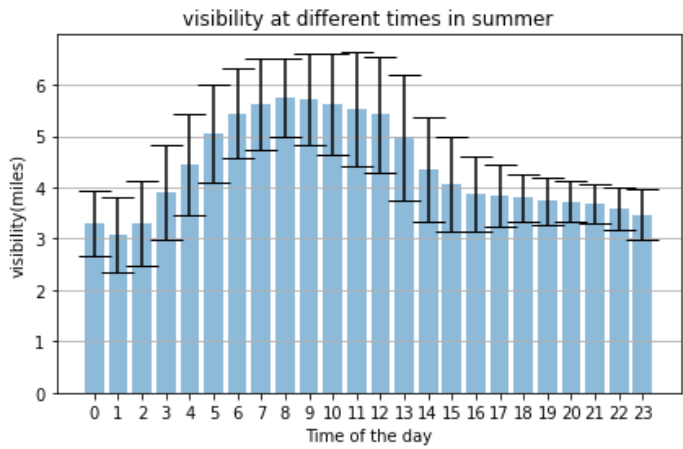


fig 3.8(c) visibility in summer

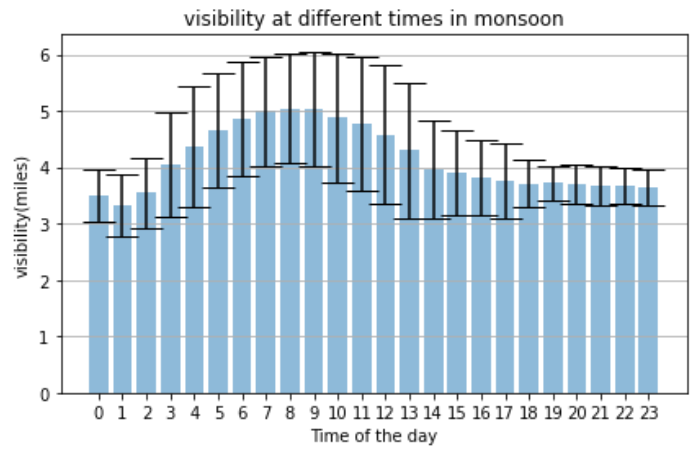


fig 3.8(d) visibility in monsoon

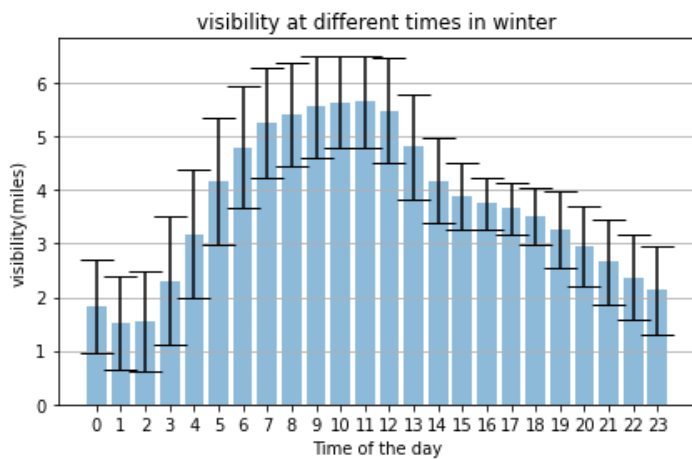


fig 3.8(e) visibility in winter

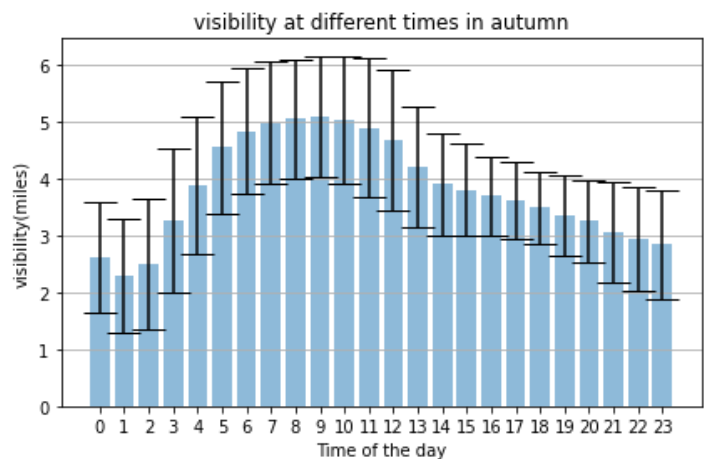


fig 3.8(f) visibility in autumn

In the above 4 plots, on x-axis, “time of the day” is in UTC and interval between two consecutive “time of the day” is 1 hour.

In winter, visibility is generally highest around 3:30 pm and in summer it’s about 12:30 pm. In autumn and monsoon, visibility is highest around 2:30 pm.

### Visibility (miles) data for airport VECC

| No. of samples | Mean | Median | Mode | std dev | max  | min  | range |
|----------------|------|--------|------|---------|------|------|-------|
| 26280          | 1.9  | 1.99   | 1.99 | 0.47    | 4.96 | 0.02 | 4.93  |

Table 11: visibility data for airport VECC

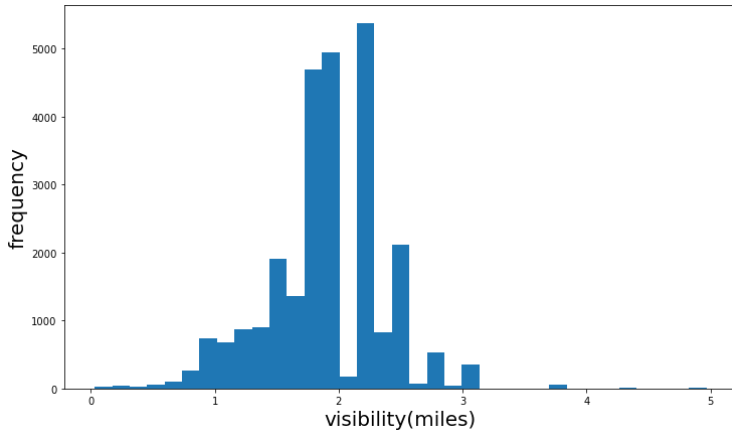


fig 3.9(a) histogram of visibility

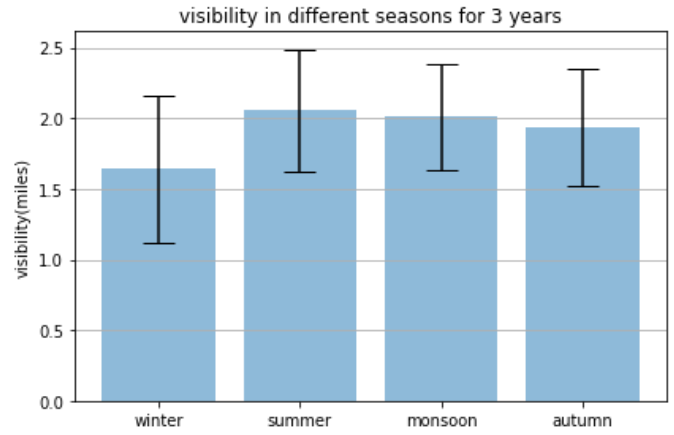


fig 3.9(b) visibility in different seasons

We can see that visibility is generally highest in summer. For most times, visibility is confined to about 3.5 miles.

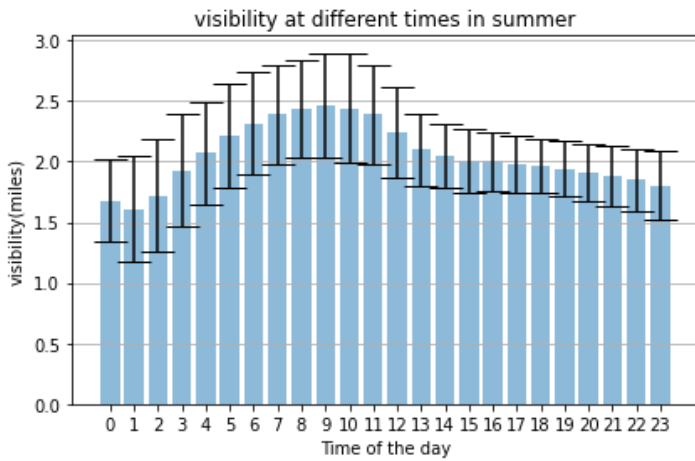


fig 3.9(c) visibility in summer

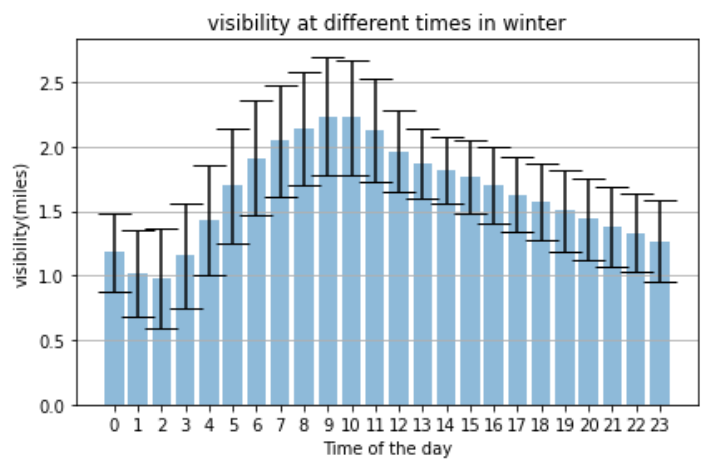


fig 3.9(d) visibility in winter

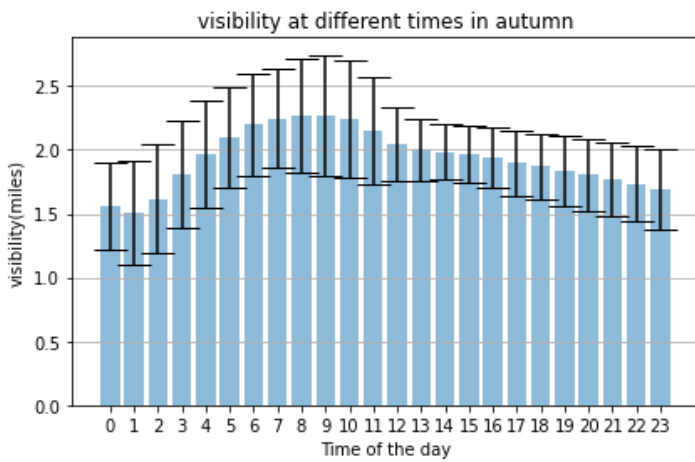


fig 3.9(e) visibility in autumn

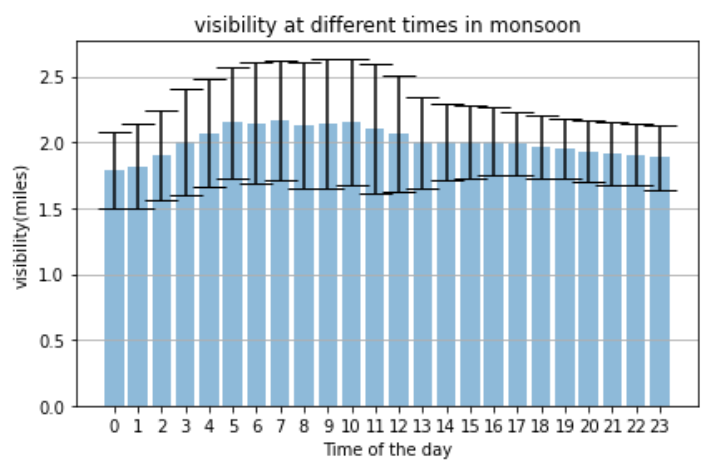


fig 3.9(f) visibility in monsoon

In the above 4 plots, on x-axis, “time of the day” is in UTC and interval between two consecutive “time of the day” is 1 hour.

In all the seasons, visibility is generally highest around 2:30 pm.

### Visibility (miles) data for airport VIDP

| No. Of samples | Mean | Median | Mode | std dev | max  | min | range |
|----------------|------|--------|------|---------|------|-----|-------|
| 26280          | 1.66 | 1.74   | 2.17 | 0.69    | 4.34 | 0   | 4.34  |

Table 12: visibility data for airport VIDP

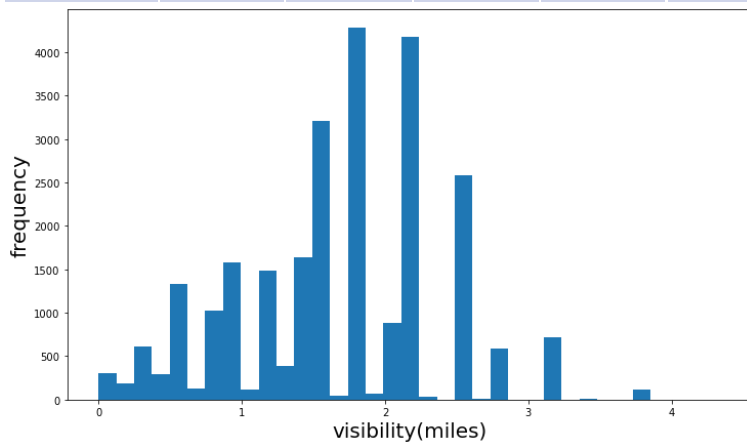


fig 3.10(a) histogram of visibility

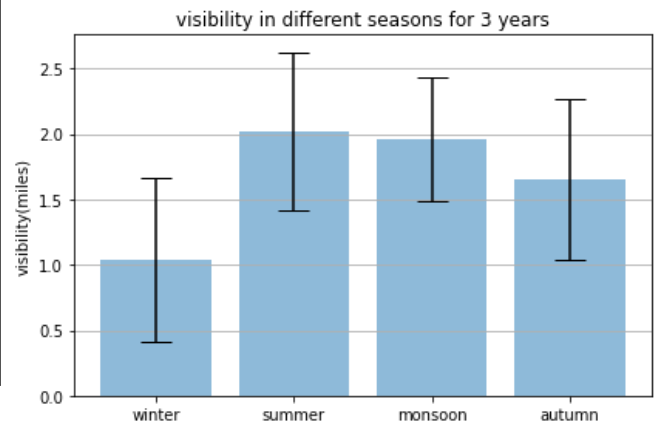


fig 3.10(b) visibility in different seasons

We can see that visibility is generally highest in summer. For most times, visibility is confined to about 3.6 miles.

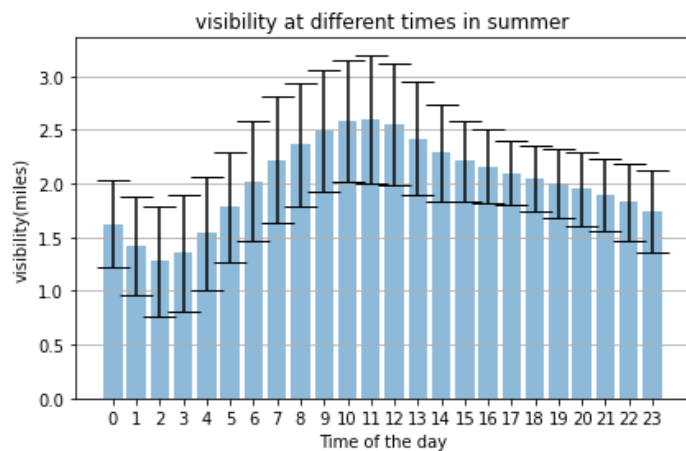


fig 3.10(c) visibility in summer

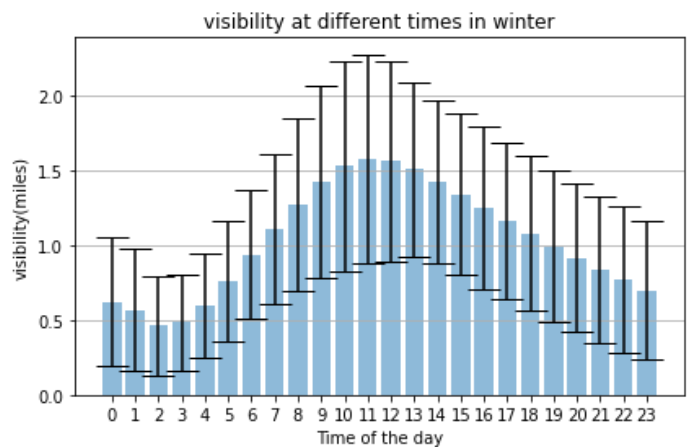


fig 3.10(d) visibility in winter

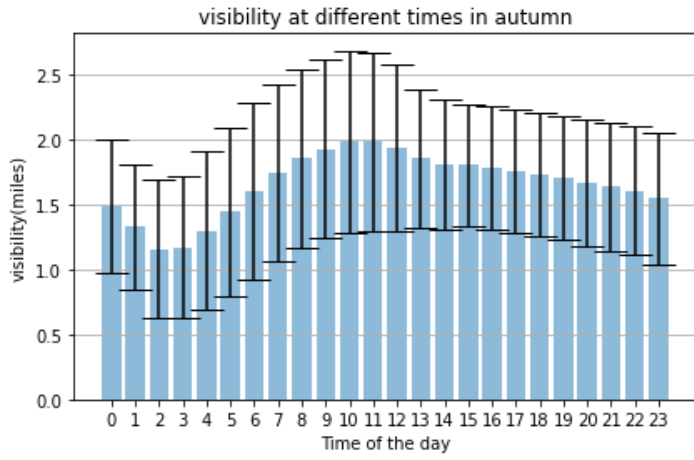


fig 3.10(e) visibility in autumn

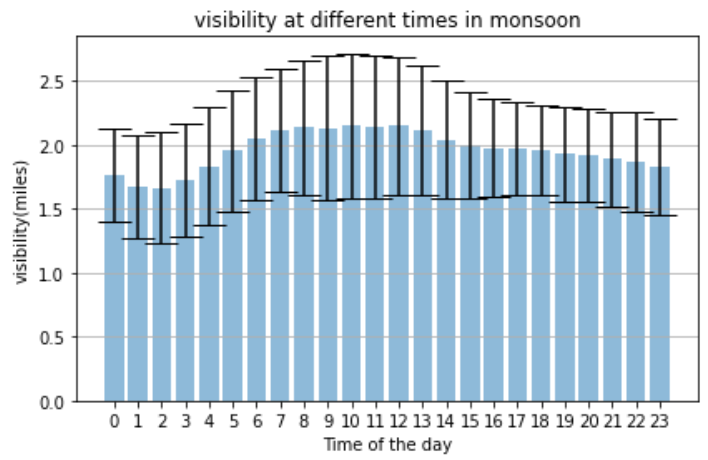


fig 3.10(f) visibility in monsoon

In the above 4 plots, on x-axis, “time of the day” is in UTC and interval between two consecutive “time of the day” is 1 hour.

In winter and summer, visibility is generally highest around 4:30 pm. In autumn and monsoon, visibility is highest around 3:30 pm.

# Chapter 4- Methodology

I have used ERA-5 reanalysis dataset having values of variable ‘geopotential’ with  $0.25^\circ \times 0.25^\circ$  spatial resolution stretching (from  $63^\circ$  in the west and  $102^\circ$  in the east and  $3^\circ$  in the south to  $42^\circ$  in the north) as input and metar observations with hourly temporal resolution for 5 stations as target.

The data taken is for a total of 3 years from 01/01/2018 to 30/12/2020. In this work I have used 4 models. One is a 6 layer (layers with learnable parameters) 2D CNN trained from scratch and the others are pretrained VGG16 and Resnet-50 (both trained on imagenet dataset) for transfer learning. Mean squared error (MSE) is used as loss function while MAE is used as metric to assess the effectiveness of the models.

## VGG16, 2D CNN, 3D CNN

VGG16 is a CNN architecture that is basic and extensively used. The VGG16 Architecture was designed by Andrew Zisserman and Karen Simonyan of the Oxford University in their 2014 paper "Very Deep Convolutional Networks for Large-Scale Image Recognition". The acronym 'VGG' refers for Visual Geometry Group, a Oxford university group of scholars that designed this architecture, and the number '16' denotes the architecture's 16 layers. The VGG16 model achieved 92.7 percent top 5 test accuracy on ImageNet, a dataset of over 14 million images belonging to 1000 classes. It outperforms AlexNet by replacing large sized filters (11 and 5 in the first and second convolutional layers, respectively) with a series of three-three kernel-sized filters.

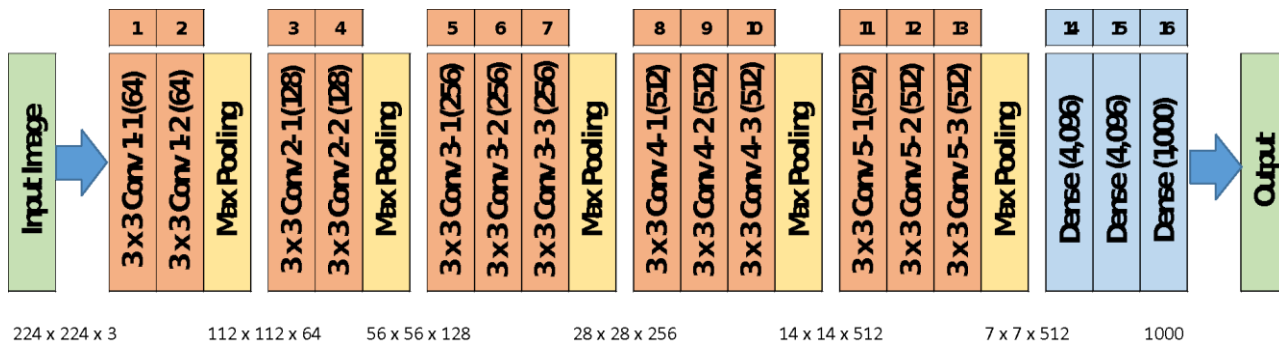


Fig 4.1 VGG16

Credit: <https://www.mygreatlearning.com/blog/introduction-to-vgg16/#VGG%2016%20Architecture>

It was discovered that increasing representation depth enhances classification accuracy, and that utilising a typical ConvNet architecture with greatly increased depth, cutting-edge performance on the ImageNet dataset may be achieved. VGG16, which is popular due to its ease of use, is used in several deep learning image categorization approaches. Training these models from scratch takes long time, so it may turn out better to use pretrained weights.

**2D CNN-** For the 5 layer 2D CNN employed in the trials, a 3x3 kernel is used in each convolution layer followed by a 2x2 max pooling layer. RMSprop is used as optimizer with learning rate 0.001. Following the convolution processes, a fully connected layer with no activation function is utilized to connect the output (real number). As a simple non machine learning baseline performance, i have used mean absolute error (MAE) of mean of absolute of the difference between historical observation and actual target. Here we make a comparison of the effectiveness of the simple 2D CNN and the pretrained model VGG16 for the problem of predicting wind velocity and visibility for the airports given ERA-5 geopotential data as input and METAR observations (wind velocity and visibility) as target. Both ERA-5 and metar observational data require lot of time in data processing. Also initially the plan was to predict only the precipitation values but after searching and processing(lots of trial and error) we concluded that due to insufficient data available we needed to concentrate on other variables like wind velocity and visibility the data for which were readily available. The reason for choosing wind velocity and visibility is that these variables greatly affect the normal functioning of the airports.

**3D CNN-** With 3D CNN, we are predicting wind speed and visibility in the next 6 hour. The 3D CNN is trained by combining the input dataset into groups of 6 consecutive images. This aggregation represents the evolution of the atmosphere over the course of a 6-hour period. The neural network can then extract information from the temporal dimension by using the observation that corresponds to the series' last image as an output.

## Hyperparameters used:

|        | Number of convolution layers | Number of dense layers | dropout rate | pooling used | optimizer         | batch size | no. of epochs |
|--------|------------------------------|------------------------|--------------|--------------|-------------------|------------|---------------|
| 2D CNN | 5                            | 1                      | 0.4          | 4 Max-pool   | RMSprop(lr=0.001) | 128        | 100           |
| VGG-16 | 13                           | 1                      | 0.4          | 5 Max-pool   | RMSprop(lr=0.001) | 128        | 100           |
| 3D CNN | 2                            | 1                      | 0.4          | 2 Max-pool   | RMSprop(lr=0.001) | 16         | 20            |

Table 13: hyperparameters used

No. of filters used in 2D CNN are 32 -> 64 -> 128 -> 256 -> 512, in 3D CNN are 64 ->128.

## Chapter 5- Results

Climatology: Long-term average of a given variable.

### Result (Mean Absolute Error) for Visibility:

| Airports | Visibility climatology<br>(miles) | 2D CNN<br>(miles) | VGG16<br>(miles) | 3D CNN<br>(miles) |
|----------|-----------------------------------|-------------------|------------------|-------------------|
| VABB     | 0.414                             | 0.47              | 0.545            | 0.67              |
| VOTV     | 0.761                             | 1.14              | 0.64             | 0.56              |
| VOBL     | 1.086                             | 0.89              | 0.952            | 1.61              |
| VECC     | 0.92                              | 0.261             | 0.338            | 0.35              |
| VIDP     | 1.23                              | 0.31              | 0.513            | 0.96              |

Table 14: Visibility forecasting accuracy for several stations comparing 2D CNN, 3D CNN and pretrained model VGG16 with the reference accuracy of climatology. The metric used is mean absolute error (MAE).

**For station VABB,**

**With 2D CNN,**

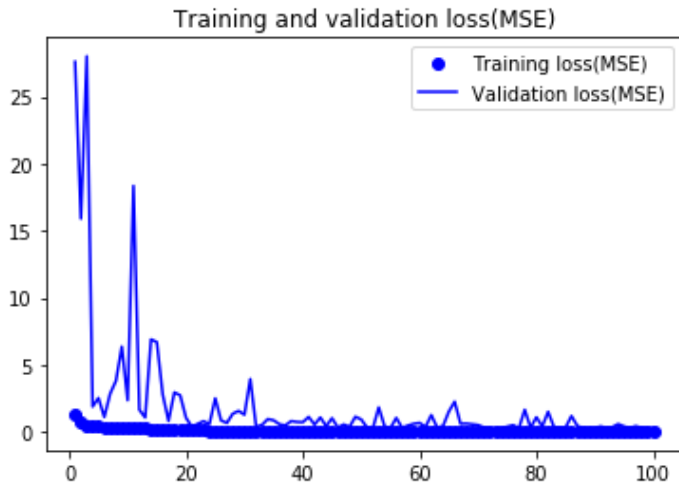


fig 5.1(a) epoch Vs loss

On the x-axis we have no. of epochs and on y-axis loss value (unit = miles squared).

This is the plot of loss Vs epochs. We can see that with continuous training, loss decreases.

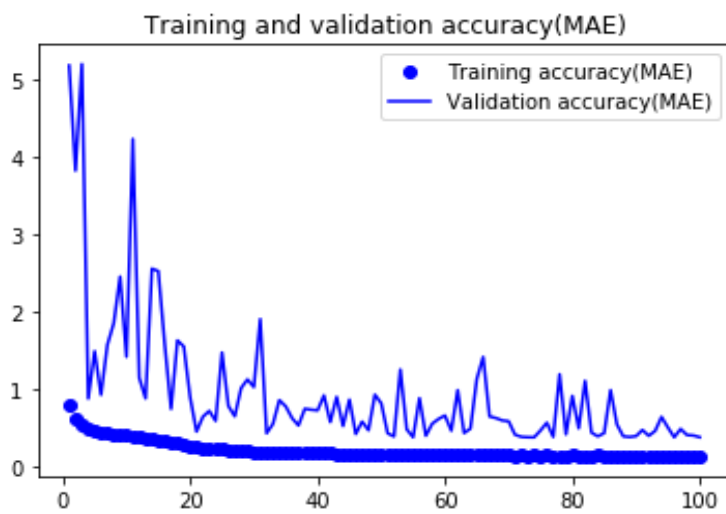


fig 5.1(b) epoch Vs accuracy

x-axis = no. of epochs, y-axis = accuracy value (unit = miles).

We can see that accuracy improves with subsequent training process.

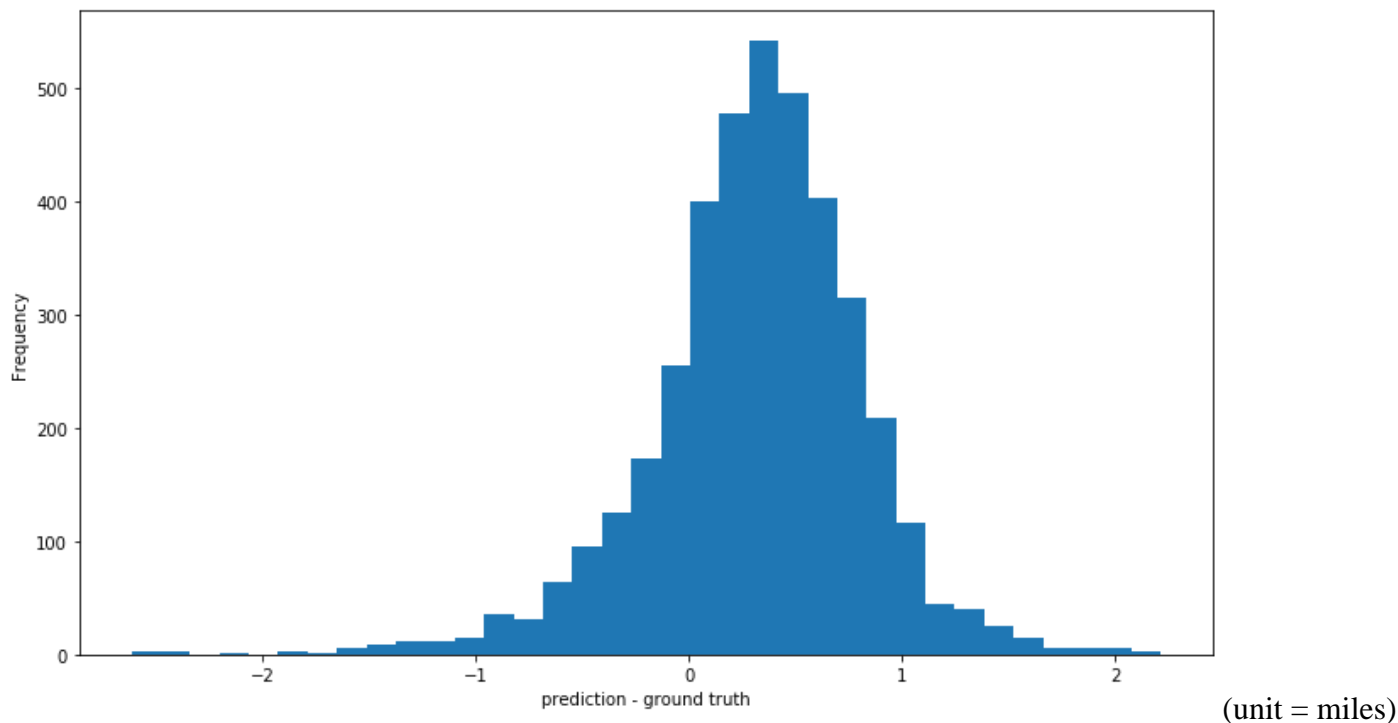


Fig 5.1(c) histogram of errors

This is the histogram of the errors (prediction – observation) that we get after evaluating our model on validation dataset. There were 3942 data points (15 % of the whole dataset of 3 years). The train, validation and test dataset split is in the ratio of 70%, 15% and 15% respectively of the whole dataset of 3 years from January 2018 to December 2020. We can see that most of the predictions are closer to ground truth i.e., errors are mostly concentrated around 0. Most of the errors are within about 1 miles.

Correlation matrix,

```
[[1.    0.56]
 [0.56  1.]]
```

The correlation coefficient between prediction and actual observation (i.e., ground truth) is 0.55. So there is only moderate correlation between the two.

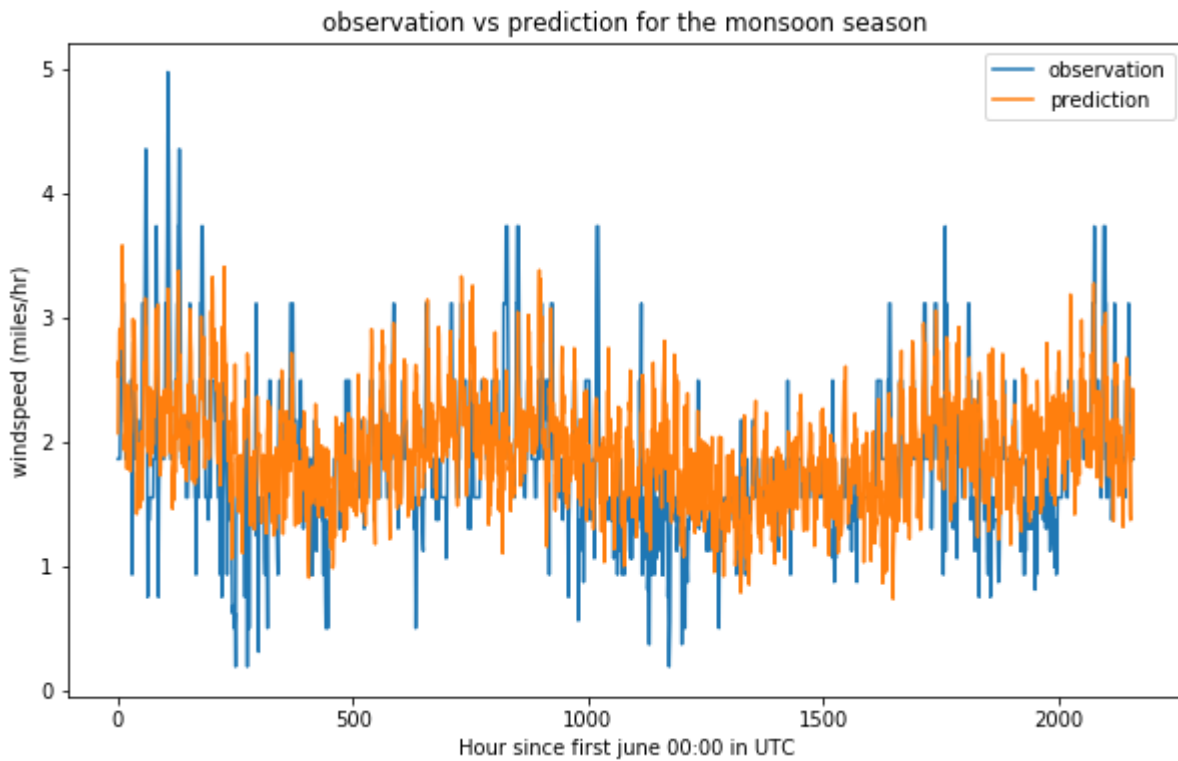
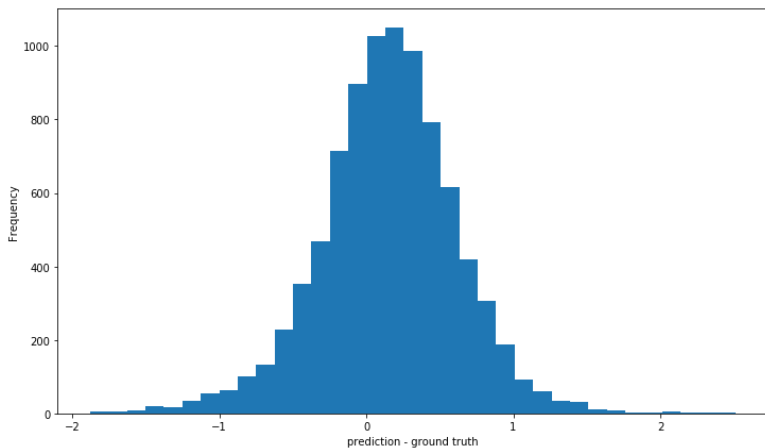


Fig 5.1(d) observation and prediction plot for monsoon season

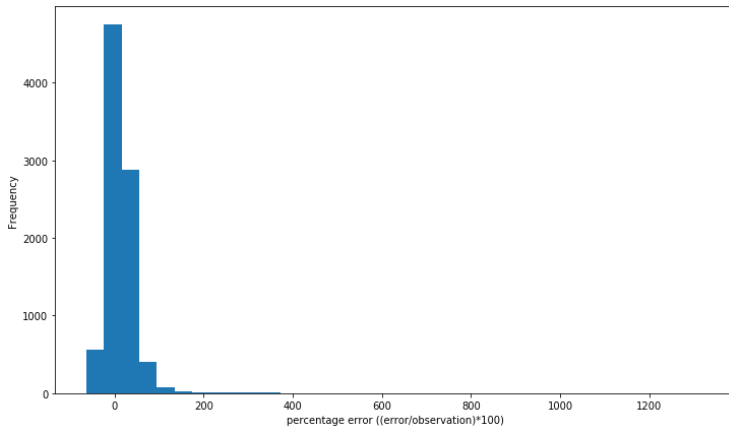
In this, observation and prediction are put in the same plot. The data taken was for 3 months from 1<sup>st</sup> june 2021 to 31<sup>st</sup> august 2021. We first find the prediction made by our model on this 3 month input data. This is a time-series data.



Unit on the x-axis is miles.

Fig 5.1(e) histogram of errors on 1 year independent dataset

We have the histogram of errors (prediction – ground truth) our model gives when tested on 1 year (1 march 2021 to 28 february 2022) of independent dataset. Again, most of the errors are within 1 miles.

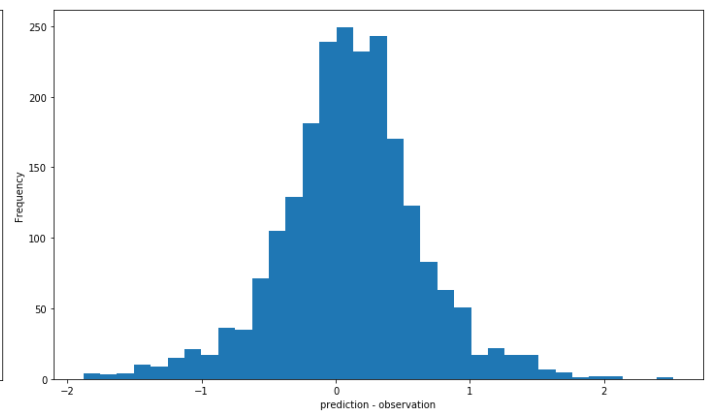
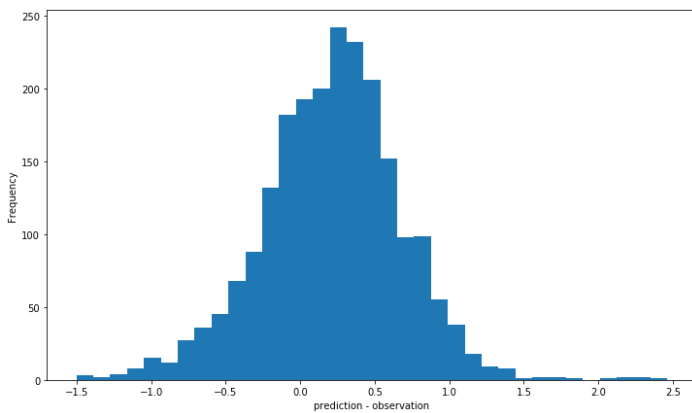


On the x-axis, percentage error has no unit.

Fig 5.1(f) percentage error for the same

We have the histogram of percentage error  $((\text{error}/\text{observation}) * 100)$  when our model is tested on 1 year (1 march 2021 to 28 february 2022) of independent dataset. As we can see, most of the data points fall under 200 % error (in miles).

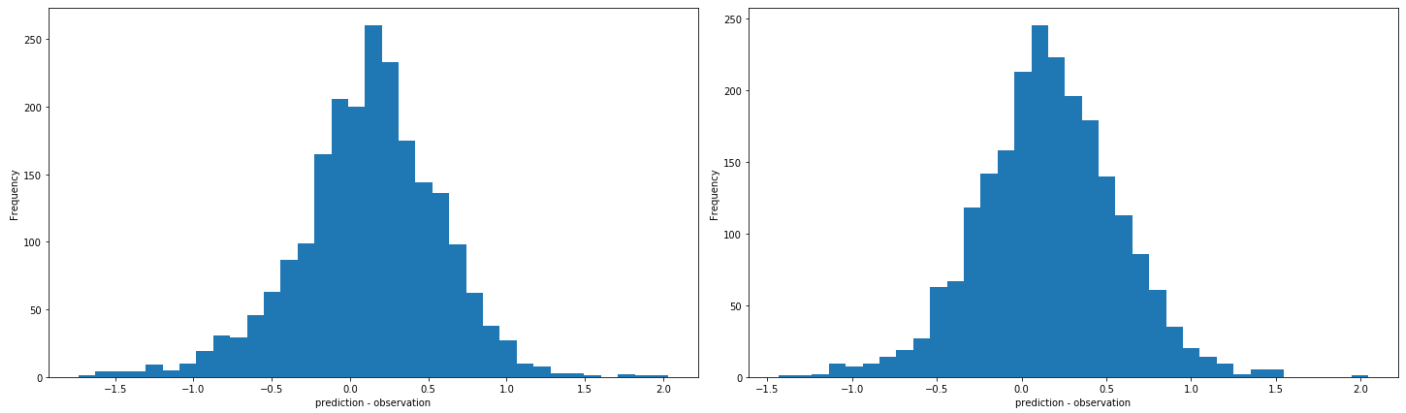
In both the plots we can see majority of predictions are closer to observation (or ground truth).



(x-axis unit = miles)

Fig 5.1(g) error histogram for summer

fig 5.1(h) error histogram for monsoon



(x-axis unit = miles)

Fig 5.1(i) error histogram for autumn

fig 5.1(j) error histogram for winter

Above 4 plots are error plots when the model is tested on 4 different seasons each of 3 month time length. 1 year of independent dataset has been broken into 4 seasons.

Summer- 1 March to 31 May

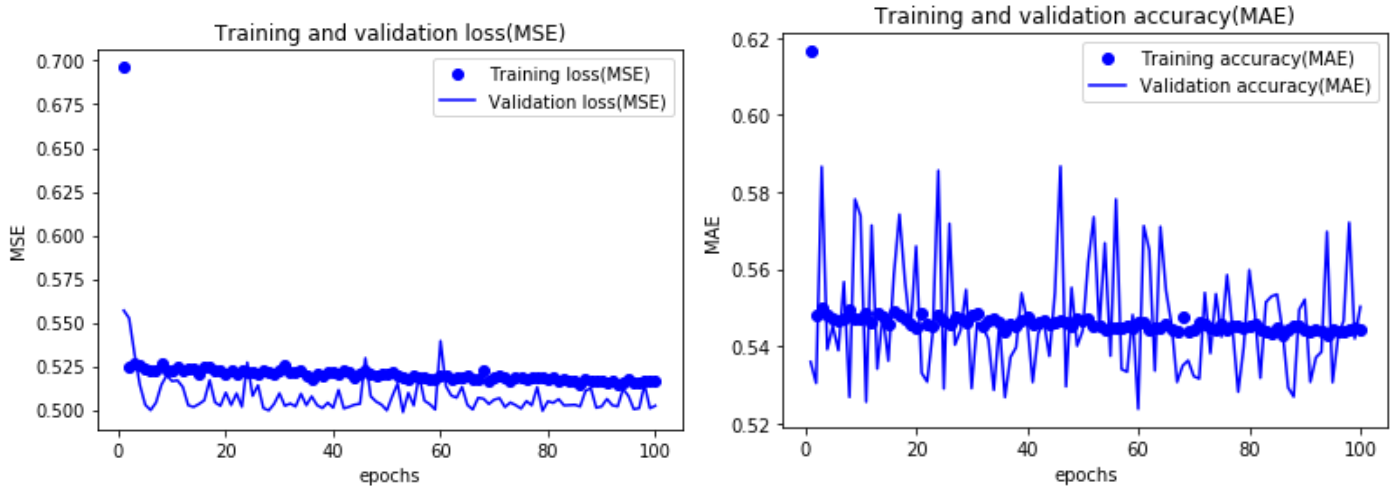
Monsoon- 1 June to 31 August

Autumn- 1 September to 30 November

Winter- 1 December to 28 February

1<sup>st</sup>, 2<sup>nd</sup>, 3<sup>rd</sup> and 4<sup>th</sup> plots are for summer, monsoon, autumn and winter datasets respectively. Most of the errors are spread over 1 miles from center.

## With VGG16,



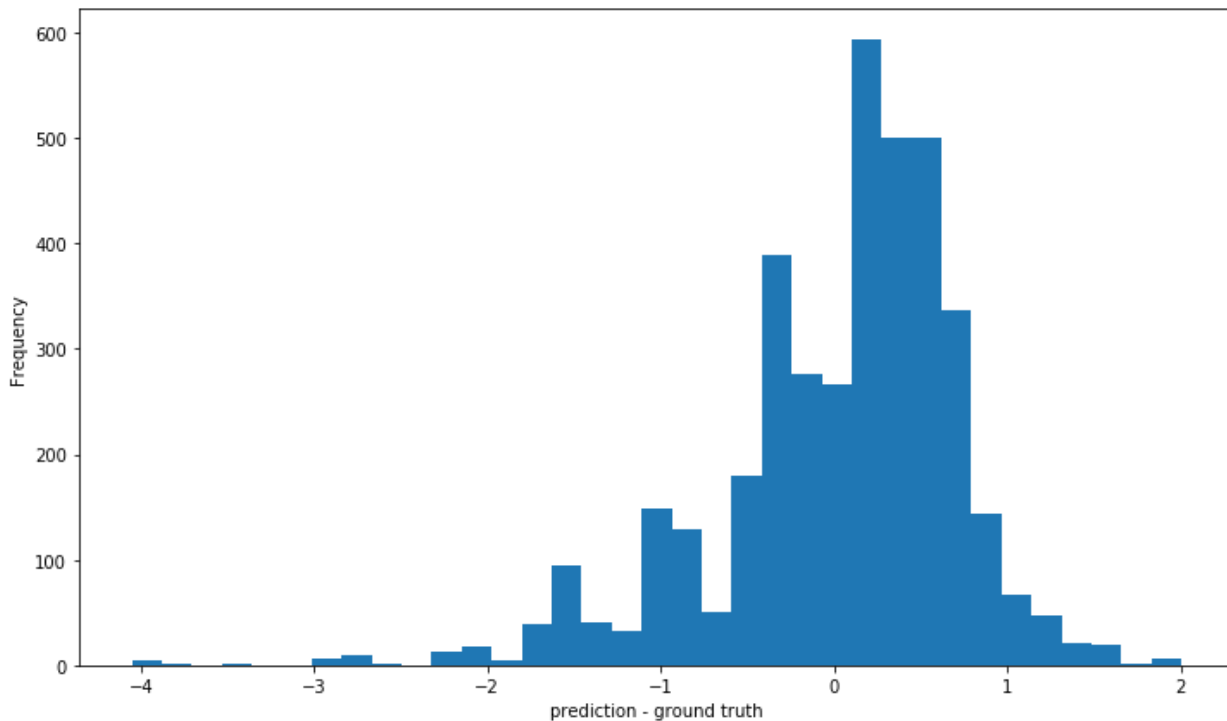
(unit of MSE = miles squared)

(unit of MAE is miles)

Fig 5.1(k) epoch Vs loss

fig 5.1(l) epoch Vs accuracy

This is the plot of epochs Vs loss. We can see that in the very beginning of the training process, loss drops fast but after just few epochs with continuous training, validation loss remains quite constant. The same way on the right side plot, accuracy becomes quite stagnant after just few epochs and we don't see any further improvement.



(unit on x-axis = miles)

Fig 5.1(m) histogram of errors

This is the histogram of the errors (prediction – observation) that we get after evaluating our model on validation dataset. We can see that most of the predictions are closer to ground truth i.e., errors are mostly concentrated around 0 miles. Most of the errors are spread within about 1 miles.

Correlation matrix,

```
[[1.    0.17939892]  
 [0.17939892  1.]]
```

The correlation coefficient between prediction and actual observation (i.e., ground truth) is 0.17. So there is only weak correlation between the two which we can see in the next plot.

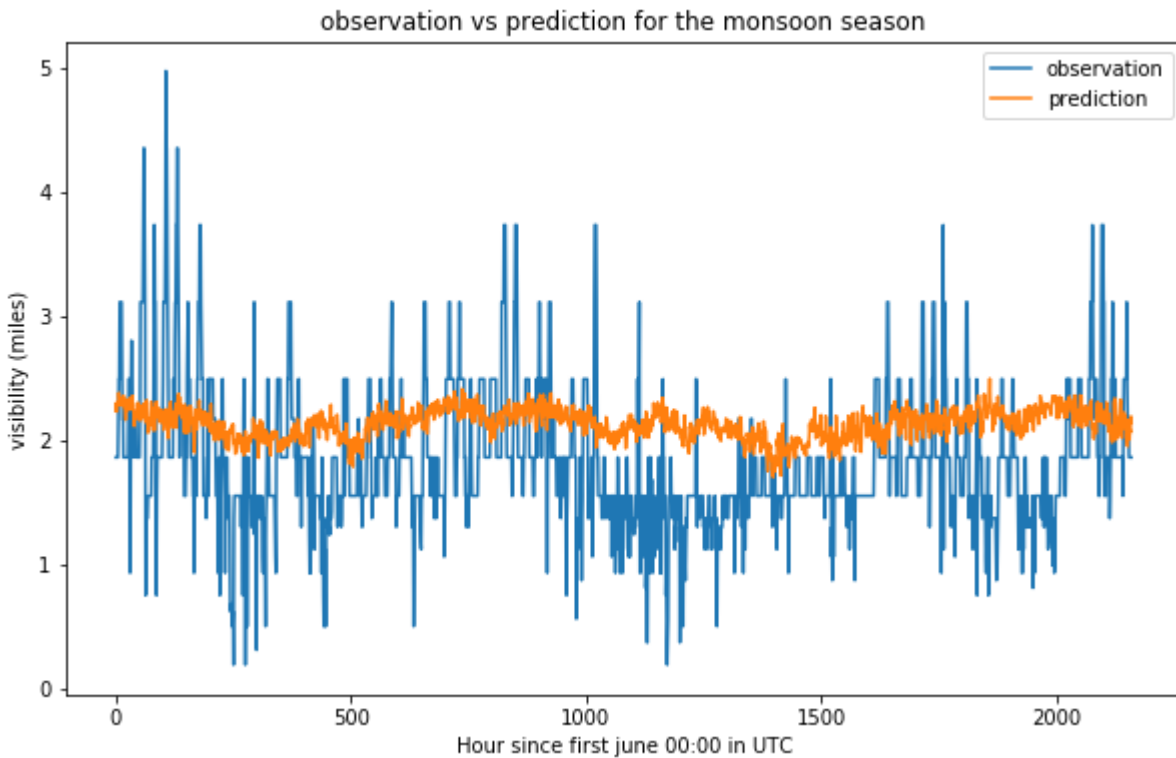
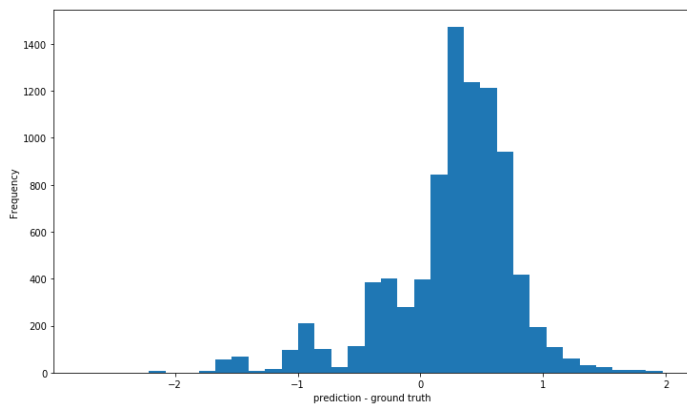
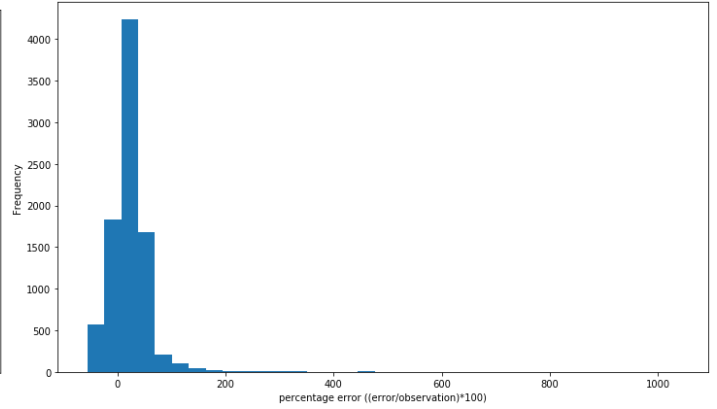


Fig 5.1(n) observation and prediction plot for monsoon season

In this, observation and prediction are put in the same plot. The data taken was for 3 months from 1<sup>st</sup> june 2021 to 31<sup>st</sup> august 2021. We first find the prediction made by our model on this 3 month independent input dataset. This is a time-series data. The plot clearly shows there is a weak correlation between the predictions made by VGG16 model and observations made for the 3 month monsoon season.



(unit = miles)



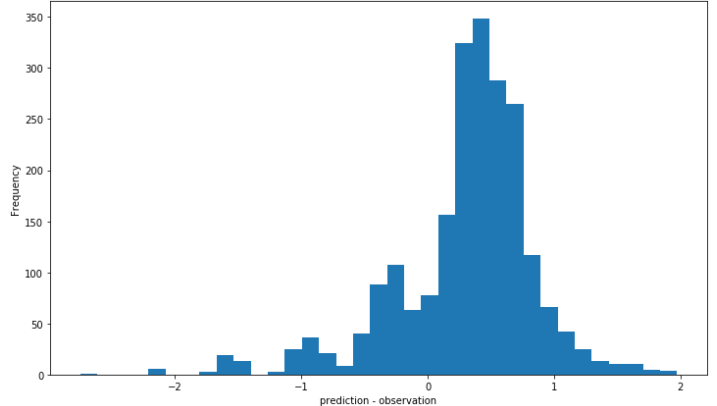
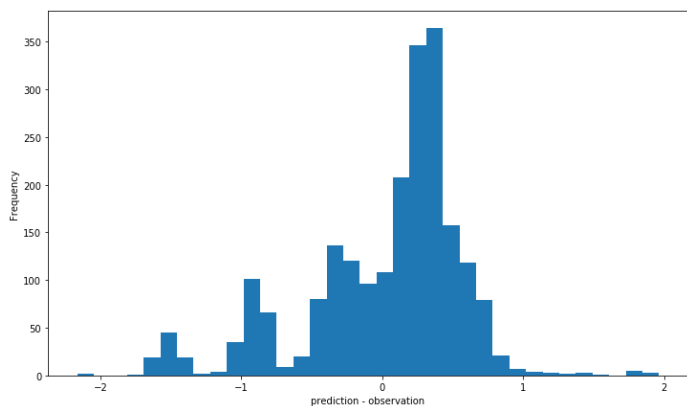
(unitless)

fig 5.1(o) error histogram for independent dataset

fig 5.1(p) percentage histogram for the same

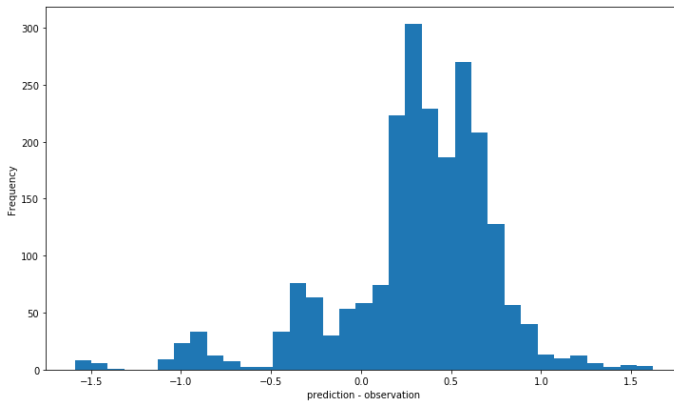
On the left side we have the histogram of errors (prediction – ground truth) our model gives when tested on 1 year (1 march 2021 to 28 february 2022) of independent dataset. Again, most of the errors are within 1 miles from the center.

On the right side we have the histogram of percentage error  $((\text{error}/\text{observation}) * 100)$  when our model is tested on 1 year (1 march 2021 to 28 february 2022) of independent dataset. As we can see, most of the data points fall under 200 % error.



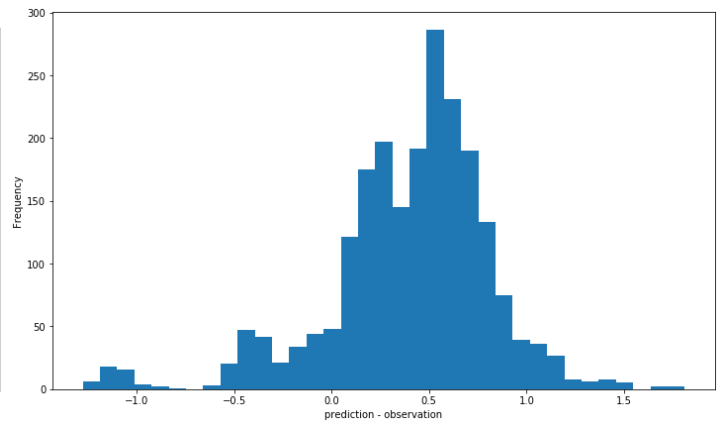
(unit = miles) error histogram for summer

Fig 5.1(q)



(unit = miles) error histogram for monsoon

fig 5.1(r)



(unit = miles) error histogram for autumn

Fig 5.1(s)

(unit = miles) error histogram for winter

fig 5.1(t)

Above 4 plots are error plots when the model is tested on 4 different seasons each of 3 month time length. 1 year of independent dataset has been broken into 4 seasons.

Summer- 1 March to 31 May

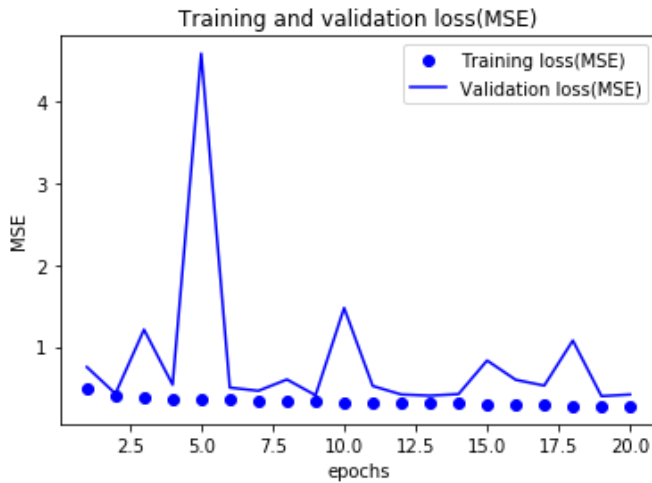
Monsoon- 1 June to 31 August

Autumn- 1 September to 30 November

Winter- 1 December to 28 February

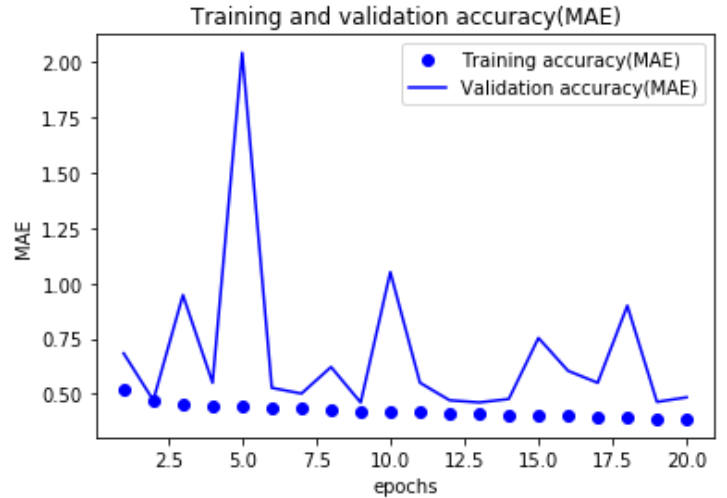
1<sup>st</sup>, 2<sup>nd</sup>, 3<sup>rd</sup> and 4<sup>th</sup> plots are for summer, monsoon, autumn and winter datasets respectively. Most of the errors are spread over 1 miles from the center.

## With 3D CNN,



(unit of MSE = miles squared)

Fig 5.1(u) epoch Vs loss



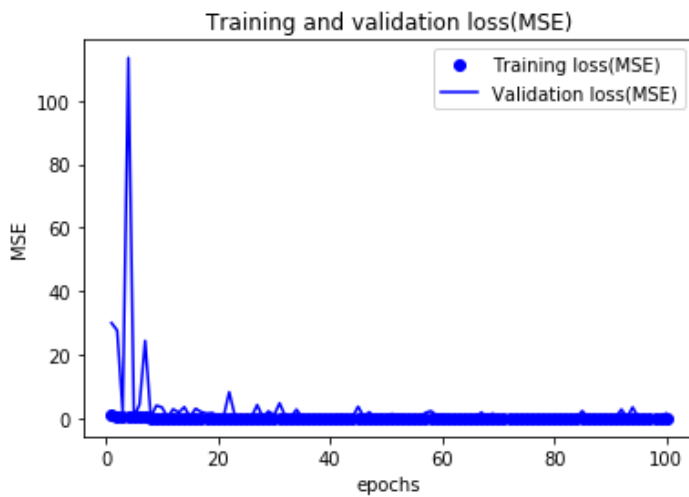
(unit of MAE = miles)

fig 5.1(v) epoch Vs accuracy

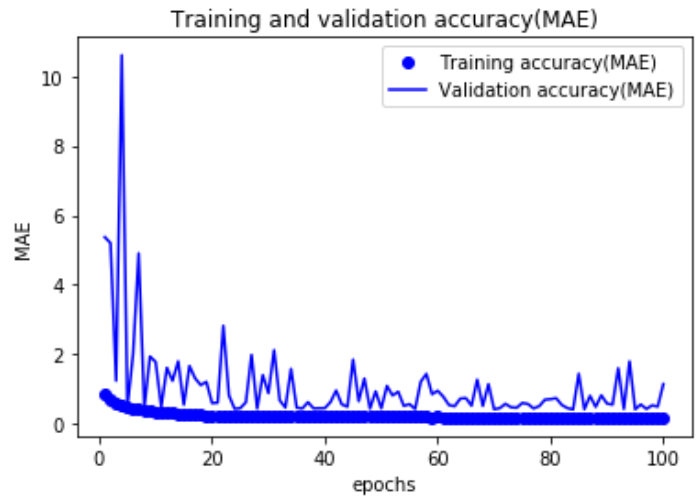
With 3D CNN, we are making predictions for 6 hours in future. With continuous training, validation loss decreases and validation accuracy improves.

## For station VOTV,

### With 2D CNN,



(Unit of MSE = miles squared)

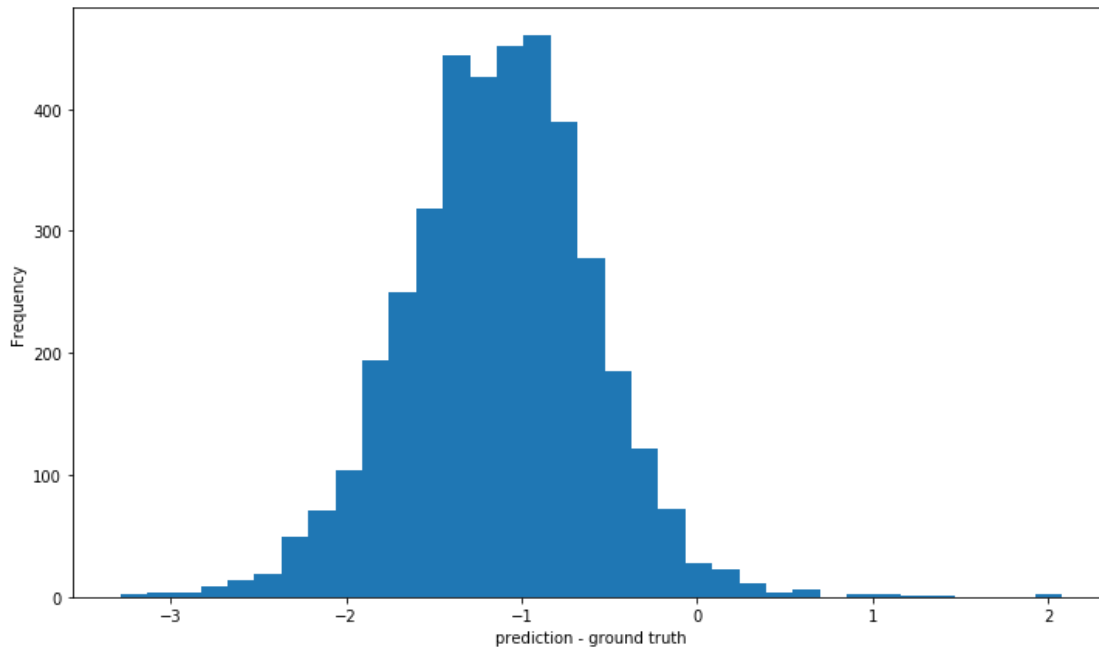


(unit of MAE = miles)

Fig 5.2(a) epoch Vs loss

fig 5.2(b) epoch Vs accuracy

This is the plot of loss Vs epochs. We can see that with continuous training, loss decreases and accuracy improves with subsequent training process.



(unit = miles)

Fig 5.2(c) histogram of errors

This is the histogram of the errors (prediction – observation) that we get after evaluating our model on validation dataset. We can see that errors are mostly concentrated around -1 miles. Most of the errors are within about 2 miles.

Correlation matrix,

```
[[1.    0.69386602]
 [0.69386602  1.]]
```

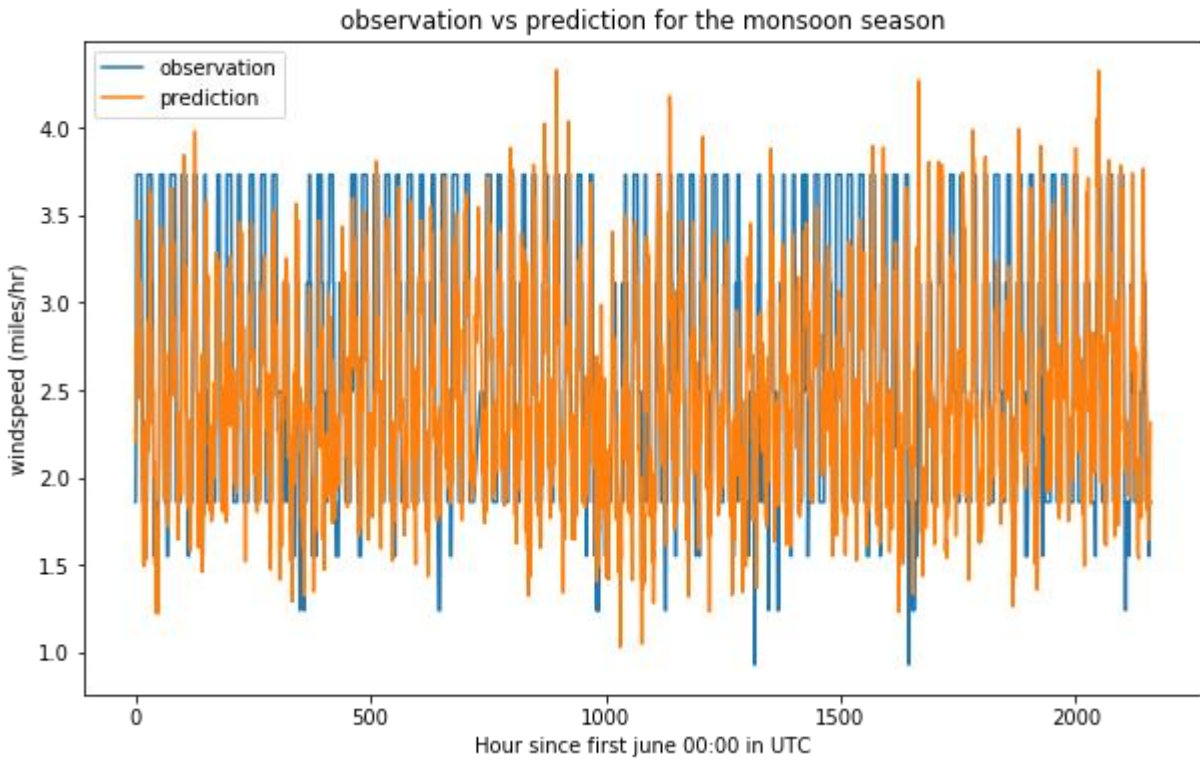
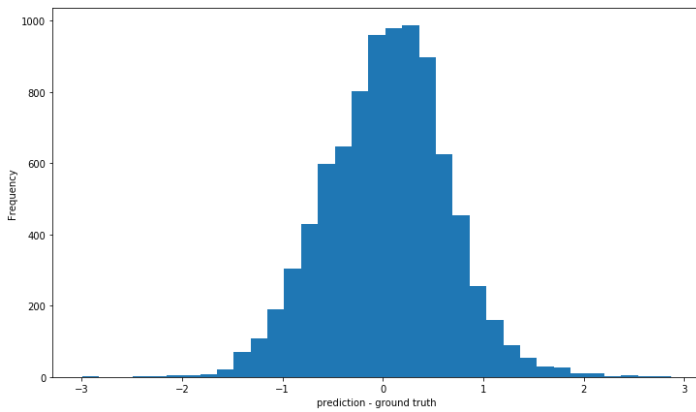
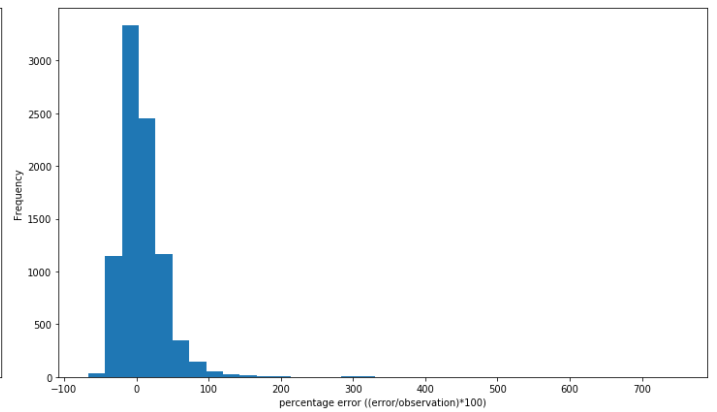


Fig 5.2(d) observation and prediction plot for monsoon season

In this, observation and prediction are put in the same plot. The data taken was for 3 months from 1st june 2021 to 31st august 2021. We first find the prediction made by our model on this 3 month input data. This is a time-series data. There is moderate correlation between observation and prediction.



(unit = miles)

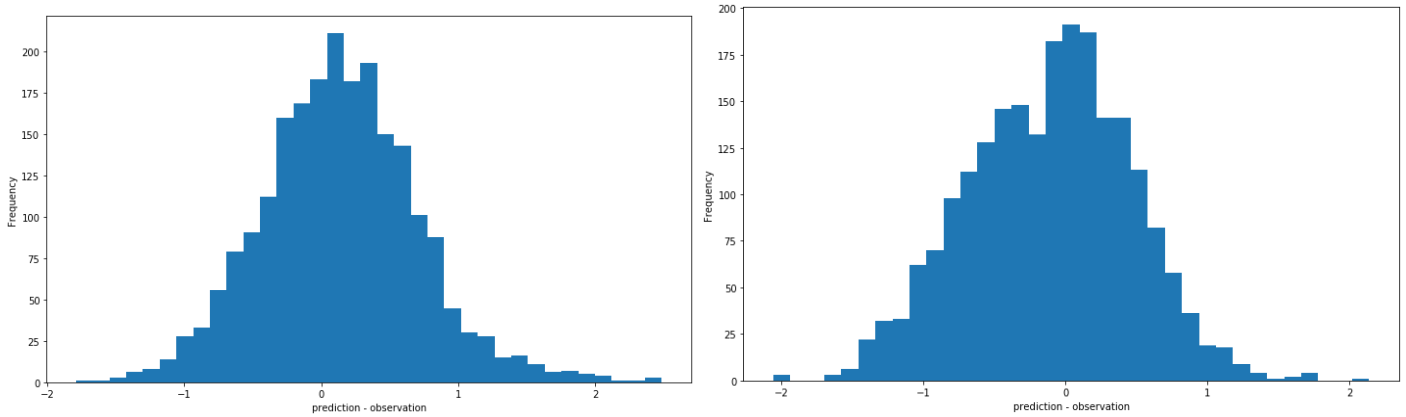


(unitless)

Fig 5.2(e) histogram of errors on 1 year independent dataset

fig 5.2(f) percentage error for the same

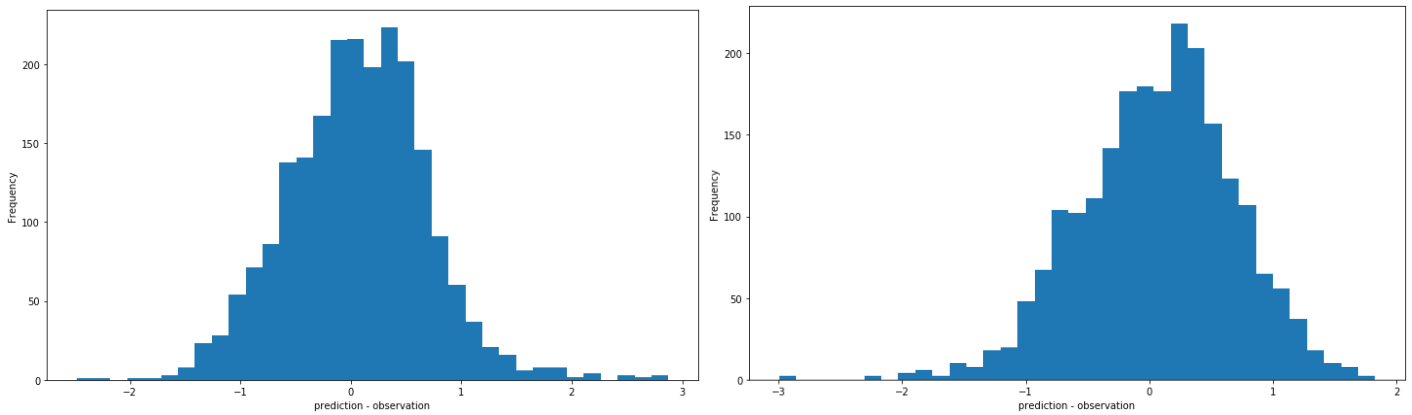
We have the histogram of errors (prediction – ground truth) and percentage error  $((\text{error}/\text{observation}) * 100)$  our model gives when tested on 1 year (1 march 2021 to 28 February 2022) of independent dataset. Again, most of the errors are within 1 miles and 100% respectively. In both the plots we can see majority of predictions are closer to observation (or ground truth).



(unit on x-axis = miles)

Fig 5.2(g) error histogram for summer

fig 5.2(h) error histogram for monsoon



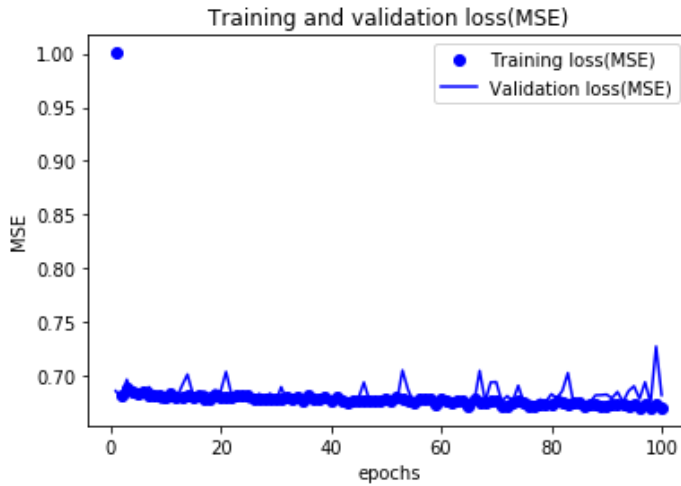
(unit on x-axis = miles)

Fig 5.2(i) error histogram for autumn

fig 5.2(j) error histogram for winter

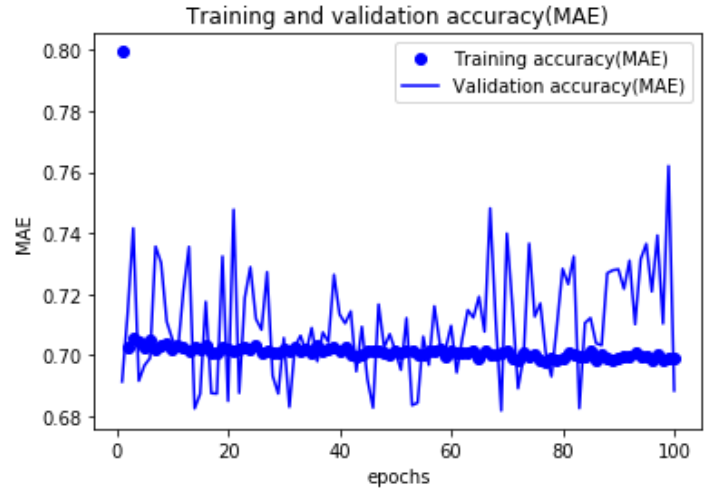
Above 4 plots are error plots when the model is tested on 4 different seasons each of 3 month time length. 1 year of independent dataset has been broken into 4 seasons. 1st, 2nd, 3rd and 4th plots are for summer, monsoon, autumn and winter datasets respectively. Most of the errors are spread over 1 miles from the center.

## With VGG16,



(unit of MSE = miles squared)

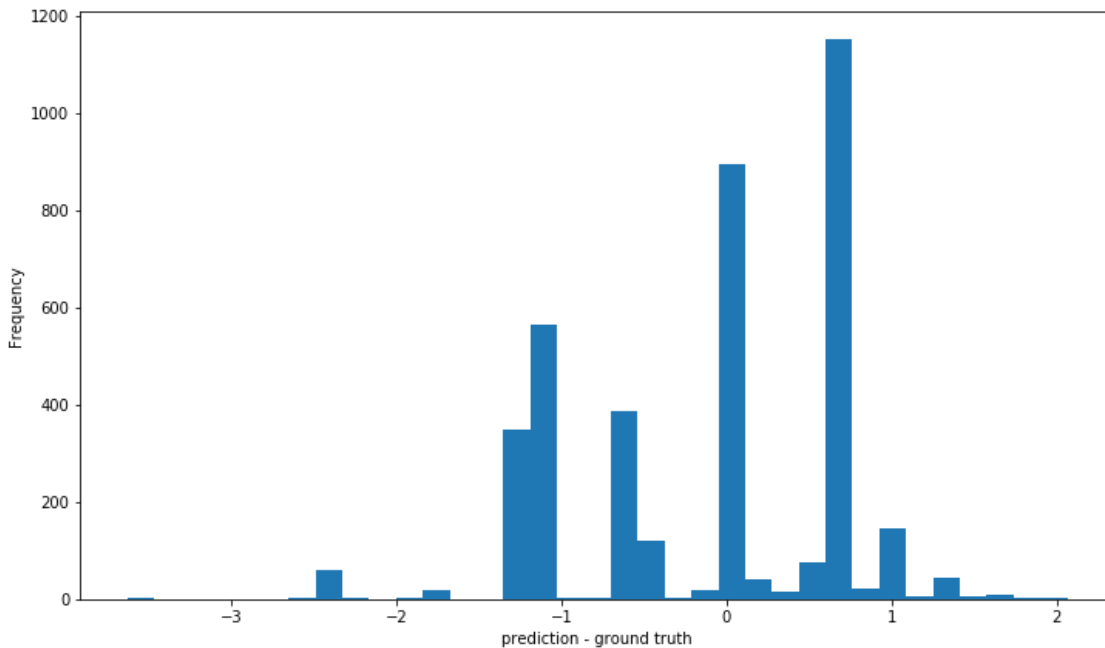
Fig 5.2(k) epoch Vs loss



(unit of MAE = miles)

fig 5.2(l) epoch Vs accuracy

This is the plot of loss Vs epochs and loss Vs accuracy. We can see that loss decreases fast in the beginning but after that becomes quite stagnant. Accuracy keeps fluctuating with continuous training and we don't see any big improvement.



(unit = miles)

Fig 5.2(m) histogram of errors

This is the histogram of the errors (prediction – observation) that we get after evaluating our model on validation dataset. We can see that most of the errors are within about 2 miles.

Correlation matrix,

```
[[1.    0.07]  
 [0.07  1.]]
```

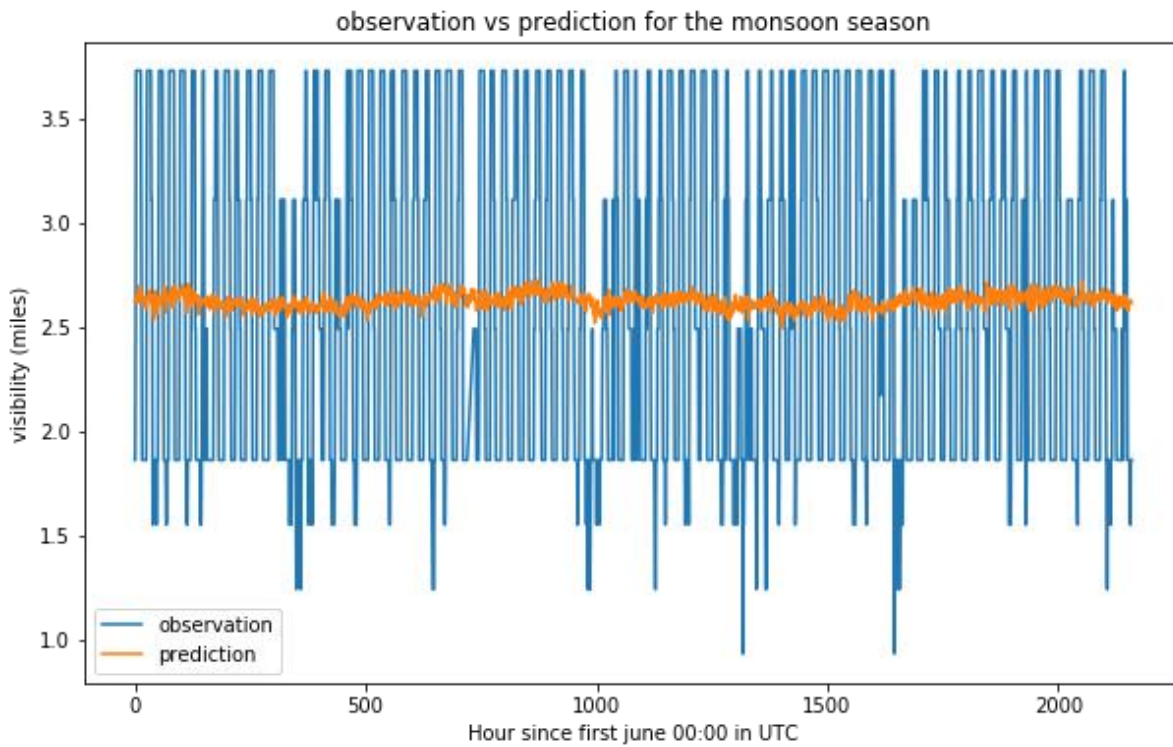
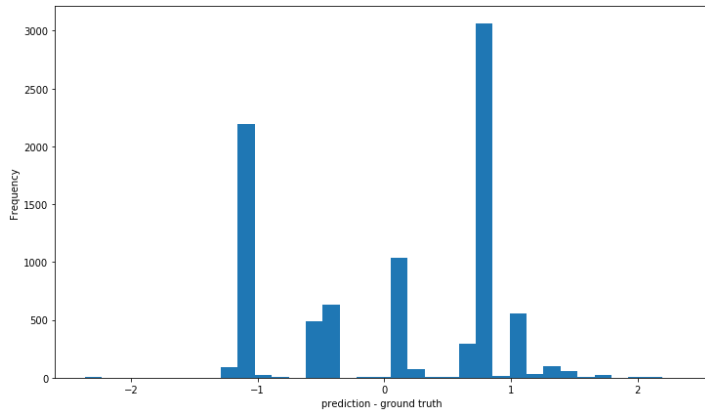
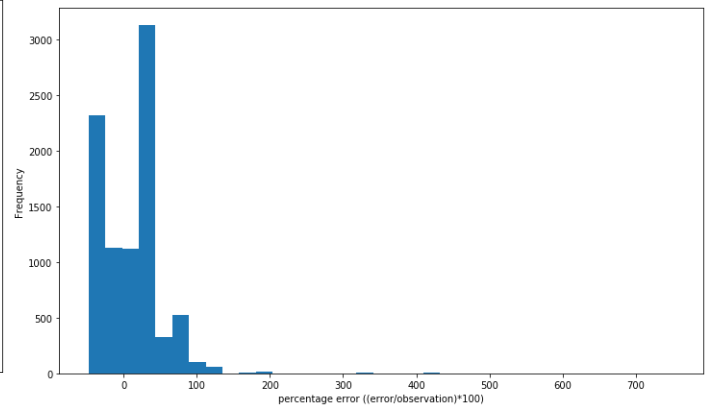


Fig 5.2(n) observation and prediction plot for monsoon season

In this, observation and prediction are put in the same plot. The data taken was for 3 months from 1st June 2021 to 31st August 2021. We first find the prediction made by our model on this 3 month independent input dataset. This is a time-series data. The plot clearly shows there is a very weak correlation between the predictions made by VGG16 model and observations made for the 3 month monsoon season.



(unit = miles)

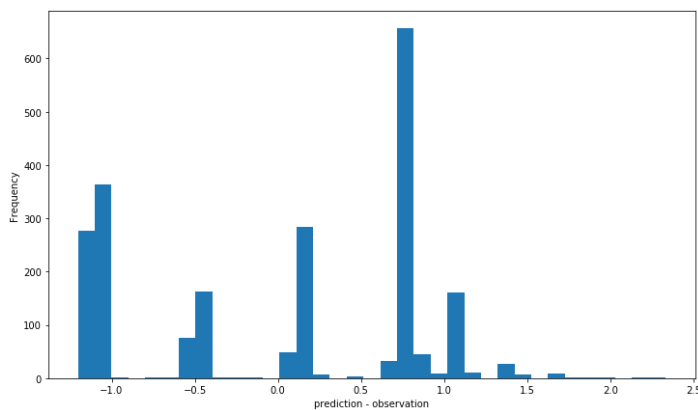


(unitless)

Fig 5.2(o) histogram of errors on 1 year independent dataset      fig 5.2(p) percentage error for the same

On the left side we have the histogram of errors (prediction – ground truth) our model gives when tested on 1 year (1 March 2021 to 28 February 2022) of independent dataset. Again, most of the errors are within 1.5 miles.

On the right side we have the histogram of percentage error  $((\text{error}/\text{observation}) * 100)$  when our model is tested on 1 year (1 March 2021 to 28 February 2022) of independent dataset. As we can see, most of the data points fall under 200 % error.



(unit = miles)

Fig 5.2(q) error histogram for summer

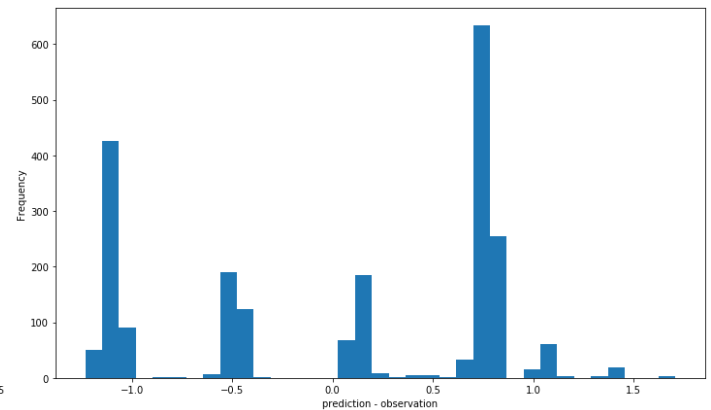
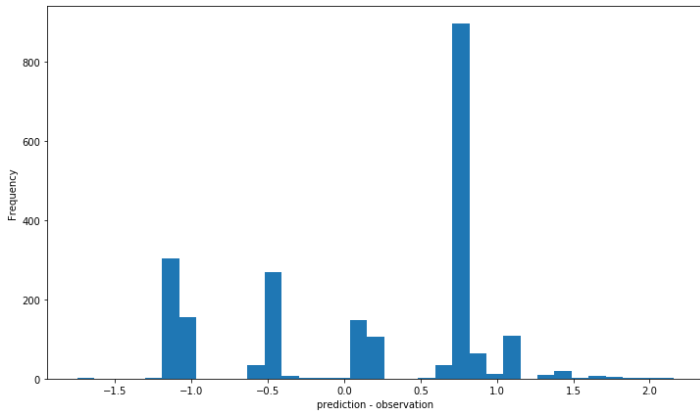


fig 5.2(r) error histogram for monsoon



(unit = miles)

Fig 5.2(s) error histogram for autumn

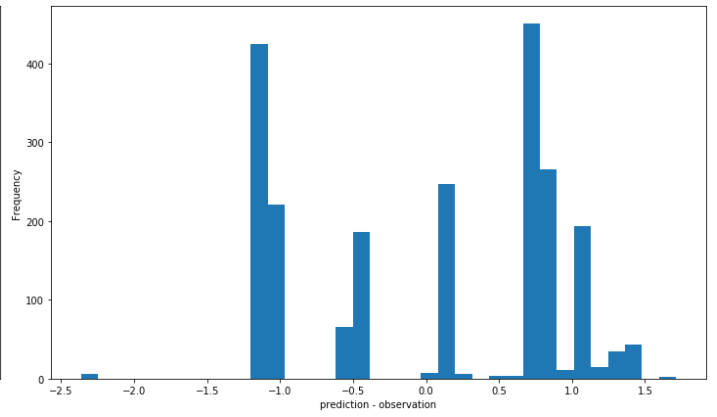
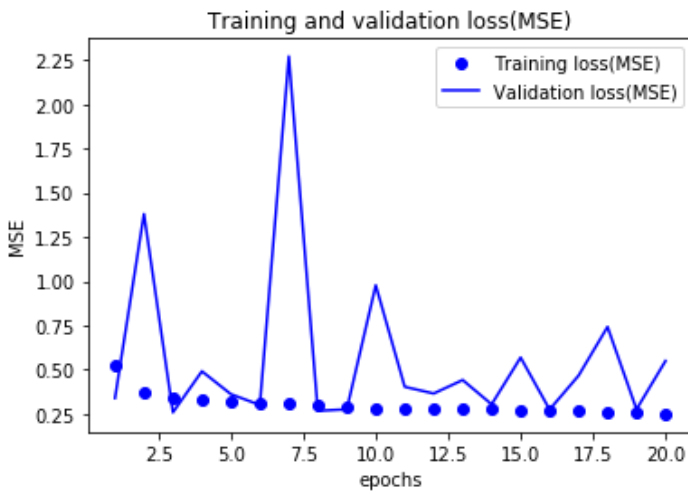


fig 5.2(t) error histogram for winter

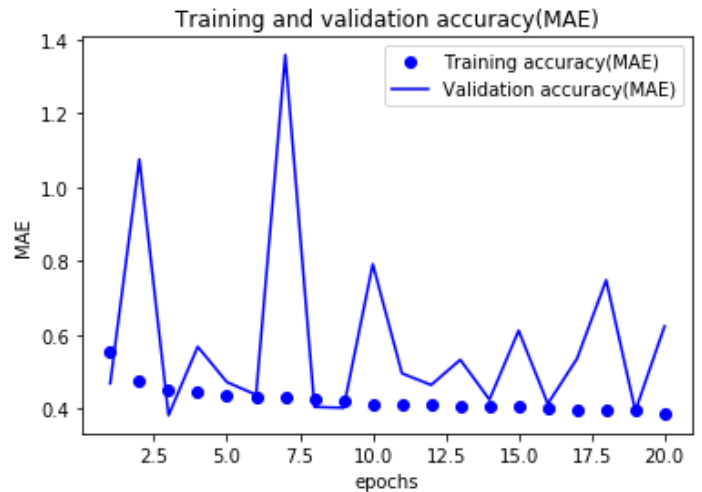
Above 4 plots are error plots when the model is tested on 4 different seasons each of 3 month time length. 1 year of independent dataset has been broken into 4 seasons. 1st , 2nd, 3rd and 4th plots are for summer, monsoon, autumn and winter datasets respectively. Most of the errors are about 1.5 miles.

### With 3D CNN,



(unit of MSE = miles squared)

Fig 5.2(u) epoch Vs loss



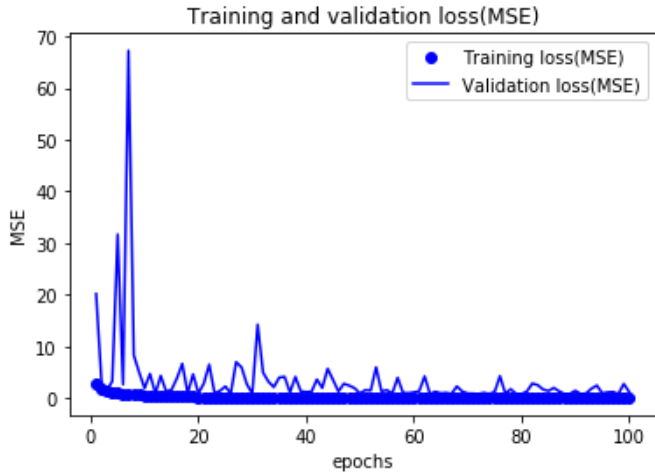
(unit of MAE = miles)

fig 5.2(v) epoch Vs accuracy

With 3D CNN, we are making predictions for 6 hours in future. With continuous training, validation loss decreases and validation accuracy improves.

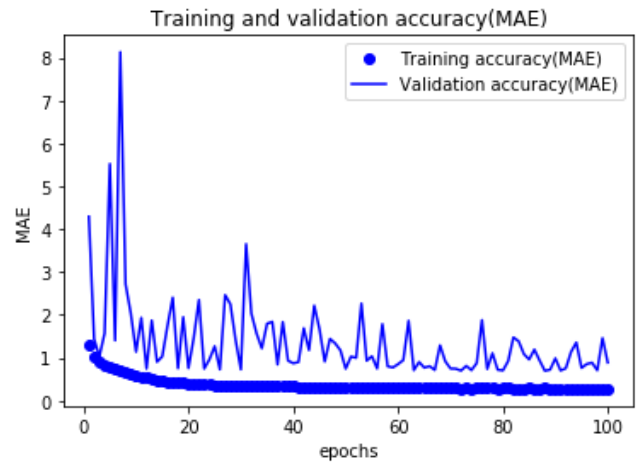
**For station VOBL,**

**With 2D CNN,**



(unit of MSE = miles)

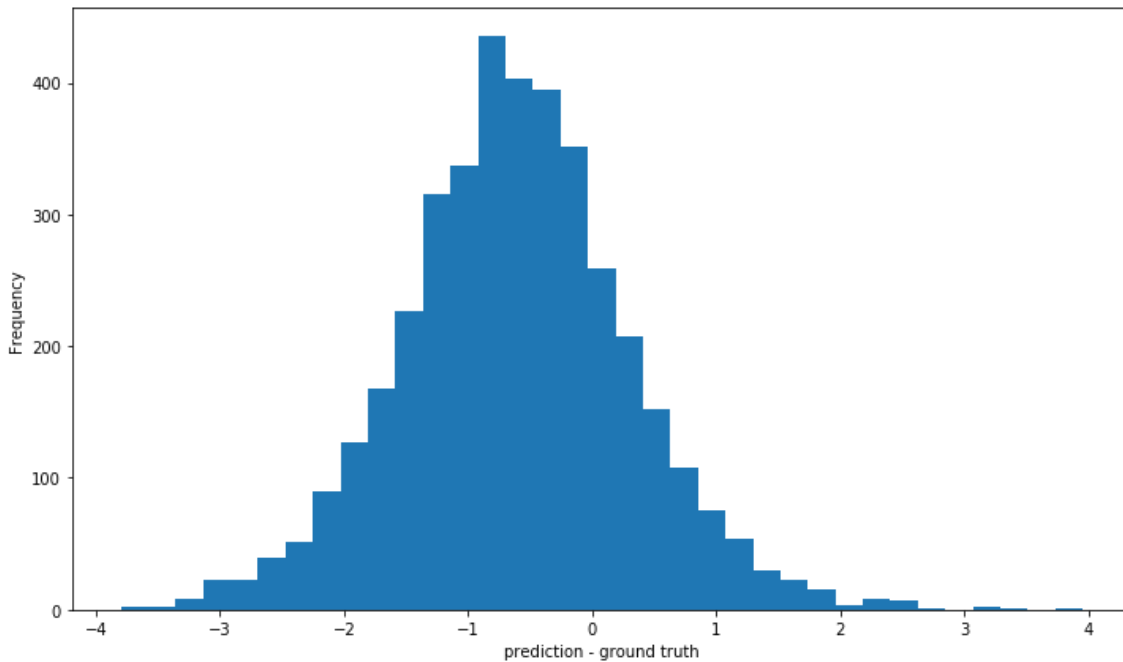
Fig 5.3(a) epoch Vs loss



(unit of MAE = miles)

fig 5.3(b) epoch Vs accuracy

This is the plot of epoch Vs epochs and epoch Vs accuracy. We can see that with continuous training, loss decreases and accuracy improves with subsequent training process.



(unit = miles)

Fig 5.3(c) histogram of errors

This is the histogram of the errors (prediction – observation) that we get after evaluating our model on validation dataset. We can see that most of the predictions are closer to ground truth i.e., errors are mostly concentrated around -1 miles. Most of the errors are within about 2 miles.

Correlation matrix,

```
[[1.    0.64763702]
 [0.64763702  1. ]]
```

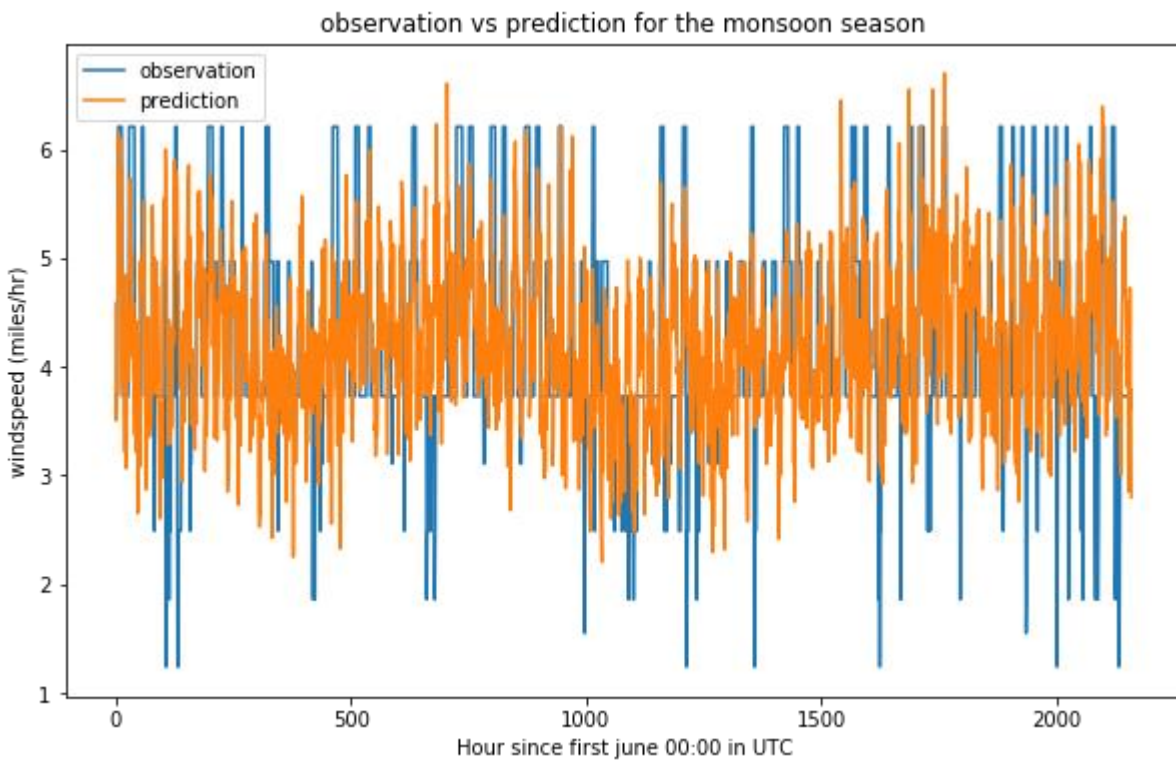
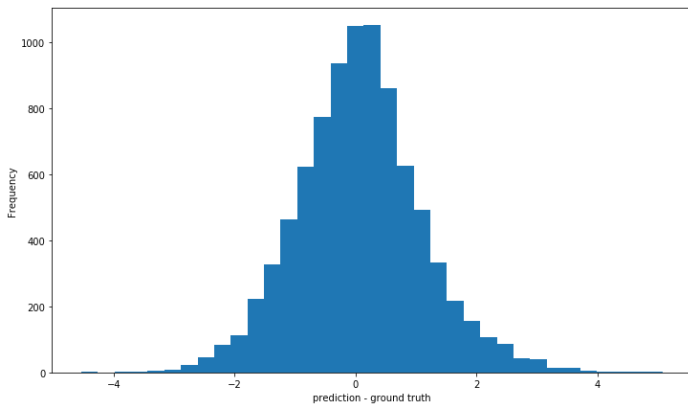
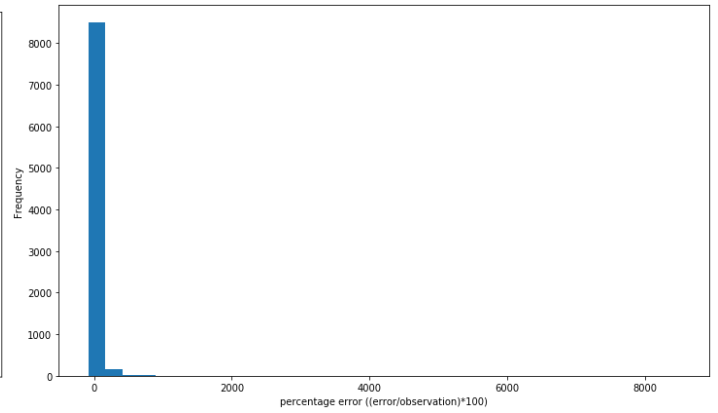


Fig 5.3(d) observation and prediction plot for monsoon season

In this, observation and prediction are put in the same plot. The data taken was for 3 months from 1st June 2021 to 31st August 2021. We first find the prediction made by our model on this 3 month input data. This is a time-series data. There is moderate correlation between observation and prediction.



(unit = miles)

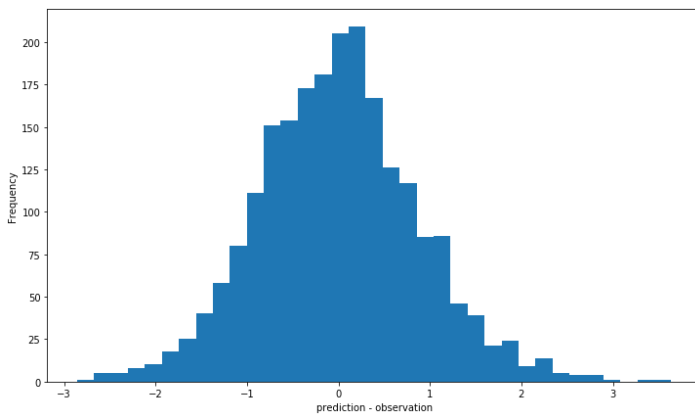


(unitless)

Fig 5.3(e) histogram of errors on 1 year independent dataset

fig 5.3(f) percentage error for the same

We have the histogram of errors (prediction – ground truth) and percentage error  $((\text{error}/\text{observation}) \times 100)$  our model gives when tested on 1 year (1 March 2021 to 28 February 2022) of independent dataset. Again, most of the errors are concentrated around 0 miles and within about 2 miles.



(unit = miles)

Fig 5.3(g) error histogram for summer

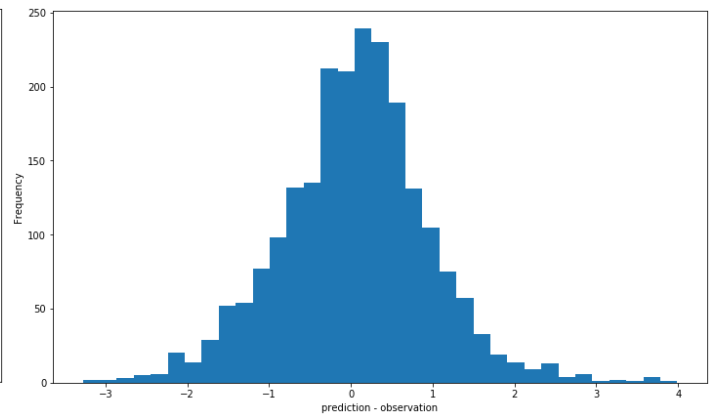
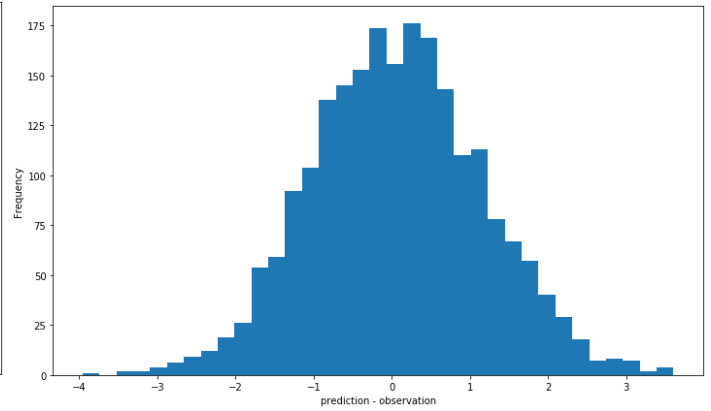
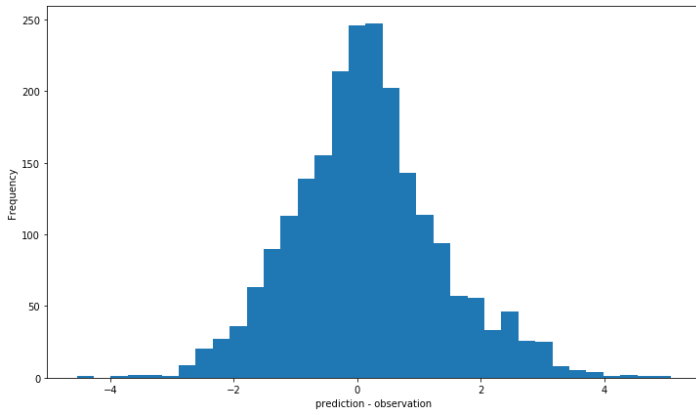


fig 5.3(h) error histogram for monsoon



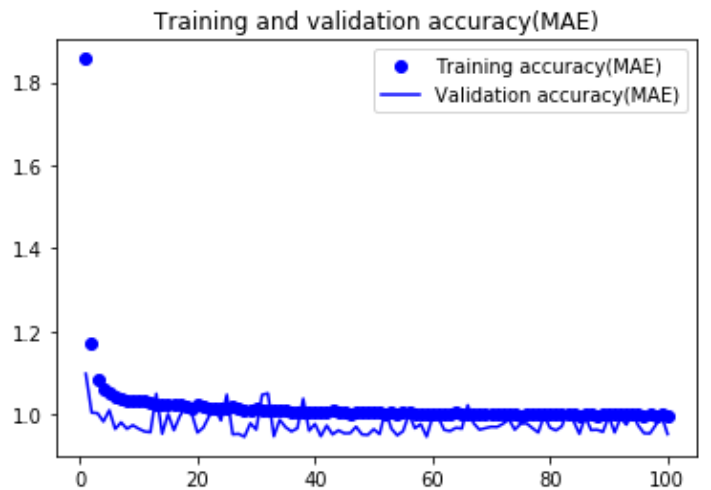
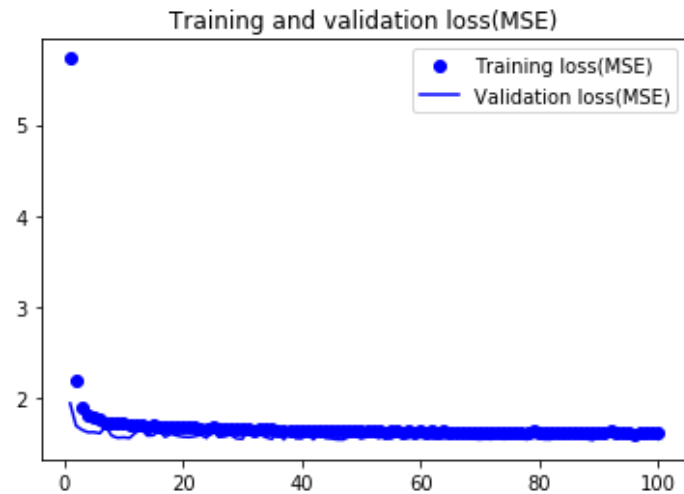
(unit = miles)

Fig 5.3(i) error histogram for autumn

fig 5.3(j) error histogram for winter

Above 4 plots are error plots when the model is tested on 4 different seasons each of 3 month time length. 1 year of independent dataset has been broken into 4 seasons. 1st, 2nd, 3rd and 4th plots are for summer, monsoon, autumn and winter datasets respectively. Most of the errors are about 2 miles.

**With vgg16,**



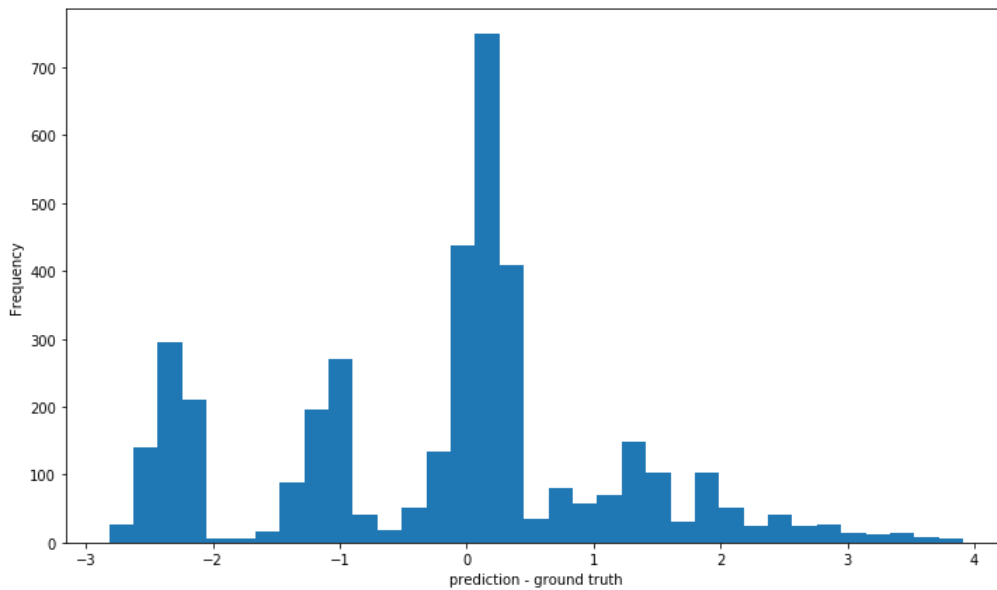
(x-axis=epochs, y-axis =MSE(unit=miles squared)),

(x-axis=epochs, y-axis=MAE(unit=miles))

Fig 5.3(k) epoch Vs loss

fig 5.3(l) epoch Vs accuracy

We can see that with continuous training, loss decreases and accuracy improves with subsequent training process.



(unit = miles)

Fig 5.3(m) histogram of errors

This is the histogram of the errors (prediction – observation) that we get after evaluating our model on validation dataset. We can see that most of the predictions are closer to ground truth i.e., errors are mostly concentrated around 0. Most of the errors are within about 3 miles.

Correlation matrix,

```
[[1.    0.15910329]
 [0.15910329  1.  ]]
```

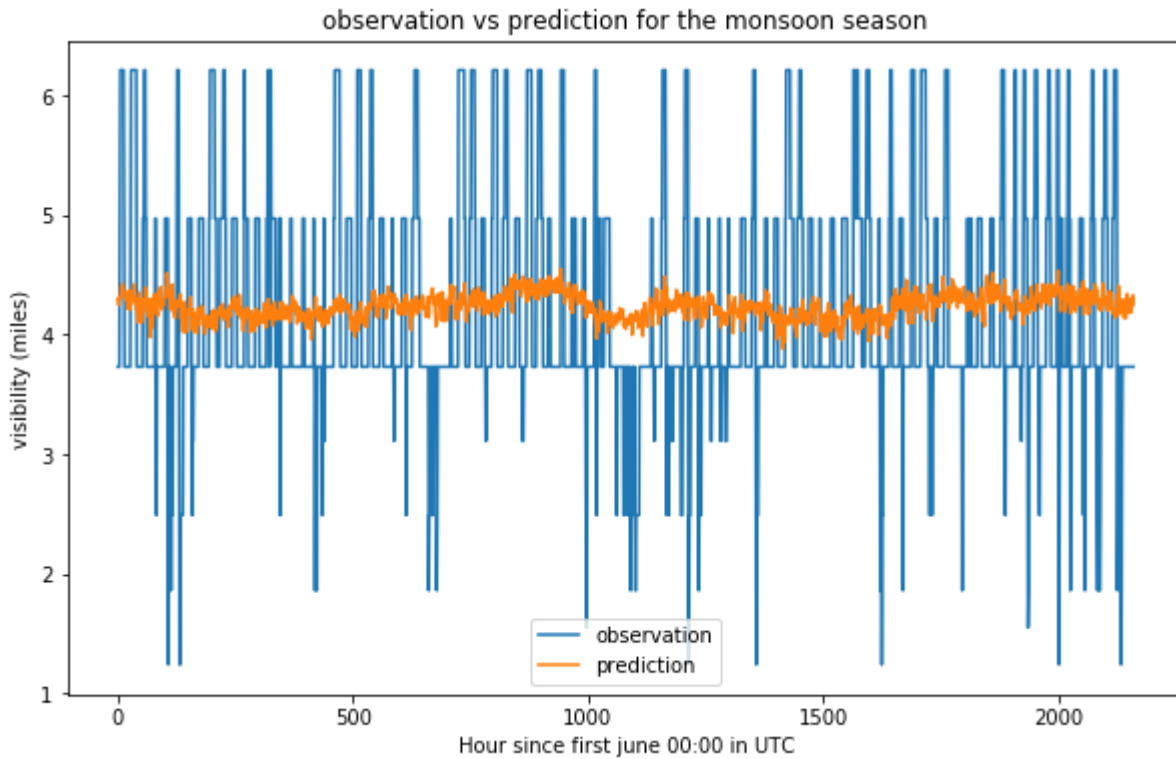


Fig 5.3(n) observation and prediction plot for monsoon season

In this, observation and prediction are put in the same plot. The data taken was for 3 months from 1st June 2021 to 31st August 2021. We first find the prediction made by our model on this 3 month independent input dataset. This is a time-series data. The plot clearly shows there is a weak correlation between the predictions made by VGG16 model and observations made for the 3 month monsoon season.

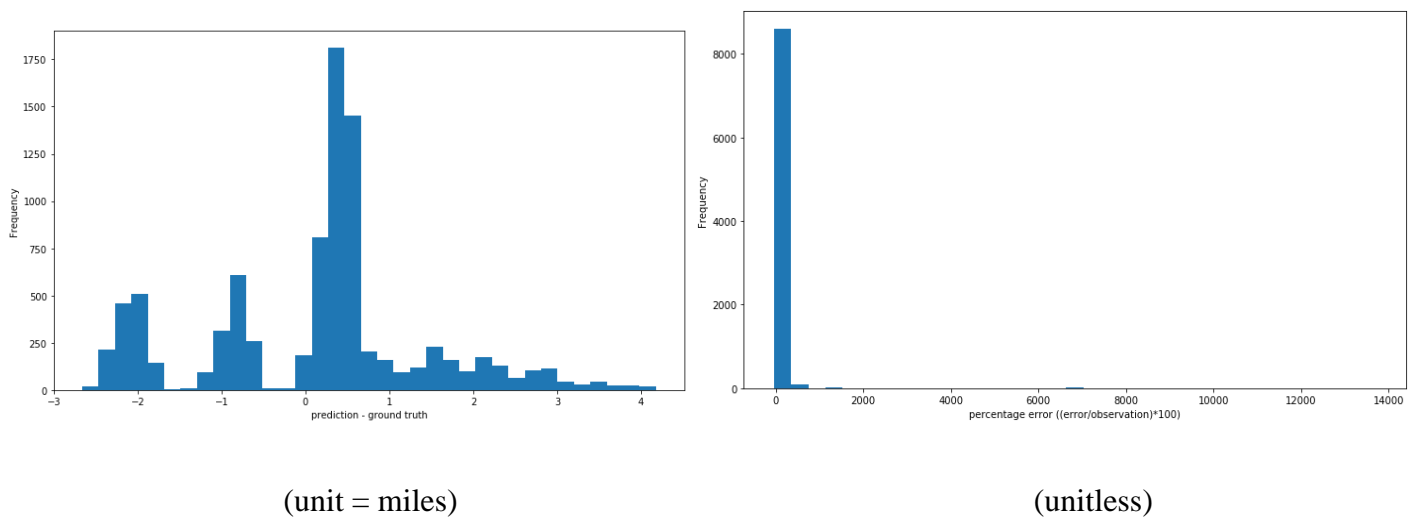
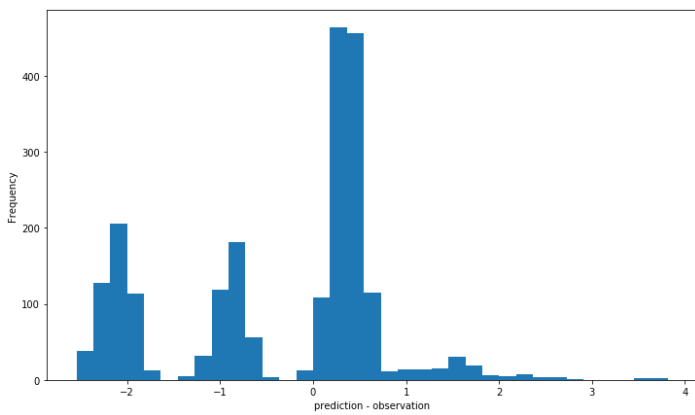


Fig 5.3(o) histogram of errors on 1 year independent dataset

fig 5.3(p) percentage error for the same

We have the histogram of errors (prediction – ground truth) and percentage error  $((\text{error}/\text{observation}) * 100)$  our model gives when tested on 1 year (1 March 2021 to 28 February 2022) of independent dataset. Again, most of the errors are concentrated around 0 miles and within about 3 miles.



(unit = miles)

Fig 5.3(q) error histogram for summer

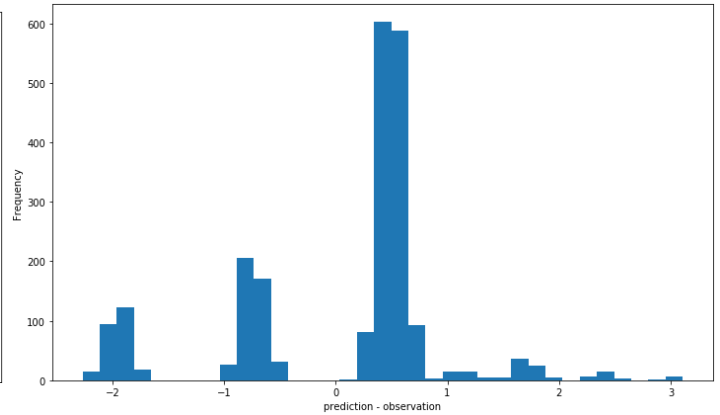
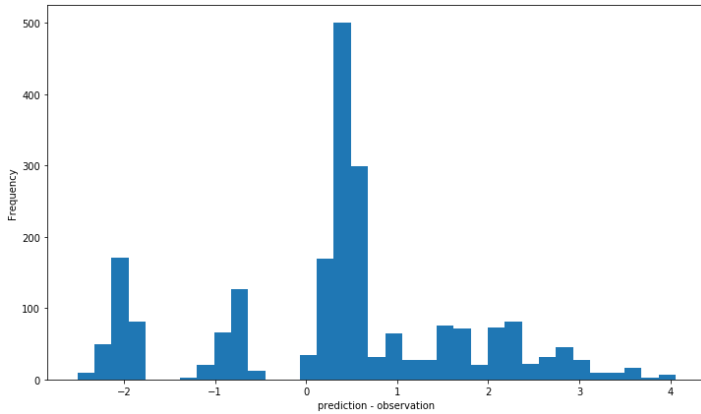


fig 5.3(r) error histogram for monsoon



(unit = miles)

Fig 5.3(s) error histogram for autumn

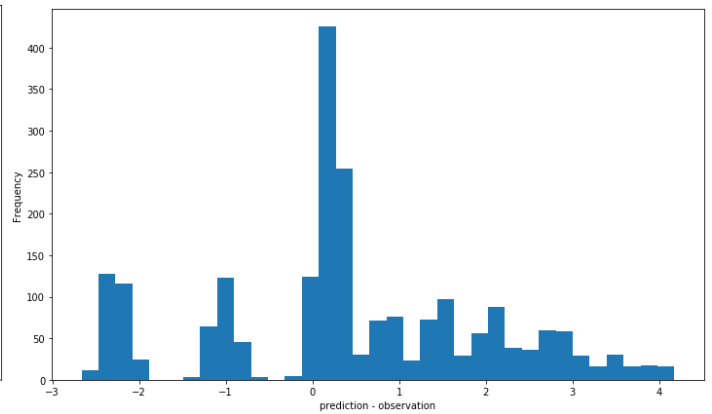
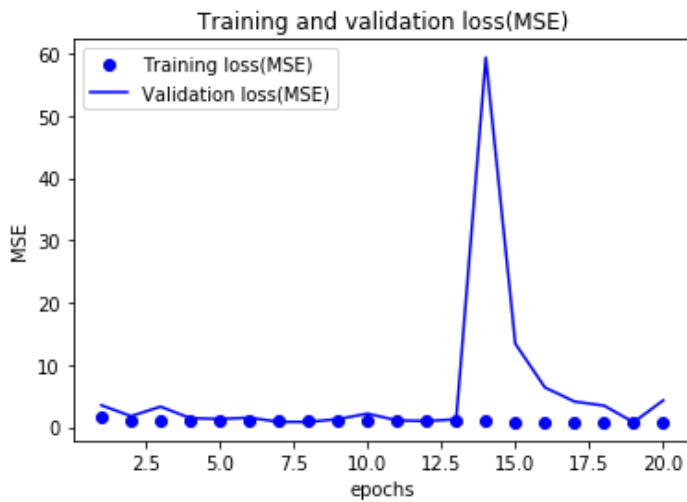


fig 5.3(t) error histogram for winter

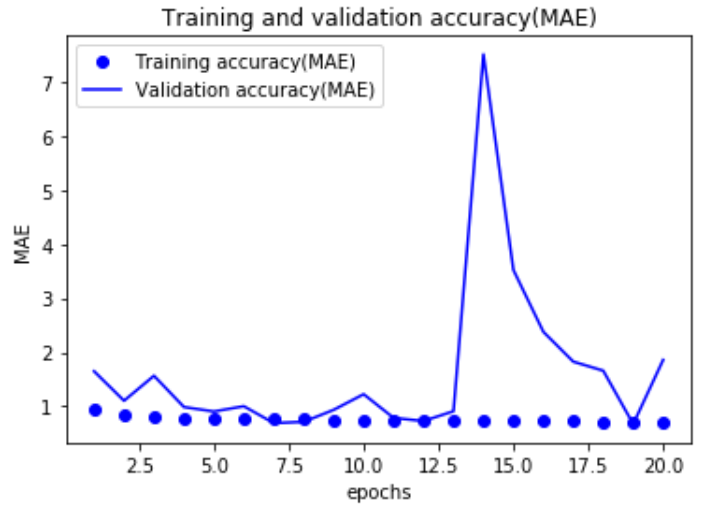
Above 4 plots are error plots when the model is tested on 4 different seasons each of 3 month time length. 1 year of independent dataset has been broken into 4 seasons. 1st, 2nd, 3rd and 4th plots are for summer, monsoon, autumn and winter datasets respectively. Most of the errors are about 3 miles.

## With 3D CNN,



(unit of MSE = miles squared)

Fig 5.3(u) epoch Vs loss



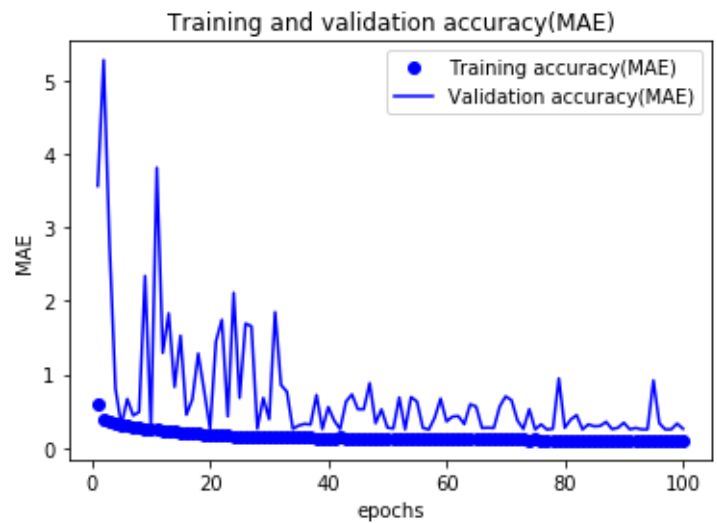
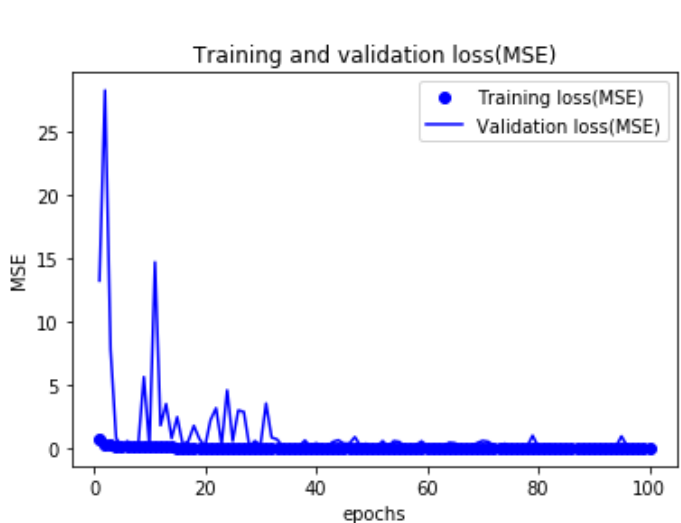
(unit of MAE = miles)

fig 5.3(v) epoch Vs accuracy

With 3D CNN, we are making predictions for 6 hours in future. With continuous training, validation loss decreases and validation accuracy improves.

## For station VECC,

## With 2D CNN,



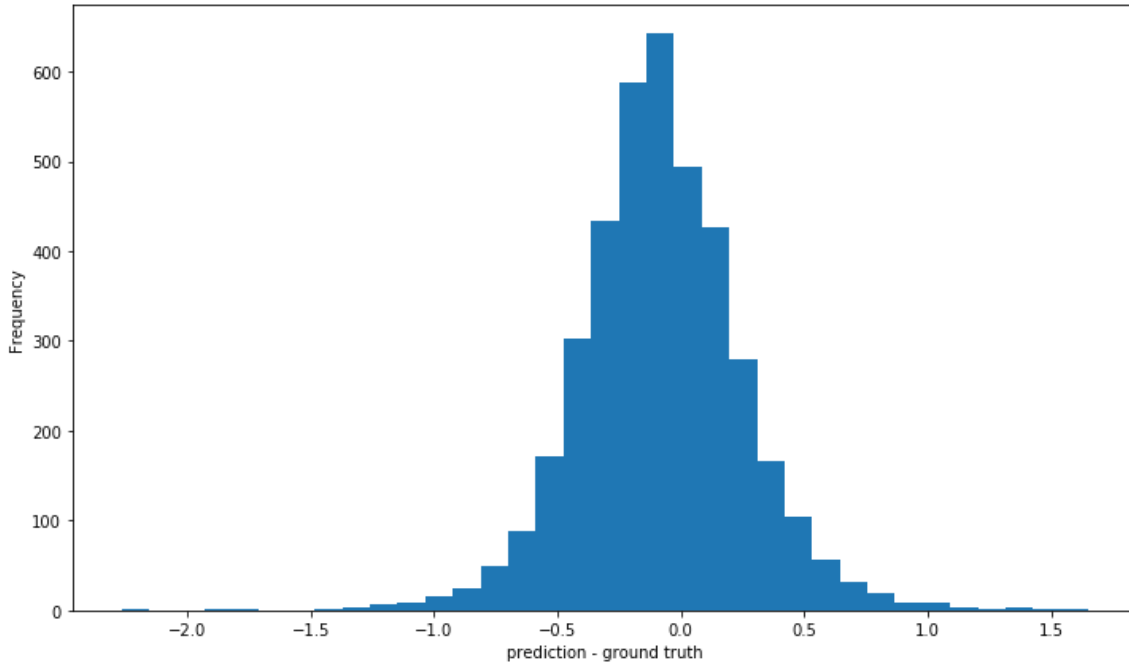
(unit of MSE = miles squared)

(unit of MAE = miles)

Fig 5.4(a) epoch Vs loss

fig 5.4(b) epoch Vs accuracy

We can see that with continuous training, loss decreases and accuracy improves with subsequent training process.



(unit = miles)

Fig 5.4(c) histogram of errors

This is the histogram of the errors (prediction – observation) that we get after evaluating our model on validation dataset. We can see that most of the predictions are closer to ground truth i.e., errors are mostly concentrated around 0. Most of the errors are within about 1 miles.

Correlation matrix,

```
[[1.    0.51972465]  
 [0.51972465  1.]]
```

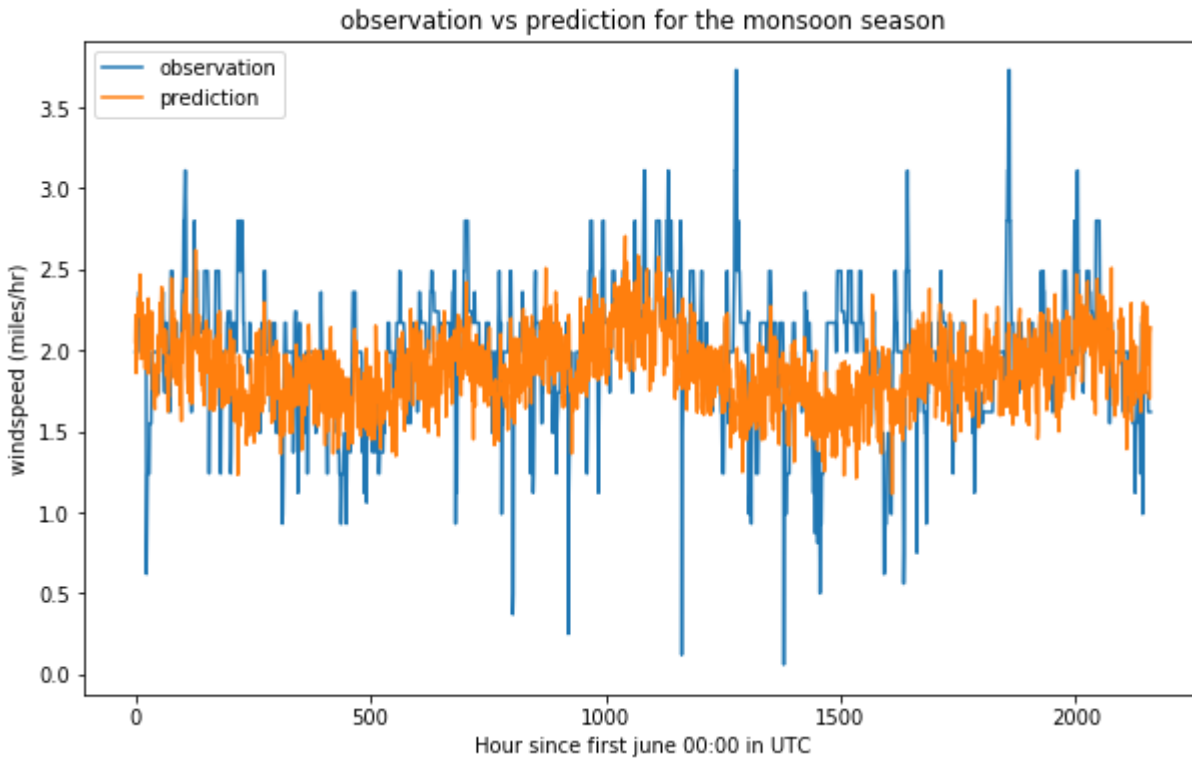
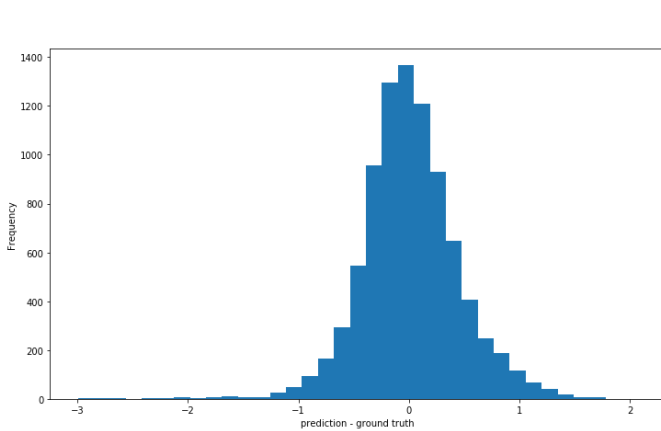
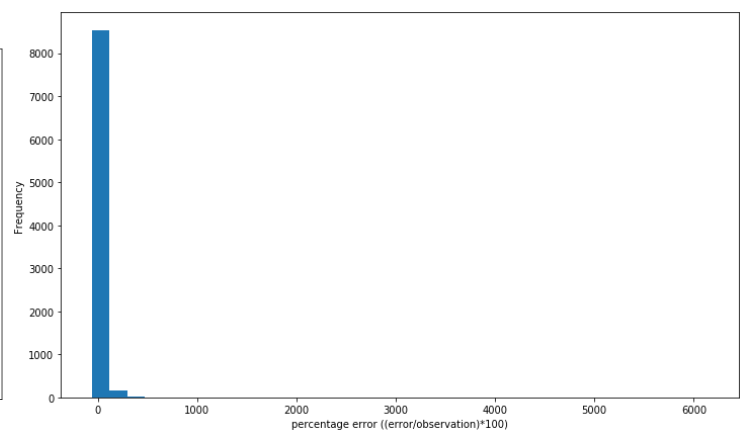


Fig 5.4(d) observation and prediction plot for monsoon season

In this, observation and prediction are put in the same plot. The data taken was for 3 months from 1st June 2021 to 31st August 2021. We first find the prediction made by our model on this 3 month input data. This is a time-series data. There is moderate correlation between observation and prediction.



(unit = miles)

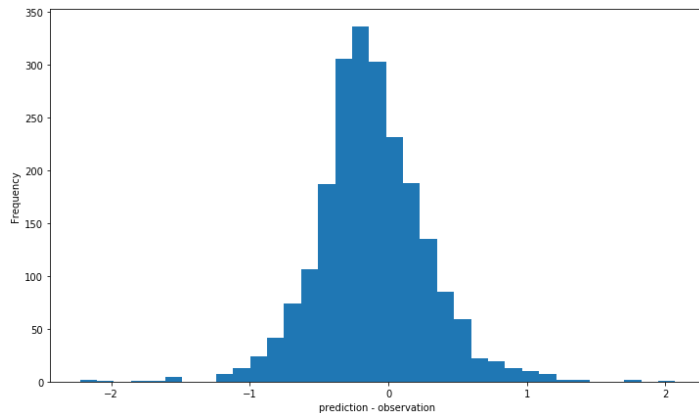
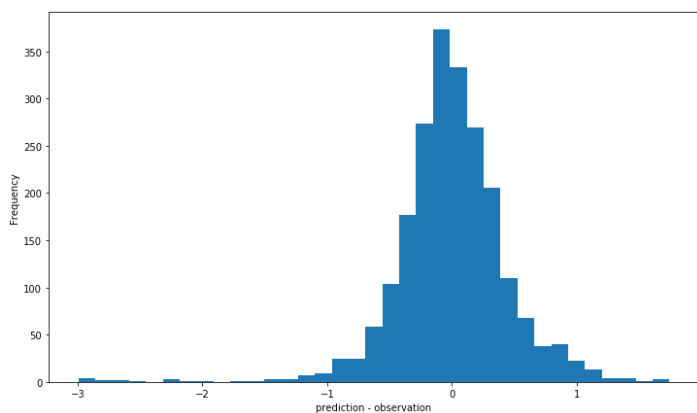


(unitless)

Fig 5.4(e) histogram of errors on 1 year independent dataset

5.4(f) percentage error for the same

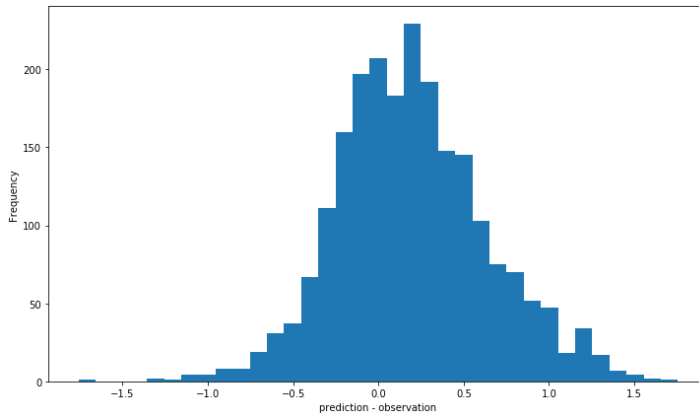
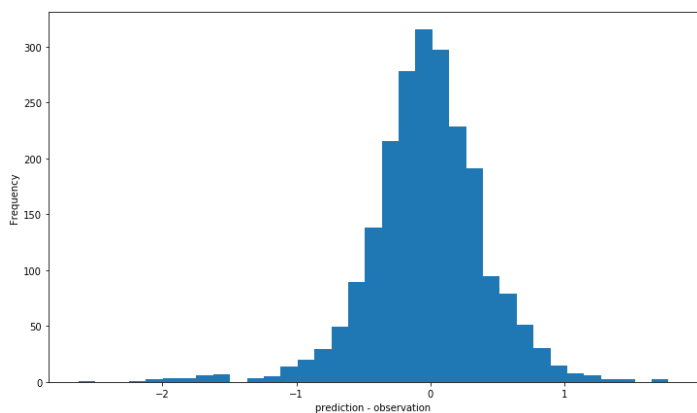
We have the histogram of errors (prediction – ground truth) and percentage error  $((\text{error}/\text{observation}) * 100)$  our model gives when tested on 1 year (1 March 2021 to 28 February 2022) of independent dataset. Again, most of the errors are concentrated around 0 miles and within about 1 miles. In both the plots we can see majority of predictions are closer to observation (or ground truth).



(x-axis unit = miles)

Fig 5.4(g) error histogram for summer

fig 5.4(h) error histogram for monsoon



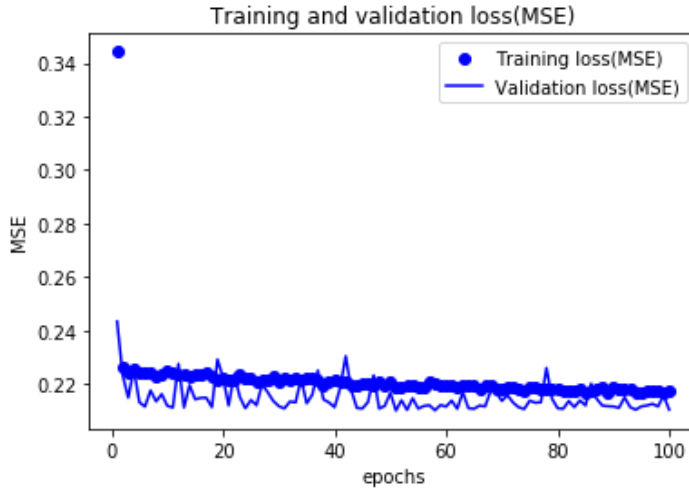
(unit = miles)

Fig 5.4(i) error histogram for autumn

fig 5.4(j) error histogram for winter

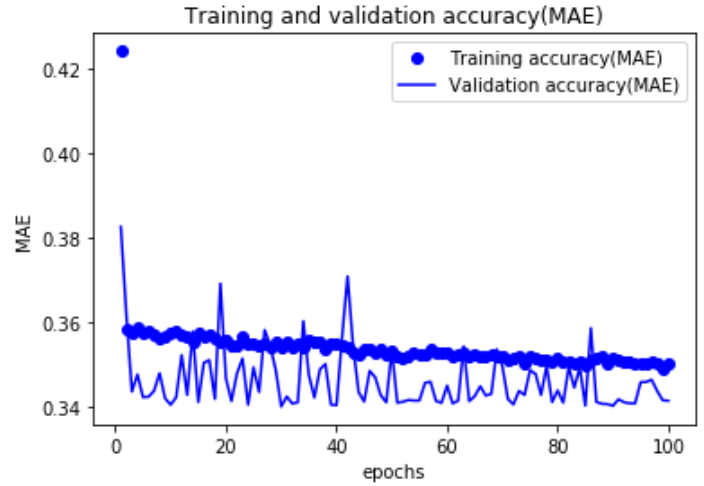
Above 4 plots are error plots when the model is tested on 4 different seasons each of 3 month time length. 1 year of independent dataset has been broken into 4 seasons. 1st, 2nd, 3rd and 4th plots are for summer, monsoon, autumn and winter datasets respectively. Most of the errors are spread over 1 miles from the center.

With vgg16,



(unit of MSE = miles squared)

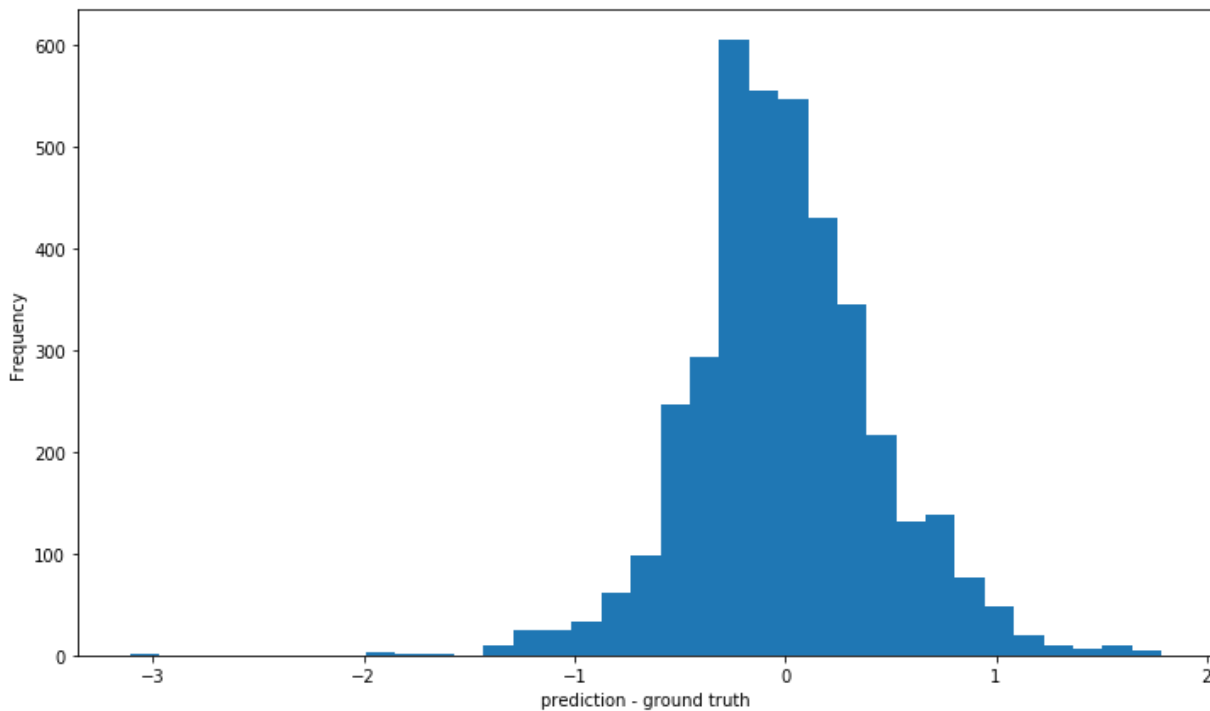
Fig 5.4(k) epoch Vs loss



(unit of MAE = miles)

fig 5.4(l) epoch Vs accuracy

We can see that with continuous training, loss decreases and accuracy improves with subsequent training process. Though the improvement is only minor.



(unit = miles)

Fig 5.4(m) histogram of errors

This is the histogram of the errors (prediction – observation) that we get after evaluating our model on validation dataset. We can see that most of the predictions are closer to ground truth i.e., errors are mostly concentrated around 0 miles. Most of the errors are within about 1 miles.

Correlation matrix,

```
[[1.    0.35146881]  
 [0.35146881  1.]]
```

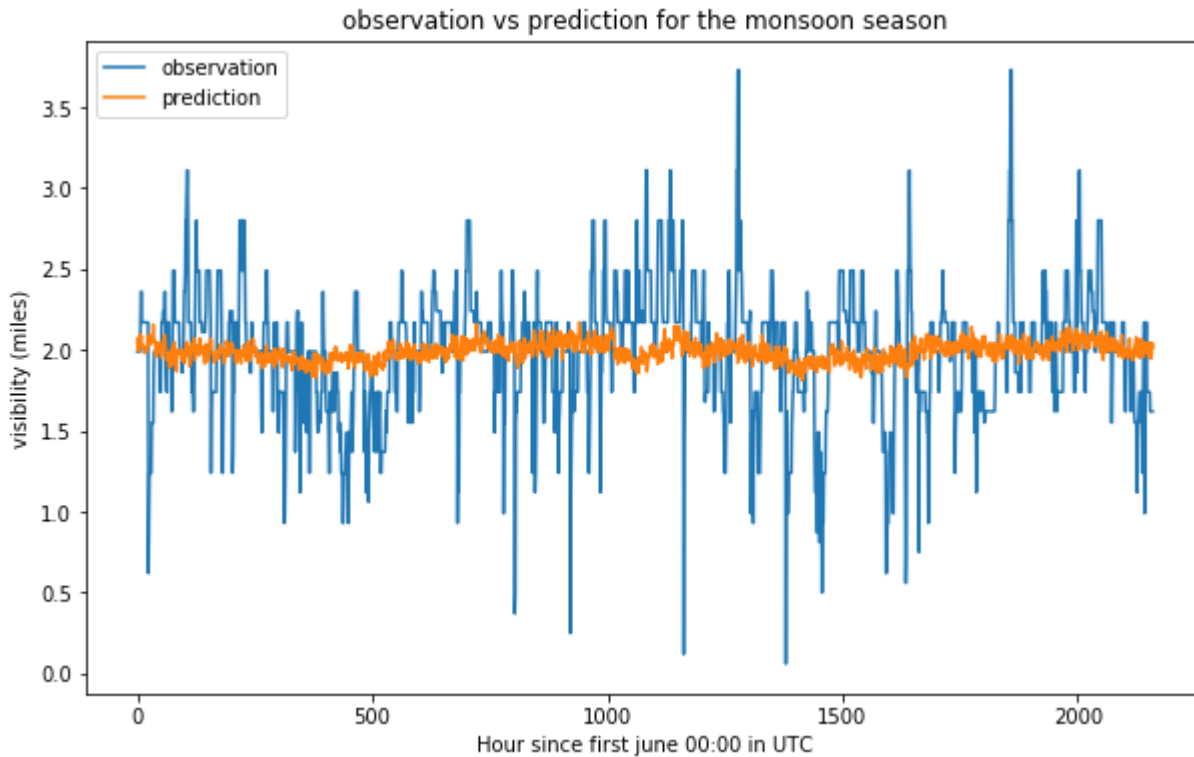
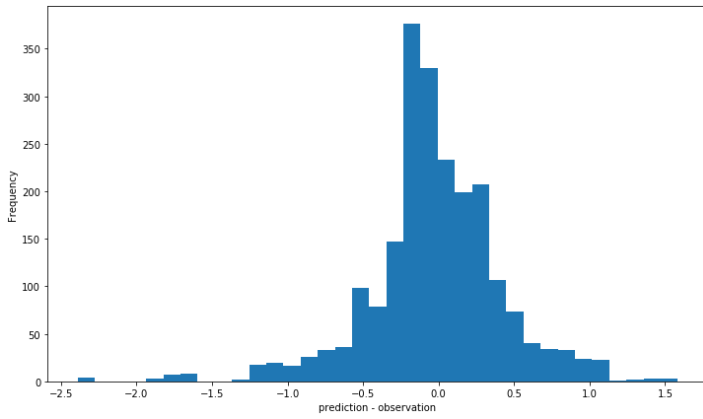


Fig 5.4(n) observation and prediction plot for monsoon season

In this, observation and prediction are put in the same plot. The data taken was for 3 months from 1st June 2021 to 31st August 2021. We first find the prediction made by our model on this 3 month independent input dataset. This is a time-series data. The plot clearly shows there is a weak correlation between the predictions made by VGG16 model and observations made for the 3 month monsoon season.





(unit = miles)

Fig 5.4(s) error histogram for autumn

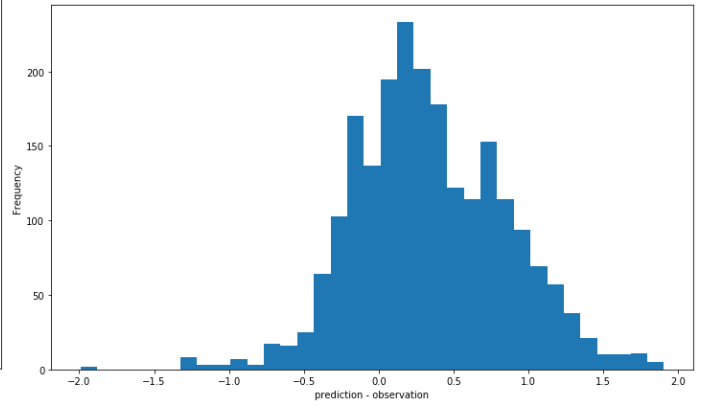
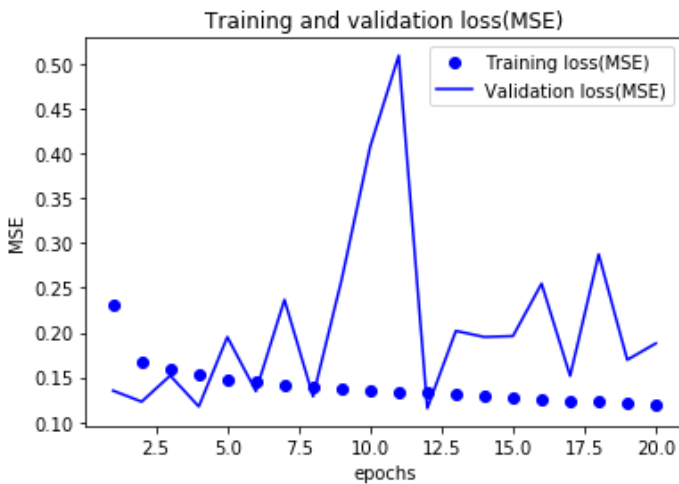


fig 5.4(t) error histogram for winter

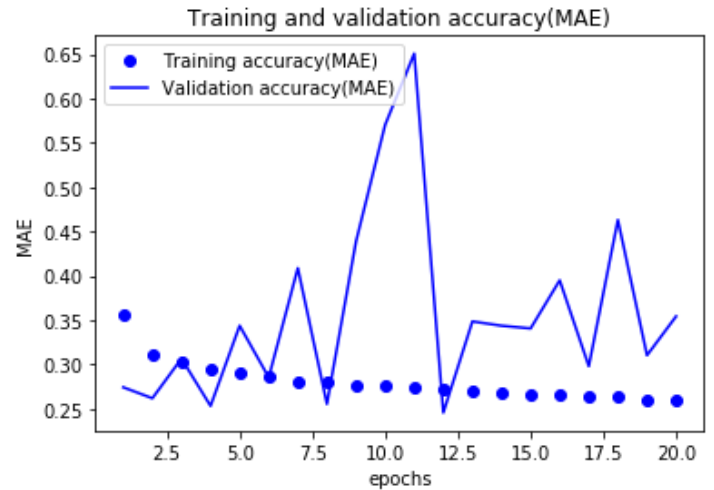
Above 4 plots are error plots when the model is tested on 4 different seasons each of 3 month time length. 1 year of independent dataset has been broken into 4 seasons. 1st, 2nd, 3rd and 4th plots are for summer, monsoon, autumn and winter datasets respectively. Most of the errors are spread over 2 miles from the center.

### With 3D CNN,



(unit of MSE = miles squared)

Fig 5.4(u) epoch Vs loss



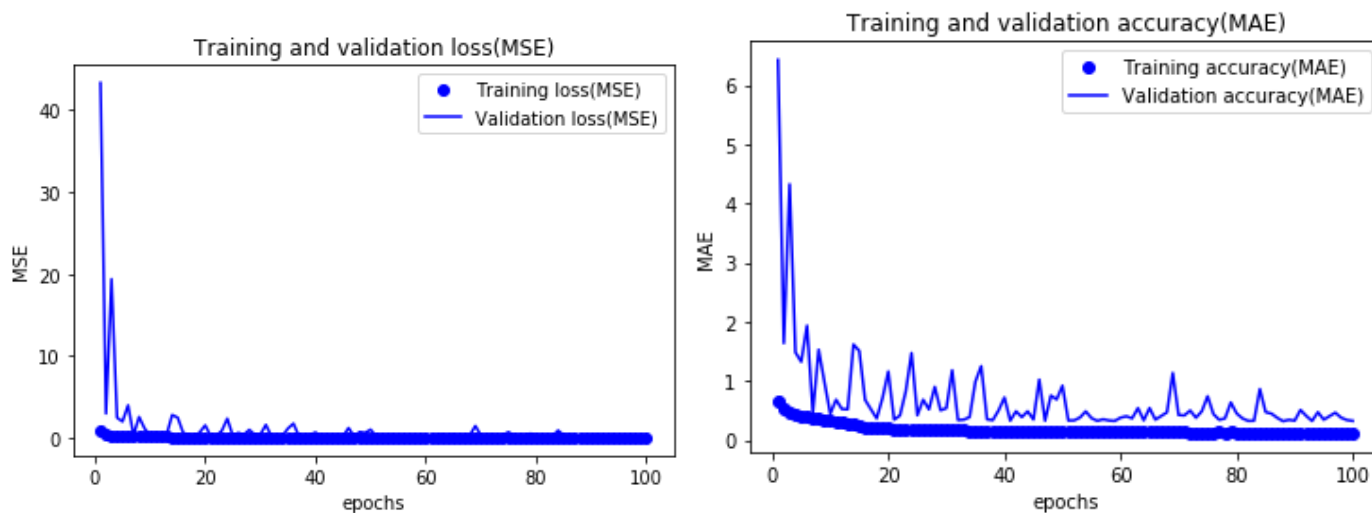
(unit of MAE = miles)

fig 5.4(v) epoch Vs accuracy

With 3D CNN, we are making predictions for 6 hours in future. With continuous training, we do not see validation loss decreasing and validation accuracy improving, they degrade. But training loss and accuracy improves. This shows there is over-fitting early on in the training process.

### For station VIDP,

With 2D CNN,



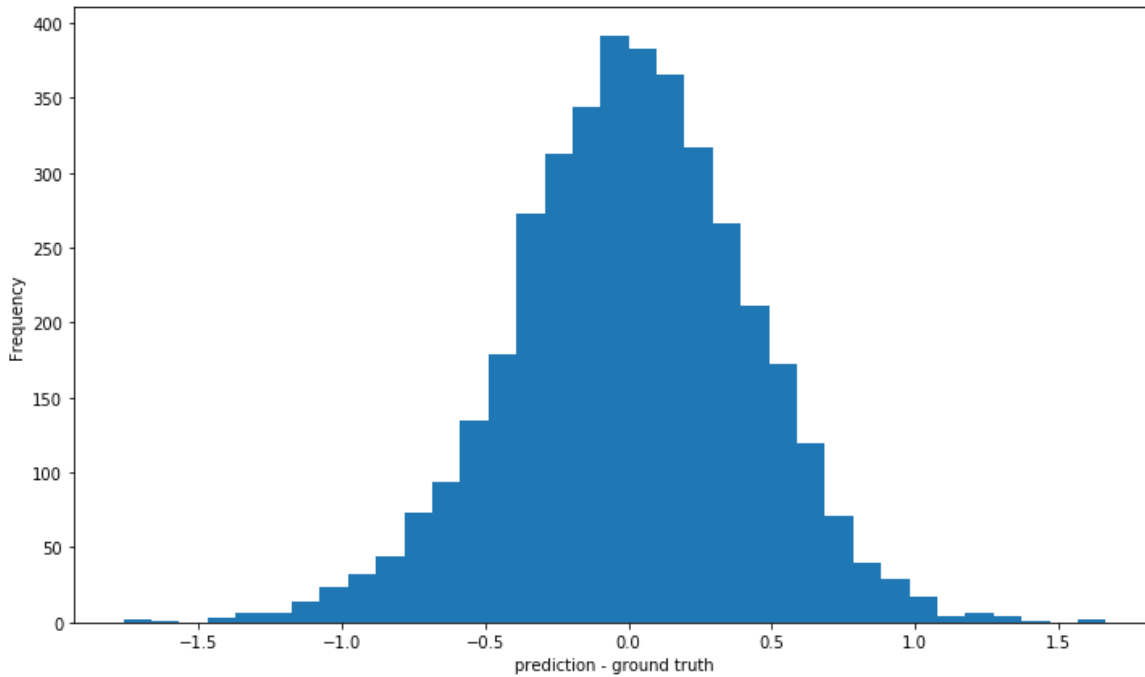
(unit of MSE = miles squared)

(unit of MAE = miles)

Fig 5.5(a) epoch Vs loss

fig 5.5(b) epoch Vs accuracy

We can see that with continuous training, loss decreases and accuracy improves with subsequent training process.



(unit = miles)

Fig 5.5(c) histogram of errors

This is the histogram of the errors (prediction – observation) that we get after evaluating our model on validation dataset. We can see that most of the predictions are closer to ground truth i.e., errors are mostly concentrated around 0 miles. Most of the errors are within about 1 miles.

Correlation matrix,

```
[[1.    0.62770413]
```

```
[0.62770413  1.]]
```

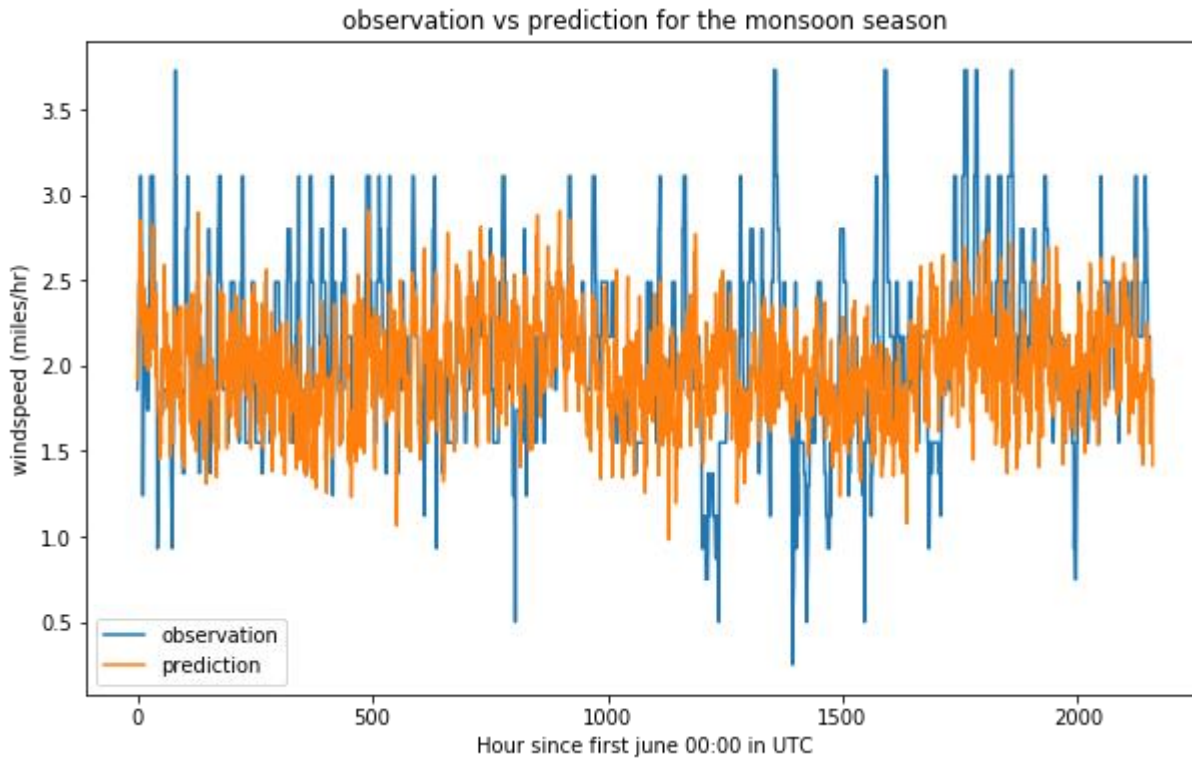
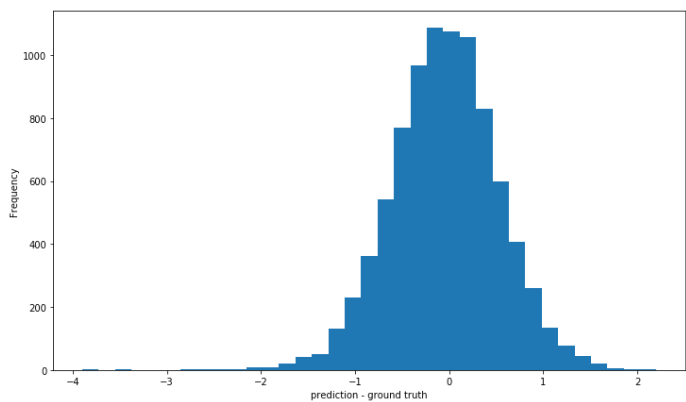
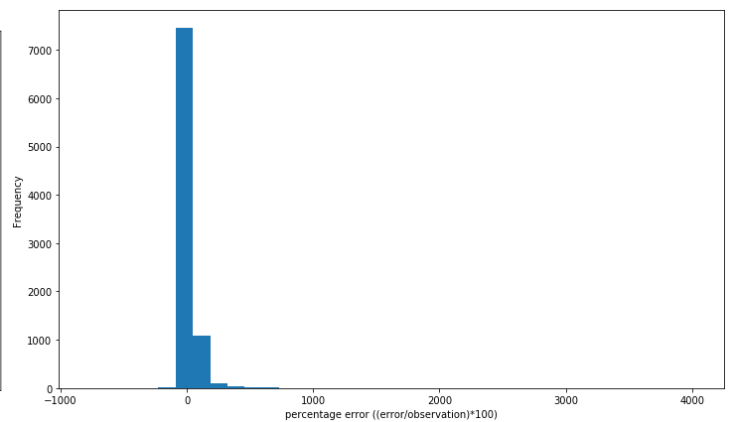


Fig 5.5(d) observation and prediction plot for monsoon season

In this, observation and prediction are put in the same plot. The data taken was for 3 months from 1st June 2021 to 31st August 2021. We first find the prediction made by our model on this 3 month input data. This is a time-series data. There is moderate correlation between observation and prediction.



(unit = miles)

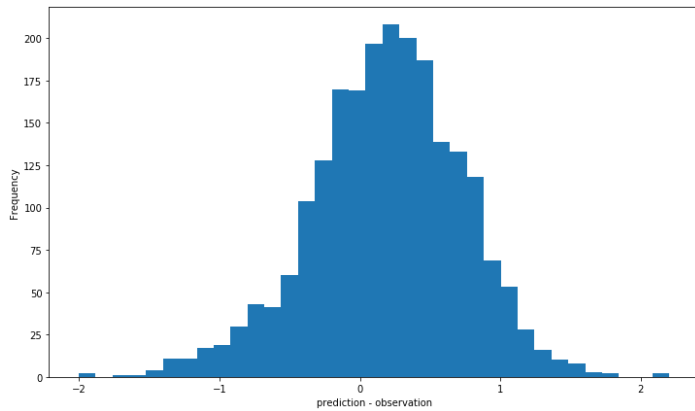


(unitless)

Fig 5.5(e) histogram of errors on 1 year independent dataset

fig 5.5(f) percentage accuracy for the same

We have the histogram of errors (prediction – ground truth) and percentage error  $((\text{error}/\text{observation}) * 100)$  our model gives when tested on 1 year (1 March 2021 to 28 February 2022) of independent dataset. Again, most of the errors are concentrated around 0 miles and within about 2 miles.



(x-axis unit = miles)

Fig 5.5(g) error histogram for summer

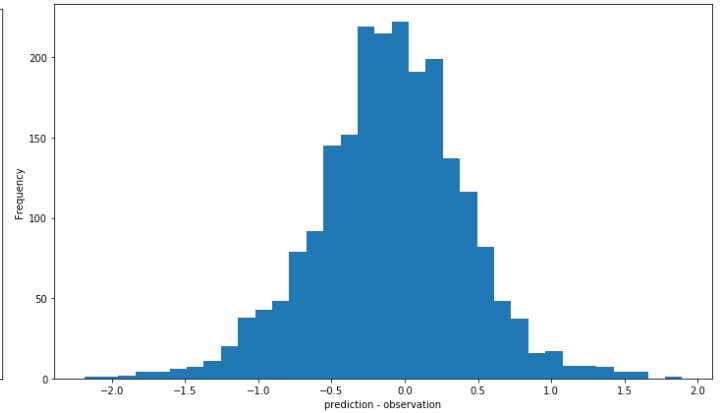
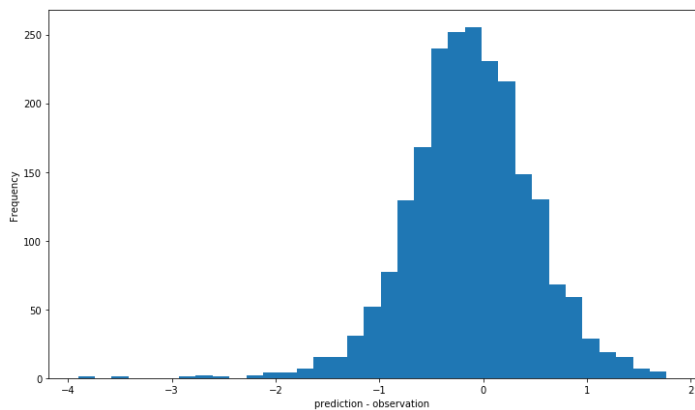


fig 5.5(h) error histogram for monsoon



(unit = miles)

Fig 5.5(i) error histogram for autumn

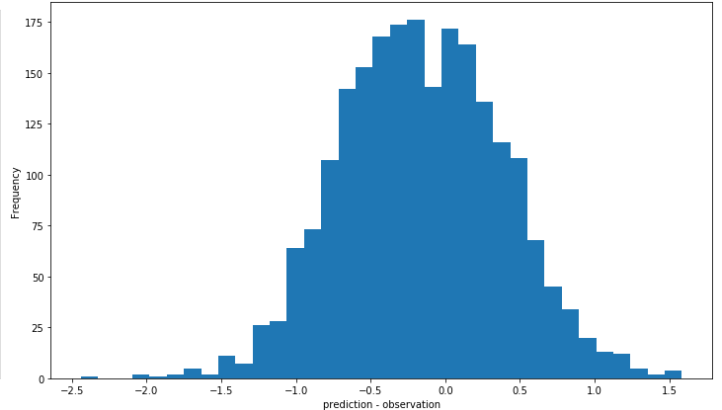
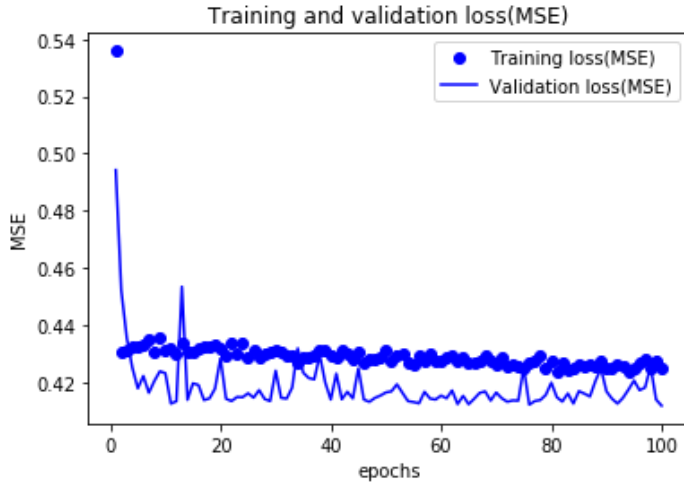


fig 5.5(j) error histogram for winter

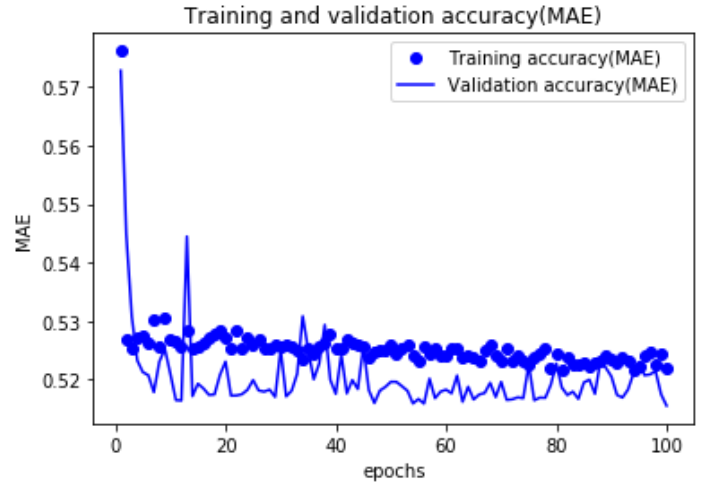
Above 4 plots are error plots when the model is tested on 4 different seasons each of 3 month time length. 1 year of independent dataset has been broken into 4 seasons. 1st, 2nd, 3rd and 4th plots are for summer, monsoon, autumn and winter datasets respectively. Most of the errors are spread over 2 miles from the center.

## With VGG16,



(unit of MSE = miles squared)

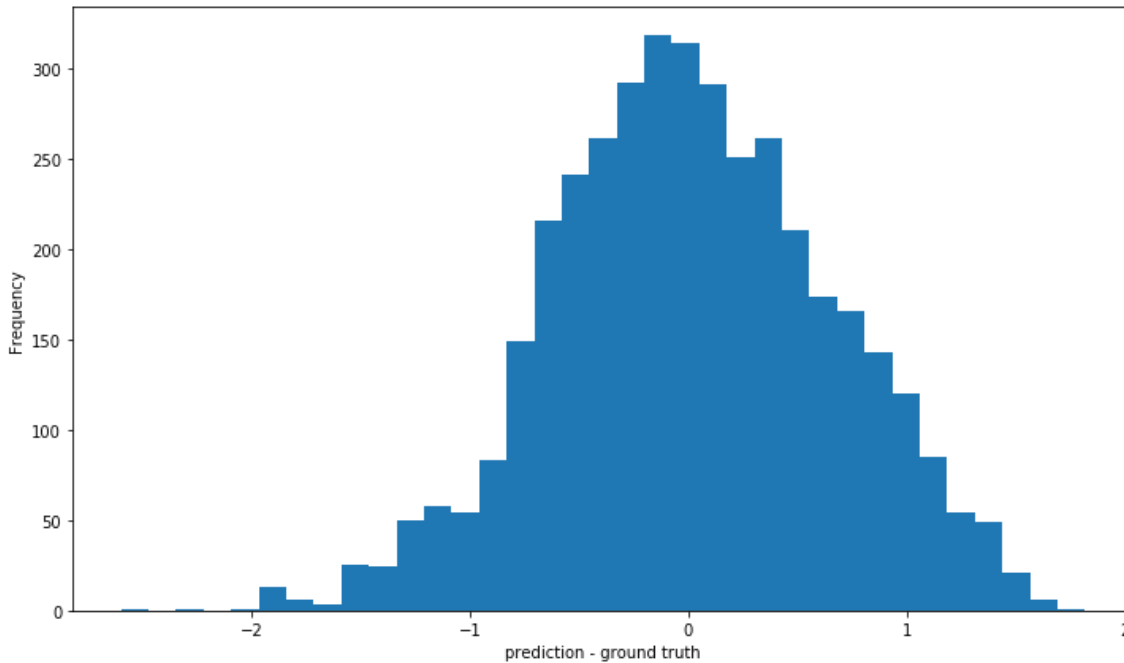
Fig 5.5(k) epoch Vs loss



(unit of MAE = miles)

fig 5.5(l) epoch Vs accuracy

We can see that with continuous training, loss decreases and accuracy improves with subsequent training process. Though the improvement is only minor.



(unit = miles)

Fig 5.5(m) histogram of errors

This is the histogram of the errors (prediction – observation) that we get after evaluating our model on validation dataset. We can see that most of the predictions are closer to ground truth i.e., errors are mostly concentrated around 0 miles. Most of the errors are within about 1.5 miles.

Correlation matrix,

```
[[1.    0.4720698]  
 [0.4720698  1. ]]
```

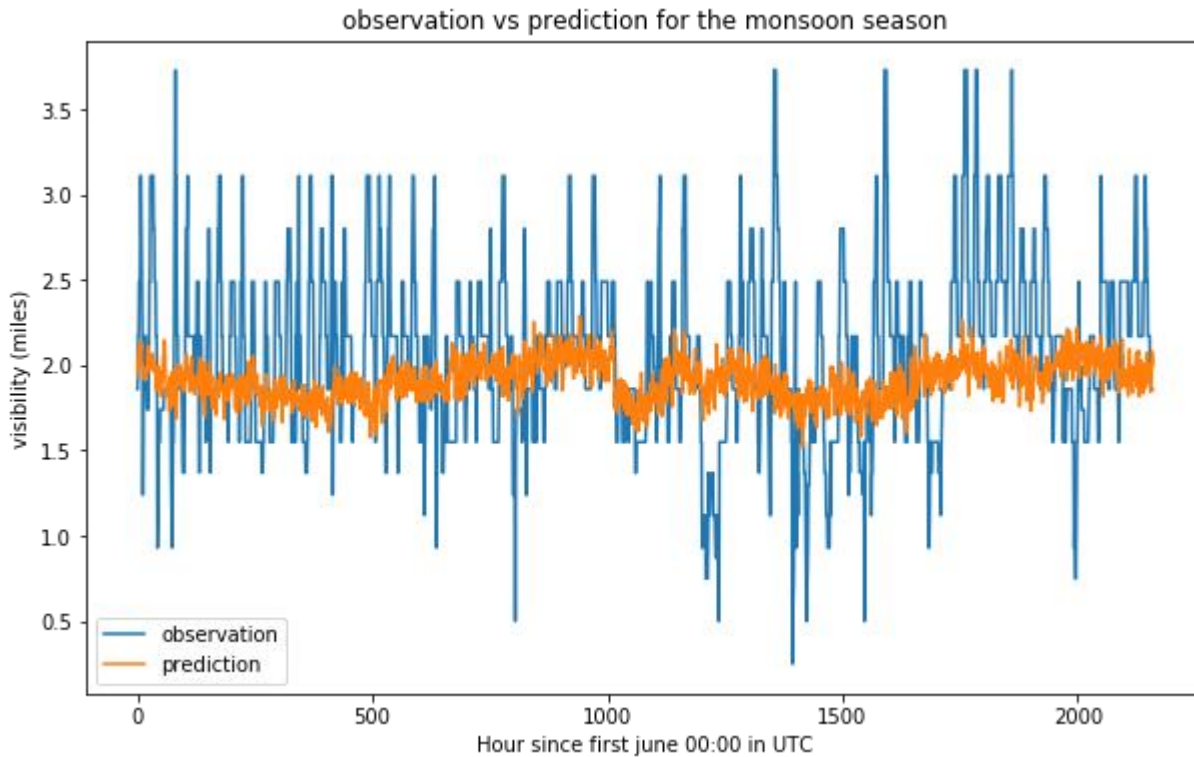
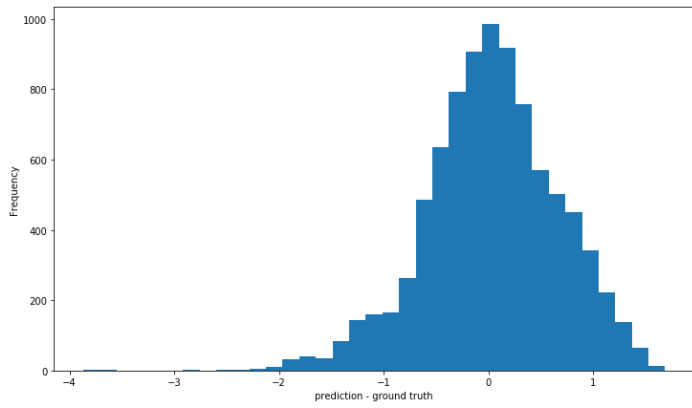
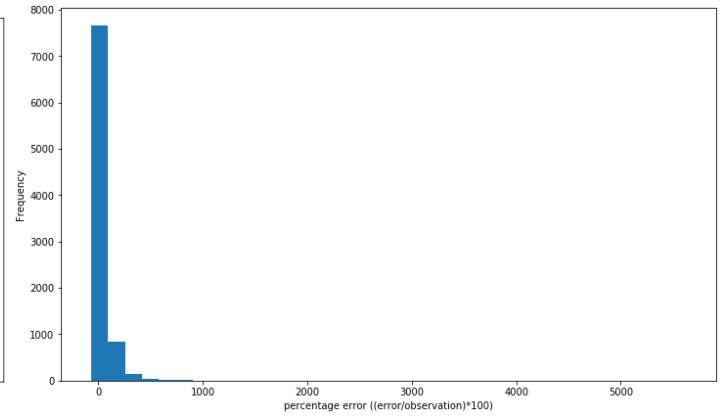


Fig 5.5(n) observation and prediction plot for monsoon season

In this, observation and prediction are put in the same plot. The data taken was for 3 months from 1st June 2021 to 31st August 2021. We first find the prediction made by our model on this 3 month independent input dataset. This is a time-series data. The plot clearly shows there is a weak correlation between the predictions made by VGG16 model and observations made for the 3 month monsoon season.



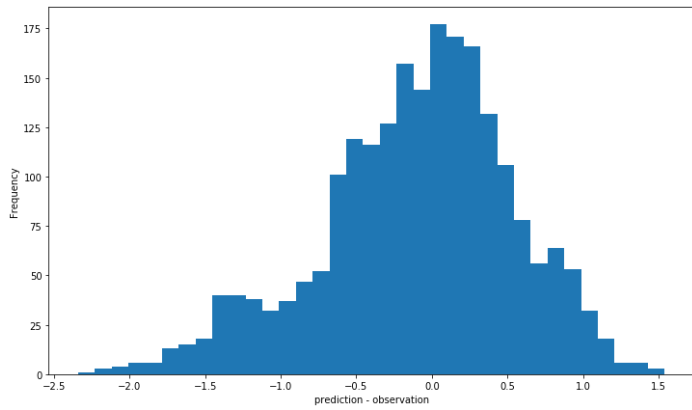
(unit= miles)



(unitless)

Fig 5.5(o) histogram of errors on 1 year independent dataset      fig 5.5(p) percentage error for the same

We have the histogram of errors (prediction – ground truth) and percentage error  $((\text{error}/\text{observation}) * 100)$  our model gives when tested on 1 year (1 March 2021 to 28 February 2022) of independent dataset. Again, most of the errors are concentrated around 0 miles and within about 2 miles.



(x-axis unit = miles)

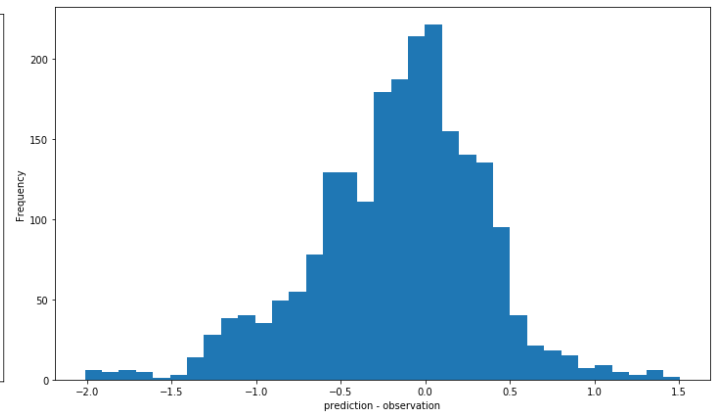
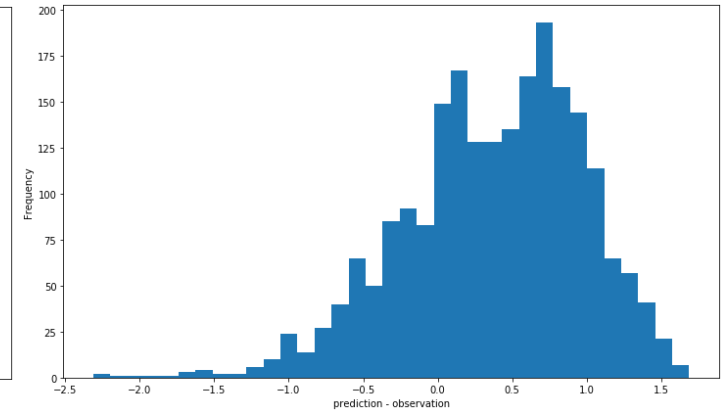
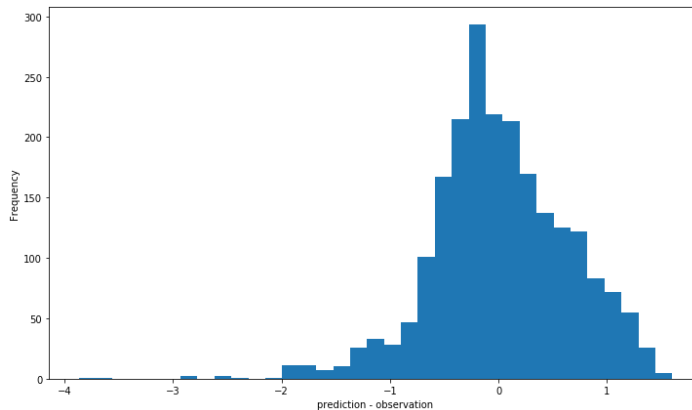


Fig 5.5(q) error histogram for summer

fig 5.5(r) error histogram for monsoon



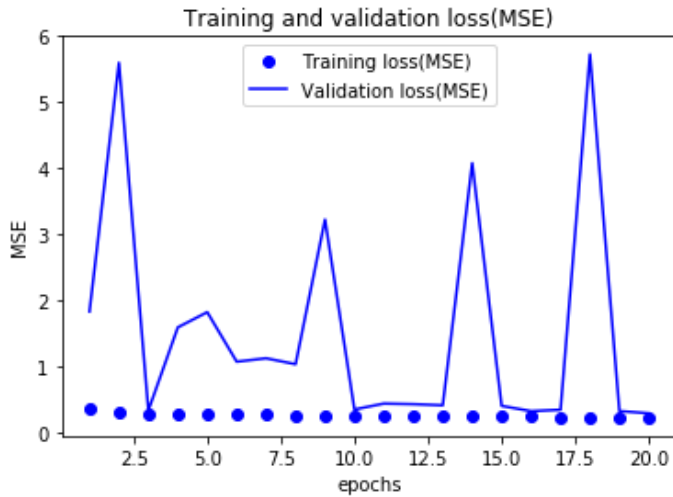
(unit= miles)

Fig 5.5(s) error histogram for autumn

fig 5.5(t) error histogram for winter

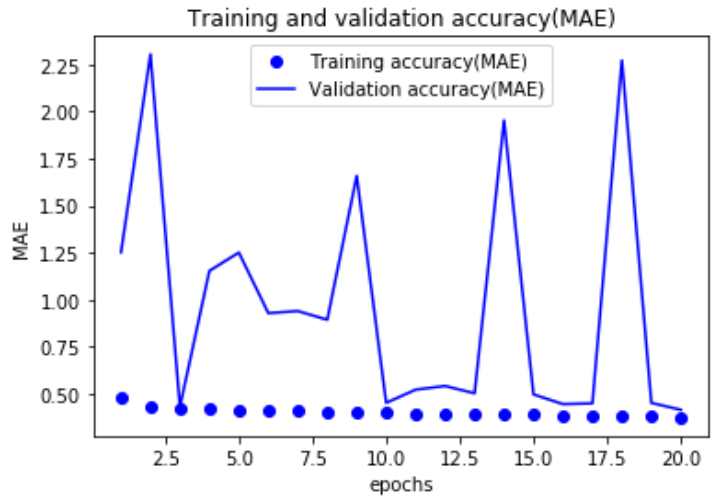
Above 4 plots are error plots when the model is tested on 4 different seasons each of 3 month time length. 1 year of independent dataset has been broken into 4 seasons. 1st, 2nd, 3rd and 4th plots are for summer, monsoon, autumn and winter datasets respectively. Most of the errors are spread over 1.5 miles from the center.

**With 3D CNN,**



(unit of MSE = miles squared)

Fig 5.5(u) epoch Vs loss



(unit of MAE = miles)

fig 5.5(v) epoch Vs accuracy

With 3D CNN, we are making predictions for 6 hours in future. With continuous training, we see validation loss and validation accuracy fluctuating (decreasing then increasing).

**Result (Mean Absolute Error) for Wind Speed:**

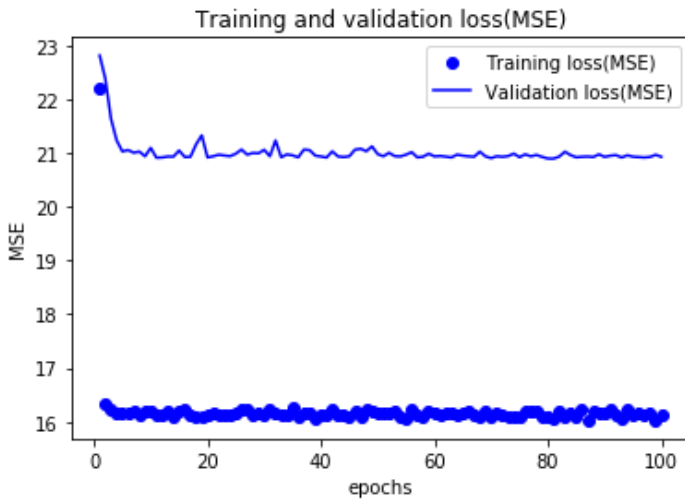
| Airports | Wind speed climatology (mph) | 2D CNN (mph) | VGG16 (mph) | 3D CNN (mph) |
|----------|------------------------------|--------------|-------------|--------------|
| VABB     | 2.32                         | 6.465        | 2.91        | 2.32         |
| VOTV     | 3.55                         | 1.95         | 2.55        | 1.78         |
| VOBL     | 5.25                         | 2.3          | 3.43        | 2.5          |
| VECC     | 4.19                         | 2.786        | 2.99        | 2.44         |
| VIDP     | 3.87                         | 4.67         | 2.79        | 2.25         |

Table 15: Wind speed forecasting accuracy for several stations comparing 2D CNN, 3D CNN and pretrained model VGG16 with the reference accuracy of climatology. The metric used is mean absolute error (MAE).

We can observe that the 2D and 3D convolutional models achieve a relative improvement over climatology.

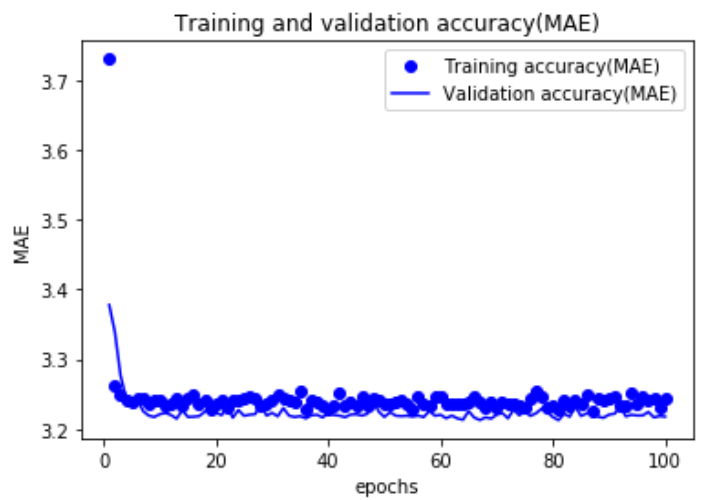
**For station VABB,**

**With vgg16,**



(unit of MSE = miles squared/hr squared)

Fig 5.6(a) epoch Vs loss



(unit of MAE = miles/hr)

fig 5.6(b) epoch Vs accuracy

This is the plot of loss Vs epochs. We can see that with continuous training, first validation loss decreases and then after it plateau before training loss. On the right side plot, validation accuracy improves with subsequent training process but it too plateaus after a while though not before training accuracy.

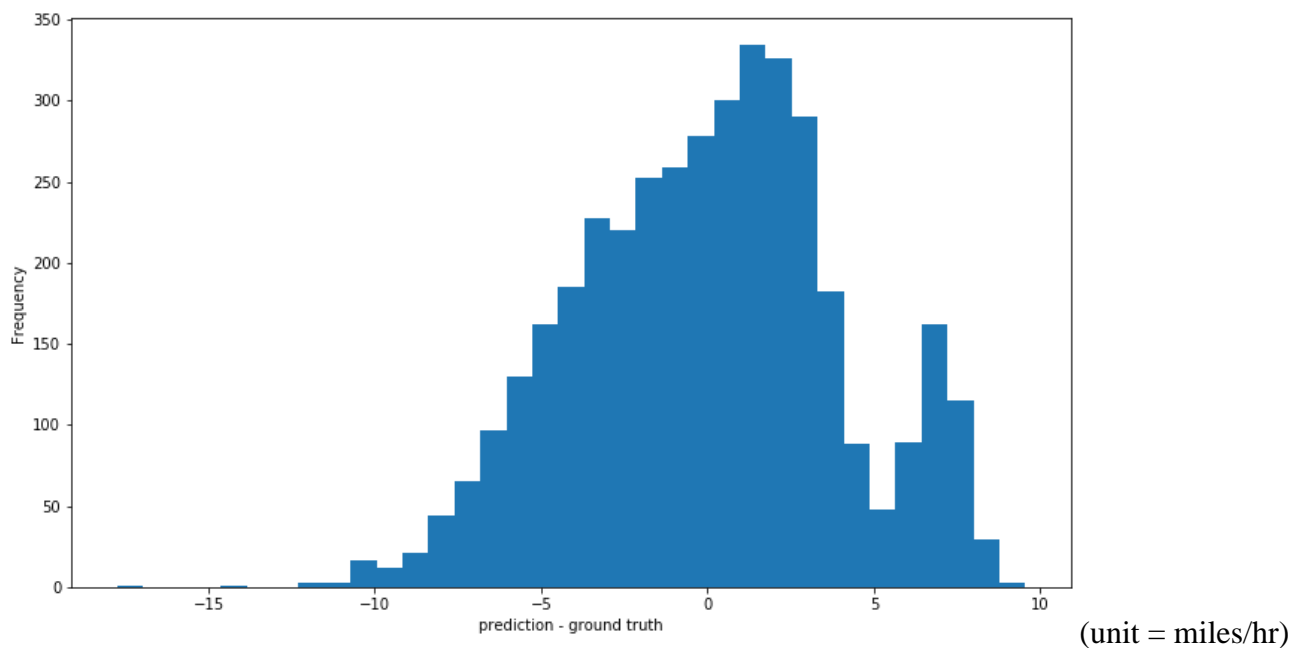


Fig 5.6(c) histogram of errors

This is the histogram of the errors (prediction – observation) that we get after evaluating our model on validation dataset. There were 3942 data points (15 % of the whole dataset of 3 years). The train, validation and test dataset split is in the ratio of 70%, 15% and 15% respectively of the whole dataset of 3 years from January 2018 to December 2020. We can see that a lot of the predictions are not close to ground truth. Errors are spread over 10 miles/hr.

Correlation matrix:

```
[[1.    0.23181734]
 [0.23181734  1.  ]]
```

The correlation coefficient between prediction and actual observation (i.e., ground truth) is 0.23. So there is only weak correlation between the two.

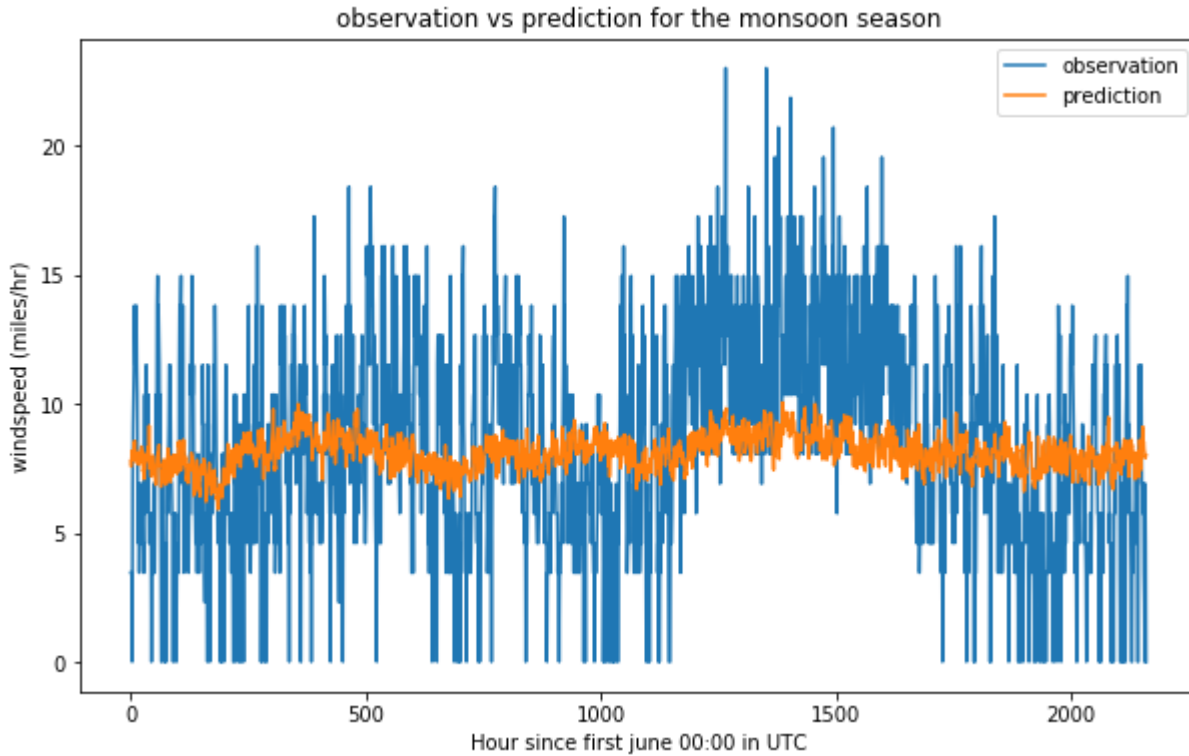
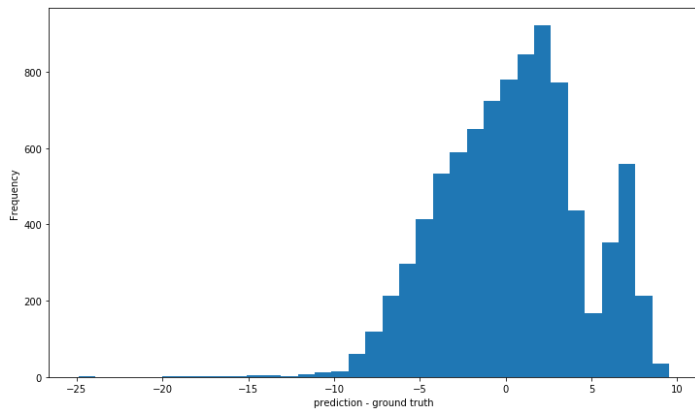
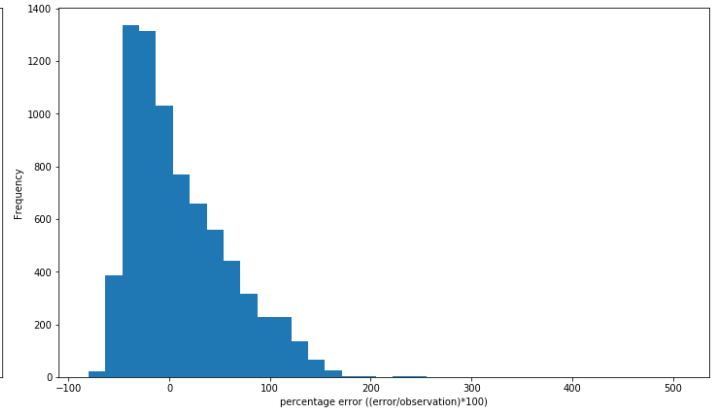


Fig 5.6(d) observation and prediction plot for monsoon season

In this, observation and prediction are put in the same plot. The data taken was for 3 months from 1<sup>st</sup> June 2021 to 31<sup>st</sup> August 2021. We first find the prediction made by our model on this 3 month input data and then plot both prediction made and the corresponding observation in this same plot together. This is a time-series data.



(unit = miles/hr)

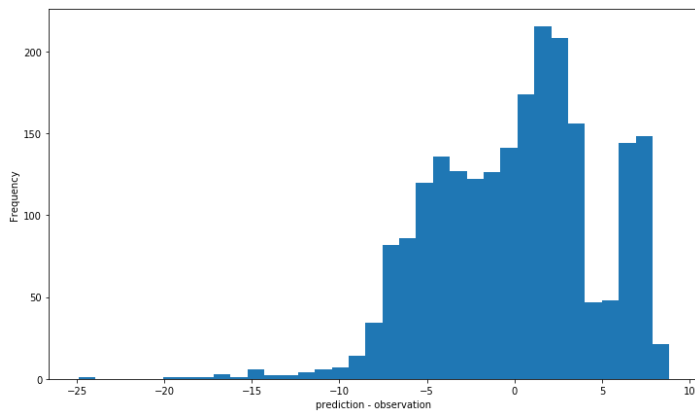


(unitless)

Fig 5.6(e) histogram of errors on 1 year independent dataset      fig 5.6(f) percentage accuracy for the same

On the left side we have the histogram of errors (prediction – ground truth) our model gives when tested on 1 year (1 March 2021 to 28 February 2022) of independent dataset. Again, most of the errors are within 10 miles/hr.

On the right side we have the histogram of percentage error  $((\text{error}/\text{observation}) * 100)$  when our model is tested on 1 year (1 March 2021 to 28 February 2022) of independent dataset. As we can see, most of the data points fall under 200 % error.



(x-axis unit = miles/hr)

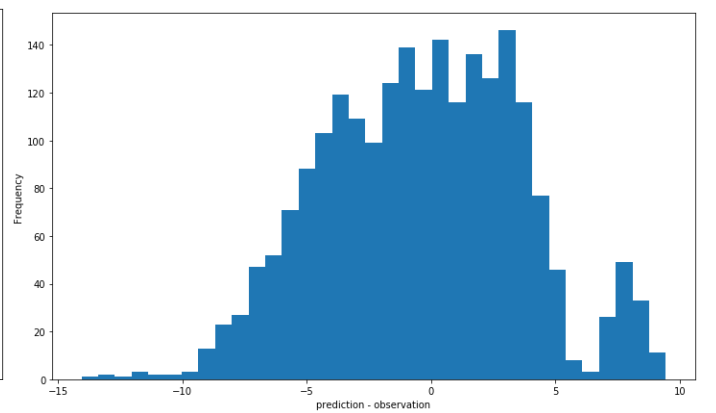
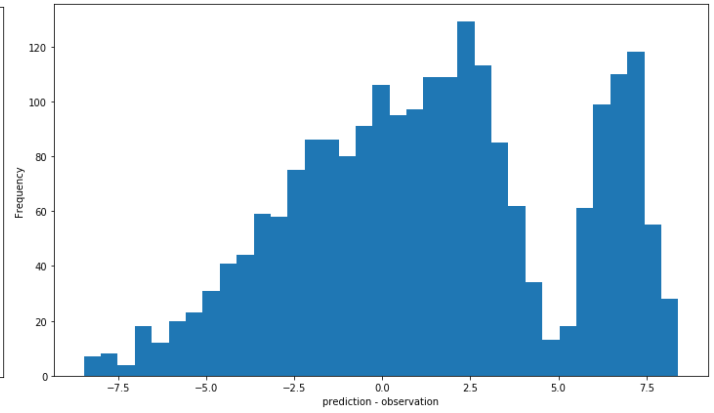
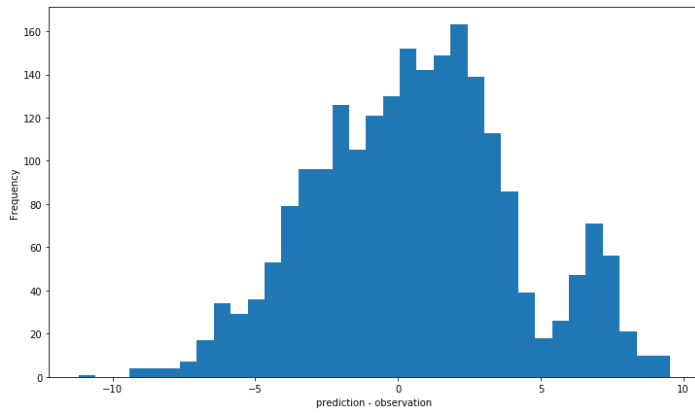


Fig 5.6(g) error histogram for summer

fig 5.6(h) error histogram for monsoon



(unit = miles/hr)

Fig 5.6(i) error histogram for autumn

fig 5.6(j) error histogram for winter

Above 4 plots are error plots when the model is tested on 4 different seasons each of 3 month time length. 1<sup>st</sup>, 2<sup>nd</sup>, 3<sup>rd</sup> and 4<sup>th</sup> plots are for summer, monsoon, autumn and winter datasets respectively. 1 year of independent dataset has been broken into 4 seasons.

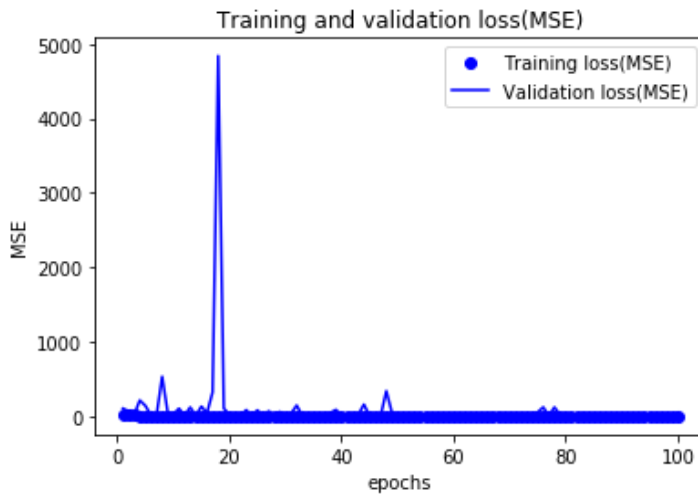
Summer- 1 March to 31 May

Monsoon- 1 June to 31 August

Autumn- 1 September to 30 November

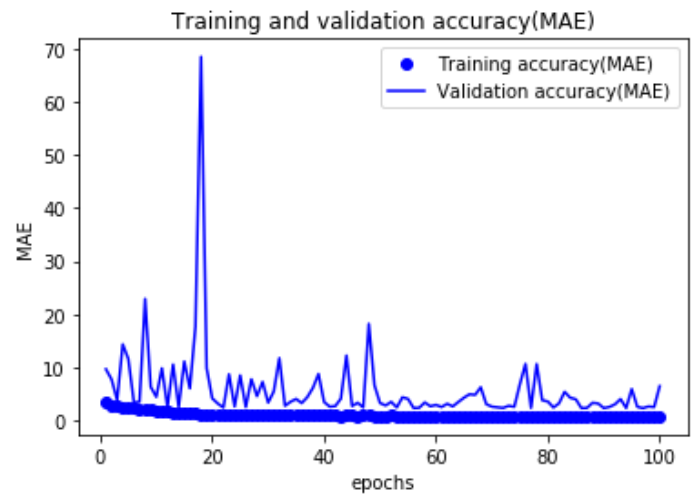
Winter- 1 December to 28 February

## With 2D CNN,



(unit of MSE = miles squared/hr squared)

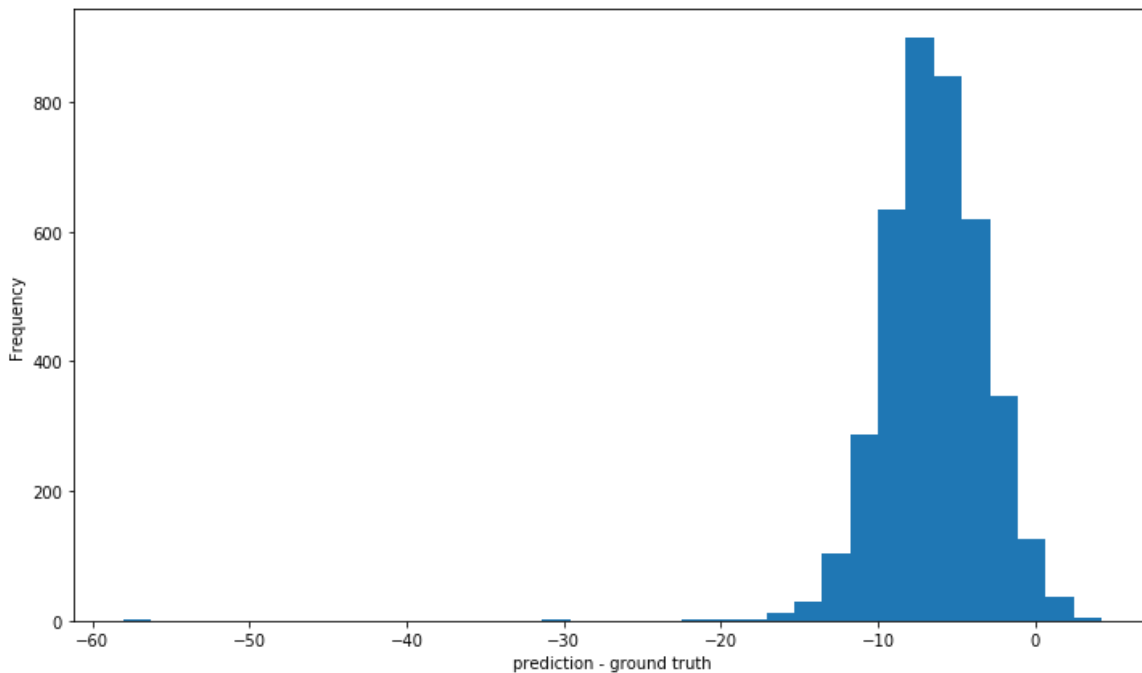
Fig 5.6(k) epoch Vs loss



(unit of MAE = miles/hr)

fig 5.6(l) epoch Vs accuracy

This is the plot of loss Vs epochs. We can see that with continuous training, loss decreases. The same way on the right side plot, accuracy improves with subsequent training process.



(unit = miles/hr)

Fig 5.6(m) histogram of errors

This is the histogram of the errors (prediction – observation) that we get after evaluating our model on validation dataset. There were 3942 data points (15 % of the whole dataset of 3 years). The train, validation and test dataset split is in the ratio of 70%, 15% and 15% respectively of the whole dataset of 3 years from January 2018 to December 2020. We can see that most of the errors are spread over 10 miles/hr.

Correlation matrix:

```
[[1.    0.58028508]  
 [0.58028508 1.    ]]
```

The correlation coefficient between prediction and actual observation (i.e., ground truth) is 0.58. So there is moderate correlation between the two.

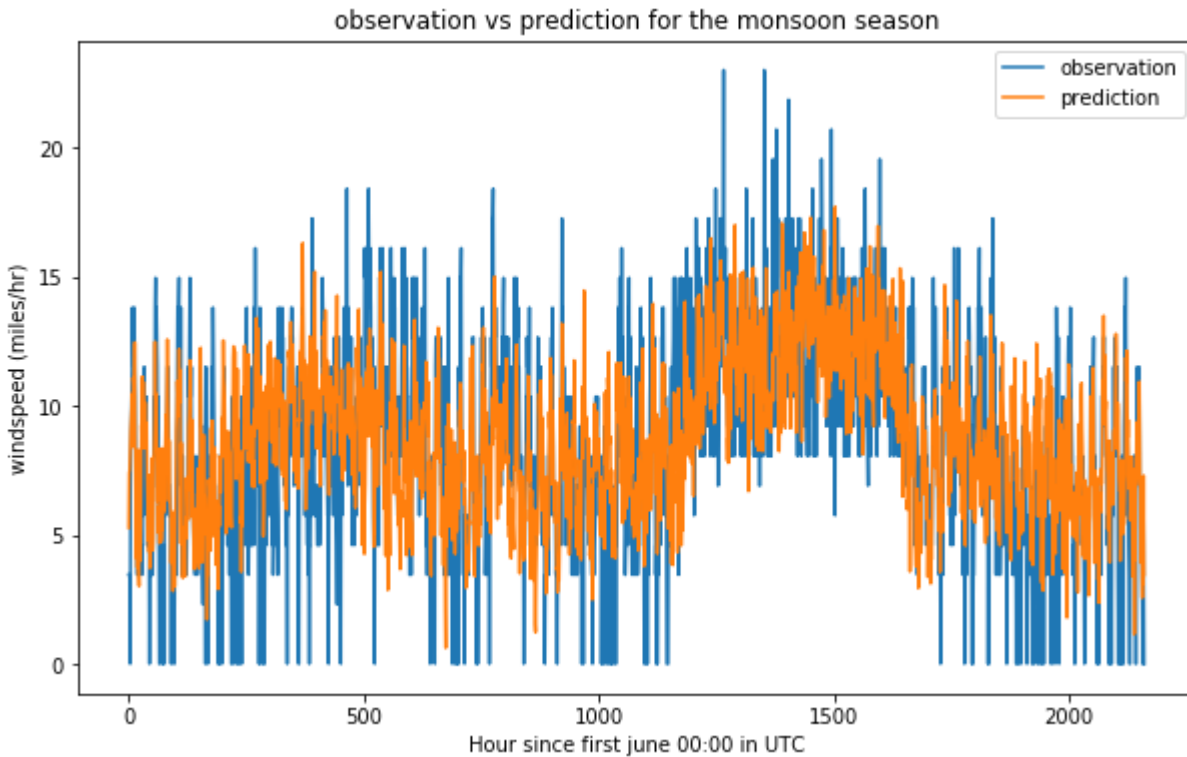


Fig 5.6(n) observation and prediction plot for monsoon season

In this, observation and prediction are put in the same plot. The data taken was for 3 months from 1<sup>st</sup> June 2021 to 31<sup>st</sup> August 2021. We first find the prediction made by our model on this 3 month input data. This is a time-

series data. From the plot we can see there is moderate level of correlation between the prediction and observation.

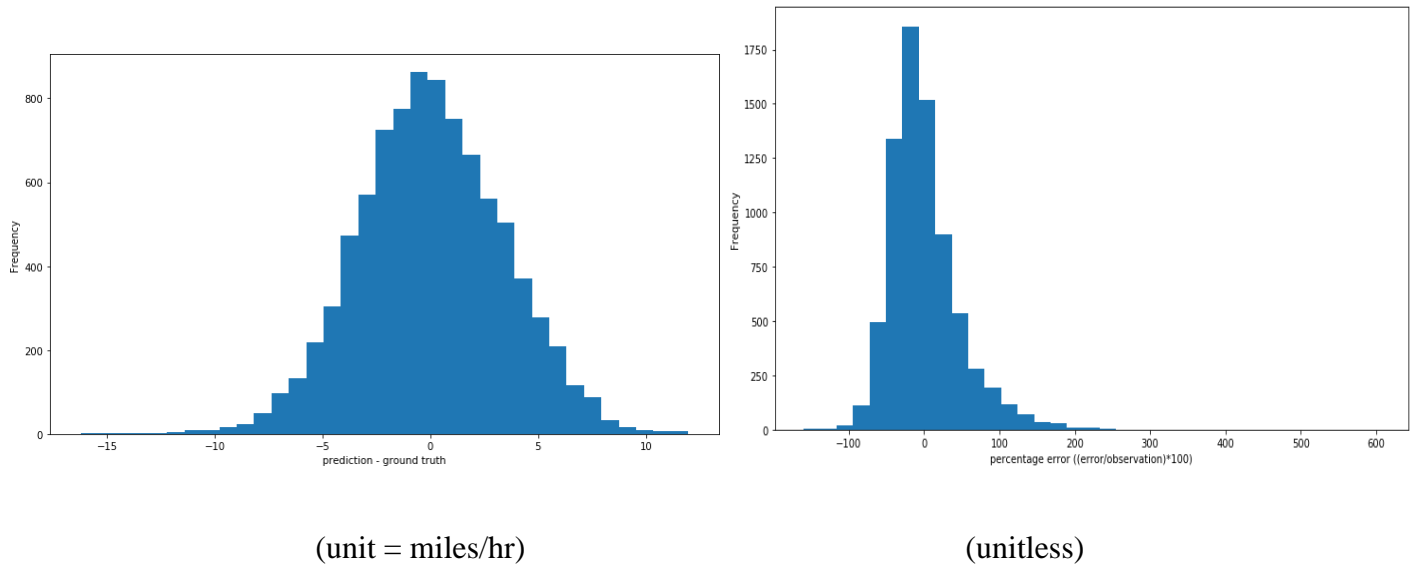
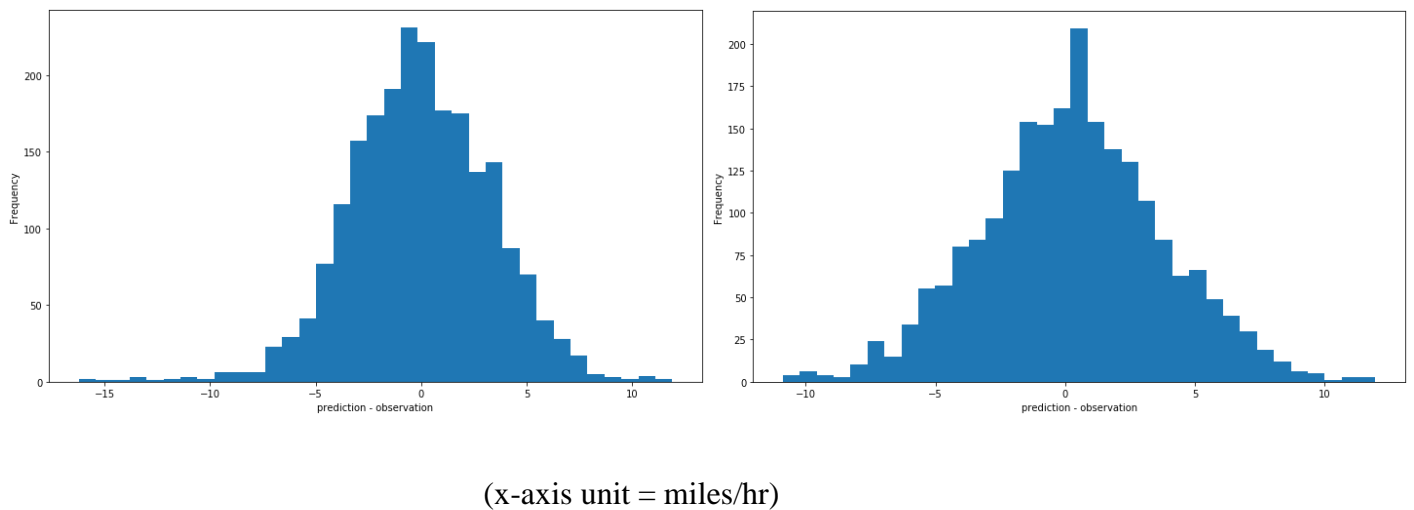


Fig 5.6(o) histogram of errors on 1 year independent dataset      fig 5.6(p) percentage accuracy for the same

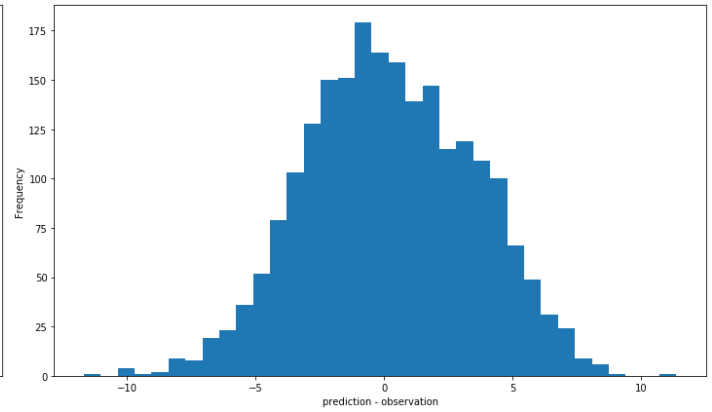
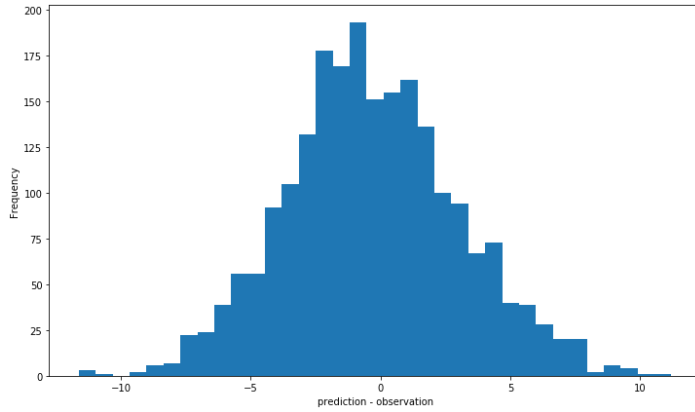
On the left side we have the histogram of errors (prediction – ground truth) our model gives when tested on 1 year (1 March 2021 to 28 February 2022) of independent dataset. Again, most of the errors are within 10 miles/hr. On the right side we have the histogram of percentage error ((error/observation)\*100) when our model is tested on 1 year (1 March 2021 to 28 February 2022) of independent dataset. As we can see, most of the data points fall under 200 % error.



(x-axis unit = miles/hr)

Fig 5.6(q) error histogram for summer

fig 5.6(r) error histogram for monsoon



(unit = miles/hr)

Fig 5.6(s) error histogram for autumn

fig 5.6(t) error histogram for winter

Above 4 plots are error plots when the model is tested on 4 different seasons each of 3 month time length. 1<sup>st</sup>, 2<sup>nd</sup>, 3<sup>rd</sup> and 4<sup>th</sup> plots are for summer, monsoon, autumn and winter datasets respectively. 1 year of independent dataset has been broken into 4 seasons.

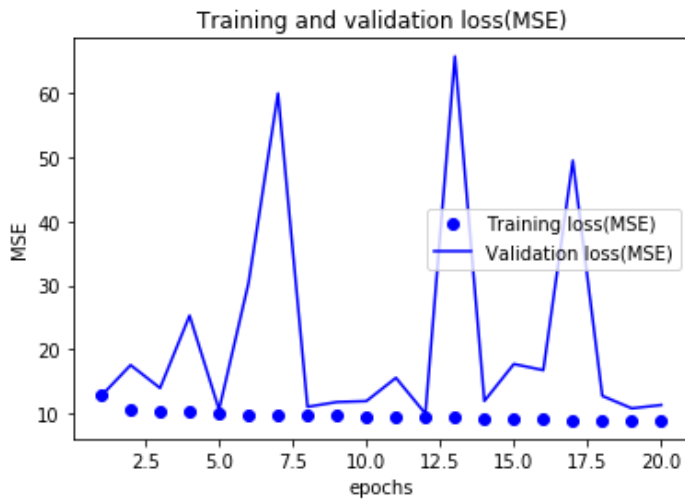
Summer- 1 March to 31 May

Monsoon- 1 June to 31 August

Autumn- 1 September to 30 November

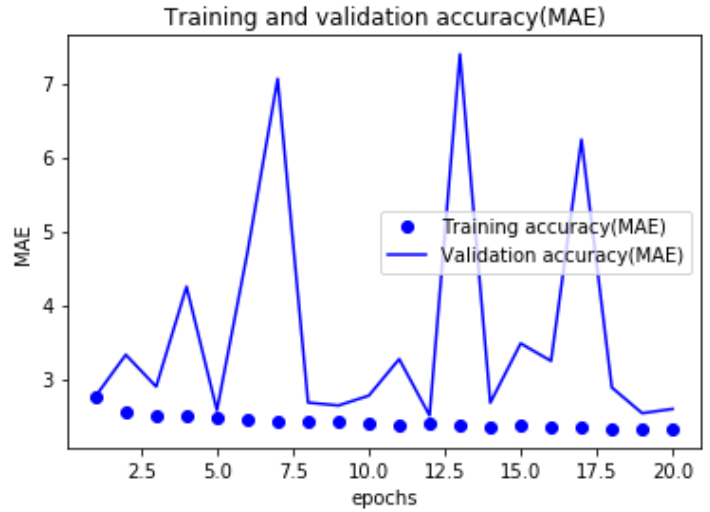
Winter- 1 December to 28 February

**With 3D CNN,**



(unit of MSE = miles squared/hr squared)

Fig 5.6(u) epoch Vs loss



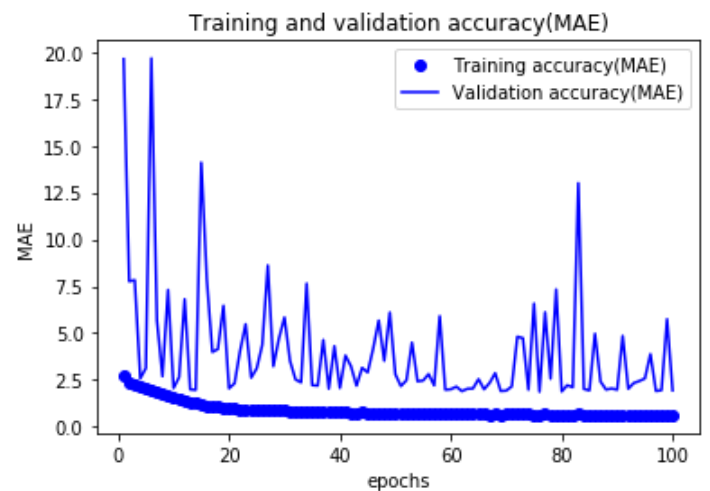
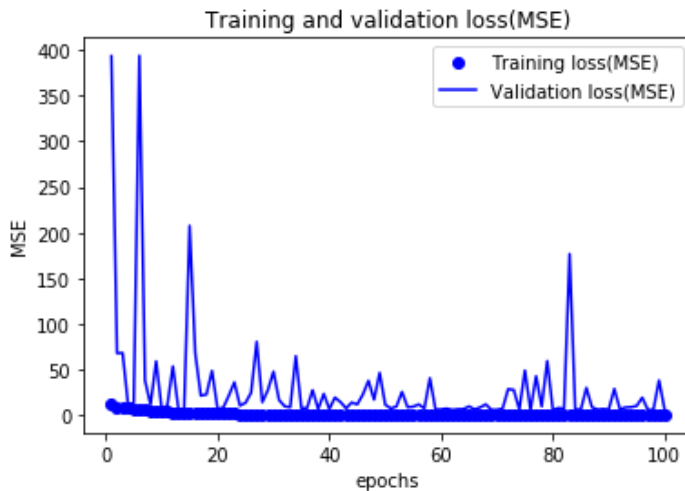
(unit of MAE = miles/hr)

fig 5.6(v) epoch Vs accuracy

With 3D CNN, we are making predictions for 6 hours in future. With continuous training, we see validation loss and validation accuracy fluctuating (decreasing then increasing).

**For station VOTV,**

**With 2D CNN,**



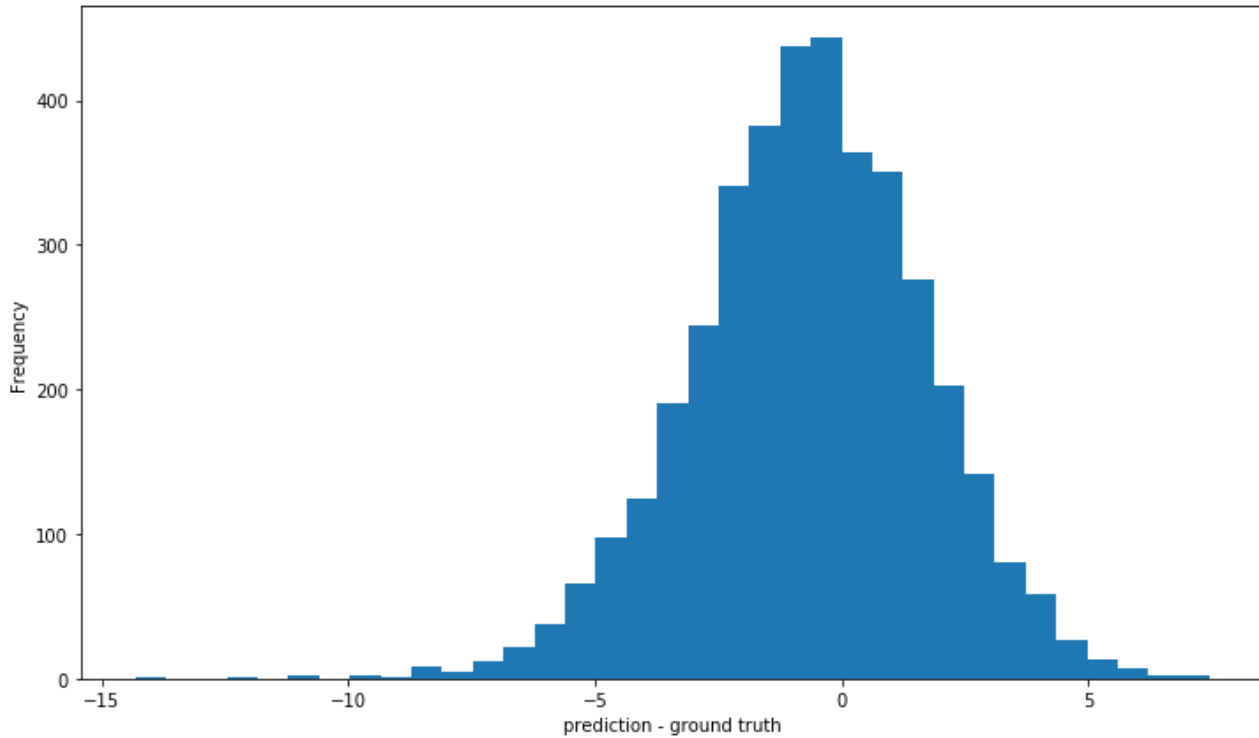
(unit of MSE = miles squared/hr squared)

(unit of MAE= miles/hr)

Fig 5.7(a) epoch Vs loss

fig 5.7(b) epoch Vs accuracy

We can see that with continuous training, loss decreases and accuracy improves with subsequent training process.



(unit = miles/hr)

Fig 5.7(c) histogram of errors

This is the histogram of the errors (prediction – observation) that we get after evaluating our model on validation dataset. We can see that most of the predictions are closer to ground truth i.e., errors are mostly concentrated around 0 miles/hr. Most of the errors are within about 5 miles/hr.

Correlation matrix

```
[[1.    0.50751333]
```

```
[0.50751333  1.]]
```

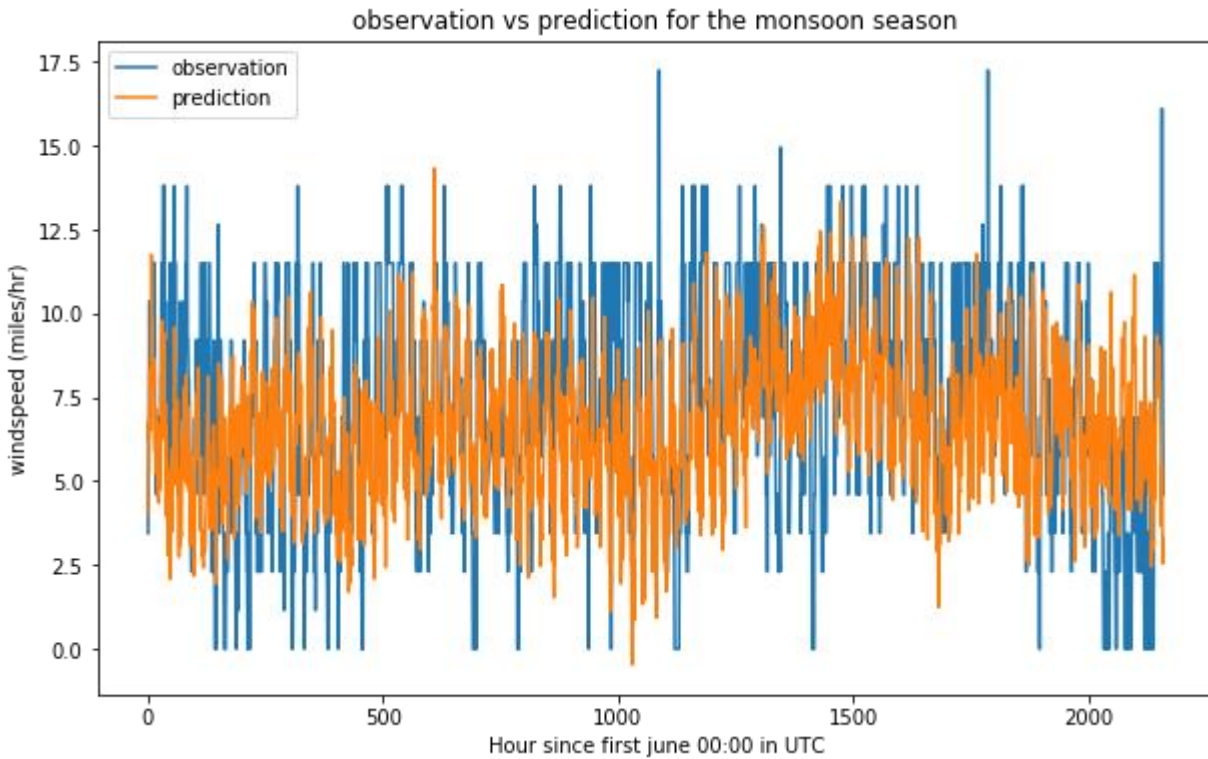
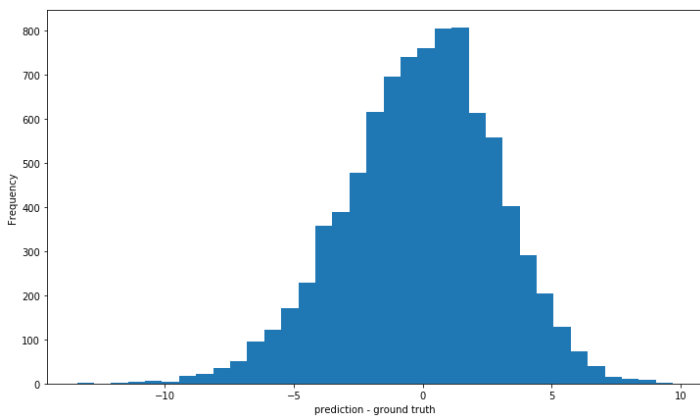
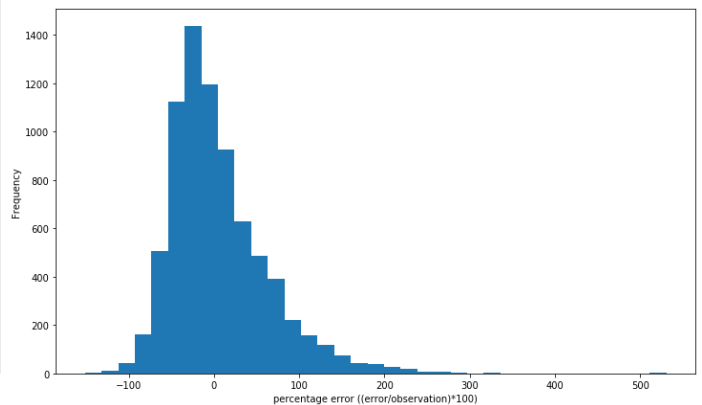


Fig 5.7(d) observation and prediction plot for monsoon season

In this, observation and prediction are put in the same plot. The data taken was for 3 months from 1st June 2021 to 31st August 2021. We first find the prediction made by our model on this 3 month input data. This is a time-series data. There is moderate correlation between observation and prediction.



(unit = miles/hr)

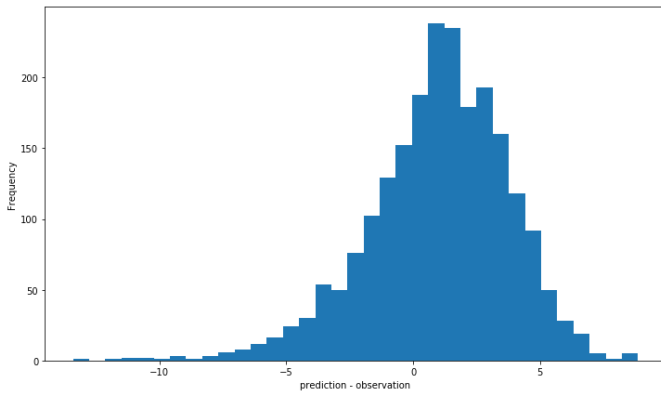


(unitless)

Fig 5.7(e) histogram of errors on 1 year independent dataset

fig 5.7(f) percentage accuracy for the same

We have the histogram of errors (prediction – ground truth) and percentage error  $((\text{error}/\text{observation}) * 100)$  our model gives when tested on 1 year (1 March 2021 to 28 February 2022) of independent dataset. Again, most of the errors are concentrated around 0 miles/HR and within about 5 miles/hr and 200% error.



(x-axis unit = miles/hr)

Fig 5.7(g) error histogram for summer

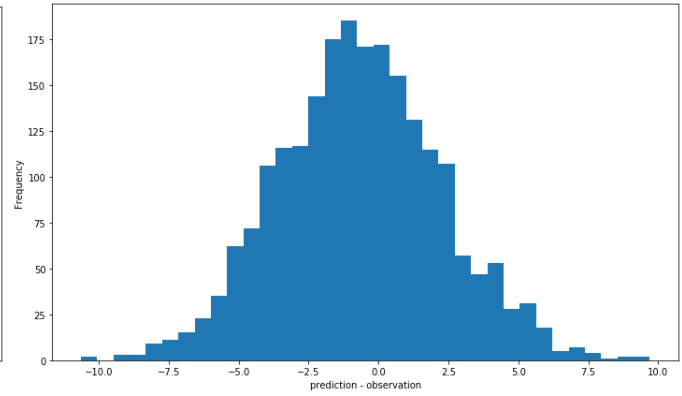


fig 5.7(h) error histogram for monsoon

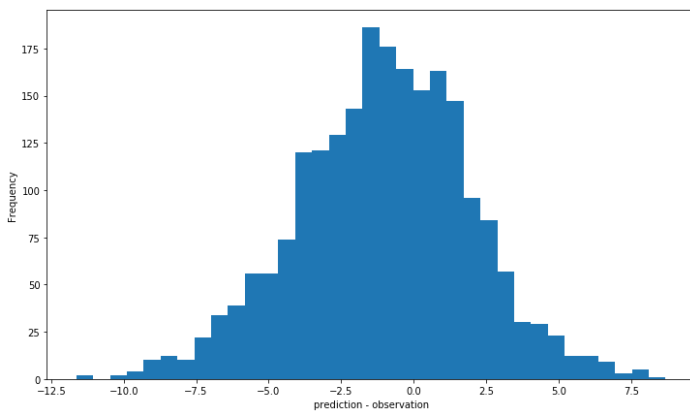


Fig 5.7(i) error histogram for autumn

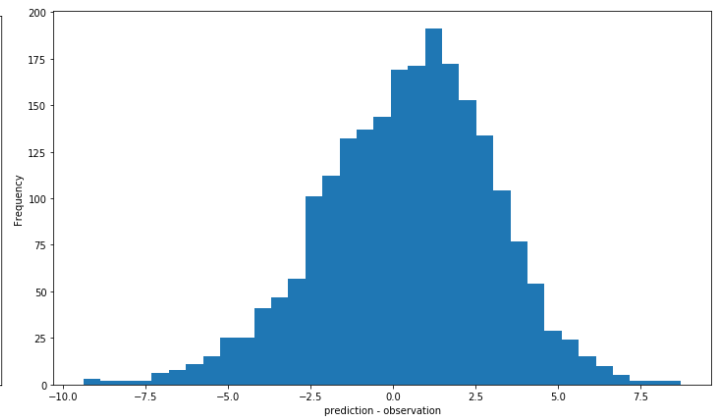
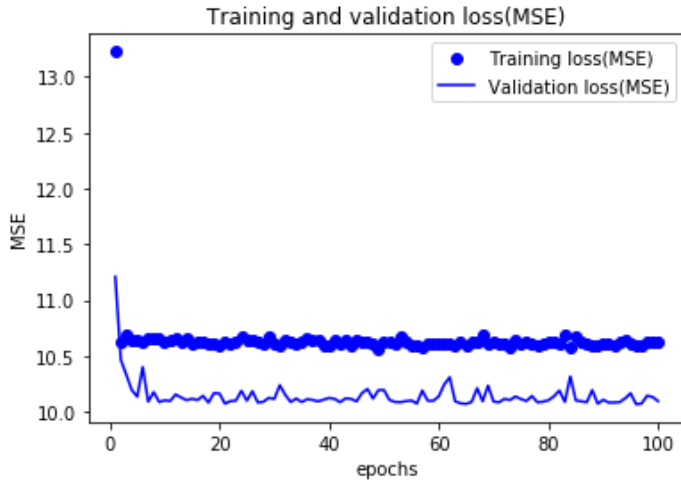


fig 5.7(j) error histogram for winter

(unit = miles/hr)

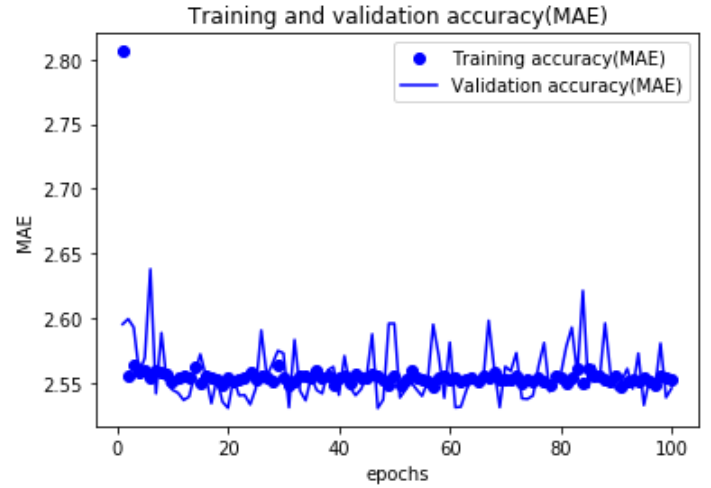
Above 4 plots are error plots when the model is tested on 4 different seasons each of 3 month time length. 1 year of independent dataset has been broken into 4 seasons. 1st, 2nd, 3rd and 4th plots are for summer, monsoon, autumn and winter datasets respectively. Most of the errors are about 7.5 miles/hr.

## With VGG16,



(unit of MSE = miles squared/hr squared)

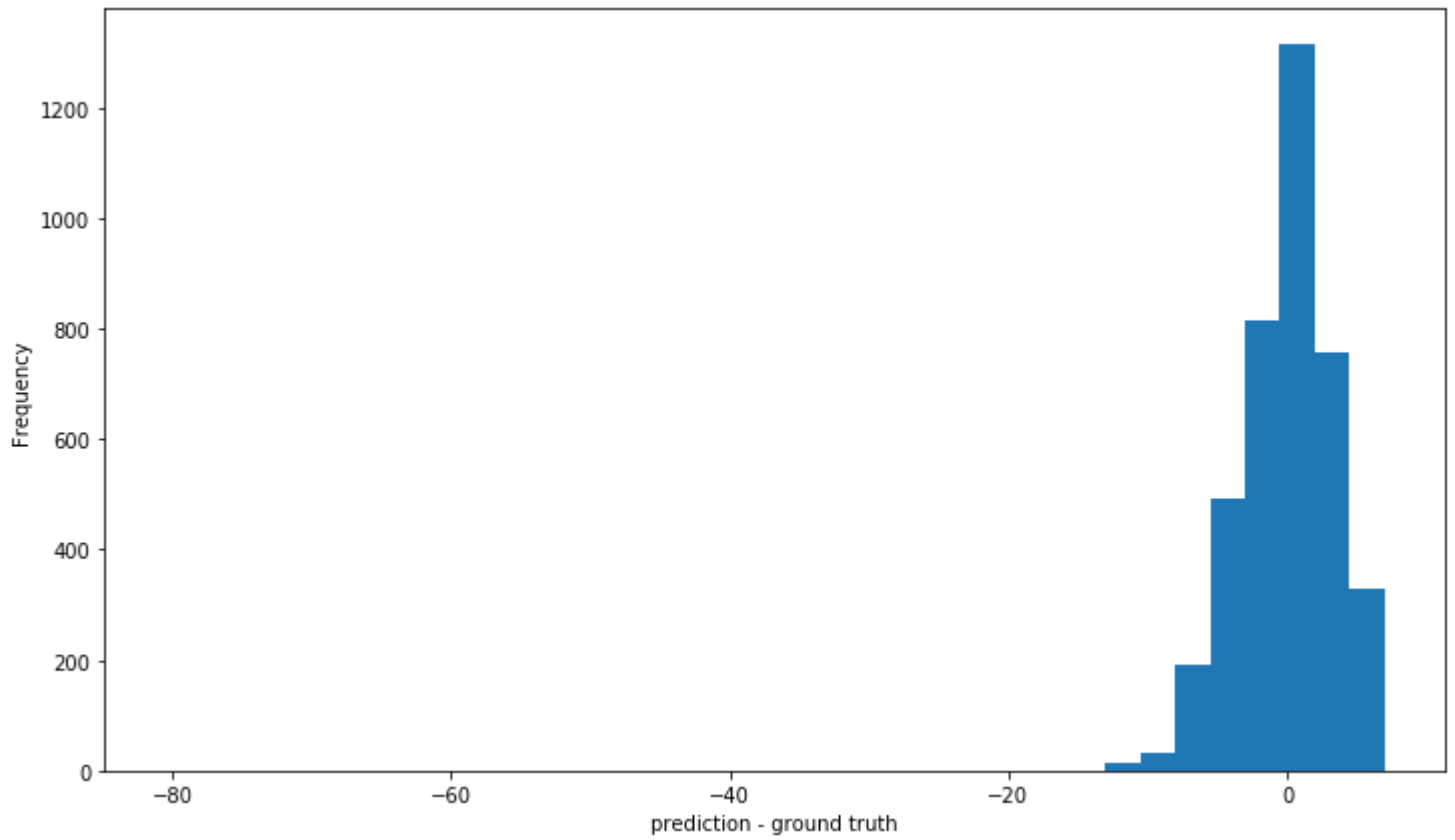
Fig 5.7(k) epoch Vs loss



(unit of MAE = miles/hr)

fig 5.7(l) epoch Vs accuracy

We can see that with continuous training, loss and accuracy improves only a little. They plateau at the very start.



(unit = miles/hr)

Fig 5.7(m) histogram of errors

This is the histogram of the errors (prediction – observation) that we get after evaluating our model on validation dataset. We can see that most of the predictions are closer to ground truth i.e., errors are mostly concentrated around 0. Most of the errors are within about 15 miles/hr.

Correlation matrix,

```
[[1.    0.29230694]
 [0.29230694  1.]]
```

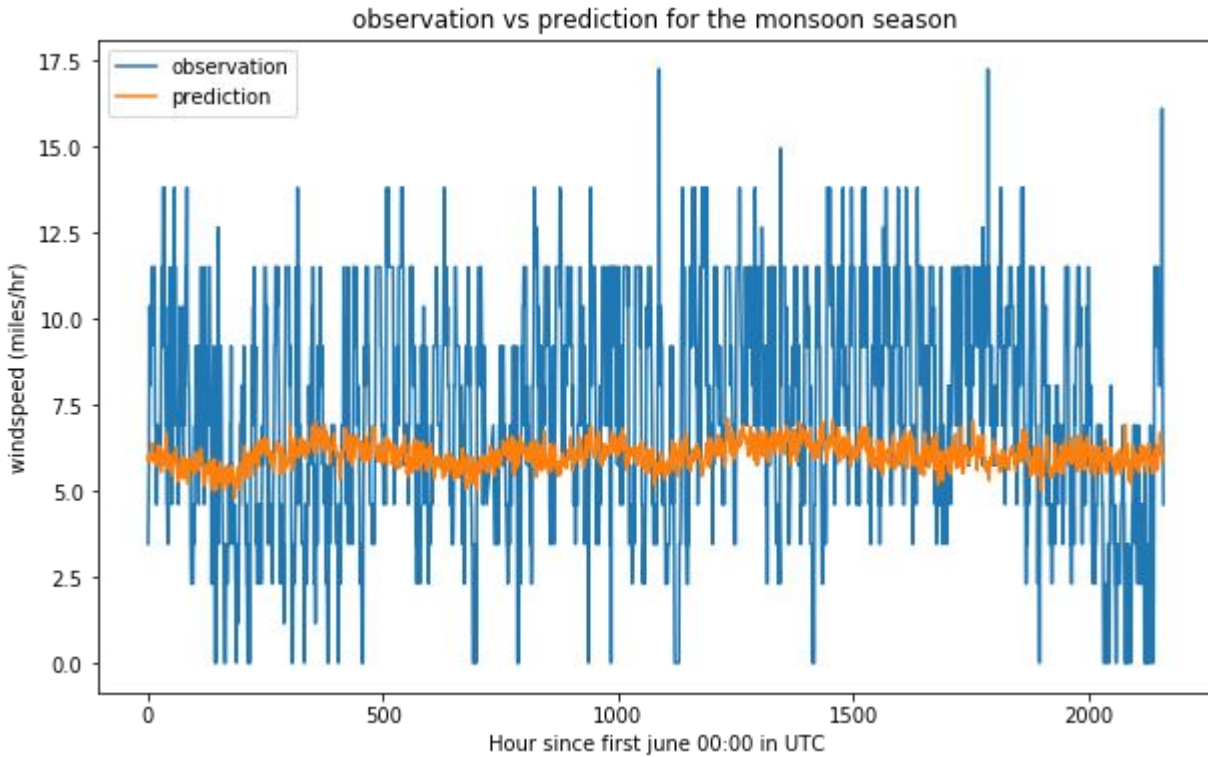
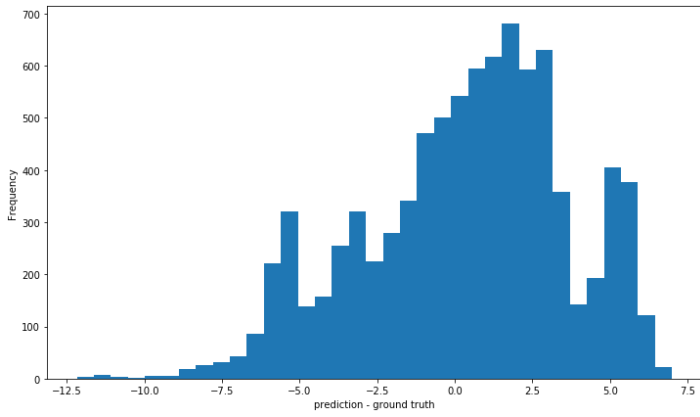
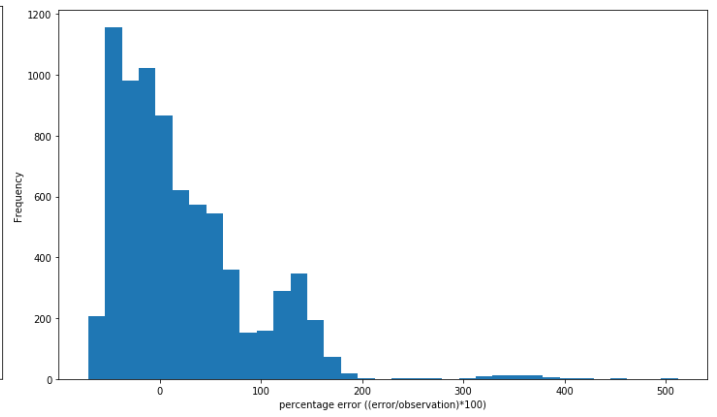


Fig 5.7(n) observation and prediction plot for monsoon season

In this, observation and prediction are put in the same plot. The data taken was for 3 months from 1st June 2021 to 31st August 2021. We first find the prediction made by our model on this 3 month independent input dataset. This is a time-series data. The plot clearly shows there is a weak correlation between the predictions made by VGG16 model and observations made for the 3 month monsoon season.



(unit = miles/hr)

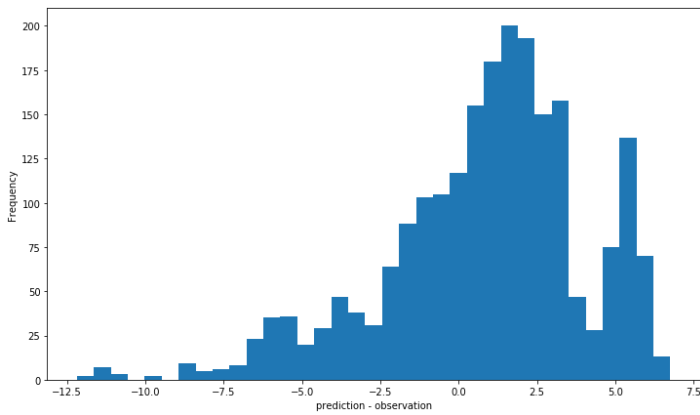


(unitless)

Fig 5.7(o) histogram of errors on 1 year independent dataset

fig 5.7(p) percentage error for the same

We have the histogram of errors (prediction – ground truth) and percentage error  $((\text{error}/\text{observation}) \times 100)$  our model gives when tested on 1 year (1 March 2021 to 28 February 2022) of independent dataset. Again, most of the errors are concentrated around 0 miles/hr and within about 7.5 miles/hr and 200% error.



(x-axis unit = miles/hr)

Fig 5.7(q) error histogram for summer

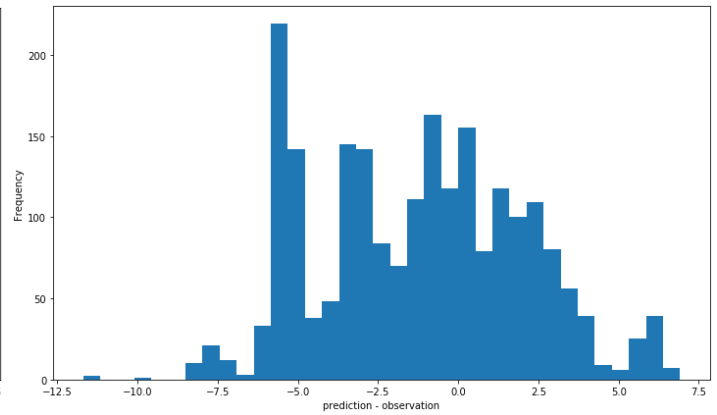
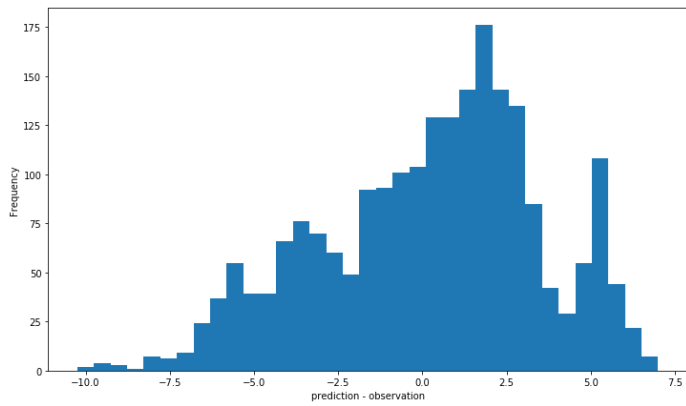


fig 5.7(r) error histogram for monsoon



(unit = miles/hr)

Fig 5.7(s) error histogram for autumn

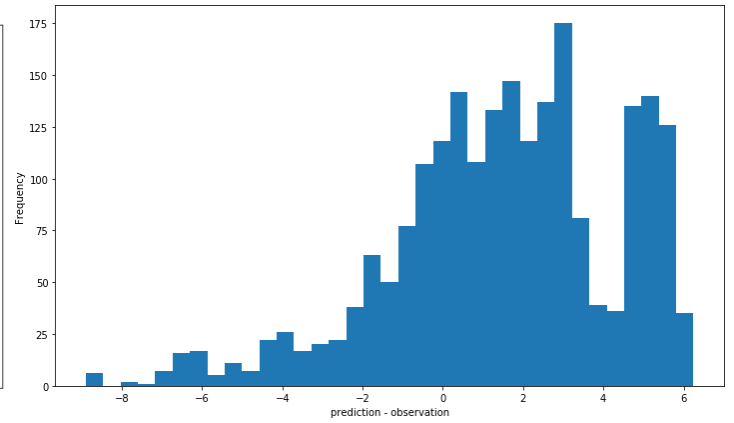
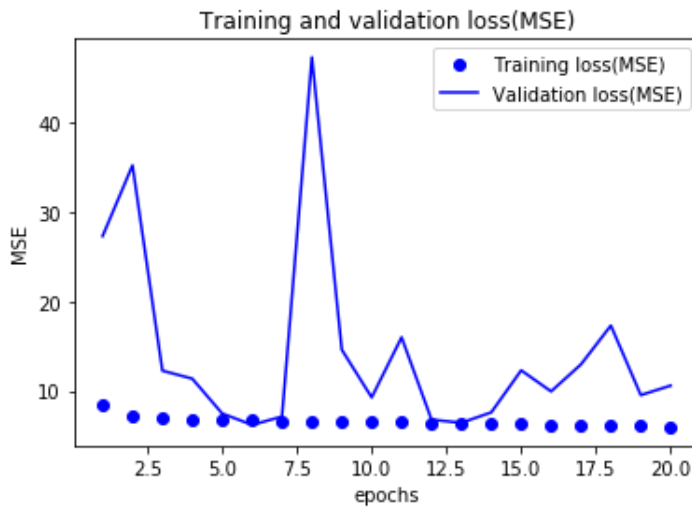


fig 5.7(t) error histogram for winter

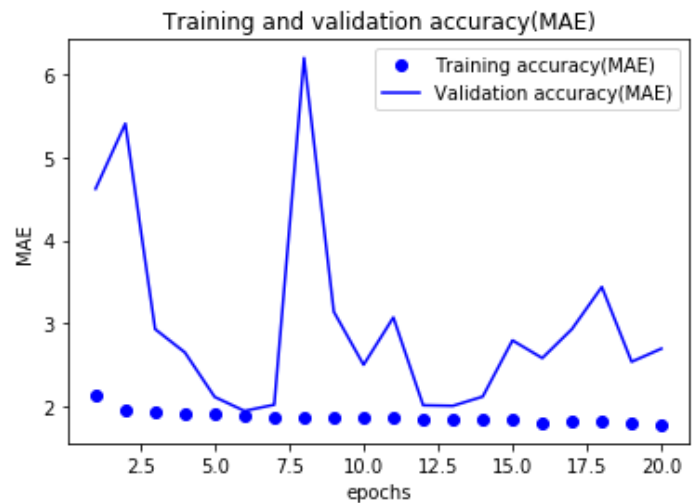
Above 4 plots are error plots when the model is tested on 4 different seasons each of 3 month time length. 1 year of independent dataset has been broken into 4 seasons. 1st, 2nd, 3rd and 4th plots are for summer, monsoon, autumn and winter datasets respectively. Most of the errors are spread over 7.5 miles/hr from the center.

**With 3D CNN,**



(unit of MSE = miles squared/hr squared)

Fig 5.7(u) epoch Vs loss



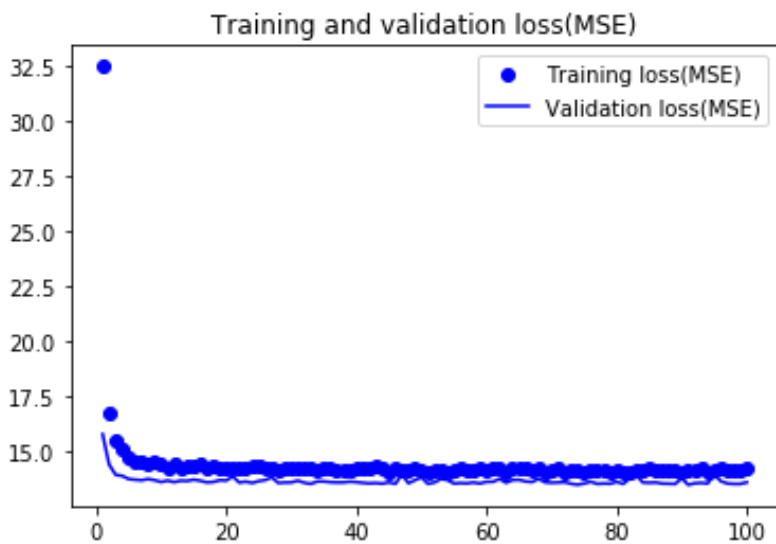
(unit of MAE = miles/hr)

fig 5.7(v) epoch Vs accuracy

With 3D CNN, we are making predictions for 6 hours in future. With continuous training, validation loss decreases and validation accuracy improves at first but then after few epochs over- fitting of the data starts happening.

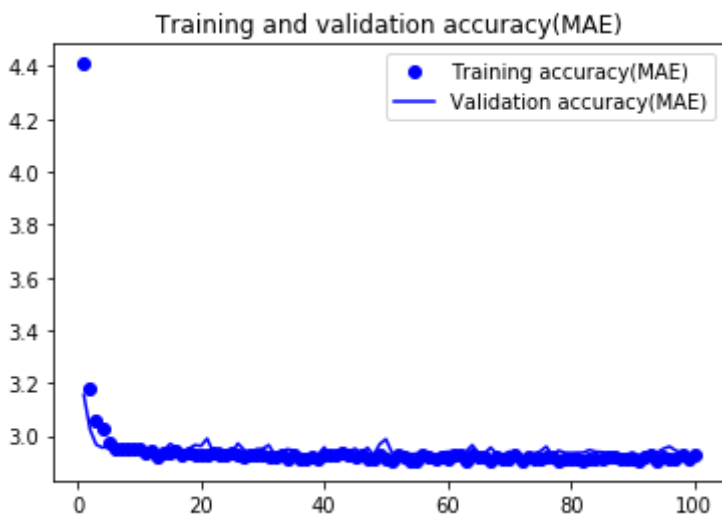
**For station VOBL,**

**With vgg16,**



(x-axis = epochs, y-axis = MSE(unit = miles squared/hr squared))

Fig 5.8(a) epoch Vs loss



(x-axis = epochs, y-axis = MAE(unit = miles/hr))

Fig 5.8(b) epoch Vs accuracy

We can see that with continuous training, loss decreases and accuracy improves. Though the improvement is only minor.

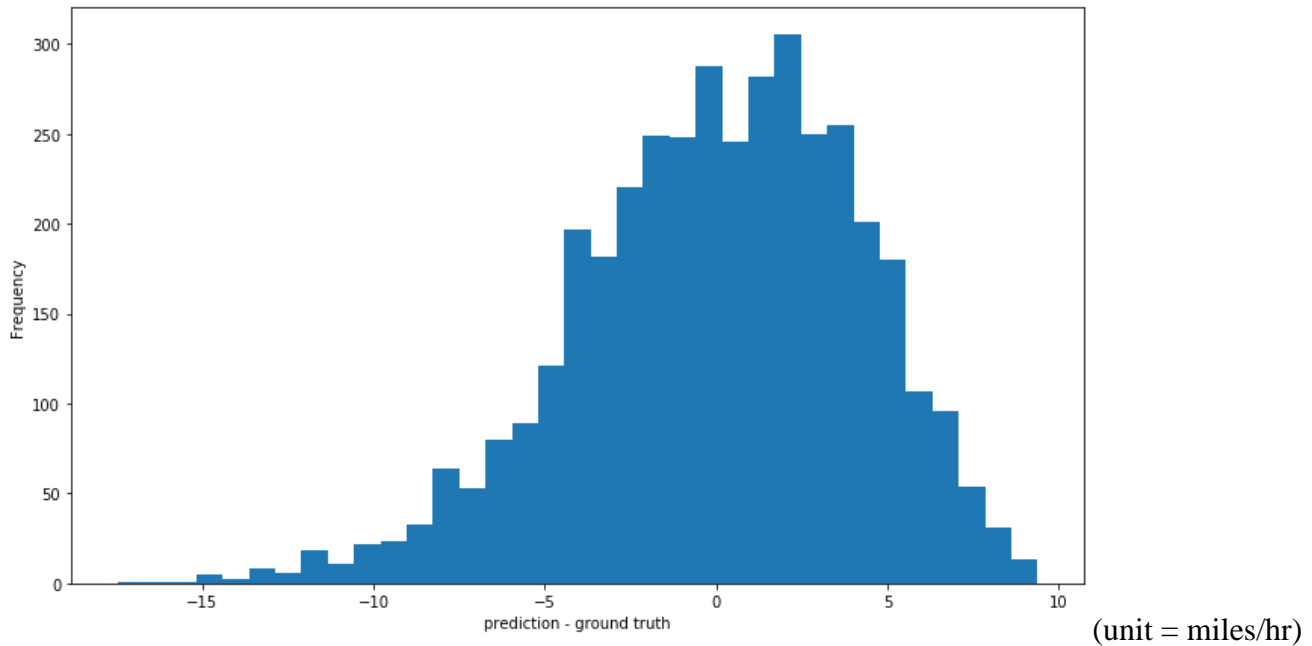


Fig 5.8(c) histogram of errors

This is the histogram of the errors (prediction – observation) that we get after evaluating our model on validation dataset. We can see that most of the predictions are closer to ground truth i.e., errors are mostly concentrated around 0. Most of the errors are within about 10 miles/hr.

Correlation matrix,

```
[[1.    0.43166513]
 [0.43166513 1. ]]
```

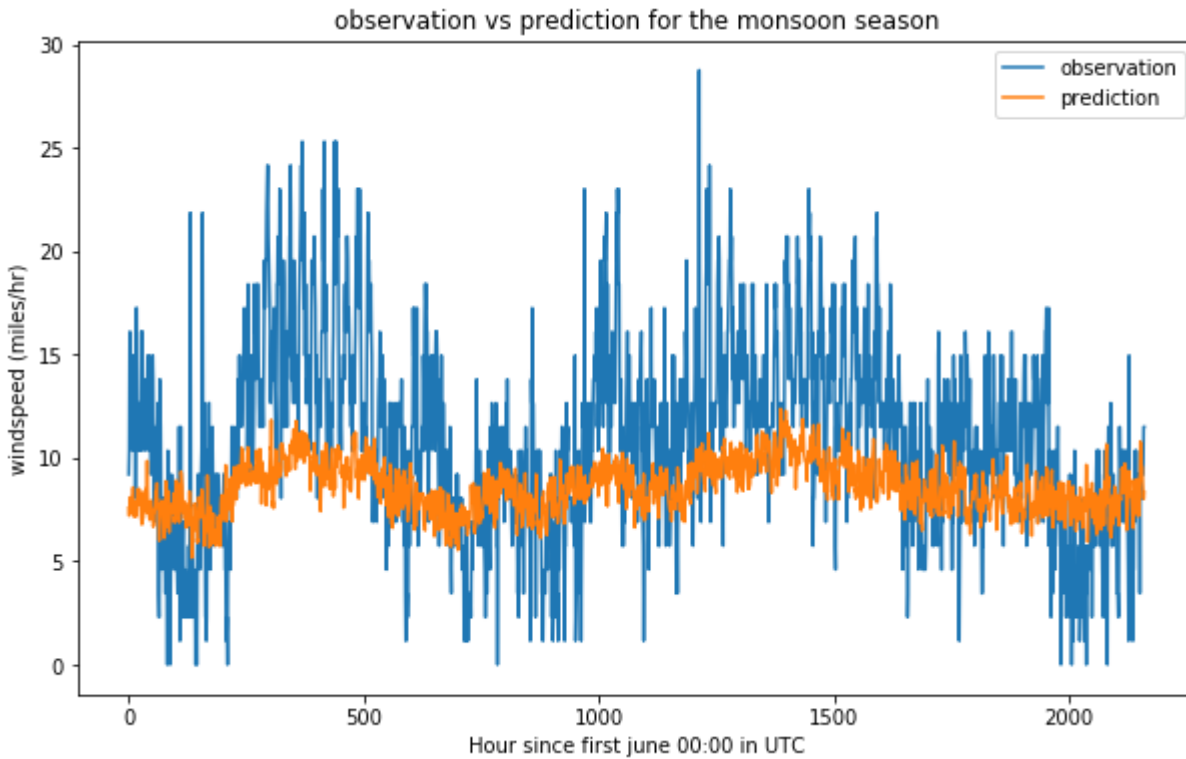
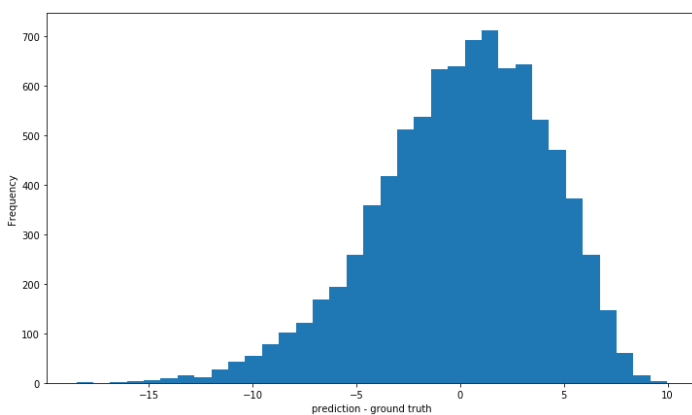
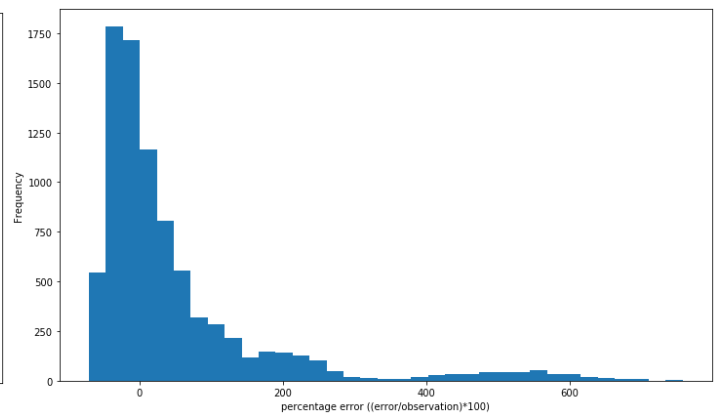


Fig 5.8(d) observation and prediction plot for monsoon season

In this, observation and prediction are put in the same plot. The data taken was for 3 months from 1st June 2021 to 31st August 2021. We first find the prediction made by our model on this 3 month independent input dataset. This is a time-series data. The plot clearly shows there is a weak correlation between the predictions made by VGG16 model and observations made for the 3 month monsoon season.



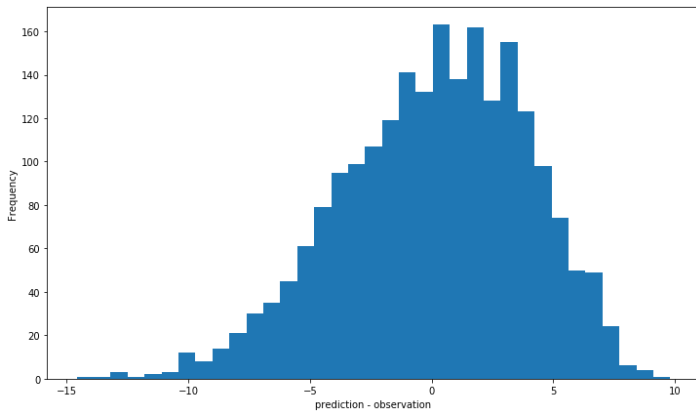
(miles/hr)



(unitless)

Fig 5.8(e) histogram of errors on 1 year independent dataset    fig 5.8(f) percentage accuracy for the same

We have the histogram of errors (prediction – ground truth) and percentage error  $((\text{error}/\text{observation}) * 100)$  our model gives when tested on 1 year (1 March 2021 to 28 February 2022) of independent dataset. Again, most of the errors are concentrated around 0 miles/hr and within about 10 miles/hr and 250% error.



(x-axis unit = miles/hr)

Fig 5.8(g) error histogram for summer

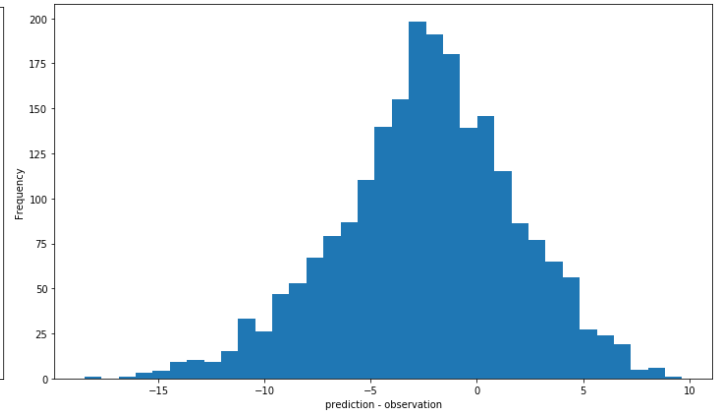
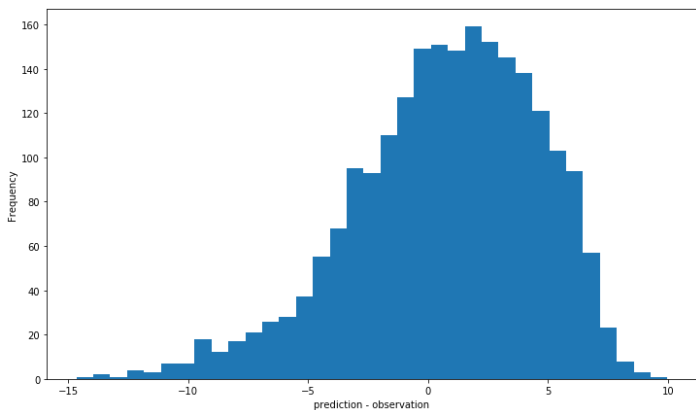


fig 5.8(h) error histogram for monsoon



(unit= miles/hr)

Fig 5.8(i) error histogram for autumn

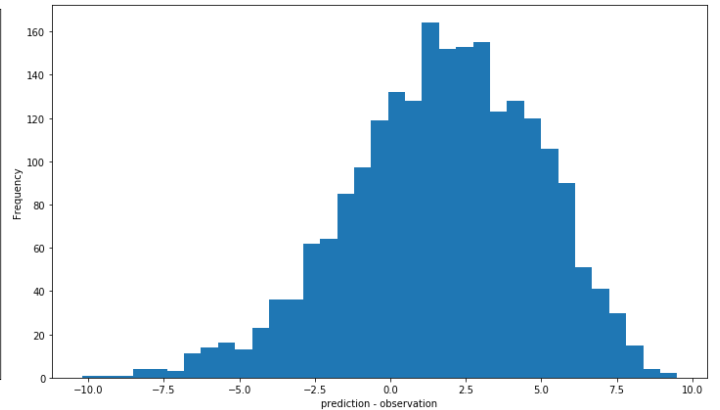
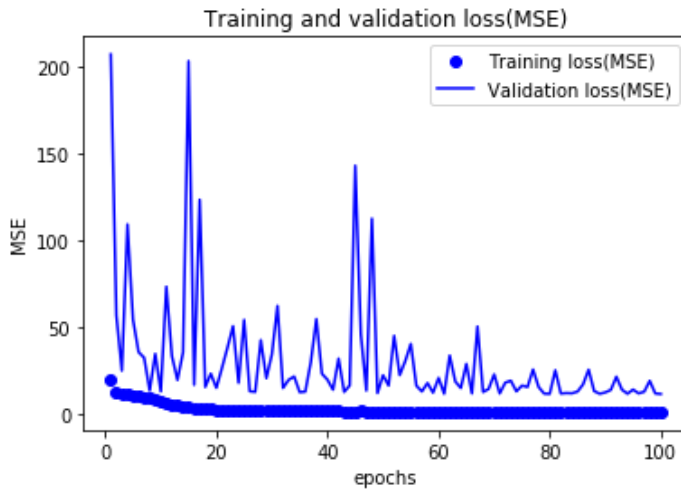


fig 5.8(j) error histogram for winter

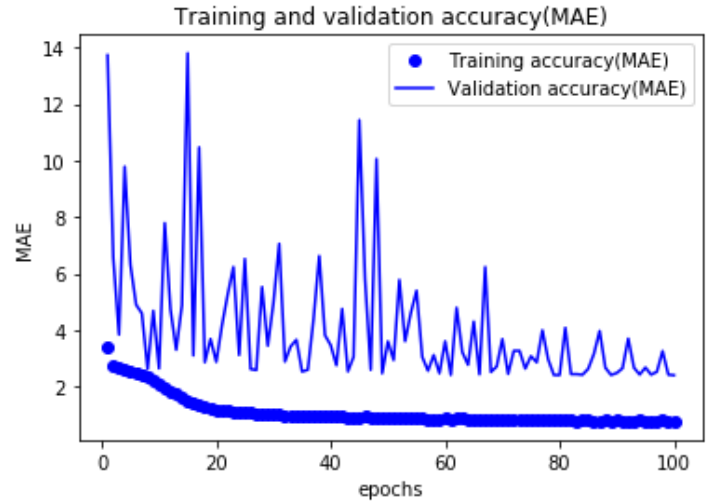
Above 4 plots are error plots when the model is tested on 4 different seasons each of 3 month time length. 1 year of independent dataset has been broken into 4 seasons. 1st, 2nd, 3rd and 4th plots are for summer, monsoon, autumn and winter datasets respectively. Most of the errors are spread over 15 miles/hr from the center.

## With 2D CNN,



(unit of MSE = miles squared/hr squared)

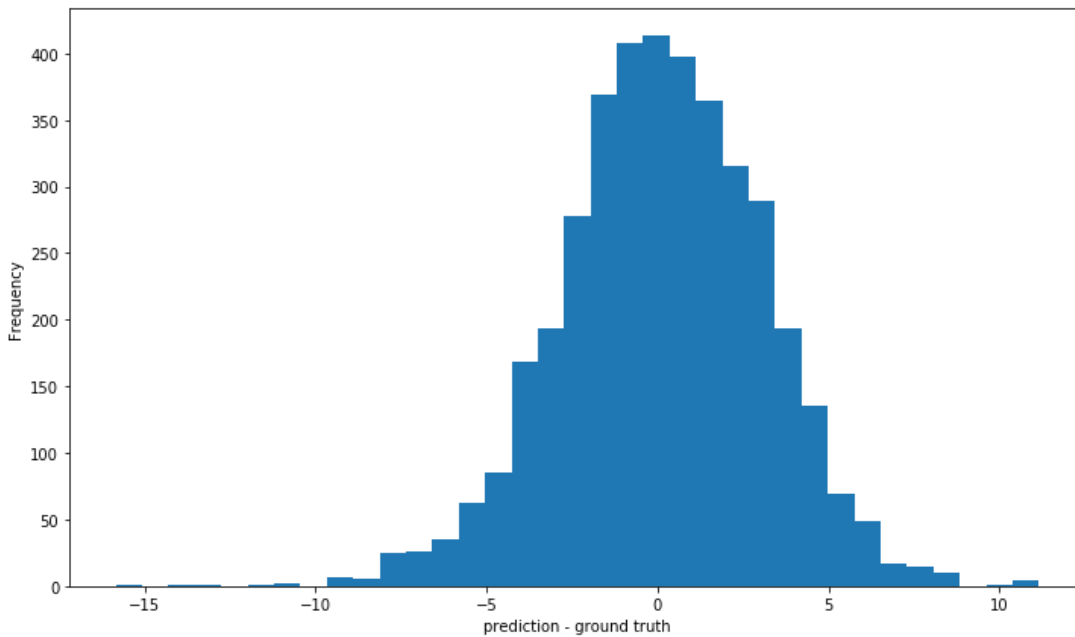
Fig 5.8(k) epoch Vs loss



(unit of MAE = miles/hr)

fig 5.8(l) epoch Vs accuracy

We can see that with continuous training, loss decreases and accuracy improves.



(unit = miles/hr)

Fig 5.8(m) histogram of errors

This is the histogram of the errors (prediction – observation) that we get after evaluating our model on validation dataset. We can see that most of the predictions are closer to ground truth i.e., errors are mostly concentrated around 0. Most of the errors are within about 10 miles/hr.

Correlation matrix

```
[[1.    0.64836289]  
 [0.64836289  1.]]
```

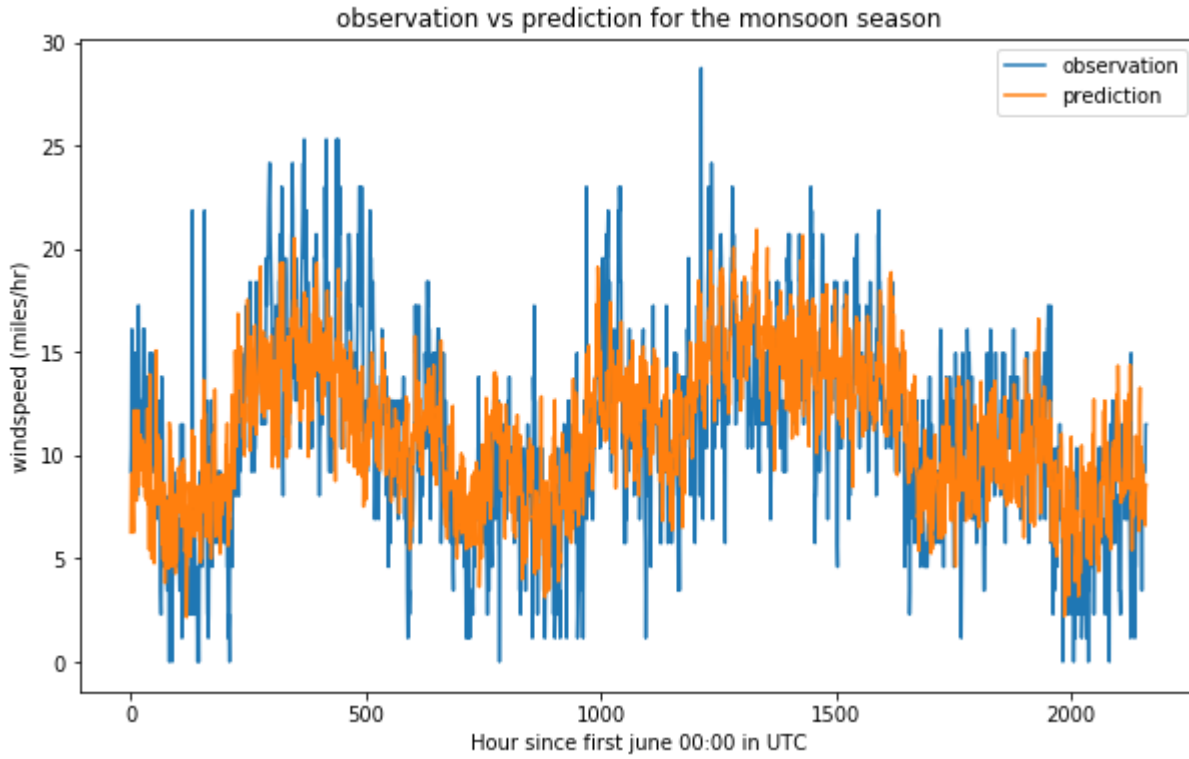
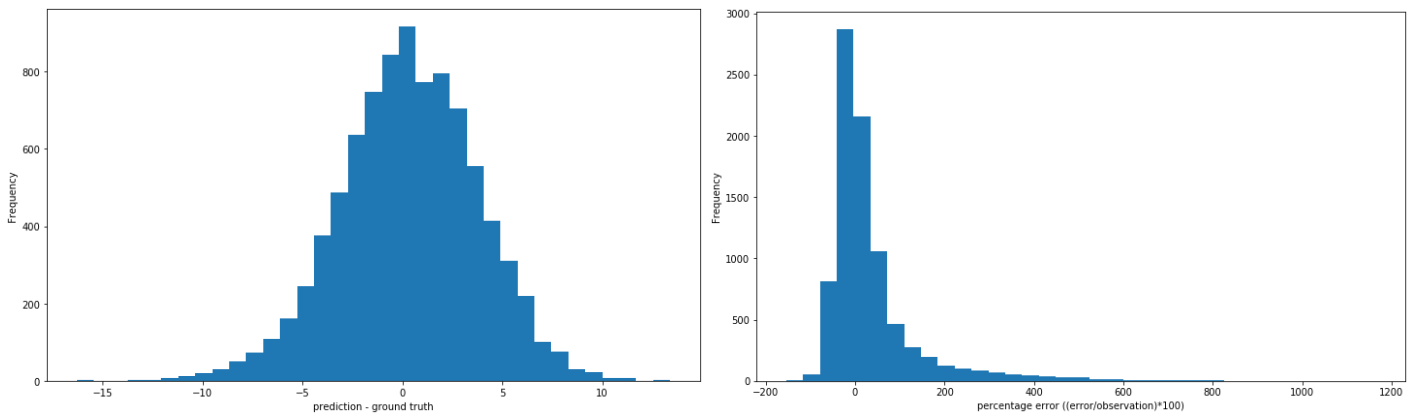


Fig 5.8(n) observation and prediction plot for monsoon season

In this, observation and prediction are put in the same plot. The data taken was for 3 months from 1st June 2021 to 31st August 2021. We first find the prediction made by our model on this 3 month input data. This is a time-series data. There is moderate correlation between observation and prediction.



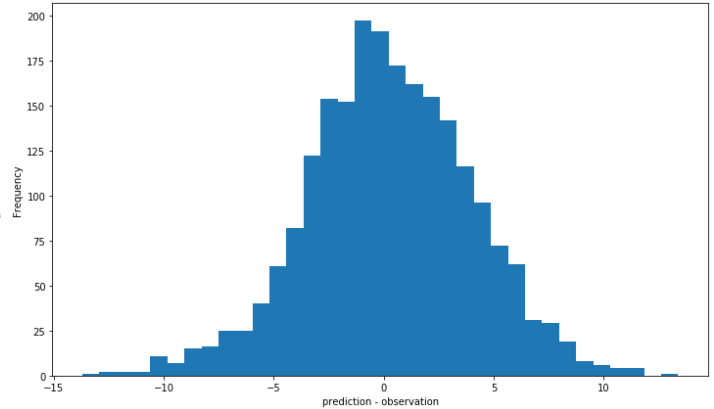
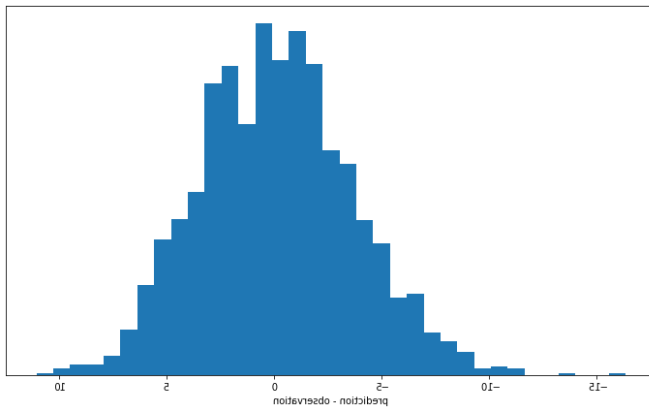
(unit = miles/hr)

(unitless)

Fig 5.8(o) histogram of errors on 1 year independent dataset

fig 5.8(p) percentage error for the same

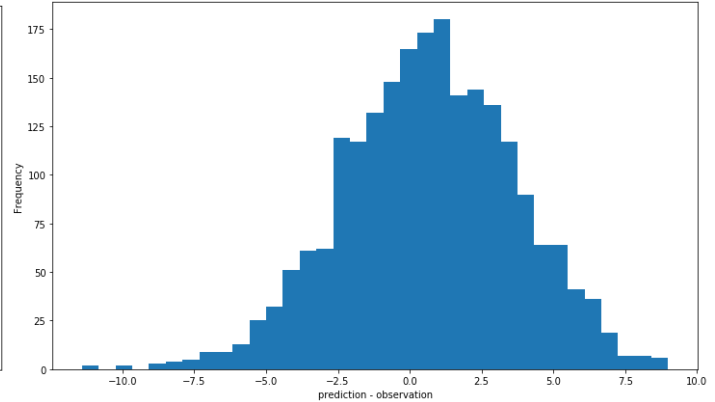
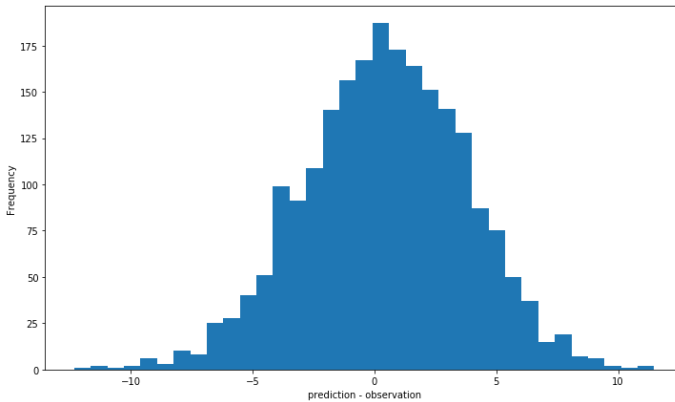
We have the histogram of errors (prediction – ground truth) and percentage error  $((\text{error}/\text{observation}) * 100)$  our model gives when tested on 1 year (1 March 2021 to 28 February 2022) of independent dataset. Again, most of the errors are concentrated around 0 miles/hr and within about 10 miles/hr and 250% error.



(x-axis unit= miles/hr)

Fig 5.8(q) error histogram for summer

fig 5.8(r) error histogram for monsoon



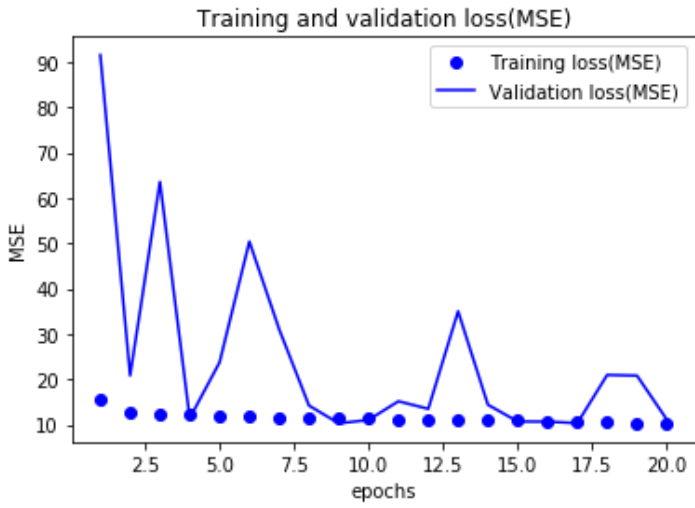
(unit = miles/hr)

Fig 5.8(s) error histogram for autumn

fig 5.8(t) error histogram for winter

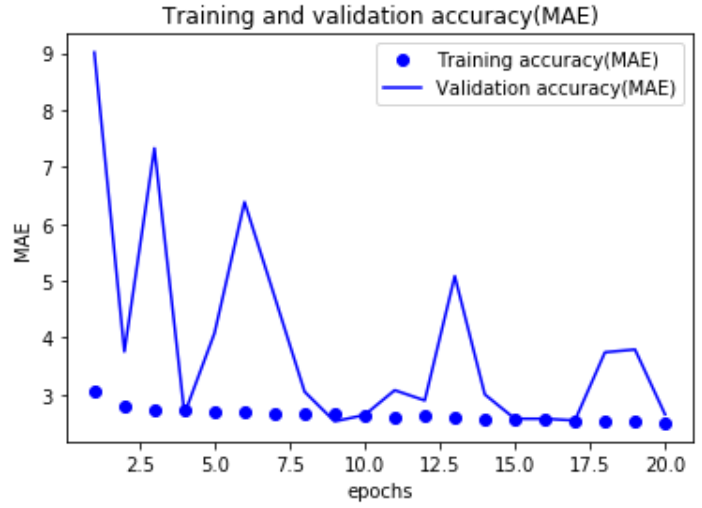
Above 4 plots are error plots when the model is tested on 4 different seasons each of 3 month time length. 1 year of independent dataset has been broken into 4 seasons. 1st, 2nd, 3rd and 4th plots are for summer, monsoon, autumn and winter datasets respectively. Most of the errors are spread over about 10 miles/hr from the center.

**With 3D CNN,**



(unit of MSE = miles squared/hr squared)

Fig 5.8(u) epoch Vs loss



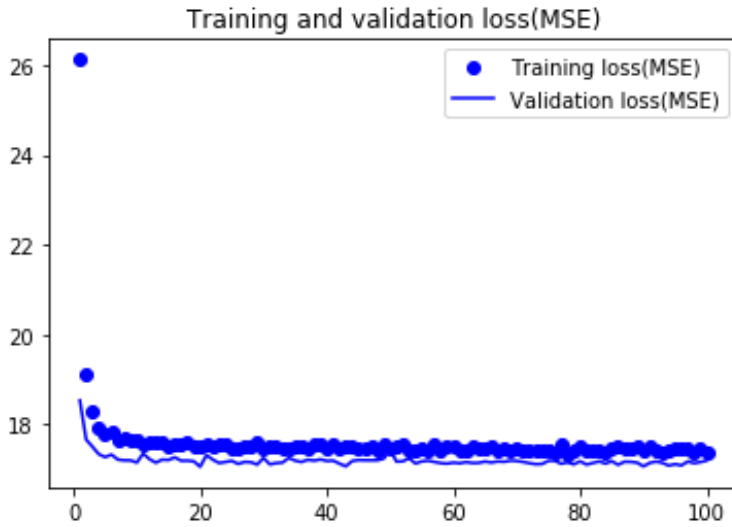
(unit of MAE = miles/hr)

fig 5.8(v) epoch Vs accuracy

We can see that with continuous training, loss decreases and accuracy improves with some fluctuation.

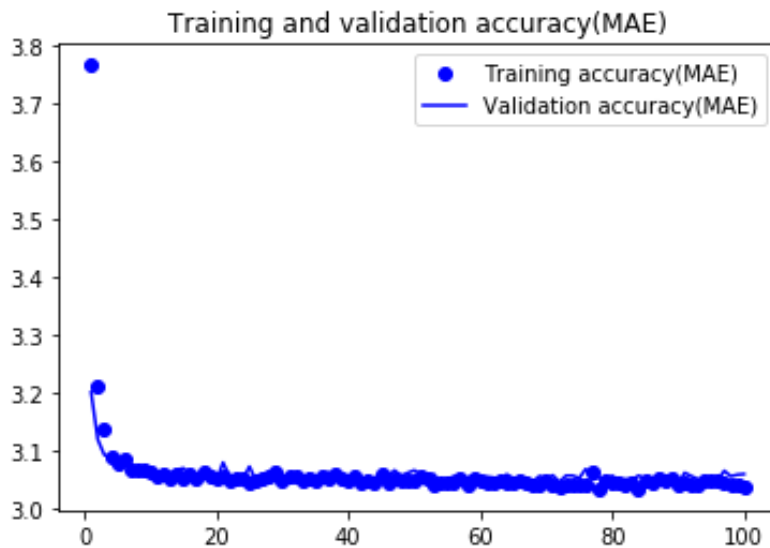
**For station VECC,**

**With VGG16,**



(x-axis= epochs, y-axis = MSE(unit = miles squared/hr squared))

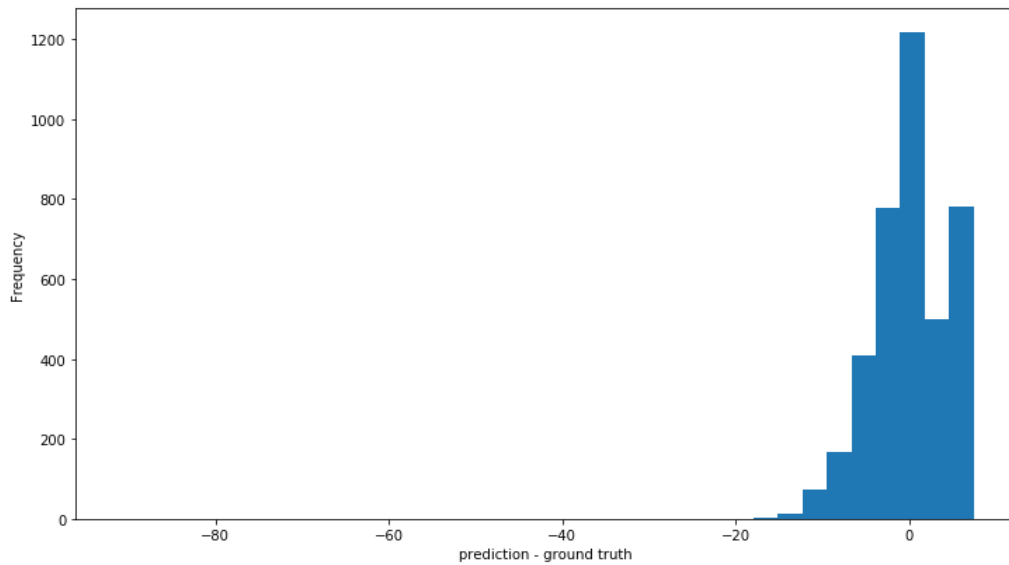
Fig 5.9(a) epoch Vs loss



(x-axis= epochs, y-axis = MAE(unit = miles/hr))

Fig 5.9(b) epoch Vs accuracy

We can see that with continuous training, loss decreases and accuracy improves. Though the improvement is only minor.



(unit = miles/hr)

Fig 5.9(c) histogram of errors

This is the histogram of the errors (prediction – observation) that we get after evaluating our model on validation dataset. We can see that most of the predictions are closer to ground truth i.e., errors are mostly concentrated around 0. Most of the errors are within about 15 miles/hr.

Correlation matrix,

```
[[1.      0.18223773]
 [0.18223773  1. ]]
```

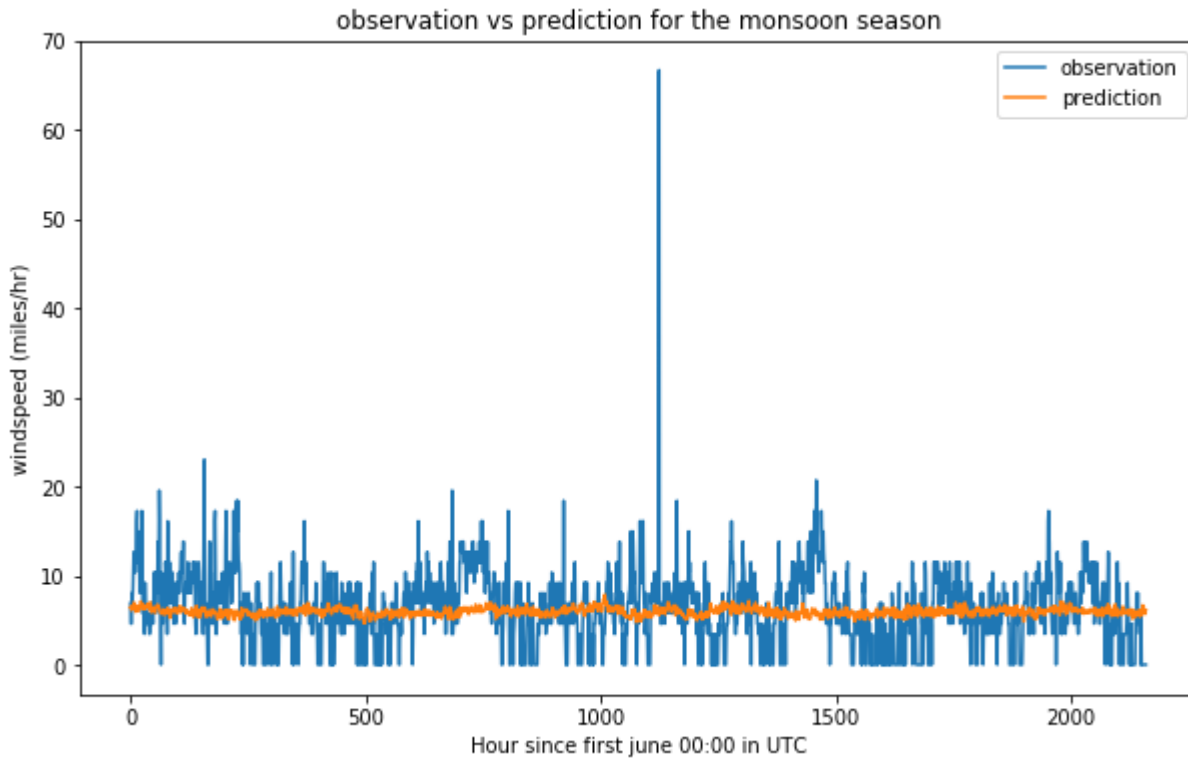


Fig 5.9(d) observation and prediction plot for monsoon season

In this, observation and prediction are put in the same plot. The data taken was for 3 months from 1st June 2021 to 31st August 2021. We first find the prediction made by our model on this 3 month independent input dataset. This is a time-series data. The plot clearly shows there is a very weak correlation between the predictions made by VGG16 model and observations made for the 3 month monsoon season.

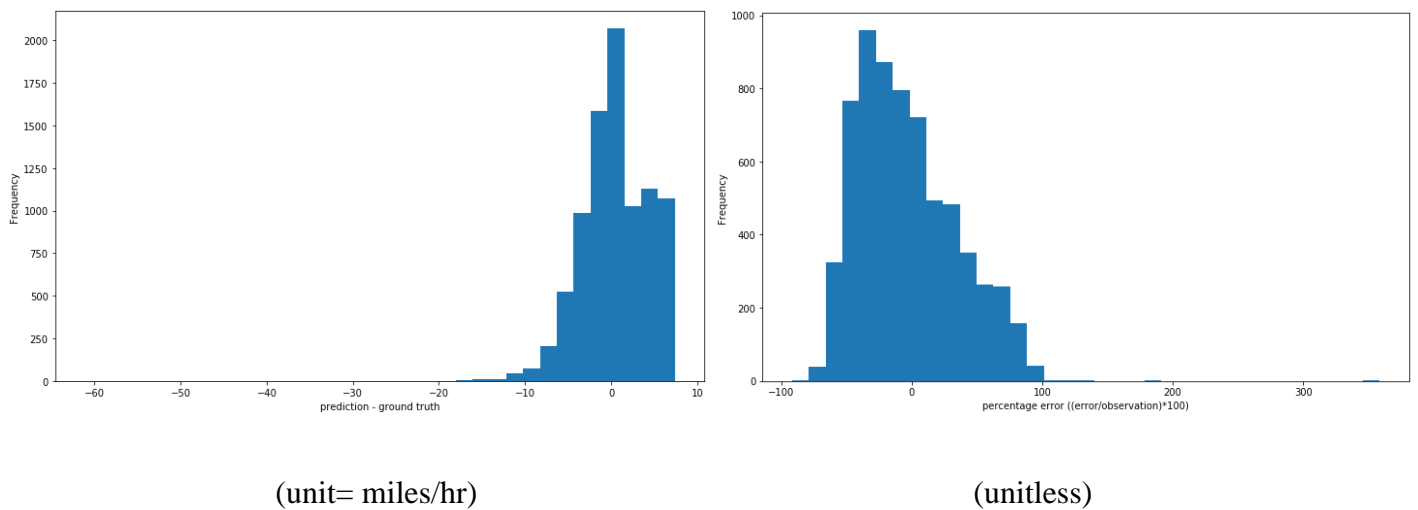
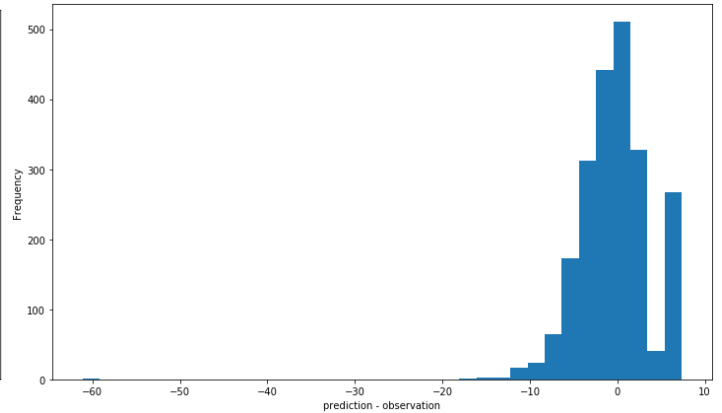
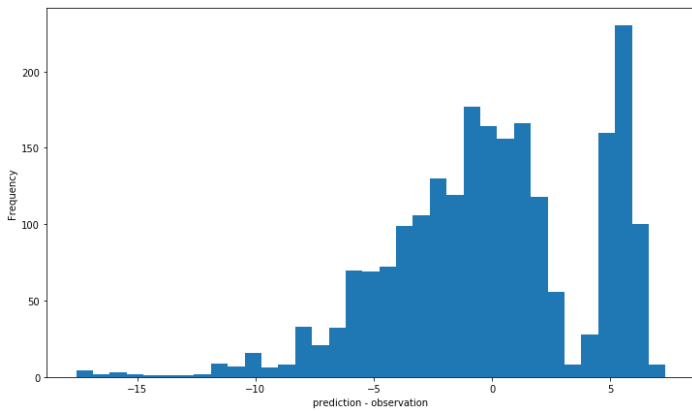


Fig 5.9(e) histogram of errors on 1 year independent dataset    fig 5.9(f) percentage error for the same

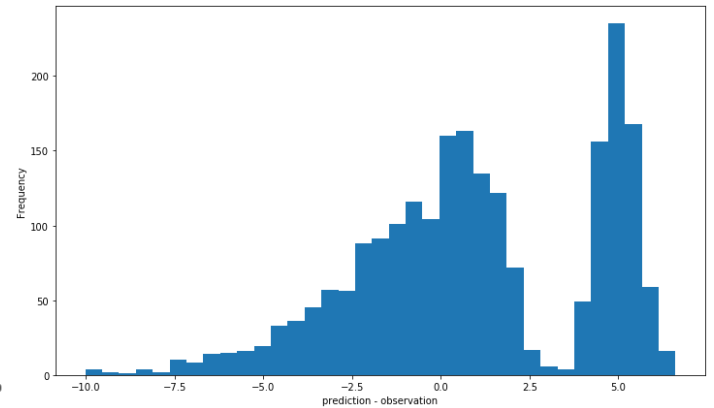
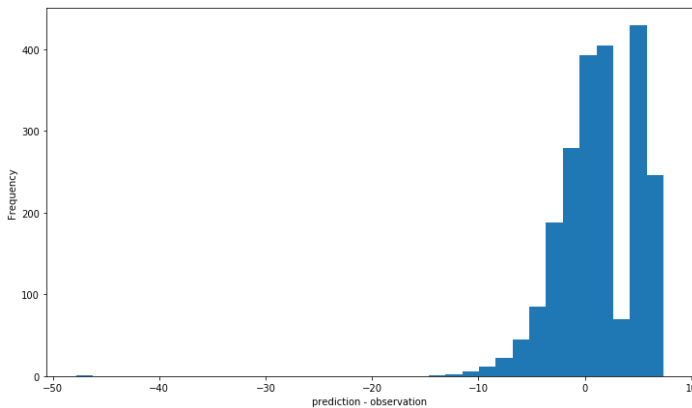
We have the histogram of errors (prediction – ground truth) and percentage error  $((\text{error}/\text{observation}) * 100)$  our model gives when tested on 1 year (1 March 2021 to 28 February 2022) of independent dataset. Again, most of the errors are concentrated around 0 miles/hr and within about 10 miles/hr and 100 % error.



(x-axis unit = miles/hr)

Fig 5.9(g) error histogram for summer

fig 5.9(h) error histogram for monsoon



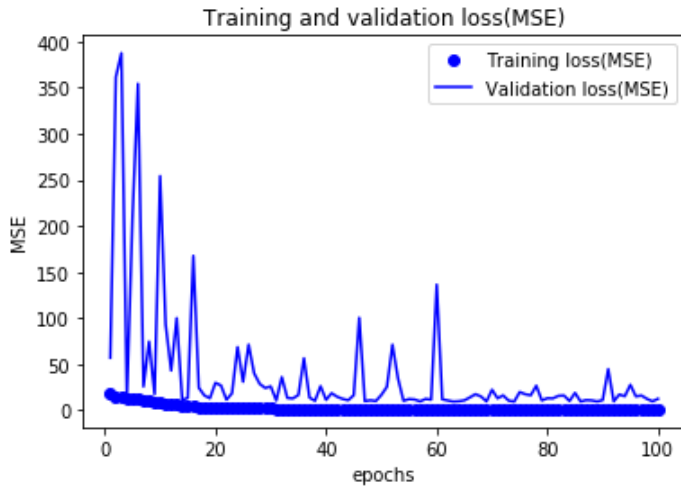
(unit= miles/hr)

Fig 5.9(i) error histogram for autumn

fig 5.9(j) error histogram for winter

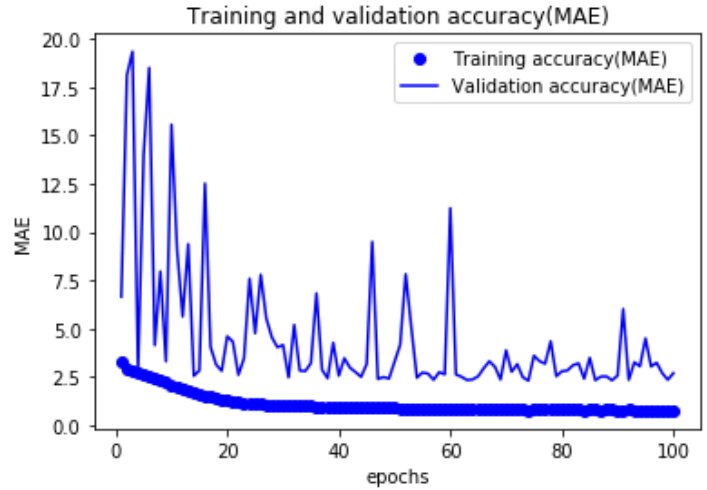
Above 4 plots are error plots when the model is tested on 4 different seasons each of 3 month time length. 1 year of independent dataset has been broken into 4 seasons. 1st, 2nd, 3rd and 4th plots are for summer, monsoon, autumn and winter datasets respectively. Most of the errors are spread over 10 miles/hr from the center.

## With 2D CNN,



(unit of MSE = miles squared/hr squared)

Fig 5.9(k) epoch Vs loss



(unit of MAE = miles/hr)

fig 5.9(l) epoch Vs accuracy

We can see that with continuous training, loss decreases and accuracy improves.

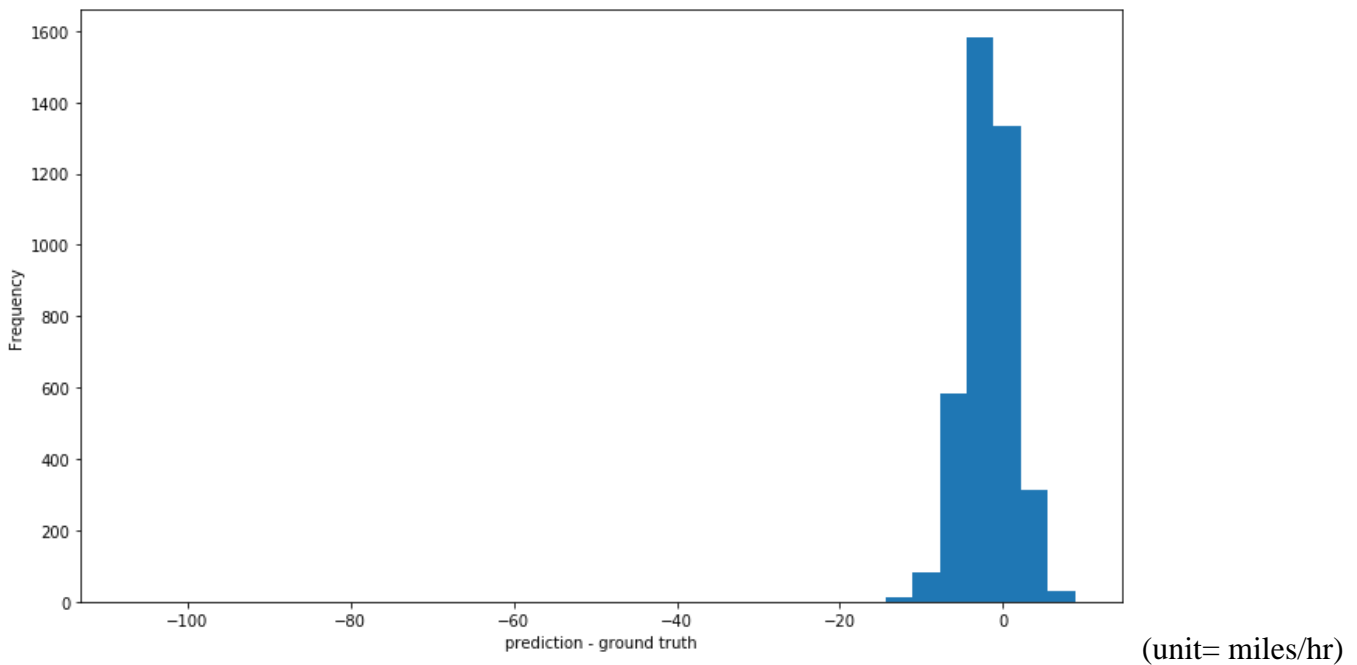


Fig 5.9(m) histogram of errors

This is the histogram of the errors (prediction – observation) that we get after evaluating our model on validation dataset. We can see that most of the predictions are closer to ground truth i.e., errors are mostly concentrated around 0. Most of the errors are within about 15 miles/hr.

Correlation matrix :

```
[[1.    0.40316432]  
 [0.40316432  1. ]]
```

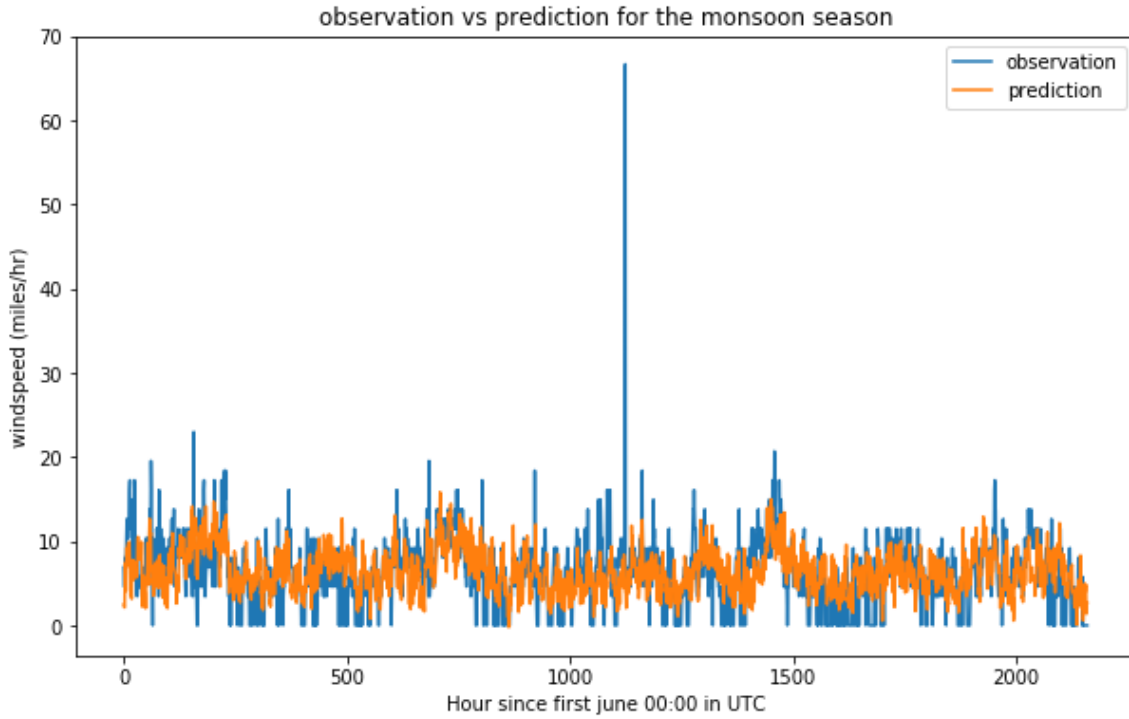
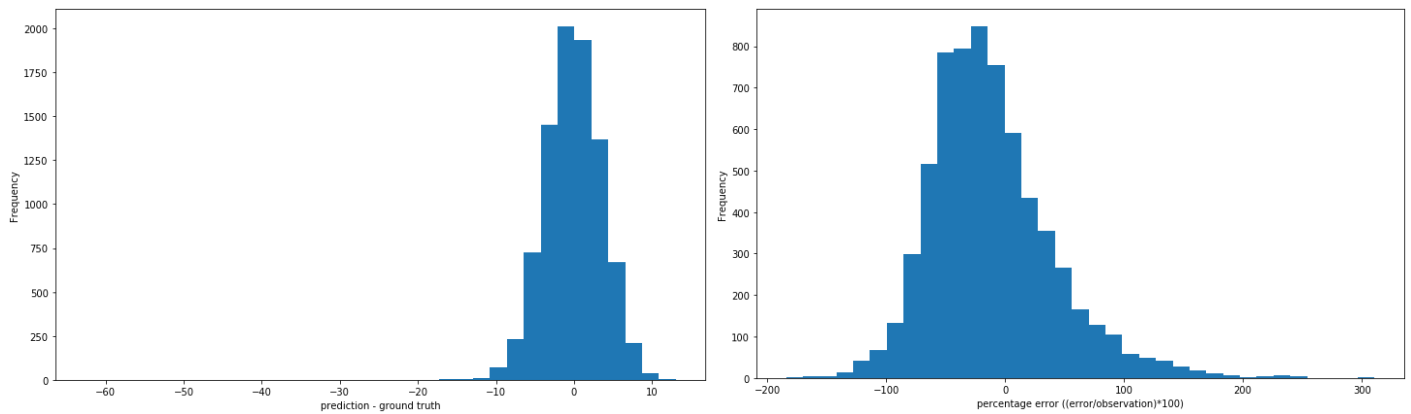


Fig 5.9(n) observation and prediction plot for monsoon season

In this, observation and prediction are put in the same plot. The data taken was for 3 months from 1st June 2021 to 31st August 2021. We first find the prediction made by our model on this 3 month input data. This is a time-series data. There is moderate correlation between observation and prediction.

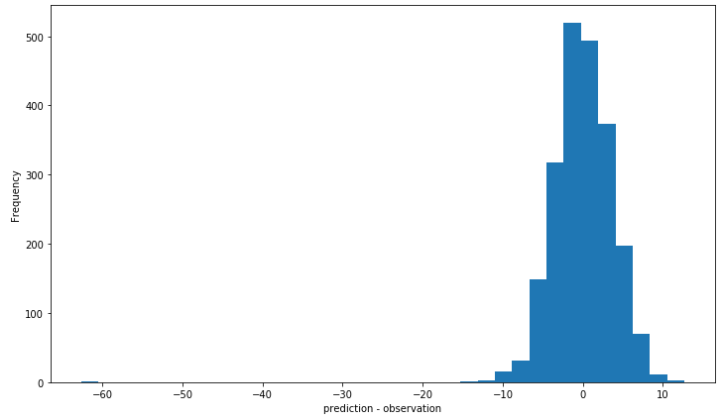
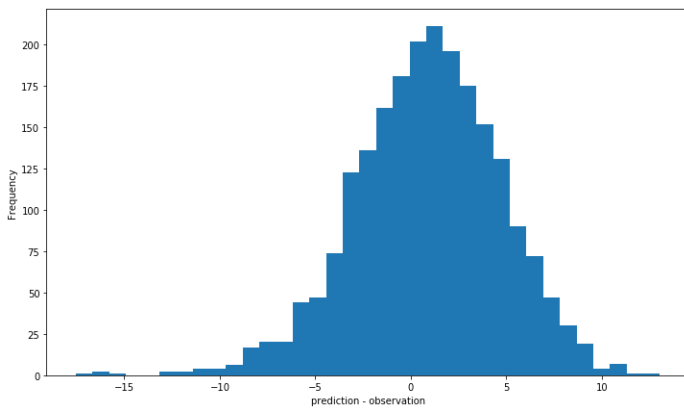


(unit= miles/hr)

(unitless)

Fig 5.9(o) histogram of errors on 1 year independent dataset    fig 5.9(p) percentage error for the same

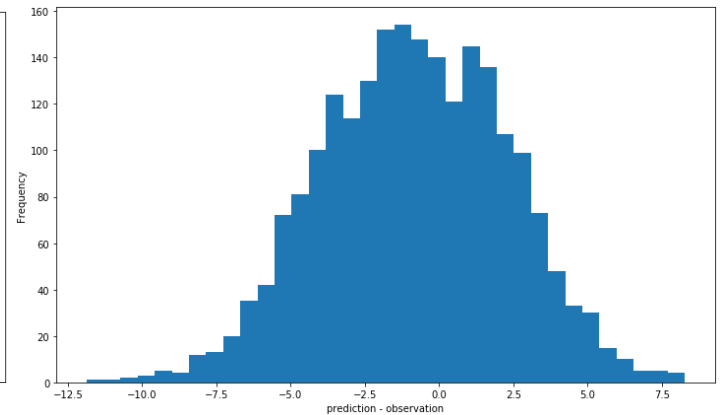
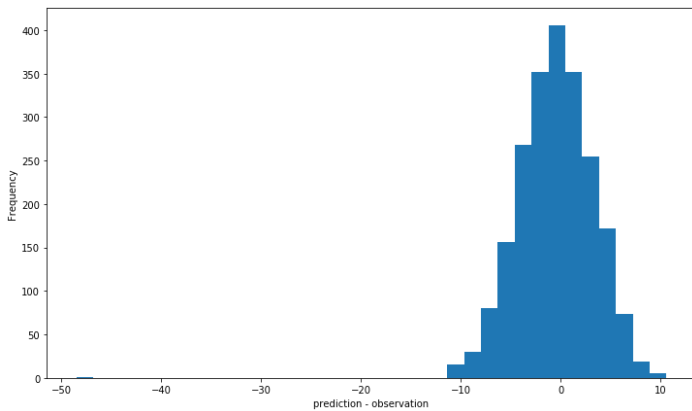
We have the histogram of errors (prediction – ground truth) and percentage error  $((\text{error}/\text{observation}) * 100)$  our model gives when tested on 1 year (1 March 2021 to 28 February 2022) of independent dataset. Again, most of the errors are concentrated around 0 miles/hr and spread within about 10 miles/hr and 100% error.



(x-axis unit = miles/hr)

Fig 5.9(q) error histogram for summer

fig 5.9(r) error histogram for monsoon



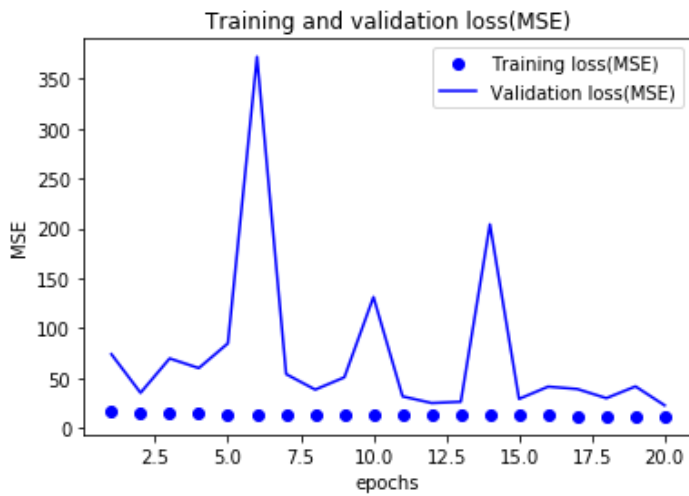
(unit= miles/hr)

Fig 5.9(s) error histogram for autumn

fig 5.9(t) error histogram for winter

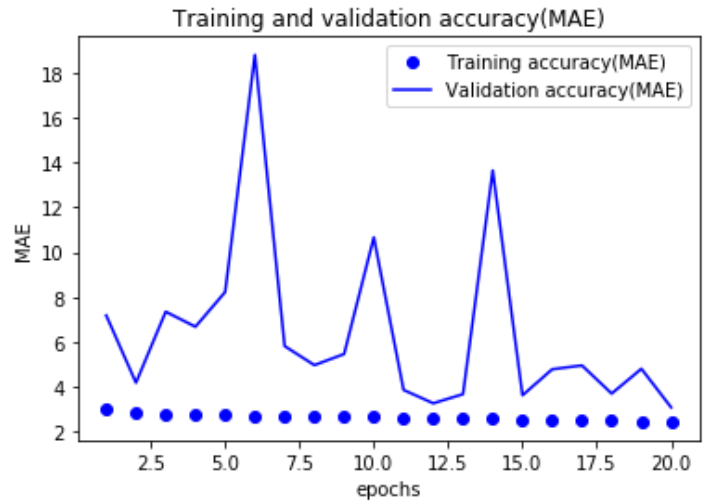
Above 4 plots are error plots when the model is tested on 4 different seasons each of 3 month time length. 1 year of independent dataset has been broken into 4 seasons. 1st, 2nd, 3rd and 4th plots are for summer, monsoon, autumn and winter datasets respectively. Most of the errors are about 10 miles/hr.

**With 3D CNN,**



(unit of MSE = miles squared/hr squared)

Fig 5.9(u) epoch Vs loss



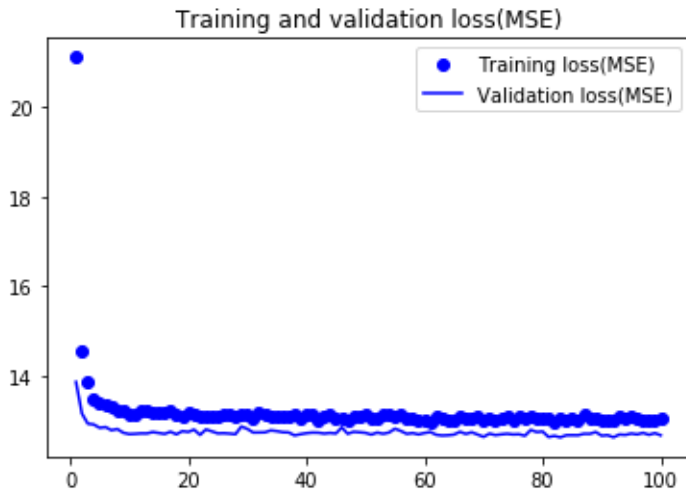
(unit of MAE = miles/hr)

fig 5.9(v) epoch Vs accuracy

With 3D CNN, we are making predictions for 6 hours in future. With continuous training, though validation loss decreases and validation accuracy improves but it also fluctuates meaning there is some over-fitting of the data.

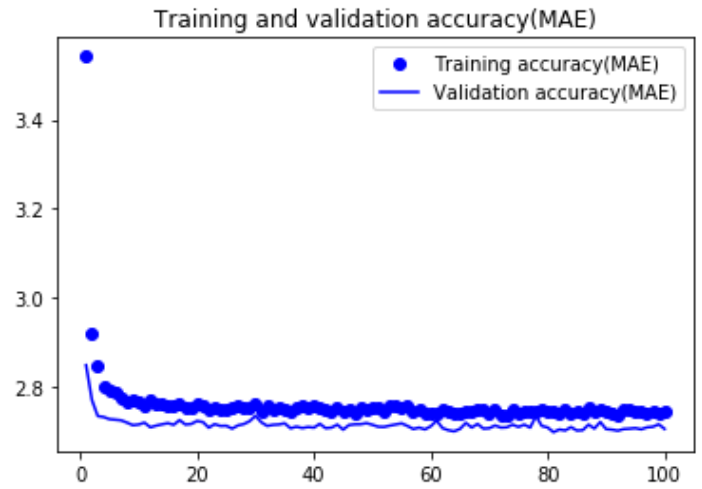
**For station VIDP,**

**With VGG16,**



(unit of MSE = miles squared/hr squared)

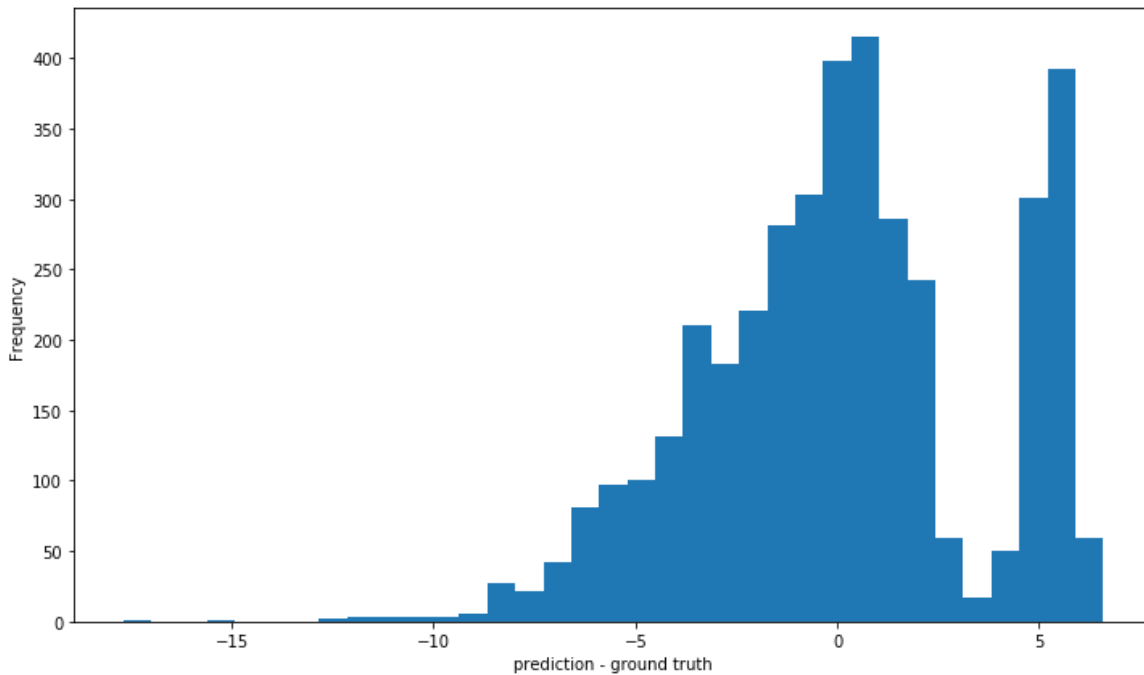
Fig 5.10(a) epoch Vs loss



(unit of MAE = miles/hr)

fig 5.10(b) epoch Vs accuracy

We can see that with continuous training, loss decreases and accuracy improves. Though the improvement is only minor.



(unit = miles/hr)

Fig 5.10(c) histogram of errors

This is the histogram of the errors (prediction – observation) that we get after evaluating our model on validation dataset. We can see that most of the predictions are closer to ground truth i.e., errors are mostly concentrated around 0. Most of the errors are within about 10 miles/hr.

Correlation matrix,

```
[[1.      0.16497658]  
 [0.16497658  1. ]]
```

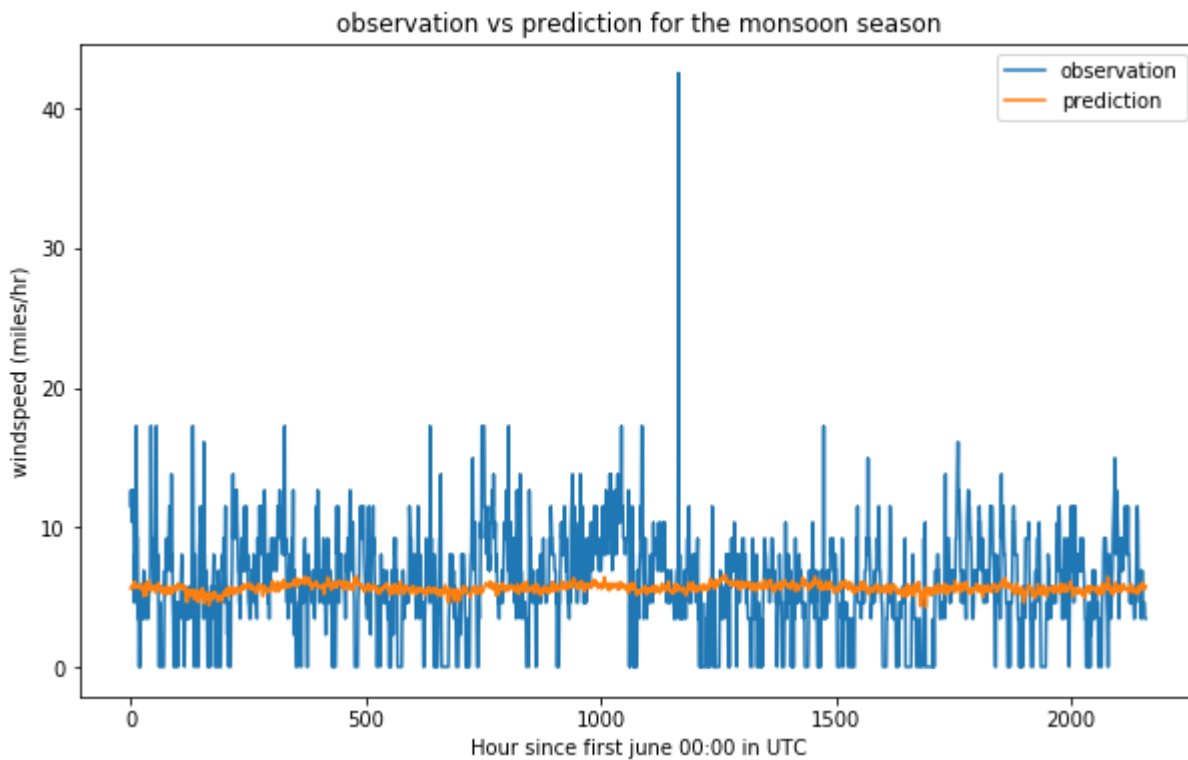
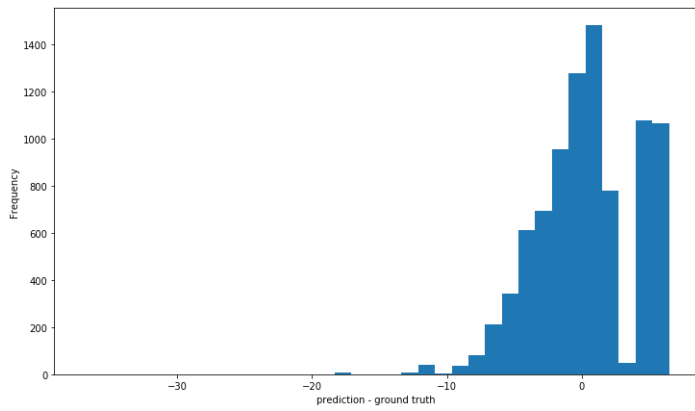
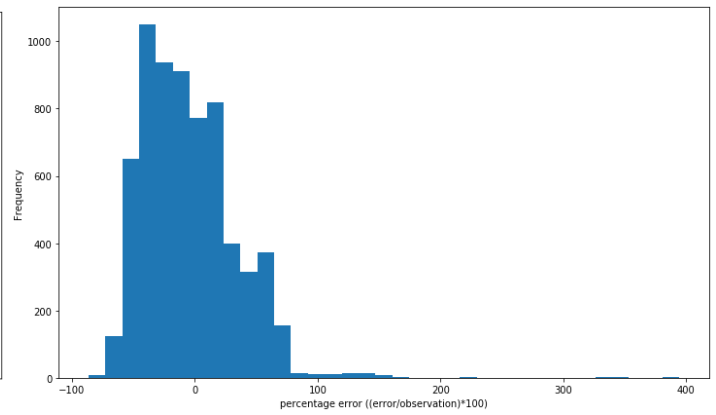


Fig 5.10(d) observation and prediction plot for monsoon season

In this, observation and prediction are put in the same plot. The data taken was for 3 months from 1st June 2021 to 31st August 2021. We first find the prediction made by our model on this 3 month independent input dataset. This is a time-series data. The plot clearly shows there is very weak correlation between the predictions made by VGG16 model and observations made for the 3 month monsoon season.



(unit = miles/hr)

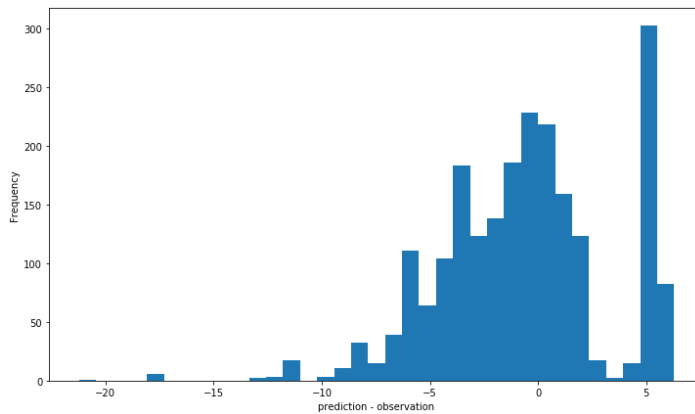


(unitless)

Fig 5.10(e) histogram of errors on 1 year independent dataset

fig 5.10(f) percentage error for the same

We have the histogram of errors (prediction – ground truth) and percentage error  $((\text{error}/\text{observation}) \times 100)$  our model gives when tested on 1 year (1 March 2021 to 28 February 2022) of independent dataset. Again, most of the errors are concentrated around 0 miles/hr and within about 10 miles/hr and 100% error.



(x-axis unit = miles/hr)

Fig 5.10(g) error histogram for summer

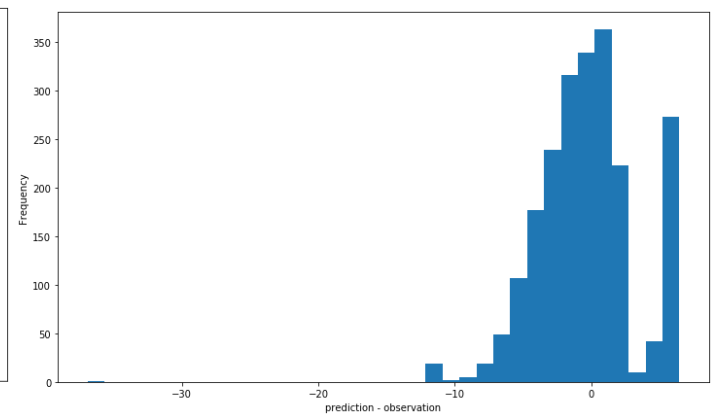
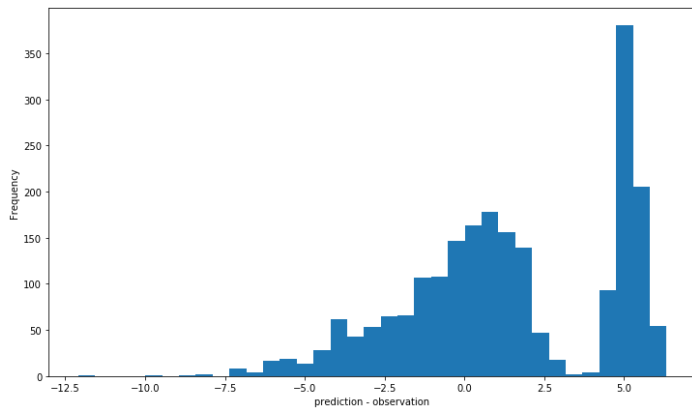


fig 5.10(h) error histogram for monsoon



(unit = miles/hr)

Fig 5.10(i) error histogram for autumn

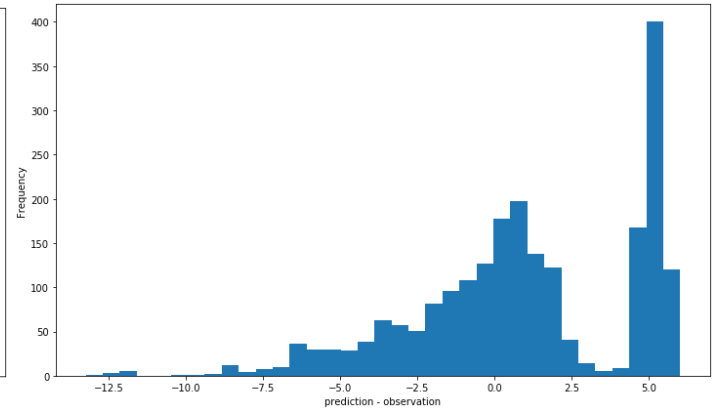
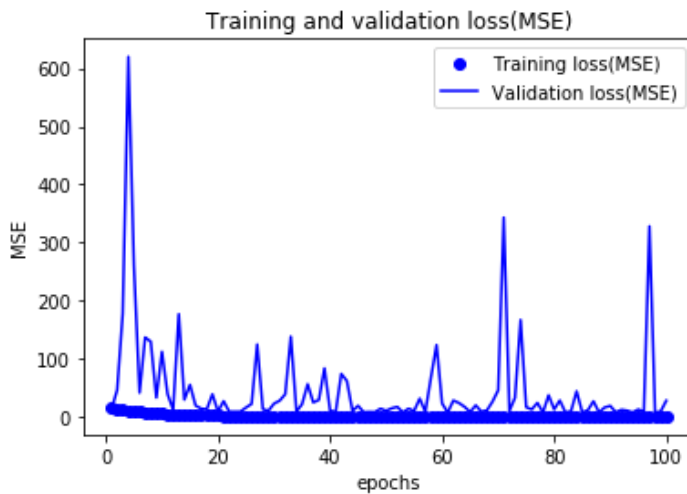


fig 5.10(j) error histogram for winter

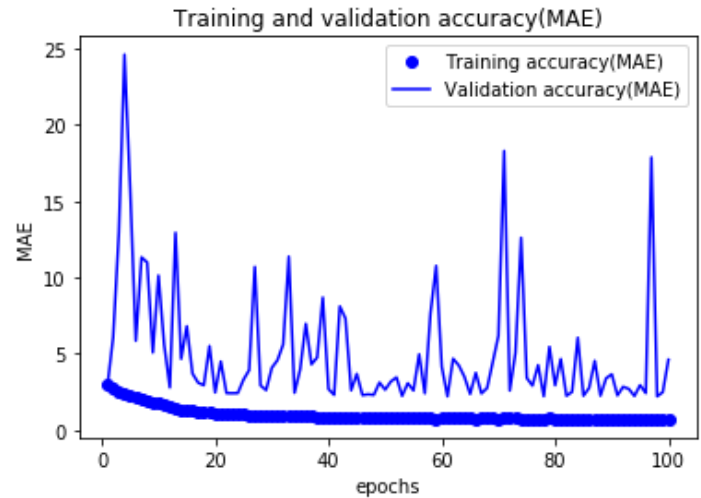
Above 4 plots are error plots when the model is tested on 4 different seasons each of 3 month time length. 1 year of independent dataset has been broken into 4 seasons. 1st, 2nd, 3rd and 4th plots are for summer, monsoon, autumn and winter datasets respectively. Most of the errors are spread over 10 miles/hr from the center.

### With 2D CNN,



(unit of MSE = miles squared/hr squared)

Fig 5.10(k) epoch Vs loss



(unit of MAE = miles/hr)

fig 5.10(l) epoch Vs accuracy

We can see that with continuous training, loss decreases and accuracy improves although there is definitely some over-fitting of the data.

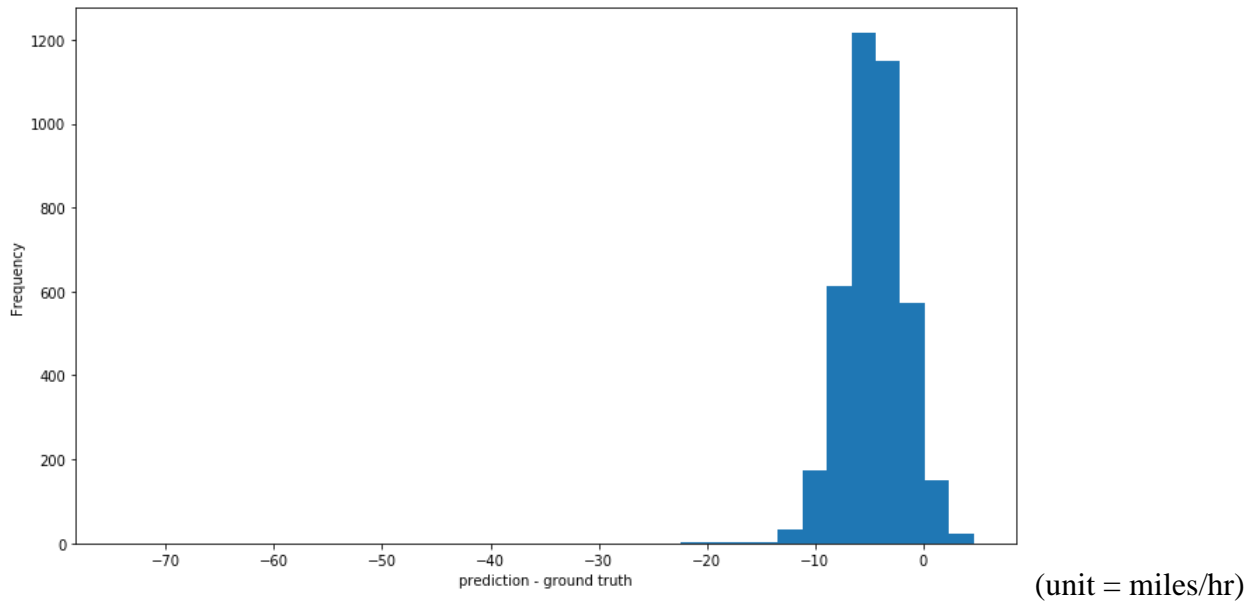


Fig 5.10(m) histogram of errors

This is the histogram of the errors (prediction – observation) that we get after evaluating our model on validation dataset. We can see that most of the predictions are closer to ground truth i.e., errors are mostly concentrated around -5 miles/hr. Most of the errors are spread over 5 miles/hr from the center.

Correlation matrix

```
[[1.    0.4289302]
 [0.4289302  1.  ]]
```

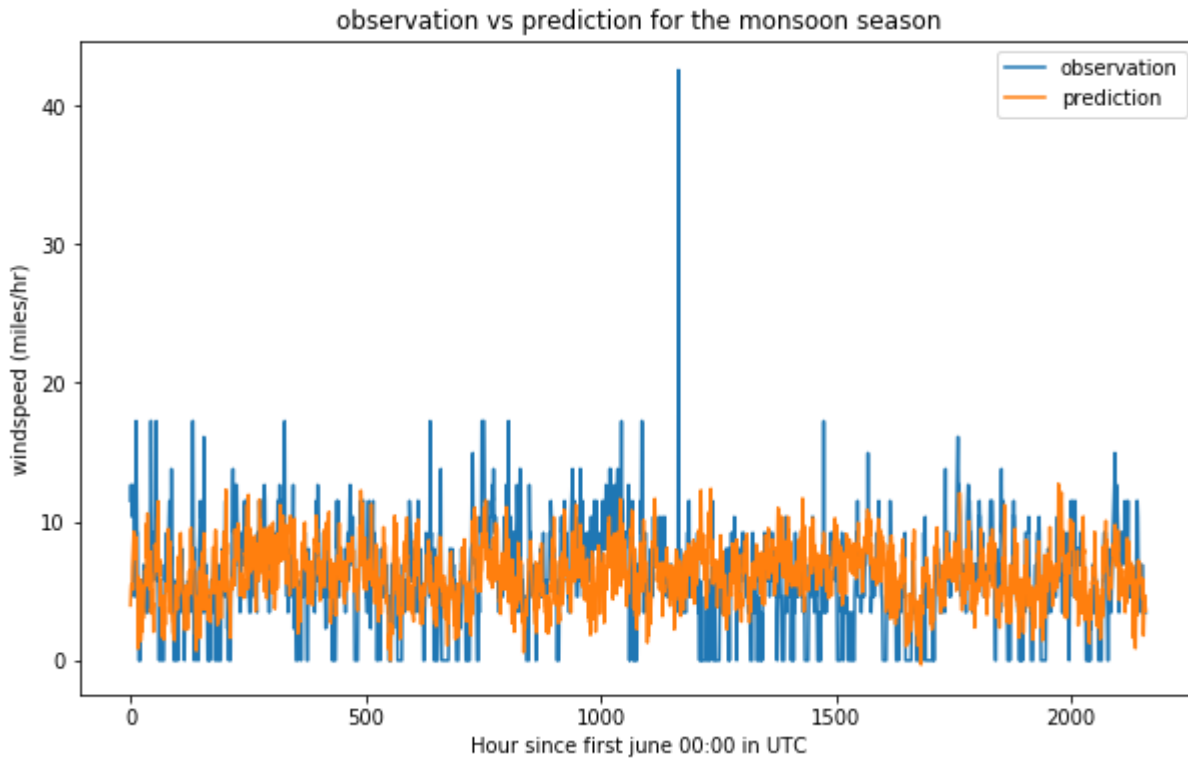
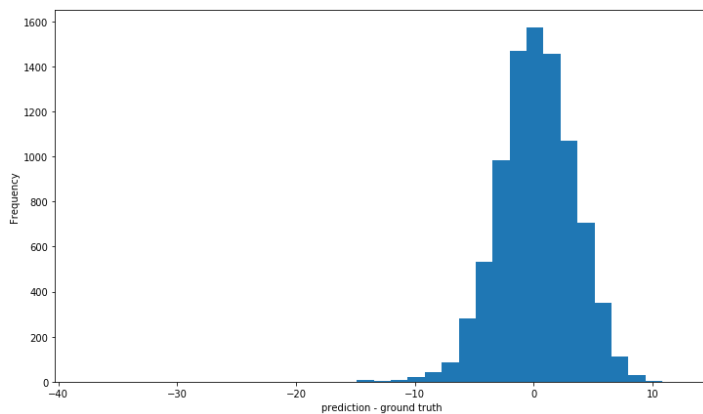
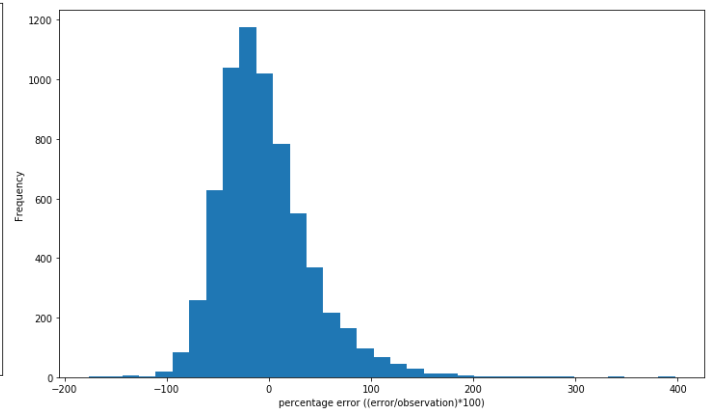


Fig 5.10(n) observation and prediction plot for monsoon season

In this, observation and prediction are put in the same plot. The data taken was for 3 months from 1st June 2021 to 31st August 2021. We first find the prediction made by our model on this 3 month input data. This is a time-series data. There is moderate correlation between observation and prediction.



(unit = miles/hr)

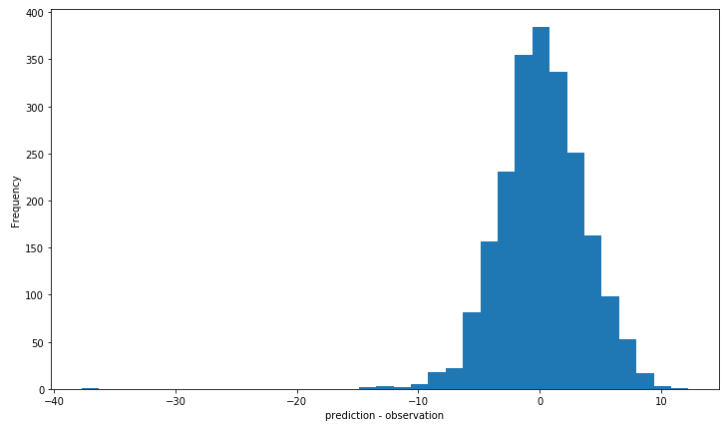
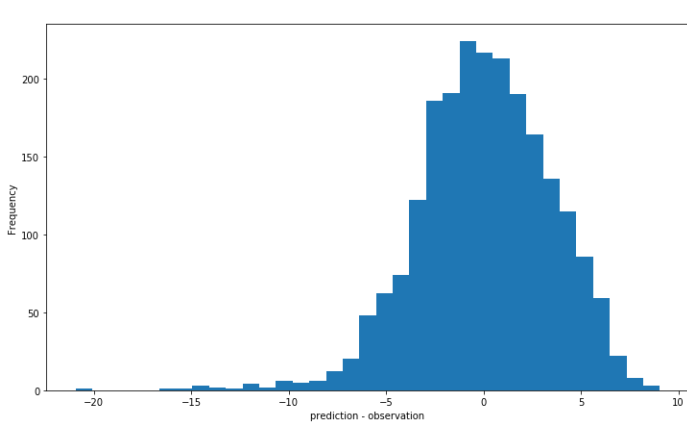


(unitless)

Fig 5.10(o) histogram of errors on 1 year independent dataset

fig 5.10(p) percentage error for the same

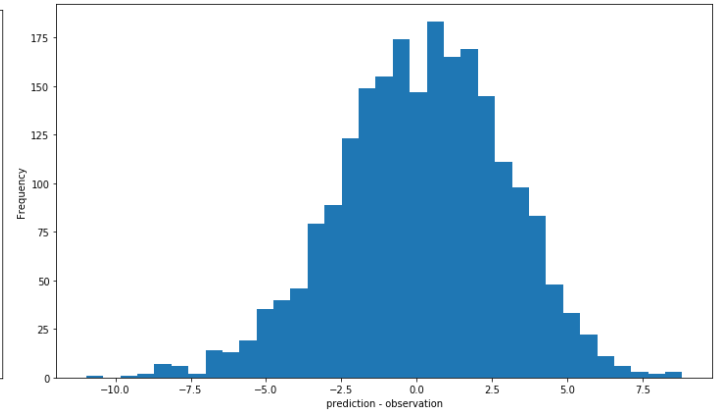
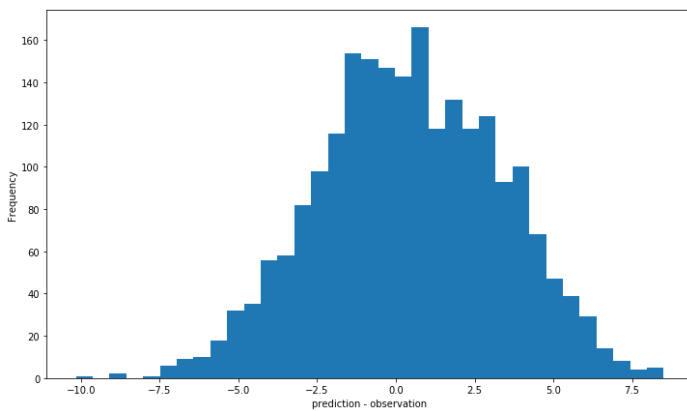
We have the histogram of errors (prediction – ground truth) and percentage error  $((\text{error}/\text{observation}) * 100)$  our model gives when tested on 1 year (1 March 2021 to 28 February 2022) of independent dataset. Again, most of the errors are concentrated around 0 miles/hr and within about 10 miles/hr and 100 % error.



(x-axis unit = miles/hr)

Fig 5.10(q) error histogram for summer

fig 5.10(r) error histogram for monsoon



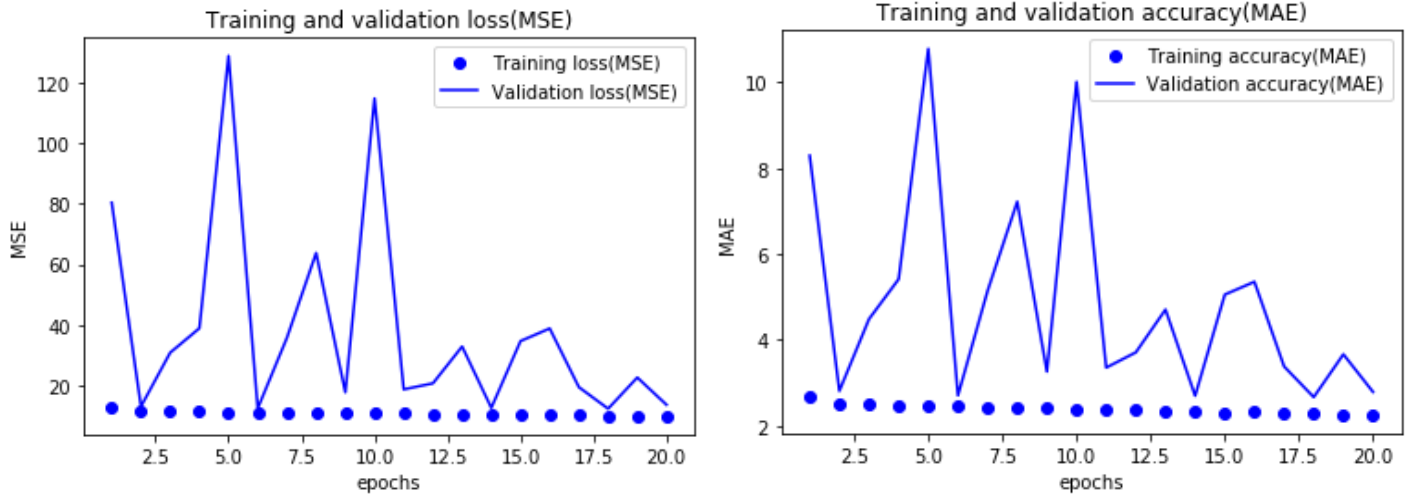
(unit = miles/hr)

Fig 5.10(s) error histogram for autumn

fig 5.10(t) error histogram for winter

Above 4 plots are error plots when the model is tested on 4 different seasons each of 3 month time length. 1 year of independent dataset has been broken into 4 seasons. 1st, 2nd, 3rd and 4th plots are for summer, monsoon, autumn and winter datasets respectively. Most of the errors are over 7.5 miles/hr from the center.

## With 3D CNN,



(unit of MSE = miles squared/hr squared)

(unit of MAE = miles/hr)

Fig 5.10(u) epoch Vs loss

fig 5.10(v) epoch Vs accuracy

With 3D CNN, we are making predictions for 6 hours in future. With continuous training, validation loss decreases and validation accuracy improves.

After all these experiments on different stations using different models, we come to the conclusion that our custom made and trained from scratch 2D CNN model performs best. Transfer learning has not worked very well in this case. We need to do more experiments with other pretrained models to conclusively say if state of the art pretrained models in computer vision can be applied in case of weather downscaling too. 3D CNN is working good for 6 hour in future prediction.

## **CHAPTER 6 – Conclusions and Future work**

This research shows that CNNs can be used to analyse the output of numerical weather models directly by using observed metar data as a target. Despite the fact that they are simple, convolutional layers can be utilised to interpret the output of numerical weather models, according to the findings. The wind speed or visibility output variable are not directly related to the NWP parameter (geopotential) employed in the studies. The goal of this initial experiment was to show that CNNs can learn certain atmospheric pressure system configurations and connect them with wind speed and visibility. These methodologies enable a new research avenue to automatically generate many derived products, in addition to weather model interpretation. Some variables in NWP are computed using statistical models rather than physical equations. So, there is a possibility that CNN-based models can be used to compute these variables, perhaps providing better results.

The code and corresponding datasets used to run all the experiments included in this work are available at the following repository: <https://github.com/AIMa-hash/Deep-Learning-for-Climate-Studies>

# REFERENCES

- 1- Duong Tran Anh, Song Pham, Thanh Duc Dang, Long Phi Hoang, March 2019, International Journal of Climatology DOI:10.1002/joc.6066
- 2- Jorge Baño-Medina, Rodrigo Manzanas, José Manuel Gutiérrez. "On the suitability of deep convolutional neural networks for continentalwide downscaling of climate change projections" , Climate Dynamics, 2021
- 3- Kevin Höhle, Michael Kern, Timothy Hewson, Rüdiger Westermann. "A comparative study of convolutional neural network models for wind field downscaling" , Meteorological Applications, 2020
- 4- Pablo Rozas Larraondo, Inaki Inza, Jose A. Lozano. Automating weather forecasts based on convolutional networks. In Proceedings of the ICML 17 Workshop on Deep Structured Prediction, Sydney, Australia, PMLR 70, 2017.
- 5- Popular networks (2018), neurohive.io/en/popular-networks/vgg16/
- 6- Slifka Sylwia Trzaska, Emilie SchnarrCenter, A Review of Downscaling Methods for Climate Change Projections, Center for International Earth Science Information Network (CIESIN), SEPTEMBER 2014
- 7- Wang, F., Tian, D., Lowe, L., Kalin, L., & Lehrter, J. (2021). Deep learning for daily precipitation and temperature downscaling. Water Resources Research, 57, e2020WR029308. doi:10.1029/2020WR029308

